

8-9-2014

Mechanistic Investigation of a Silylation-Based Kinetic Resolution Using Linear Free Energy Relationships and Its Application to Substrate Expansion and Polymer Supported Kinetic Resolutions

RAVISH K. AKHANI

University of South Carolina - Columbia

Follow this and additional works at: <https://scholarcommons.sc.edu/etd>

 Part of the [Chemistry Commons](#)

Recommended Citation

AKHANI, R. K.(2014). *Mechanistic Investigation of a Silylation-Based Kinetic Resolution Using Linear Free Energy Relationships and Its Application to Substrate Expansion and Polymer Supported Kinetic Resolutions*. (Doctoral dissertation). Retrieved from <https://scholarcommons.sc.edu/etd/2785>

This Open Access Dissertation is brought to you by Scholar Commons. It has been accepted for inclusion in Theses and Dissertations by an authorized administrator of Scholar Commons. For more information, please contact digres@mailbox.sc.edu.

MECHANISTIC INVESTIGATION OF A SILYLATION-BASED KINETIC RESOLUTION
USING LINEAR FREE ENERGY RELATIONSHIPS AND ITS APPLICATION TO
SUBSTRATE EXPANSION AND POLYMER SUPPORTED KINETIC RESOLUTIONS

by

RAVISH K. AKHANI

Bachelor of Science
Gujarat University, 2004

Master of Science
Gujarat University, 2006

Master of Science
Long Island University, 2009

Submitted in Partial Fulfillment of the Requirements

For the Degree of Doctor of Philosophy in

Chemistry

College of Arts and Sciences

University of South Carolina

2014

Accepted by:

Sheryl L. Wiskur, Major Professor

Ken D. Shimizu, Committee Member

Daniel L. Reger, Committee Member

Sondra Berger, Committee Member

Lacy Ford, Vice Provost and Dean of Graduate Studies

© Copyright by Ravish K. Akhiani, 2014
All Rights Reserved.

DEDICATION

This work is dedicated to my late father Kantilal B. Akhani, my mother Daksha K. Akhani and my wife Rajeshwari Patel.

ACKNOWLEDGEMENTS

First and foremost, I would like to thank my advisor Dr. Sheryl Wiskur. I really appreciate her support and dedicated involvement in every step throughout the process, which allowed me to bring my maximum potential out as a research scientist. I would also like to thank you for your financial support through NSF career award to do my research and attend conferences.

I would like to show gratitude to my committee members who helped me to walk through the entire process of the graduate school. I would like to thank all staff members at chemistry department, as they were very helpful and supportive people. I must also thanks to my advisor Dr. Wayne Schnatter at the Long Island University and professors at the St. Xavier's college for their guidance over the past several years. I am very thankful to the past and current members of the Wiskur lab for their help and support during this past couple years. I would like to thank Dr. Cody Sheppard and Dr. Maggie Moore for teaching me about research and helping me during my plan, proposal and seminars. I am also thankful to Robert Clark, Li Wang, Max Deaton and Julia Pribyl as they always made lab environment very energetic through various discussions. This accomplishment would have not been possible without support from so many people around the globe. Thanks to all my friends (Alpit, Niral, Satish, Kenal, Jatin, Niyati, Jay, Kunjal, Shreyas, Mansi, Vaibhav, Anuja, Anand , Pratik and many more) and family here in USA and in INDIA for always being with me and support me to pursue my dream. I want to thank my sister Ami

Trivedi and her family (Riya, Keya and Rajesh Trivedi) as they were the one who took care of my mother all the time in my absence. I would like to thank my parents in law Jaytibhai Patel and Chandrikaben Patel for always supporting me to achieve my dream. I don't have enough words to thank my mother Dakshaben Akhani, I would have not even able to think about my graduate study without her blessings and all her sacrifices for me.

Finally, I would like thank my wife Rajeshwari Patel (Roshni) for being with me in this entire journey and helping on every step of my career. I cannot even image my life without her. Roshni, Love you so much and desperately waiting for our new family member to begin a new paradigm of our life

ABSTRACT

This dissertation represents our preliminary mechanistic investigations on the silylation-based kinetic resolution of secondary alcohols, and how we use that knowledge for further expansion of this methodology. Chapter 2 describes how we came up with a preliminary mechanism of our silylation-based methodology using a linear free energy relationship and a rate study. In this chapter, several *para* substituted triphenylsilyl chlorides were prepared that varied electronically and sterically in order to understand the substituent effects on the rate and the selectivity of the reaction. Selectivity factors and initial rates were experimentally determined for the kinetic resolution reactions with the newly designed silyl chlorides. Linear free energy relationships were found to correlate both selectivity factors and initial rates.

Chapter 3 covers our ^{29}Si NMR studies in order to understand if a complex is forming between the catalyst (-)-tetramisole and Ph_3SiCl . A variety of different techniques were used including ^1H NMR titrations, ^{29}Si NMR experiments, and ^1H - ^{29}Si gHSQC 2D experiments. Finally, three different mechanisms were proposed for future study.

Chapter 4 discusses our efforts to apply the silylation-based methodology developed by the Wiskur lab to allylic alcohols, homoallylic alcohols, and 2-arylcyclohexanols. No enantiodiscrimination was obtained with allylic alcohols and homoallylic alcohols while a moderate level of selectivity was achieved with

2-arylcyclohexanols. Employing Ph_3SiCl substituted in the *para* position with an isopropyl group in the kinetic resolution reaction of 2-arylcyclohexanol resulted in a doubling of the selectivity factor. The synthesis of various substrates and employing them in our kinetic resolution is discussed.

Chapter 5 describes the use of a polymer supported triphenylsilyl chloride in our kinetic resolution reaction. Different molecular weight polymers containing triphenylsilyl chloride were prepared and tested in the kinetic resolution of 4-chromanol. Similar selectivity factors were reported in all cases. Reaction optimization along with future work for this project is discussed.

Finally, Chapter 6 explores our attempt toward the development of a kinetic resolution of amines by transforming them into imines and employing them in an asymmetric aza-Diels-Alder reaction. Various chiral Lewis acids were attempted to achieve selectivity in the aza-Diels-Alder reaction.

TABLE OF CONTENTS

DEDICATION	iii
ACKNOWLEDGEMENTS	iv
ABSTRACT	vi
LIST OF TABLES	xi
LIST OF FIGURES	xiii
LIST OF SCHEMES	xvi
CHAPTER 1: BACKGROUND AND INTRODUCTION TO THE SILYLATION-BASED KINETIC RESOLUTION	1
1.1 INTRODUCTION	1
1.2 METHODS TO OBTAIN ENANTIOMERICALLY PURE COMPOUNDS	3
1.3 ACYLATION	12
1.4 SILYLATION	19
1.5 CONCLUSIONS	25
1.6 REFERENCES	28
CHAPTER 2 MECHANISTIC INVESTIGATION OF SILYLATION-BASED KINETIC RESOLUTION USING LINEAR FREE ENERGY RELATIONSIPS AND RATE STUDY	34
2.1 INTRODUCTION	34
2.2 BACKGROUND: NUCLEOPHILIC ASSISTED SILYLATION AND LINEAR FREE ENERGY RELATIONSHIPS (LFER)	36
2.3 LFER IN ASYMMETRIC CATALYSIS	44

2.4 EXAMPLES OF LFER IN ASYMMETRIC CATALYSIS	46
2.5 UNDERSTANDING THE MECHANISM OF OUR Silylation-BASED KINETIC RESOLUTION THROUGH LINEAR FREE ENERGY RELATIONSHIPS USING SELECTIVITY FACTORS AND A RATE STUDY	50
2.6 SYNTHESIS OF <i>P</i> -SUBSTITUTED TRIPHENYLSilyL CHLORIDES	53
2.7 RATE STUDY USING FAST REACTING ENANTIOMER WITH DIFFERENT PARA SUBSTITUTED TRIPHENYLSilyL CHLORIDES.....	54
2.8 KINETIC RESOLUTION OF TETRALOL AND 4-CHROMANOL USING DIFFERENT PARA SUBSTITUTED TRIPHENYLSilyL CHLORIDES.....	59
2.9 CONCLUSIONS	69
2.10 EXPERIMENTAL	70
2.11 REFERENCES.....	107
CHAPTER 3 COMPLEX FORMATIONS STUDY OF TRIPHENYLSilyL CHLORIDE AND (-)- TETRAMISOLE USING $^1\text{H}/^{29}\text{Si}$ NMR FOR THE ENANTIOSELECTIVE SilyLATION REACTION .	
3.1 INTRODUCTION.....	112
3.2 BACKGROUND	114
3.3 RE-EXAMINATION OF COMPLEX FORMATION	120
3.4 CONCLUSIONS	132
3.5 EXPERIMENTAL	135
3.6 REFERENCES.....	139
CHAPTER 4 SUBSTRATE EXPANSION: KINETIC RESOLUTION OF ALLYLIC ALCOHOLS, HOMO ALLYLIC ALCOHOLS AND 2-ARYLCYCLOHEXANOLS USING OUR SilyLATION BASED METHODOLOGY	
4.1 INTRODUCTION	142
4.2 BACKGROUND	143
4.3 SilyLATION BASED KINETIC RESOLUTION OF ALLYLIC AND HOMOALLYLIC ALCOHOLS.....	146

4.4 CONCLUSIONS	162
4.5 EXPERIMENTAL	164
4.6 REFERENCES.....	171
CHAPTER 5 A SILYLATION BASED KINETIC RESOLUTION OF SECONDARY ALCOHOLS USING POLYMER SUPPORTED TRIPHENYLSILYL CHLORIDE	175
5.1 INTRODUCTION	175
5.2 BACKGROUND	176
5.3 RESEARCH DESIGN.....	182
5.4 RESULT AND DISCUSSION.....	184
5.5 FUTURE DIRECTION	192
5.6 CONCLUSIONS	193
5.7 EXPERIMENTAL	194
5.8 REFERENCES.....	201
CHAPTER 6 KINETIC RESOLUTIONS OF AMINES VIA IMINES USING AN AZA DIELS-ALDER REACTION	204
6.1 INTRODUCTION	204
6.2 BACKGROUND	205
6.3 RESEARCH DESIGN.....	212
6.4 RESULT AND DISCUSSION.....	214
6.5 EXPERIMENTAL	222
6.6 REFERENCES.....	230

LIST OF TABLES

Table 1.1 Comparison of the conversion required to obtain 80%, 90% and 99% <i>ee</i> of the recovered starting material for kinetic resolution with different selectivity factors	11
Table 2.1 Hammett substituent constants	39
Table 2.2 Charton steric parameter for various substituents.....	43
Table 2.3 Swain-Lupton parameter for various substituents	44
Table 2.4 Effect of substitution on different position (<i>ortho</i> , <i>meta</i> and <i>para</i>) of triphenylsilyl chloride in kinetic resolution of 4-chromanol	53
Table 2.5 Rate study employing the fast reacting enantiomer (<i>R</i>) using different <i>para</i> substituted triphenylsilyl chlorides	55
Table 2.6 Kinetic resolution using different <i>para</i> substituted triphenylsilyl chloride.....	60
Table 2.7 Rate of slow reacting enantiomer (<i>S</i>)- 2.15 for different <i>para</i> substituted triphenylsilyl chloride	68
Table 3.1 Previous data of $^1\text{H}/^{29}\text{Si}$ gHSQC NMR of complex 1.14 / Ph_3SiX	119
Table 3.2 ^1H - ^{29}Si gHSQC NMR analysis after saturation of ^1H NMR titration of $\text{Ph}_3\text{SiCl}/\textbf{1.14}$ complex	124
Table 3.3 Rate study comparison of deuterated versus non-deuterated tetralol	130
Table 4.1 Kinetic resolution of structurally different allylic & homoallylic alcohols.....	148
Table 6.1 Reaction of phenyl imine and Danishefsky's Diene in the presence of different Lewis acids.....	215
Table 6.2 (<i>S</i>)-BINOL/ $\text{B}(\text{OPh})_3$ at different temperatures	216

Table 6.3 Reaction of phenyl imine with different (S)-BINOL/Boron-Metal Complex .218

Table 6.4 Reaction of imine **6.21** with Danishefsky's diene in the presence of different
chiral Lewis Acids219

LIST OF FIGURES

Figure 1.1 Enantiomer of limonene	1
Figure 1.2 The enantiomers of thalidomide and naproxen	2
Figure 1.3 Enantiomerically pure compounds obtained from nature	4
Figure 1.4 Secondary chiral alcohol moiety in pharmaceutical drugs.....	12
Figure 1.5 Examples of kinetic resolution of secondary alcohols reported in literature using chiral DMAP & PPY derivatives as a catalyst.....	15
Figure 2.1 Five coordinated silicon species reported by Yoder.....	37
Figure 2.2 Taft's correlation for the development of steric parameter	41
Figure 2.3 Asymmetric catalysis through Curtis-Hammett principle.....	45
Figure 2.4 Correlation of electronic effect and enantioselectivity in Mn(III)-catalyzed epoxidation reaction.....	47
Figure 2.5 Correlation of the steric effect of the ligand and enantioselectivity in Nozaki- Hiyama-Kishi reaction of an allylic halide with both aldehyde and ketones	49
Figure 2.6 3D surface evaluation of steric and electronic effect vs measured enantioselectivity	50
Figure 2.7 Hammett plot employing the parameter σ_{para} versus the log of rates for the kinetic resolution of the fast reacting enantiomer (<i>R</i>) of alcohol 2.15	57
Figure 2.8 Comparison of the experimental $\log(k_x/k_H)$ using the rate data from Table 2.5 versus the predicated $\log(k_x/k_H)$ calculated from Eq.2.5	58

Figure 2.9 Hammett plots employing the parameter σ_{para} versus the log of the selectivity factors for the kinetic resolution of alcohols 2.15 and 2.10	62
Figure 2.10 Hammond postulate diagram explaining electronic effect on selectivity factors.....	63
Figure 2.11 Charton analysis of alcohols (A.) 2.15 , (B.) 2.10 , and (C.) selected alkyl substituted silyl chlorides (2.13a,g-j) in the silylation-based kinetic resolution.....	65
Figure 2.12 Comparison of the experimental log(<i>s</i>) using the selectivity data for 2.15 from Table 2.6 versus the predicted log(<i>s</i>) calculated from Eq. 2.6.....	66
Figure 2.13 Hammett plot employing the parameter σ_{para} versus the log of the calculated rates for the kinetic resolution of the slow reacting enantiomer (<i>s</i>)- 2.15	69
Figure 3.1 Two possible mechanistic pathways for our enantioselective silylation.....	114
Figure 3.2 Comparison of the bicyclic ring protons of the catalyst and the precipitate which formed from 1.14 and 2.13a	116
Figure 3.3 An nOe-difference experiment spectrum of precipitate obtained from 1.14 and Ph ₃ SiCl in THF	117
Figure 3.4 Pentavalent silicon reported by the Wagler group	118
Figure 3.5 Pentavalent silicon reported in the literature	118
Figure 3.6 ¹ H NMR of a solution of 1.14 and Ph ₃ SiCl (1:1 ratio) at different concentrations	121
Figure 3.7 ¹ H NMR study of 1.14 /Ph ₃ SiCl at different concentration.....	123
Figure 3.8 ¹ H- ²⁹ Si gHSQC possible complex formation at -18.5 ppm.....	127
Figure 3.9 ¹ H- ²⁹ Si HSQC NMR of Ph ₃ SiOH/ 1.14 at room temperature.....	129
Figure 4.1 2-Arylcycloalkanols moiety in bioactive compounds	152
Figure 4.2 Data from the kinetic resolution of (±)- <i>cis</i> and (±)- <i>trans</i> -2-(3-methoxy)cyclohexanol	160
Figure 4.3 Commercially available 2-arylcycloalkanols	161
Figure 5.1 Graphical presentation of the kinetic resolution using polymer supported chlorosilane	176

Figure 6.1 Chiral amines in pharmaceutical drugs	206
Figure 6.2 Other chiral Lewis acid catalysis.....	218
Figure 6.3 Catalyst with hydrogen bonding capability	220

LIST OF SCHEMES

Scheme 1.1 General scheme showing asymmetric reaction	4
Scheme 1.2 Asymmetric hydrogenation reported by Knowles and a synthesis L-DOPA at commercial scale using Knowles's catalytic asymmetric hydrogenation.....	5
Scheme 1.3 Synthesis of (<i>S</i>)-naproxen Noyori's asymmetric hydrogenation	6
Scheme 1.4 Sharpless asymmetric epoxidation	7
Scheme 1.5 General reaction scheme of kinetic resolution reaction	9
Scheme 1.6 First chiral DMAP catalyzed kinetic resolution reactions using acylation developed by Vedej's and Chen	13
Scheme 1.7 Kinetic resolution of secondary alcohol using Fu's chiral DMAP derivatized catalyst	14
Scheme 1.8 Kinetic resolution of secondary alcohols using Vedejs bicyclic phosphine catalyst 1.11	16
Scheme 1.9 Kinetic resolution of secondary alcohols using various amidine-based catalyst	17
Scheme 1.10 Additional kinetic resolution of secondary alcohols via acylation with amidine-based catalysts	19
Scheme 1.11 Recent development in asymmetric silylation	21
Scheme 1.12 First enantioselective silylation developed by Wiskur lab.....	22
Scheme 1.13 Silylation based kinetic resolution of monofunctional secondary alcohols	23

Scheme 1.14 One-pot reaction linking asymmetric catalysis and kinetic resolution	24
Scheme 1.15 Kinetic resolution of α -hydroxyl lactones and lactams	25
Scheme 2.1 Previously reported silylation based kinetic resolution of monofunctional secondary alcohols	35
Scheme 2.2 Nucleophilic assisted silylation mechanism proposed by Corriu	36
Scheme 2.3 Nucleophilic assisted silylation mechanism proposed by Chojnowski, Bassindale, and Frye	37
Scheme 2.4 Ionization of substituted benzoic acids in water at 25 °C	38
Scheme 2.5 Previously reported importance of triphenylsilyl chloride	51
Scheme 2.6 Synthesis of <i>p</i> -Substituted triphenylsilylchlorides	54
Scheme 2.7 Proposed mechanism of the silylation reaction	57
Scheme 3.1 Previously reported silylation-based kinetic resolution by the Wiskur lab ..	113
Scheme 3.2 Plausible tetravalent or pentavalent silicon complex formations between (-)-tetramisole and Ph ₃ SiCl in our enantioselective silylation	115
Scheme 3.3 Plausible general base catalysis mechanism in our silylation-based methodology	130
Scheme 3.4 Three Potential mechanisms for our silylation-based kinetic resolution	132
Scheme 4.1 Kinetic resolution of allylic alcohols developed by the Fu group and its application to the synthesis of (-)-baclofen and epoethilone A	144
Scheme 4.2 Kinetic resolution of allylic alcohols reported by the Vedejs group and the Birman group	146
Scheme 4.3 Silylation based kinetic resolution of (-)-carveol	150
Scheme 4.4 Common structural topology in previously studied kinetic resolution	151
Scheme 4.5 Non-enzymatic kinetic resolution reported in literature for 2-arylcycloalkanols	153
Scheme 4.6 Investigation of a catalyst using (\pm)- <i>trans</i> -2-phenylcyclohexanol	155
Scheme 4.7 Synthesis of chlorotris(4-isopropylphenyl)silane	156

Scheme 4.8 Kinetic resolution using 1.31 and 1.14 catalyst with chlorotris(4-isopropylphenyl)silane	157
Scheme 4.9 Synthesis of 2-arylcycloalkanols.....	159
Scheme 4.10 NaBH ₄ reduction of 2-(3-methoxyphenyl)cyclohexanone.....	160
Scheme 4.11 Two-step synthesis of 2-arylcycloalkanols	162
Scheme 5.1 Kinetic resolution of secondary alcohols using a polymer supported proline-based catalyst by Janda et al	178
Scheme 5.2 Kinetic resolution of amines using a polymer supported enantioselective N-acetylation	179
Scheme 5.3 Polymer supported kinetic resolution of N-heterocycles reported by the Bode group	180
Scheme 5.4 Kinetic resolution of a secondary alcohols using chiral polymeric silane ...	181
Scheme 5.5 Synthesis of polymer supported triphenylsilyl chloride from pendant type polymer	183
Scheme 5.6 Synthesis of polymer supported triphenylsilyl chloride using a silane monomer polymerization	183
Scheme 5.7 Attempted synthesis of triphenylsilane based polymer from homo and random co-polymer	185
Scheme 5.8 Synthesis of <i>p</i> -diphenylsilane styrene as a monomer.....	186
Scheme 5.9 Synthesis of polymer supported triphenylsilyl chloride using monomer polymerization method	187
Scheme 5.10 Preliminary study using polymer supported chlorosilane in the kinetic resolution reaction.....	188
Scheme 5.11 Synthesis of polymer supported chlorosilane using different method	189
Scheme 5.12 Screening of catalyst in the polymer supported kinetic resolution of 4-chromanol	191
Scheme 5.13 Screening of different molecular weight polymers in the kinetic resolution of 4-chromanol.....	191

Scheme 6.1 Basic protocol for the kinetic resolution of amines via imines	205
Scheme 6.2 Catalytic non-enzymatic kinetic resolution of amines	208
Scheme 6.3 Kinetic resolution of amine derivatives	209
Scheme 6.4 (a) Copper catalyzed [3+2] kinetic resolution of imines (b) Kinetic resolution of Imines using Rhodium/diphosphine catalyzed hydrogenation	211
Scheme 6.5 Aza-Diels-Alder reaction	212
Scheme 6.6 Kinetic resolution of an imine using an aza-Diels-Alder reaction reported by the Yamamoto and his co-worker	213
Scheme 6.7 Imine formation from amines using a Dean-Stark procedure	214
Scheme 6.8 Asymmetric reaction of benzyl imine and Danishefsky's diene	221

CHAPTER 1

BACKGROUND AND INTRODUCTION TO SILYLATION-BASED KINETIC RESOLUTIONS

1.1 Introduction

Chirality is one of the most important concepts in organic chemistry. A molecule with a non-superimposable mirror image is a chiral compound, and the mirror image of this chiral compound is known as an enantiomer. A 50:50 mixture of two enantiomers is called a racemic mixture.¹ In general, enantiomers display the identical physical and chemical properties but can display different biological properties. Two enantiomers of the same molecule can have completely different biological properties. This fundamental difference can be illustrated by using the naturally occurring enantiomers of limonene (Figure 1.1). The *R* enantiomer of limonene smells like oranges while its mirror image (*S*)-limonene smell like lemons.²

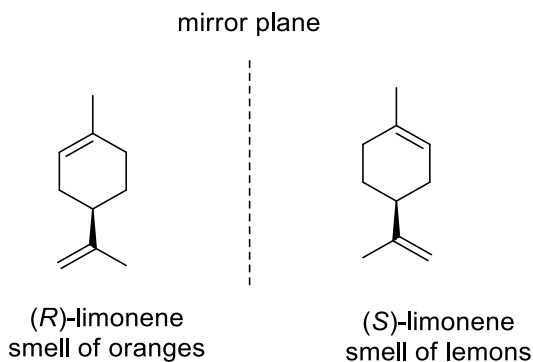


Figure 1.1 Enantiomers of limonene

Due to this difference in biological activity of enantiomers, enantiomerically pure compound has gained more attention within the pharmaceutical industry. Thalidomide is an example that shows the importance of enantiomerically pure drugs in pharmaceuticals.³ In this case, (*R*)-thalidomide acts as a potential drug for morning sickness in pregnant woman while (*S*)-thalidomide causes severe birth defects (Figure 1.2(A)). Another example is naproxen⁴; the (*S*)-enantiomer of naproxen is used as an anti-inflammatory agent while its (*R*)-enantiomer of naproxen can be toxic to the liver (Figure 1.2(B)). Therefore, the sale of chiral drugs in their single enantiomer form has grown dramatically in the pharmaceutical industry over the past several years. Using a drug in its single enantiomeric form will allow it to utilize its maximum potential of effectiveness and avoid any dangers associated with a racemic mixture.

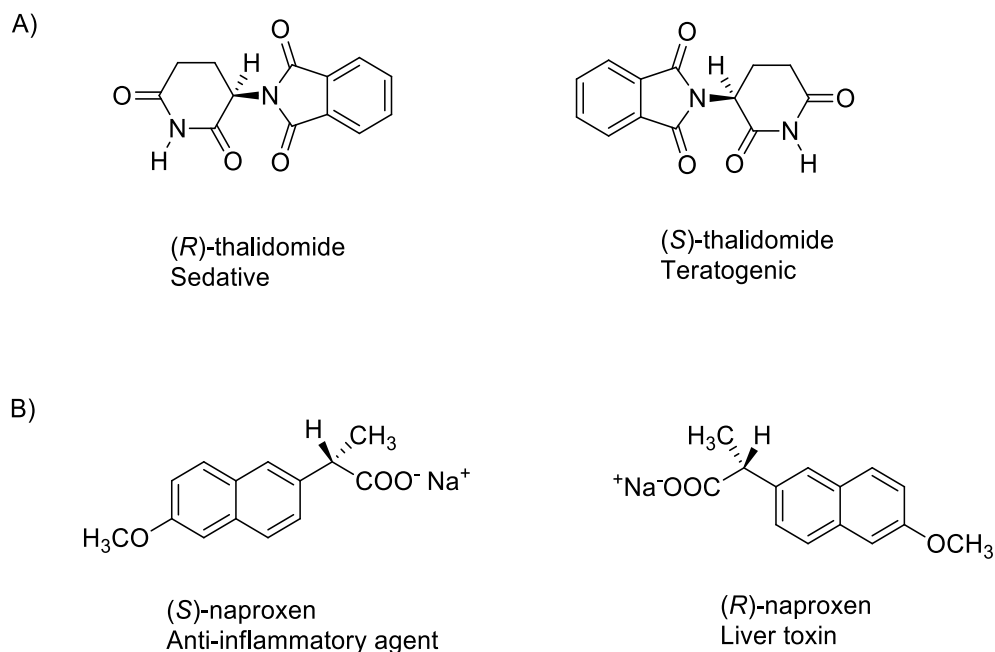


Figure 1.2 The enantiomers of thalidomide and naproxen

According to the US Food and Drug Administration, pharmaceutical companies are required to have an enantiomeric purity of 99% or more in order to be sold as a compound

in single enantiomer form. If a drug's purity is less than 99%, or it is used as a racemic mixture, the biological activity of both enantiomers must be analyzed before selling as a drug.⁵ In both cases, a drug manufacturer must synthesize and analyze the biological activity of both enantiomers. As a result, the demand for enantiomerically pure compounds has increased dramatically. Thus, an accurate method to obtain enantiomerically enriched compounds has become an essential tool. Chiral technology is expected to reach a value of \$5.1 billion (US) market globally by 2017, according to a Global Industry Analyst, Inc report.⁶ It is really important to understand enantiomeric purity, which can be measured in terms of enantiomeric excess (*ee*). The percentage difference between the major and minor enantiomers is known as enantiomeric excess (Equation 1.1). A higher *ee* value represents higher purity of one enantiomer.

$$\% ee = 100 * ([R] - [S]) / ([R] + [S]) \quad \text{Equation 1.1}$$

An *ee* value over 95% or more can be classified as an enantiomerically pure compound and *ee* can be determined by using chiral HPLC or GC. There are several ways to obtain enantiomerically pure compounds.

1.2 Methods to obtain enantiomerically pure compounds

1.2.1 Nature (As a chiral pool)

Nature is a source of enantiomerically pure compounds. It is considered one of the best sources because the requisite starting material or target itself is produced by nature and laboratory syntheses are very expensive. Nature has a limitations, nature offers a limited scope of compounds and often as a single enantiomer. In that case, if one is

interested in the other form of the enantiomer, a laboratory synthesis becomes mandatory. Examples of enantiomerically pure compounds obtained from nature are shown in Figure 1.3.

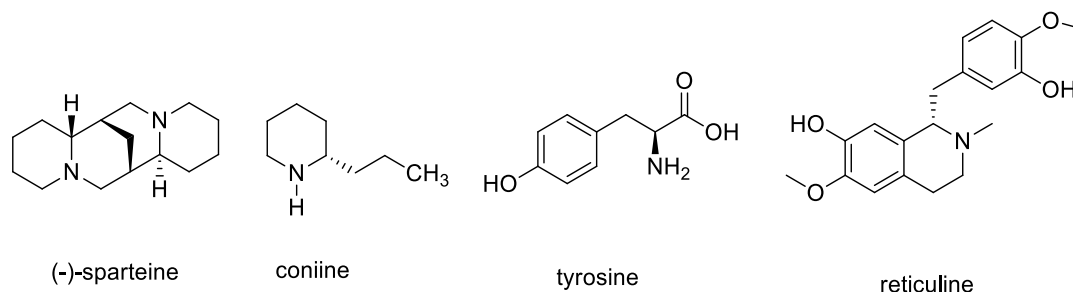
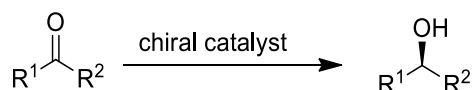


Figure 1.3 Enantiomerically pure compounds obtained from nature

1.2.2 Asymmetric catalysis

Asymmetric catalysis is one of the most widely used synthetic ways to obtain enantiomerically enriched compounds. In this method, chirality is introduced to a prochiral substrate using chiral auxiliaries or chiral catalysts (Scheme 1.1).⁷ The main advantage of this method involves the possibility to achieve up to > 99% yield with > 99% *ee*.

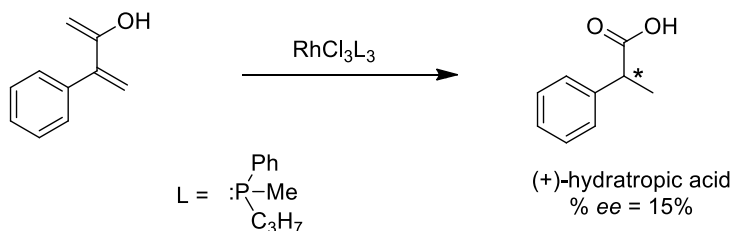


Scheme 1.1 General scheme showing an asymmetric reaction

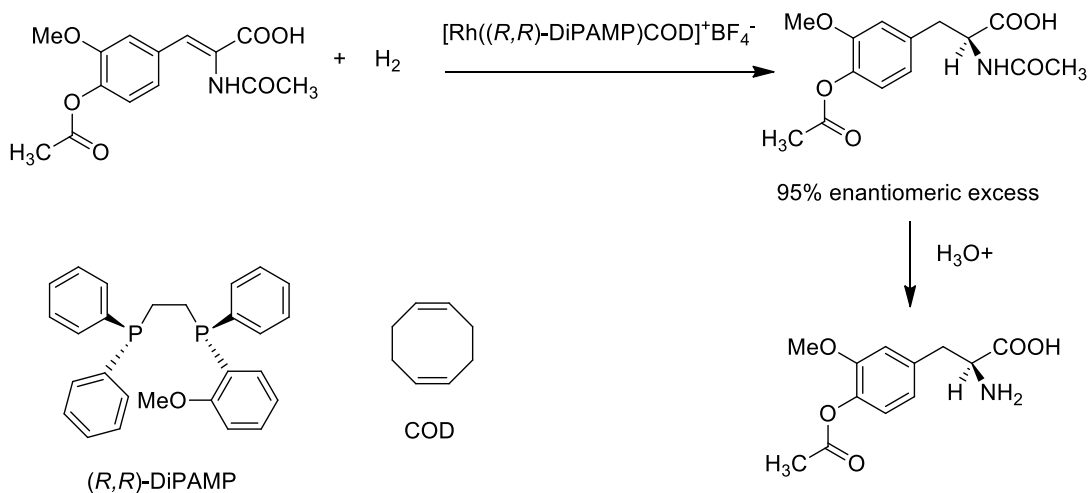
Numerous examples of asymmetric catalysis are reported in the literature.⁸⁻¹¹ Asymmetric hydrogenation is one of them. A breakthrough in asymmetric hydrogenation was reported in 1968 when Knowles¹² at Monsanto Company in St. Louis reported the conversion of a prochiral substrate to a chiral product with an excess of one enantiomer using a chiral transition metal (Rh) catalyst. In order to verify this, Knowles used prochiral styrene and converted that into (+)-hydratropic acid with 15% *ee* using enantiomerically pure methypropylphenylphosphine (69% *ee*) (Scheme 1.2(A)). Knowles' success was

commercialized in 1974 to synthesis L-DOPA, a drug use in the treatment of Parkinson disease (Scheme 1.2 (B)).¹³

A)

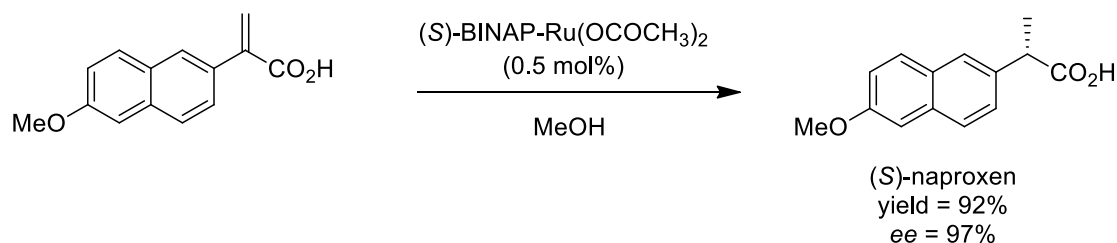


B)



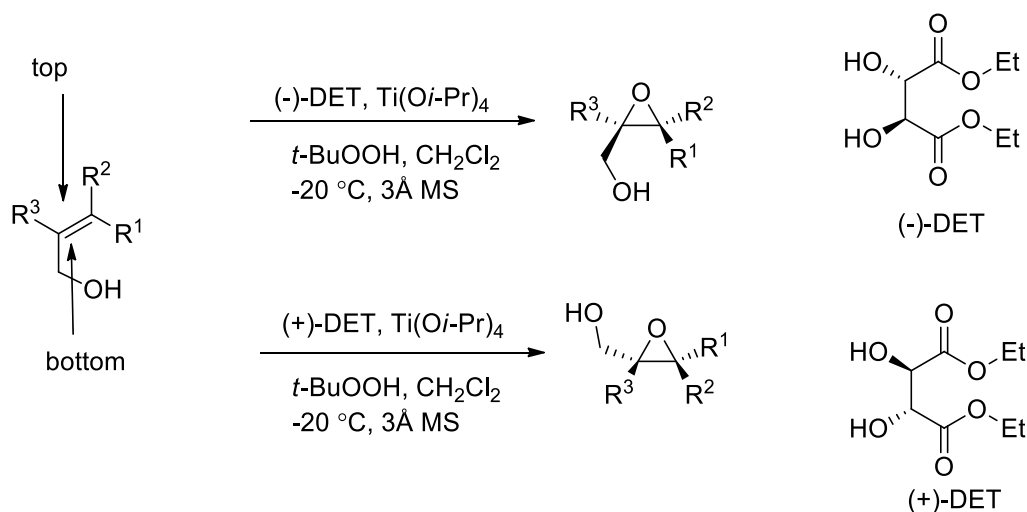
Scheme 1.2 (A) Asymmetric hydrogenation reported by Knowles and (B) a synthesis L-DOPA at commercial scale using Knowles's catalytic asymmetric hydrogenation

Another important discovery in asymmetric catalysis involves the BINAP-Ru (II) chiral catalyst for asymmetric hydrogenation that was reported by Noyori. A variety of functionalized ketones and olefins can be hydrogenated using Noyori's catalyst.¹⁴⁻¹⁷ The synthesis of (*S*)-naproxen from an α,β -unsaturated carboxylic acid represents a great example of Noyori's asymmetric hydrogenation of double bond. In this reaction, (*S*)-naproxen was obtained in 92% yield with 97% *ee* (Scheme 1.3).¹⁸



Scheme 1.3 Synthesis of (*S*)-naproxen via Noyori's asymmetric hydrogenation

In the 1980, Barry Sharpless invented an important asymmetric oxidation reaction known as the Sharpless epoxidation reaction.^{19,20} This reaction represents an important transformation to convert allylic alcohols into epoxy alcohols with excellent enantioselectivities (Scheme 1.4). All reagents used in this system are commercially available which includes ((+) or (-)-diethyl tartrate (DET), titanium tetrakisopropoxide and *tert*-butyl hydroperoxide). In this method, the epoxide oxygen is delivered with high chiral induction by using titanium bound enantiomerically pure tartrate. In the epoxidation, delivery of oxygen occurs from the top side of the olefin when (-)-DET used as a ligand while delivery of oxygen occurs from the bottom side of the olefin when (+)-DET used as a ligand. Several structurally diverse allylic alcohols were reported with yields ranging from 77-87% with enantiomeric excess $\geq 90\%$. For this exceptional work in asymmetric catalysis Knowles, Noyori and Sharpless were awarded the Nobel Prize in 2001.



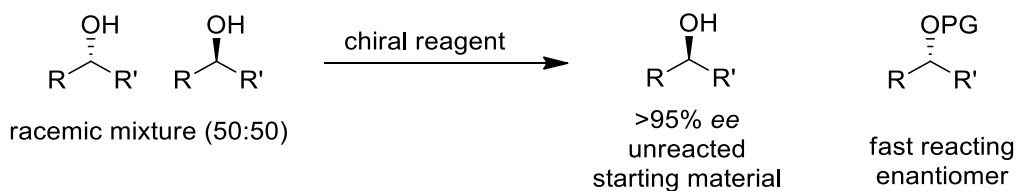
Scheme 1.4 Sharpless asymmetric epoxidation

Even though numerous reactions are reported in the literature using asymmetric catalysis, it still has certain limitations. One of the major drawbacks of asymmetric catalysis is that the enantiomeric excess of the product generally remains the same throughout the reaction. In asymmetric catalysis, different substrates will result in different *ee*'s, which means that substrates with lower *ee*'s require further optimization to get highly enriched products. Therefore, using asymmetric catalysis at industrial scale can sometimes be limiting, which may require adoption of completely different systems which can untimely increase the overall cost. Due to this limitations, it is really important to look at alternative methods to obtain enantiomerically pure compounds.

1.2.3 Resolutions

A resolution is the selective separation of one enantiomer from a mixture of an enantiomers.⁷ Resolutions have several advantages in contrast to the previously discussed two methods. Resolutions can be classified into three classes which include classical resolution, chiral chromatography, and kinetic resolutions. A classical resolution²¹ is a technique where an equimolar mixture of enantiomers, known as a racemic mixture, is

separated by simply converting them into diastereomers. A stoichiometric amount of an enantiomerically pure chiral resolving reagent is used to convert enantiomers into a pair of diastereomers through a salt formation. The diastereomers are then simply separated by selective crystallization from each other followed by cleavage of the chiral resolving reagent to obtain an enantiomerically pure compound. A variety of amines and carboxylic acids can be separated through classical resolutions. The main limitation of this technique is the use of a chiral reagent in stoichiometric amounts. Another method of resolutions involves the use of chiral chromatography. In this technique, a preparative scale chromatography is employed using a chiral stationary phase. One enantiomer interacts with the chiral stationary phase while the other enantiomer remains in the mobile phase. This technique often comes with the limitations of long retention times, large volumes of solvents, high cost of chiral columns, and limited chiral stationary phase availability. Finally, the last technique and the major focus of this dissertation is kinetic resolution. A kinetic resolution is a technique to separate a racemic mixture by the selective derivatization of one enantiomer over the other (Scheme 1.5).⁷ In this technique, enantioselectivity is the result of the difference in the reactivity of the two enantiomers towards a derivatization where one enantiomer reacts faster than the other enantiomer. In the kinetic resolution, most desired product is the unreacted starting material. There are several ways to do the kinetic resolution including epoxidation, reduction and carbonylations etc.



Scheme 1.5 General reaction scheme of a kinetic resolution reaction

The most attractive aspect of the kinetic resolution method over asymmetric catalysis is that *ee* changes over the course of the reaction. Therefore in kinetic resolutions, an achievement of an *ee* over 99% for the unreacted starting material can be possible for a variety of different substrates using the same methodology without any further optimization. Also, due to the wide range of availability of compounds found as racemic mixtures, it is viable option to use a kinetic resolution as a separation technique. In kinetic resolutions, since *ee* changes over the course of the reaction, it is hard to compare one reaction to other just by comparing *ee*'s. To measure the efficiency of the kinetic resolution, the selectivity factor (*s*) is used as a measuring parameter.²²

$$s = k_{\text{fast}}/k_{\text{slow}} = e^{\Delta\Delta G^\ddagger/RT} \quad \text{Equation 1.2}$$

Selectivity factor is the ratio of the rate of the fast reacting enantiomer over the rate of the slow reacting enantiomer. In other words, the selectivity factor is the measurement of the energy difference in the diastereomeric transition state of the selectivity determining step ((Equation 1.2). If one enantiomer reacts 50 times faster than the other one, then the selectivity factor is 50. The higher the selectivity factor the more selective the reaction is at derivatizing one enantiomer over the other. A selectivity factor ≥ 10 is considered as a benchmark for any kinetic resolution reaction considered to be practical. Selectivity can

be calculated (equation 1.3) using conversion (obtained from HPLC) and the *ee* of starting material or product. The most common way of calculating the conversion is to use both the *ee* of the starting material and *ee* of the product as shown in Eq. 1.3

$$C = \frac{ee_s}{ee_s + ee_p} \quad \text{Equation 1.3}$$

$$s = \frac{\ln[(1-C)(1-ee_s)]}{\ln[(1-C)(1+ee_s)]} \quad \begin{array}{l} ee_s = ee \text{ of unreacted starting material} \\ ee_p = ee \text{ of product} \end{array}$$

$$s = \frac{\ln[(1-C)(1+ee_p)]}{\ln[(1-C)(1-ee_p)]}$$

In a kinetic resolution, it is easy to obtain the recovered starting material in over 99% *ee*, even for a kinetic resolution with a low selectivity factor by allowing the reaction to proceed higher conversion. Table 1.1 shows the percent conversion required in order to achieve 80%, 90%, or 99% *ee* with different selectivity factors. Even with a selectivity factor of 2, one can always achieve over 99% *ee* just by simply pushing the conversion close to completion (Table 1, entry 1). The major drawback of the kinetic resolution is its yield. One cannot achieve more than a 50% yield. One way to overcome the limitation of the kinetic resolution is to use the Mitsunobu²³ reaction which allows to convert stereochemistry of enantiomer to its other enantiomer or through the racemization of enantiomer.

Table 1.1 Comparison of the conversion required to obtain 80%, 90% and 99% *ee* of the unreacted starting material for kinetic resolution with different selectivity factors

Entry	s	Conv.(%) 80% <i>ee</i>	Conv.(%) 90% <i>ee</i>	Conv.(%) 99% <i>ee</i>
1	2	93.8	97.2	99.7
2	5	67.9	74.7	86.6
3	10	56.4	62.0	72.0
4	20	50.5	54.9	61.9
5	50	46.8	50.4	54.8
6	100	45.6	48.9	52.3

There are several ways to do kinetic resolution reactions, including enzymatic, metal catalysis, and organocatalysis. Each type of kinetic resolution has its own advantages and disadvantages. Amongst all of the above, organocatalyzed kinetic resolutions are getting more attention in academia as well as in industry because of the simple catalyst preparation on large scale, the air and moisture stability of the catalysts, no metal involvement, and comparable selectivities to enzyme and metal catalysis.²⁴ Chiral secondary alcohols are the most common class of functional group subjected to kinetic resolutions with numerous potential applications as chiral building blocks in the fine chemical and in pharmaceutical industries.²⁵ Acylation is the most common way to obtain enantioenriched alcohols through kinetic resolutions. Figure 1.4 shows some important chiral secondary alcohol moieties in pharmaceutical drugs.

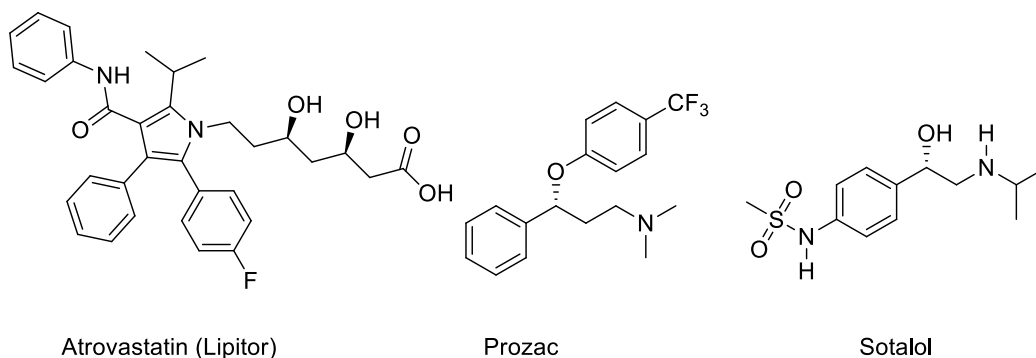
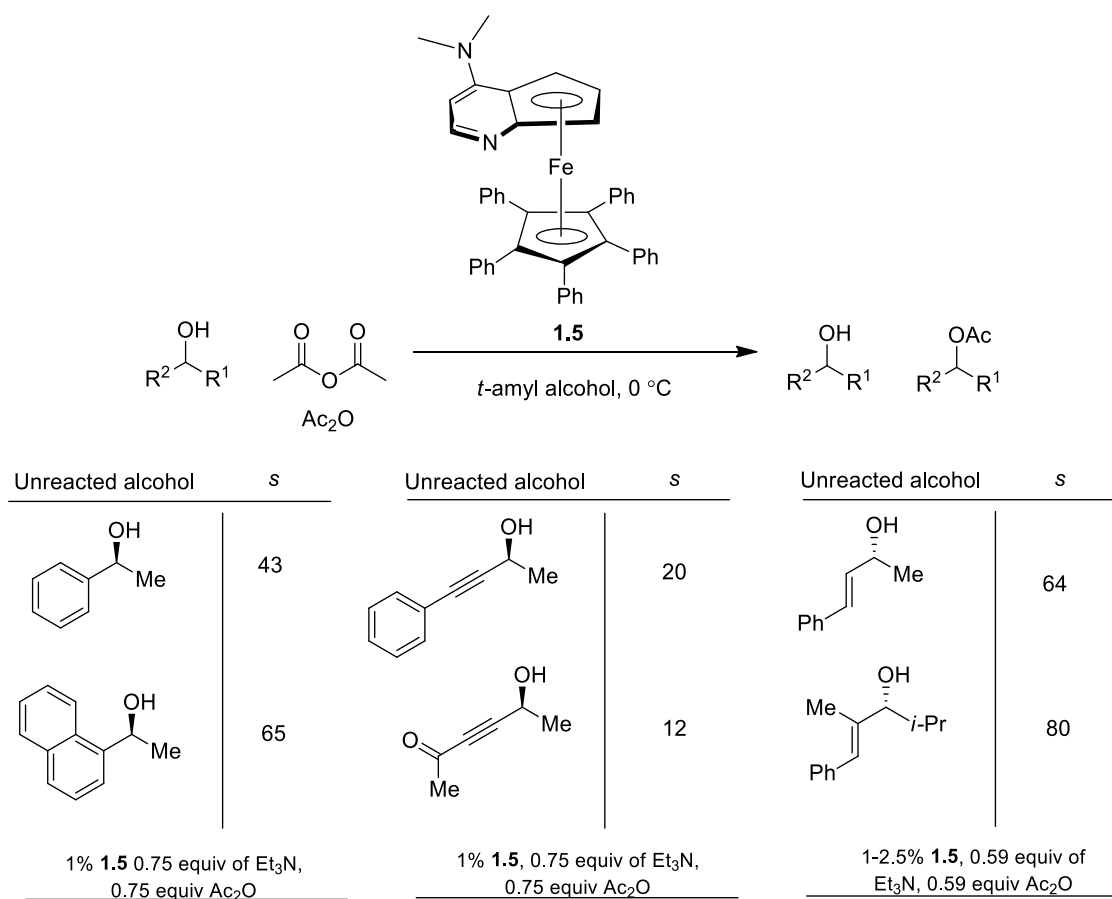


Figure 1.4 Secondary chiral alcohol moieties in pharmaceutical drugs²⁵

1.3. Acylation

Acylation is the most studied organocatalyzed reaction for the kinetic resolution of secondary alcohols, reported in the literature compared to any other reaction.²⁶ Several classes of organocatalysts have been developed to enantioenrich alcohols via an acylation reaction. Amongst all classes of catalysts, a chiral DMAP (4-dimethylaminopyridine) was proven to be one of the most successful organocatalysts.²⁷ The first example using chiral a DMAP as a catalyst for an acylation reaction to selectively resolve secondary alcohols was reported by Vedejs and Chen in 1996 (Scheme 1.6)²⁸. In this method, an acylpyridinium salt was generated by treating DMAP **1.1** with 2,2,2-trichloro-1,1-dimethylethyl chloroformate **1.2**. A stoichiometric amount of the acylpyridinium salt **1.3** was used in the kinetic resolution of alcohol **1.4** along with a Lewis acid (ZnCl_2 or MgBr_2) and a tertiary amine as a base to achieve the desired conversion. Selectivity factors of 11-53 were reported for a variety of secondary alcohols and a selectivity factor of 14 for one allylic alcohol. Besides decent selectivity factors, this method still suffers from a major drawback, i.e. the use of a catalyst in stoichiometric amount. Again, one should keep in mind it was one of the first examples showing the application of a chiral DMAP in acylation reactions.



Scheme 1.7 Kinetic resolution of secondary alcohols using Fu's chiral DMAP derivatized catalyst

The following are several other example of “chiral DMAP and PPY (pyrrolidino)” based catalysts reported in literature for the kinetic resolution of secondary alcohols via acylation (Figure 1.5).

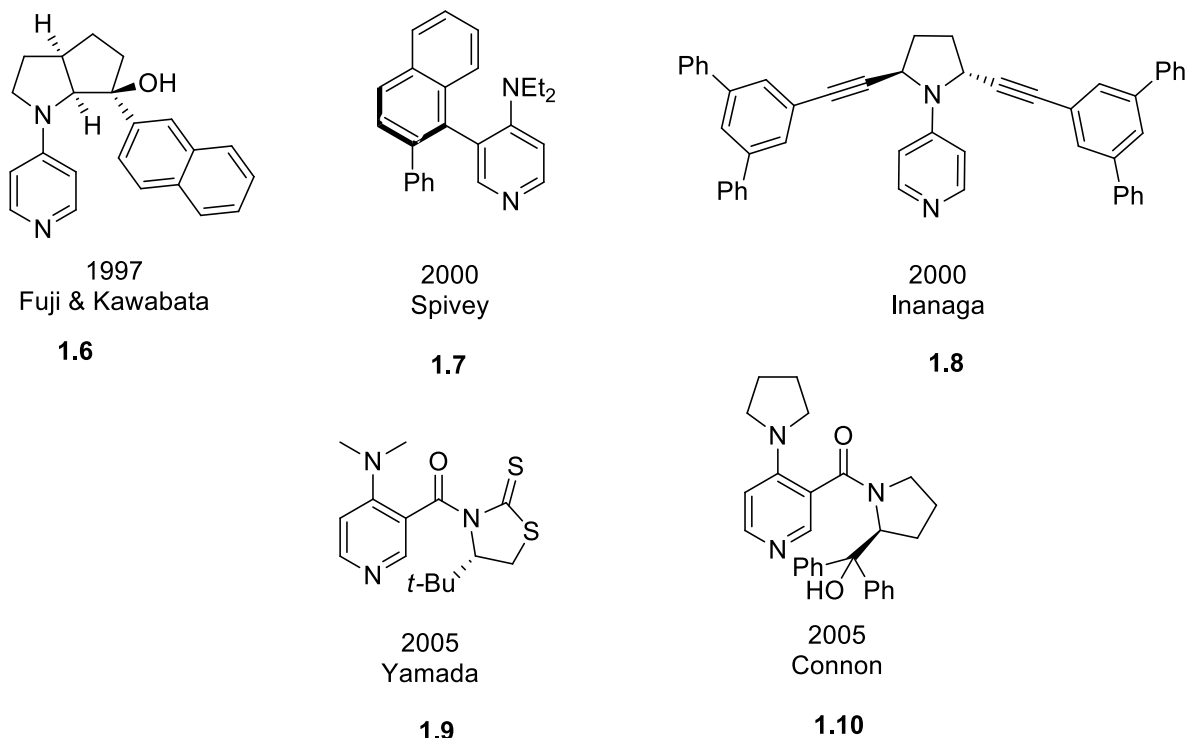
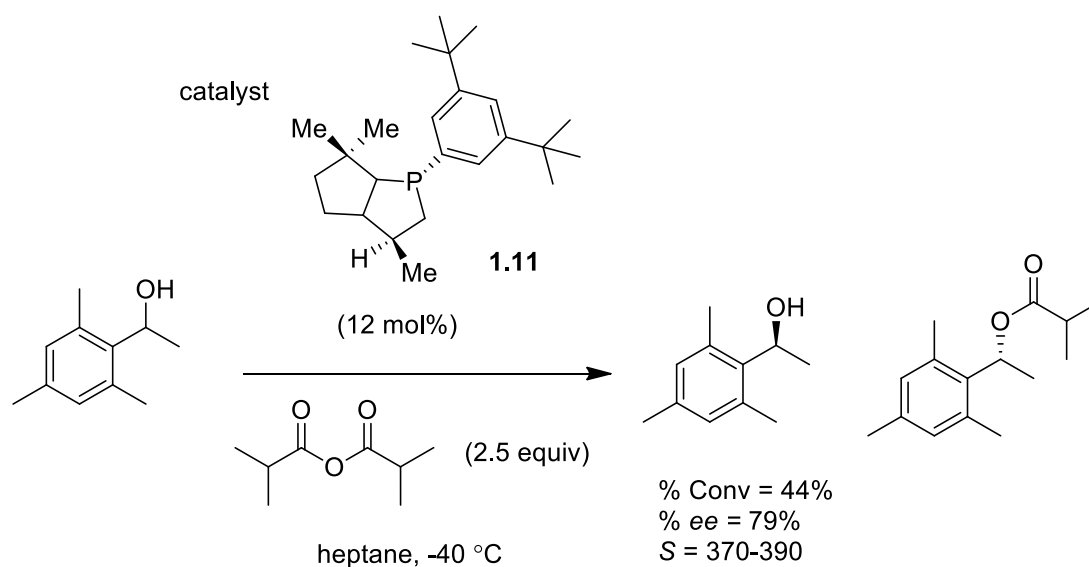


Figure 1.5 Examples of kinetic resolution of secondary alcohols reported in literature using chiral DMAP & PPY derivatives as a catalyst³⁵⁻³⁹

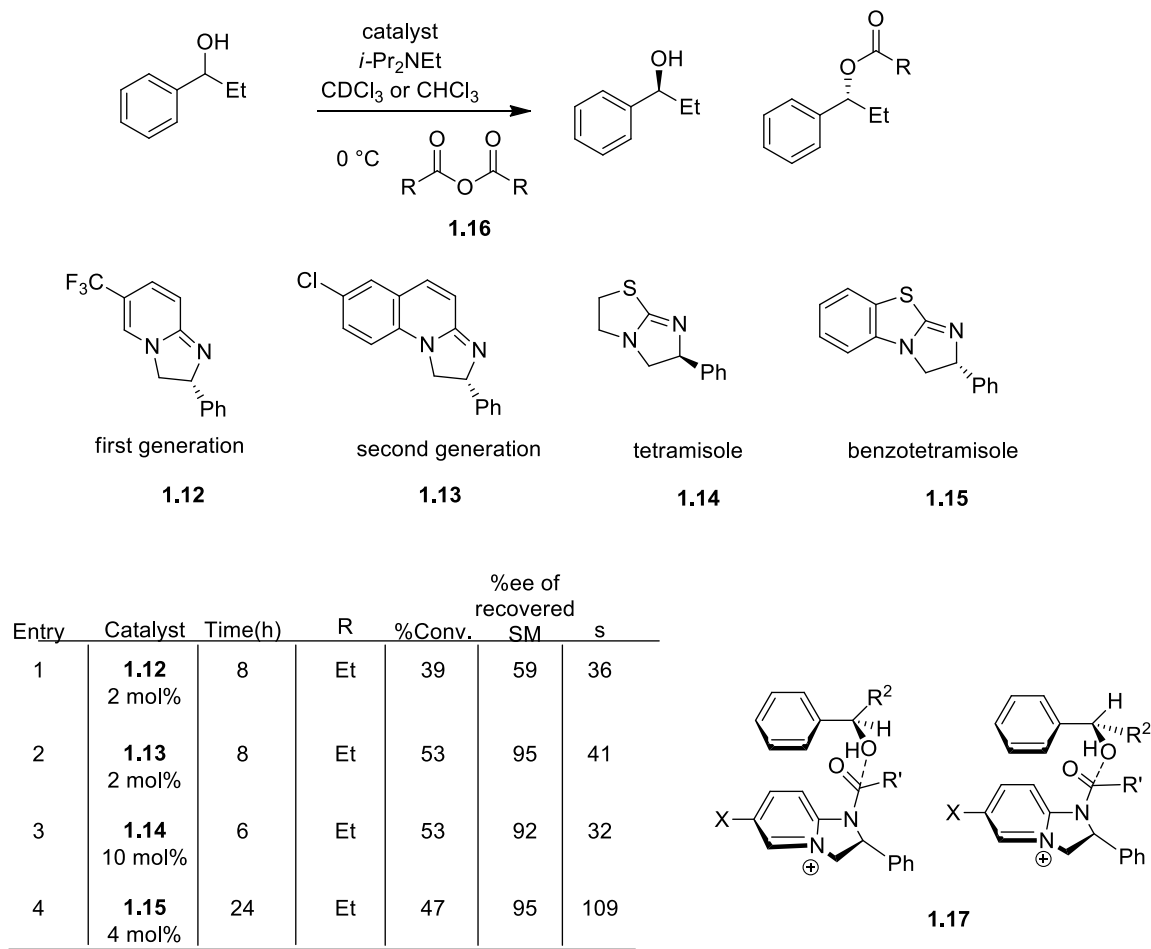
In addition to DMAP, chiral phosphines are another class of chiral catalysts for the acylation of secondary alcohols. In 1996, Vedejs et al reported a successful kinetic resolution using a phosphine based catalyst.⁴⁰ One of the interesting aspects of phosphine catalysts is that it forms similar P-acylphosphine salts as observed with DMAP.⁴¹ Among several phosphine based catalysts, the bicyclic phosphine **1.11** reported by Vedejs was found to be the most efficient catalyst in the kinetic resolution of aryl alkyl carbinols (Scheme 1.8). Selectivity factors up to almost 400 were reported for sterically hindered secondary alcohols.⁴² This is the best selectivity factor so far reported in the literature using a phosphine-based organocatalyzed system.



Scheme 1.8 Kinetic resolution of secondary alcohols using Vedejs' bicyclic phosphine catalyst **1.11**

Recently, amidine-based catalysts (ABCs) are becoming another successful class of catalyst for enantioselective acylation reactions.⁴³ In 2004, Birman's group introduced the first example showing the potential of an amidine based catalyst in the kinetic resolution of secondary alcohols.⁴⁴ In this system, the addition of *N,N*-diisopropylethyl amine was found to be useful to increase the rate of the acylation reaction which made it possible to run the reaction with a lower catalyst loading (2 mol%) at $0\text{ }^{\circ}\text{C}$. Scheme 1.9 shows the kinetic resolution of (\pm)-phenylethylcarbinol using first generation **1.12** amidine based catalyst with a selectivity factor 36. Selectivity factors up to 85 were reported using propanoic anhydride **1.16** as an acylating reagent. The selectivity was explained by the formation of, a π - π or π -cation interaction in the transition state (**1.17**) between π system of substrate (benzene ring) and pyridinium ring of the *N*-acylated catalyst. Based on the proposed transition state, the fast reacting enantiomer was predicted to be the one with less or minimize steric repulsion. Soon after that, a second generation catalyst **1.13** was

reported by Birman group where the pyridine moiety was replaced by a quinoline moiety.⁴⁵ An increased in selectivity factor was reported compared to first generation catalyst (**1.12**) which demonstrate significant role of π system in the selectivity determination. Furthermore, this extended π system of the catalyst allowed to achieve better selectivity factor with trans-cinnamyl alcohols due to better π interaction with quinolone moiety.

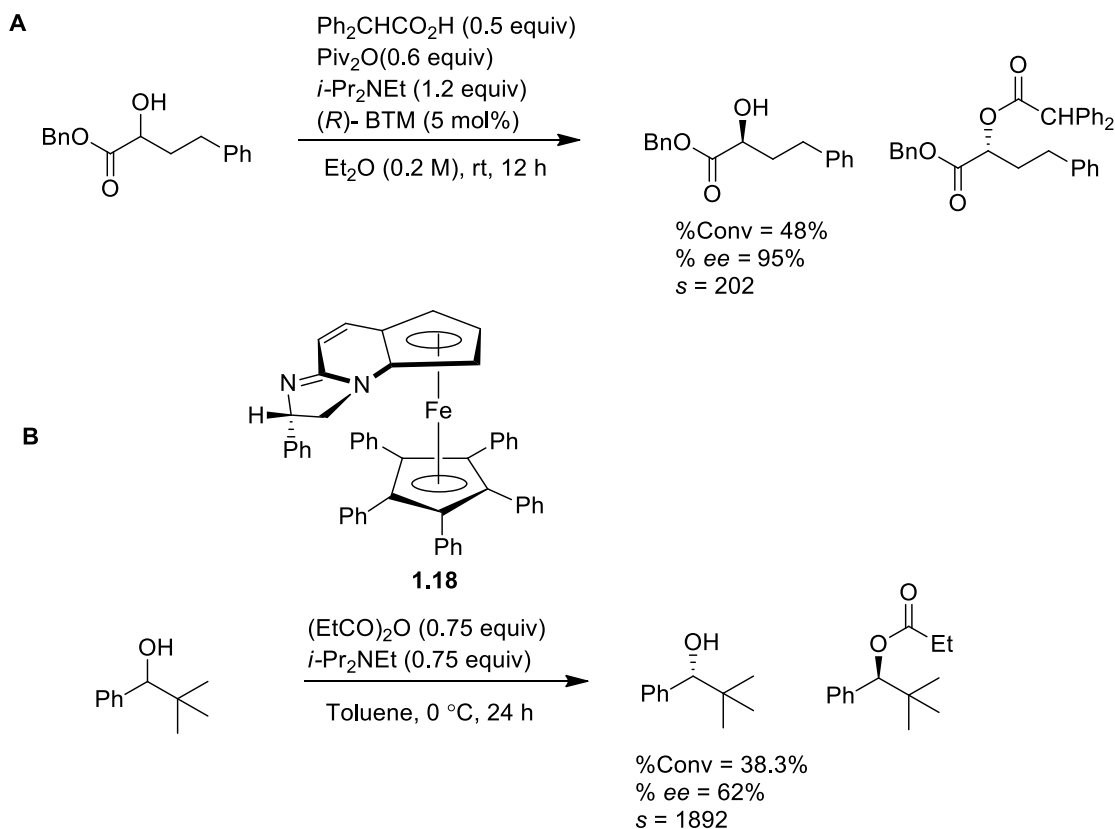


Scheme 1.9 Kinetic resolution of secondary alcohols using various amidine-based catalyst

In 2006, a major breakthrough was achieved when the Birman group used tetramisole (**1.14**) and benzotetramisole (**1.15**) as acylation catalysts.⁴⁶ Enormous increases in selectivity factors were reported using benzotetramisole as a catalyst in the kinetic resolution of benzylic alcohols ($s = 100$ -355) with isobutyric anhydride as the acylation

source in some cases. Benzotetramisole **1.15** was also proven to be the best catalyst to resolve propargylic alcohols.⁴⁷ In 2008, the Birman group also introduced an extended version of the amidine-based catalysts called homotetramisole and homobenzotetramisole.^{48,49} This version of catalyst was employed to resolve aryl cycloalkanols.

More recently, the Shinna group has reported a system to resolve a variety of different classes of alcohols using the amidine-based catalysts **1.14** and **1.15** and a free carboxylic acid coupled with an anhydride as the acylating source.^{50,51} In this method, mixed anhydrides were generated through transacylation, which was further catalytically activated by a nucleophilic catalyst (Scheme 1.10). Finally, a selective reaction with racemic alcohols generated an optically active carboxylic ester and an enantioenriched alcohol. Using this methodology, the kinetic resolution of benzylic alcohols (*s* up to 88), 2-hydroxyalkanoates (*s* up to 202)⁵², 2-hydroxy- γ -butyrolactones (*s* up to over 1000)⁵³ were achieved. More recently, another planar chiral acylation catalyst (**1.18**, Fc-PIP) was introduced by the Deng and Fossey group for enantioselective acylation.⁵⁴ Selectivity factors close to 2000 were reported for the kinetic resolution of secondary alcohols (arylalkyl carbinols).



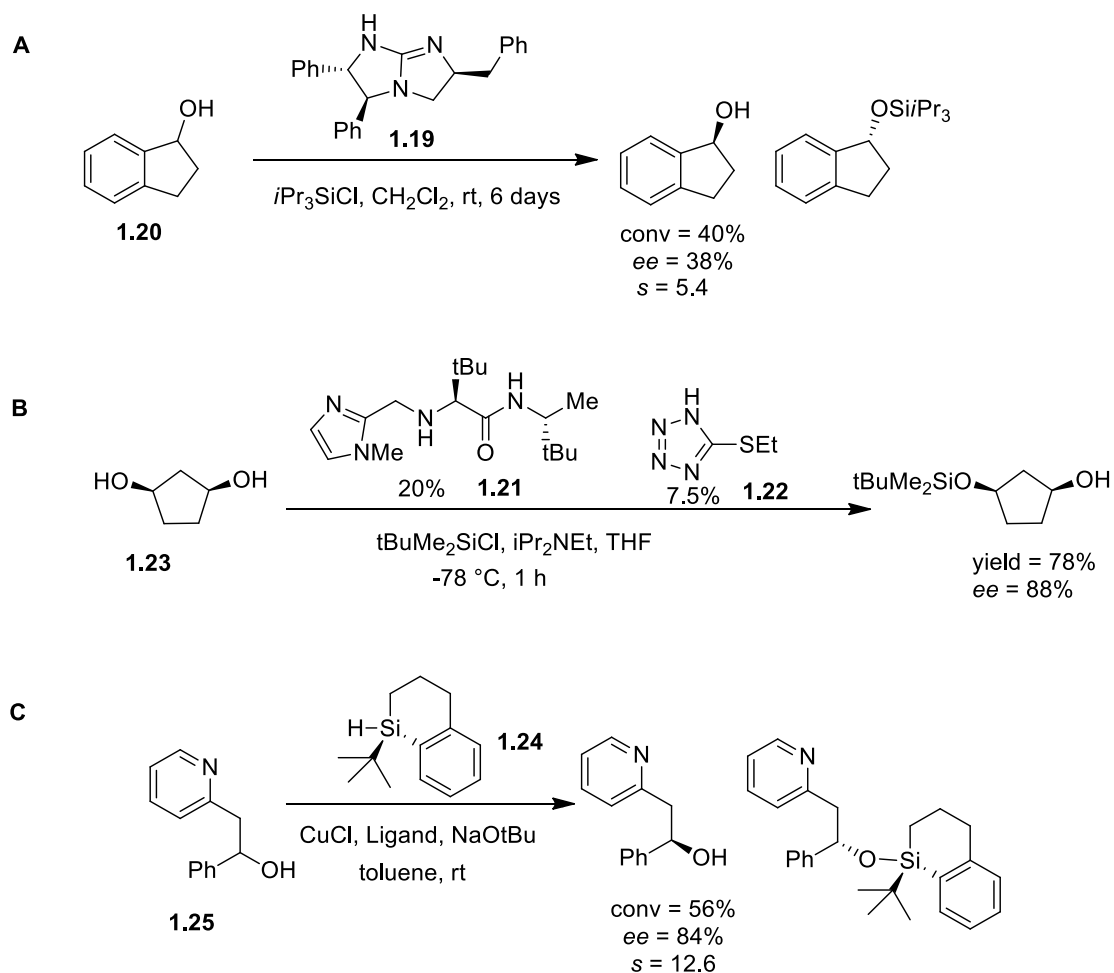
Scheme 1.10 Additional kinetic resolutions of secondary alcohols via acylation with amidine-based catalysts

1.4 Silylation

A silylation-based kinetic resolution is an alternative reaction to acylation to obtain enantiomerically enriched alcohols. Silylation has many advantages over acylation including tunable reactivity, orthogonality to other protecting groups and tolerance to a wide range of other functional groups.⁵⁵ Due to these advantages, silylation has become an active area of research over the past several years. In 2001, the first silylation based kinetic resolution was introduced by Ishikawa.⁵⁶ In this kinetic resolution, a secondary alcohol **1.20** (Scheme 1.11(A)) was used as a substrate, a guanidine catalyst **1.19** was employed and triisopropylsilyl chloride (TIPSCl) as a silicon source. A stoichiometric amount of chiral catalyst and TIPSCl was used in the reaction and a 40% conversion was reported

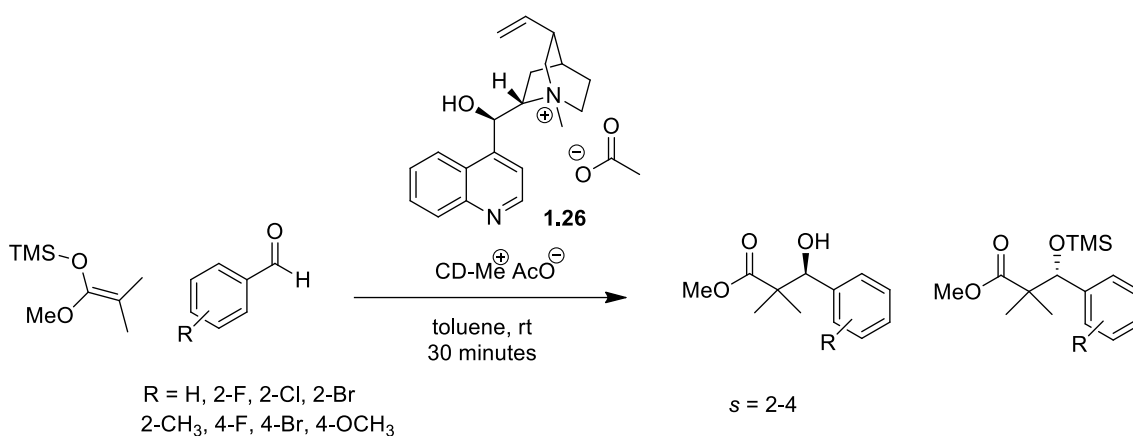
after 6 days. This report was a significant contribution to asymmetric silylation since it was the first example of using silicon as a means of separation in a kinetic resolution process. Lower conversion and stoichiometric amounts of catalyst were found to be a major drawbacks in Ishikawa's silylation based kinetic resolution. This issue of stoichiometric amount of catalyst in silylation was resolved when Hoveyda and Snapper reported the enantioselective silylation of meso diols **1.23** (Scheme 1.11(B)) using the imidazole based peptide like chiral catalyst **1.21**.⁵⁷ A number of substrates were successfully resolved using this methodology, including racemic 1,2-diols⁵⁸, meso diols⁵⁹ and triols⁶⁰. However, a high catalyst loading and long reaction times were required to obtain higher conversion. Recently, this problem was eliminated with the addition of the structurally similar, achiral co-catalyst **1.22** which can act as a nucleophilic promoter along with imidazole peptide like chiral catalyst or as a Brønsted base.⁶¹

In 2005, the Oestreich group reported the first successful copper(I)-catalyzed silylation-based kinetic resolution using distereoselective dehydrogenative coupling of racemic alcohol and chiral silanes.⁶² This methodology requires a two-point binding of the substrate (alcohol and pyridine nitrogen) to get better stereoselectivity which was demonstrated by using 2-pyridyl-substituted benzylic secondary alcohols **1.25** (*s* ≈ 10) (Scheme 1.11(C)). Substantially improved selectivity factor was obtained after optimization of same methodology using Rh(I) metal instead of Cu(I) metal for the nitrogen donor functionalized secondary alcohols.⁶³ The major drawbacks of this methodology is the use of a metal catalyst, the synthesis of the chiral silane **1.24** and the substrate scope. Despite all these developments, there is still plenty of room for further advancement of enantioselective silylation reactions to deliver a more robust methodology.



Scheme 1.11 Recent developments in asymmetric silylation

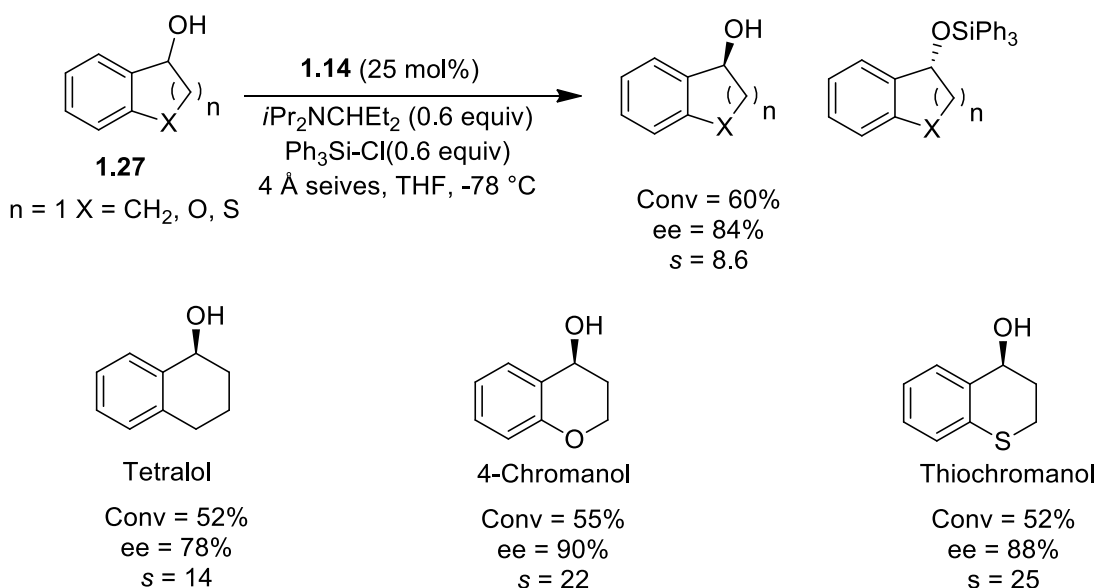
With this enticement of further development, the Wiskur group reported its first example of an enantioselective silylation (Scheme 1.12) by carrying out a Mukaiyama aldol reaction between a silyl ketene acetal and benzaldehyde in the presence of the chiral ammonium salt **1.26**.⁶⁴ This transformation was a combination of two separate reactions where the first step involves the formation of a carbon-carbon bond and the second step is a protection step.



Scheme 1.12 First enantioselective silylation developed by the Wiskur group

In this methodology, it is noteworthy to report that the enantioselectivity was arising from the second step which is the protection step instead of first step carbon-carbon bond forming step. After careful mechanistic analysis, the reaction was discovered to be a kinetic resolution where the selectivity was a result of different reactivities of the diastomeric salts (racemic alkoxide with chiral cinchonidine cation) with the silyl source which could be the silyl ketene acetal or the silyl acetate. Selectivity factors for this system were low in the 2-4 range. This informative report lead the Wiskur group to discover a more direct silylation-based kinetic resolution reaction. In 2011, the Wiskur group reported an organocatalyzed silylation-based kinetic resolution of monofunctional secondary alcohols.⁶⁵ In this system, commercially available (-)-tetramisole **1.14** was used as a small molecule nucleophilic catalyst and triphenylsilyl chloride as a silicon source. The substrates targeted in this report were monofunctional secondary alcohols **1.27**, challenging substrates to resolve due to the complete elimination of two point binding as required by the previous silylation methodologies for better selectivity. This report is the first example of a silylation based kinetic resolution of monofunctional secondary alcohols (Scheme 1.13). A variety of different secondary alcohols were investigated, ranging from

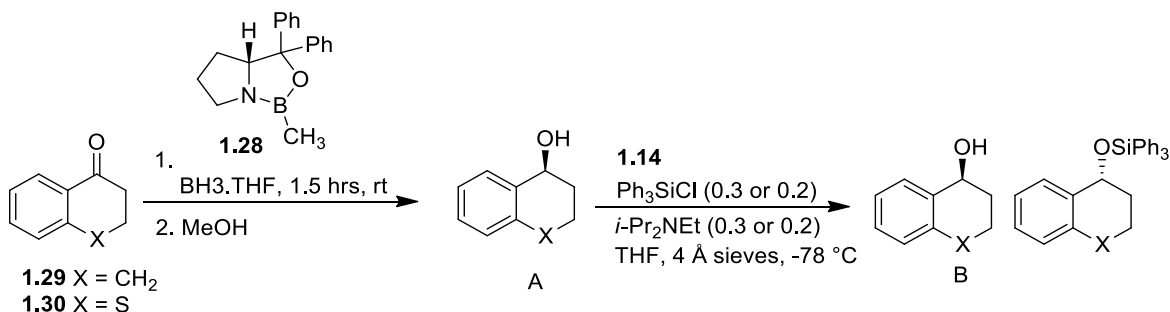
moderate to good selectivity. Good selectivity was reported with indanol ($s = 8.6$), since it is one of the most challenging substrates to resolve using a small molecule catalyst. Higher selectivity factors were obtained with tetralol ($s = 14$), chromanol ($s = 22$) and thiochromanol ($s = 25$). Overall, this methodology displays a significant contribution in the field of silylation.



Scheme 1.13 Silylation based kinetic resolution of monofunctional secondary alcohols

Soon after this discovery, the Wiskur group showed an application of our silylation-based kinetic resolution system in an *ee* polishing reaction.⁶⁶ In this report, an asymmetric enantioselective reaction and a silylation-based kinetic resolution was combined to generate (>95%) *ee* with (>50%) yield. The main advantage of combining these two reactions is to circumvent the limitation of a kinetic resolution reaction (maximum yield 50%) and an asymmetric catalysis (*ee* remains unchanged). To demonstrate this idea, α -tetralone (**1.29**) and thio-chromanone (**1.30**) were reduced first by using a Corey-Bakshi-Shibata reduction which produced the product in good yield and moderate *ee*. Then a

silylation based kinetic resolution, developed by our lab, was utilized to polish the enantioselectivity of the reaction further to obtain higher enantiomeric excess.



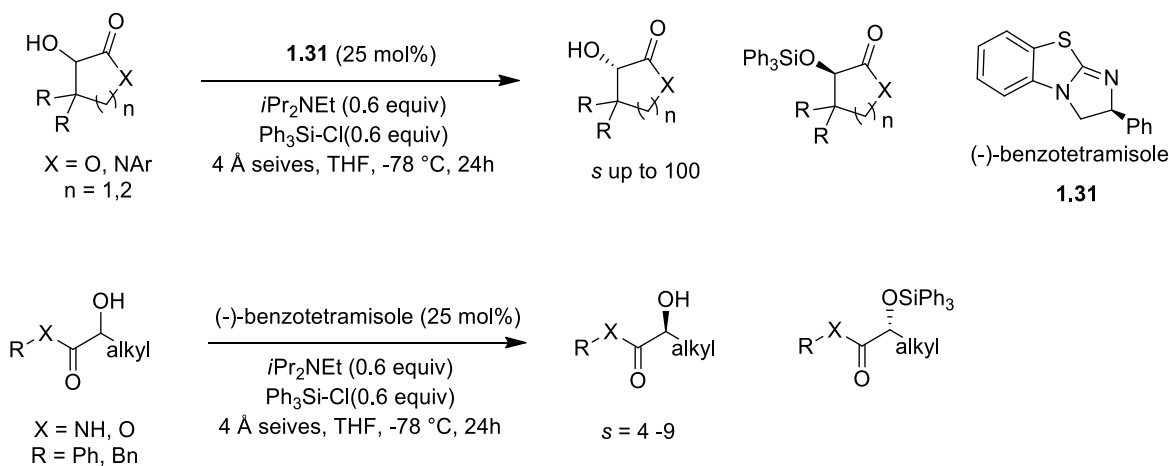
Methanol was removed after first step and THF was added to reaction prior to the kinetic resolution.

X	A	B	yield of B
CH ₂	85	96	68
S	85	95	81

Scheme 1.14 One-pot reaction linking asymmetric catalysis and a kinetic resolution

Recently, substrate expansion was taken as an initiative to show the potential of the silylation method developed by the Wiskur group. After a careful analysis of substrates, α -hydroxyl lactones and lactams were found to be the logical substrates to explore due to the common structural features compare to monofunctional secondary alcohols (Scheme 1.15). Using commercially available pantolactone, a similar optimized conditions to the previously screened monofunctional secondary alcohols were found after a little modification to the catalyst and the concentration of the substrate. Better selectivity factors were reported when (-)-tetramisole was replaced with (-)-benzotetramisole (**1.31**). A decrease in selectivity was observed when steric effects were removed from the β position

of pantolactone. As a result, several lactones with increased steric effects in the β position of pantolactone were investigated. A huge jump in selectivity was observed by changing the β position of pantolactone from dimethyl ($s = 36$) to diethyl ($s = 100$). Spiro cyclic lactones and a bicyclic lactone were also investigated with selectivity factors ranging from 8-48. Good to moderate levels of selectivity were reported when α -hydroxy lactams, amides and esters were used as a substrate class ($s = 3$ -24). In conclusion, this report is the first example of non-enzymatic based kinetic resolution of α -hydroxyl lactones and lactams.⁶⁷



Scheme 1.15 Kinetic resolution of α -hydroxy lactones and lactams

1.5 Conclusions

As we have discussed, chirality plays a crucial role in the pharmaceutical industry. Development of a more efficient method to obtain enantiomerically enriched compounds is quickly becoming a priority in both academia and industry. Among all the methods discussed, kinetic resolution is a valuable technique to meet the demand of structurally diverse chiral compounds. Among the several types of catalyst, organocatalyzed kinetic

resolutions show more practicality and economic viability towards large scale reactions. Due to the wide range of applications, more attention has been given to chiral secondary alcohols. Acylation was reported to be the most common way of obtaining chiral secondary alcohols via kinetic resolutions. On the other hand, silylation has many advantages over acylation, although enantioenriching alcohols through silylation remains underdeveloped. Therefore, the Wiskur group initiated research efforts towards development of silylation-based kinetic resolution methodology. A major breakthrough occurred in 2011, when our group reported our first successful organocatalyzed kinetic resolution of monofunctional secondary alcohols using silylation as a way of separation. Moderate to good selectivity factors were observed for various alcohols (s up to 25). Recently, expansion of this methodology was done using lactones and lactams as a substrates.

To expand the substrate class more efficiently, a detailed understanding of the mechanism becomes essential in order to make this system more applicable to a wide range of substrates. Several mechanistic studies were taken under consideration to learn about our system. The main focus of this dissertation was a preliminary investigation of silylation based kinetic resolutions using linear free energy relationships of substituted triphenylsilyl chlorides. The results and discussion of this dissertation will include the role of triphenylsilyl chloride in chirality determination, charge development in the transition state, and the influence of altering the steric and electronic of triphenylsilyl chloride on selectivity. In the third chapter, our efforts to understand a formation of the reactive intermediate in our silylation-based kinetic resolution using ^1H - ^{29}Si NMR will be discussed. In the fourth chapter, the newly obtained mechanistic information was employed to find a new substrate class with improved selectivity. In the fifth chapter, the

development of a kinetic resolution of secondary alcohols using a polymer supported triphenylsilyl chloride will be discussed. Finally, the last chapter will represent our prior attempt to develop amine-based kinetic resolutions using a Diels-Alder reaction.

1.6 References

- (1) Brown, W. H.; Foote, C. S. *Chirality. Organic Chemistry. Third Edition*; Vondeling, J., Eds.; Books/Cole: United States of America, 2002.
- (2) Solomons, T. W. G.; Fryhle, C. B. *Stereochemistry. In Organic Chemistry, 10e*; Wiley: USA, 2011; p 194.
- (3) Kim, J. H.; Scialli, A. R. Thalidomide: The tragedy of birth defects and the effective treatment of disease (vol 122, pg 1, 2011). *Toxicol. Sci.* **2012**, *125*, 613-613.
- (4) Harrington, P. J.; Lodewijk, E. Twenty years of naproxen technology. *Org. Process. Res. Dev.* **1997**, *1*, 72-76.
- (5) http://www.fda.gov/drugs/GuidanceComplianceRegulatoryInformation/Guidances/ucm_122883.htm
- (6) http://www.prweb.com/releases/chiral_technology/chiral_separation/prweb93955.htm
- (7) Keith, J. M.; Larrow, J. F.; Jacobsen, E. N. Practical considerations in kinetic resolution reactions. *Adv. Synth. Catal.* **2001**, *343*, 5.
- (8) Chen, Y.; Yekta, S.; Yudin, A. K. Modified BINOL ligands in asymmetric catalysis. *Chem. Rev.* **2003**, *103*, 3155-212.
- (9) Mukherjee, S.; Yang, J. W.; Hoffmann, S.; List, B. Asymmetric enamine catalysis. *Chem. Rev.* **2007**, *107*, 5471-5569.
- (10) Doyle, A. G.; Jacobsen, E. N. Small-molecule H-bond donors in asymmetric catalysis. *Chem. Rev.* **2007**, *107*, 5713-43.
- (11) Genet, J. P.; Ayad, T.; Ratovelomanana-Vidal, V. Electron-deficient diphosphines: the impact of DIFLUORPHOS in asymmetric catalysis. *Chem. Rev.* **2014**, *114*, 2824-2880.
- (12) Knowles, W. S.; Sabacky, M. J. Catalytic asymmetric hydrogenation employing a soluble optically active rhodium complex. *Chem. Commun.* **1968**, 1445-1446.
- (13) Knowles, W. S. Asymmetric hydrogenation. *Acc. Chem. Res.* **1983**, *16*, 106-112.
- (14) Miyashita, A.; Yasuda, A.; Takaya, H.; Toriumi, K.; Ito, T.; Souchi, T.; Noyori, R. Synthesis of 2,2'-bis(diphenylphosphino)-1,1'-binaphthyl (binap), an atropisomeric chiral bis(triaryl)phosphine, and Its use in the

- rhodium(I)-catalyzed asymmetric hydrogenation of α -(acylamino)acrylic acids. *J. Am. Chem. Soc.* **1980**, *102*, 7932-7934.
- (15) Noyori, R.; Ohkuma, T.; Kitamura, M.; Takaya, H.; Sayo, N.; Kumobayashi, H.; Akutagawa, S. Asymmetric hydrogenation of beta-keto carboxylic esters - a practical, purely chemical access to beta-hydroxy esters in high enantiomeric purity. *J. Am. Chem. Soc.* **1987**, *109*, 5856-5858.
 - (16) Noyori, R.; Ohta, M.; Hsiao, Y.; Kitamura, M.; Ohta, T.; Takaya, H. Asymmetric-synthesis of isoquinoline alkaloids by homogeneous catalysis. *J. Am. Chem. Soc.* **1986**, *108*, 7117-7119.
 - (17) Noyori, R. Asymmetric catalysis: Science and opportunities (Nobel lecture). *Angew. Chem., Int. Ed.* **2002**, *41*, 2008-2022.
 - (18) Ohta, T.; Takaya, H.; Kitamura, M.; Nagai, K.; Noyori, R. Asymmetric hydrogenation of unsaturated carboxylic-acids catalyzed by binap-ruthenium(ii) complexes. *J. Org. Chem.* **1987**, *52*, 3174-3176.
 - (19) Katsuki, T.; Sharpless, K. B. The 1st practical method for asymmetric epoxidation. *J. Am. Chem. Soc.* **1980**, *102*, 5974-5976.
 - (20) Finn, M. G.; Sharpless, K. B. Mechanism of asymmetric epoxidation .2. Catalyst structure. *J. Am. Chem. Soc.* **1991**, *113*, 113-126.
 - (21) Porter, W. H. Resolution of chiral drugs. *Pure Appl. Chem.* **1991**, *63*, 119-1122.
 - (22) Kagan, H. B.; Fiaud, J. C. Kinetic resolution. *Top. Stereochem.* **1988**, *18*, 249-330.
 - (23) Mitsunob.O; Yamada, M. Preparation of esters of carboxylic and phosphoric acid via quaternary phosphonium salts. *Bull. Chem. Soc. Jpn.* **1967**, *40*, 2380-2382.
 - (24) Gaunt, M. J.; Johansson, C. C. C.; McNally, A.; Vo, N. T. Enantioselective organocatalysis. *Drug Discov Today* **2007**, *12*, 8-27.
 - (25) Xu, G. C.; Yu, H. L.; Xu, J. H. Facile access to chiral alcohols with pharmaceutical relevance using a ketoreductase newly mined from *pichia guilliermondii*. *Chin. J. Chem.* **2013**, *31*, 349-354.
 - (26) Muller, C. E.; Schreiner, P. R. Organocatalytic enantioselective acyl transfer onto racemic as well as meso alcohols, amines, and thiols. *angew. Chem., Int. Ed.* **2011**, *50*, 6012-6042.

- (27) Wurz, R. P. Chiral dialkylaminopyridine catalysts in asymmetric synthesis. *Chem. Rev.* **2007**, *107*, 5570-5595.
- (28) Vedejs, E.; Chen, X. H. Kinetic resolution of secondary alcohols. Enantioselective acylation mediated by a chiral (dimethylamino)pyridine derivative. *J. Am. Chem. Soc.* **1996**, *118*, 1809-1810.
- (29) Ruble, J. C.; Fu, G. C. Chiral pi-complexes of heterocycles with transition metals: A versatile new family of nucleophilic catalysts. *J. Org. Chem.* **1996**, *61*, 7230-7231.
- (30) Ruble, J. C.; Latham, H. A.; Fu, G. C. Effective kinetic resolution of secondary alcohols with a planar-chiral analogue of 4-(dimethylamino)pyridine. Use of the Fe(C(5)Ph(5)) group in asymmetric catalysis. *J. Am. Chem. Soc.* **1997**, *119*, 1492-1493.
- (31) Fu, G. C. Asymmetric catalysis with "planar-chiral" derivatives of 4-(dimethylamino)pyridine. *Acc. Chem. Res.* **2004**, *37*, 542-547.
- (32) Ruble, J. C.; Tweddell, J.; Fu, G. C. Kinetic resolution of arylalkylcarbinols catalyzed by a planar-chiral derivative of DMAP: A new benchmark for nonenzymatic acylation. *J. Org. Chem.* **1998**, *63*, 2794-2795.
- (33) Bellemin-Laponnaz, S.; Tweddell, J.; Ruble, J. C.; Breitling, F. M.; Fu, G. C. The kinetic resolution of allylic alcohols by a non-enzymatic acylation catalyst; application to natural product synthesis. *Chem. Commun.* **2000**, 1009-1010.
- (34) Tao, B. T.; Ruble, J. C.; Hoic, D. A.; Fu, G. C. Nonenzymatic kinetic resolution of propargylic alcohols by a planar-chiral DMAP derivative: Crystallographic characterization of the acylated catalyst. *J. Am. Chem. Soc.* **1999**, *121*, 5091-5092.
- (35) Kawabata, T.; Nagato, M.; Takasu, K.; Fuji, K. Nonenzymatic kinetic resolution of racemic alcohols through an "induced fit" process. *J. Am. Chem. Soc.* **1997**, *119*, 3169-3170.
- (36) Yamada, S.; Misono, T.; Iwai, Y. Kinetic resolution of sec-alcohols by a new class of pyridine catalysts having a conformation switch system. *Tetrahedron Lett.* **2005**, *46*, 2239-2242.
- (37) Spivey, A. C.; Fekner, T.; Spey, S. E. Axially chiral analogues of 4-(dimethylamino)pyridine: Novel catalysts for nonenzymatic enantioselective acylations. *J. Org. Chem.* **2000**, *65*, 3154-3159.

- (38) Naraku, G.; Shimomoto, N.; Hanamoto, T.; Inanaga, J. Synthesis of enantiomerically pure C-2-symmetric 4-pyrrolidinopyridine derivative as a chiral acyl transfer catalyst for the kinetic resolution of secondary alcohols. *Enantiomer* **2000**, *5*, 135-138.
- (39) O Dalaigh, C.; Connon, S. J. Nonenzymatic acylative kinetic resolution of Baylis-Hillman adducts. *J. Org. Chem.* **2007**, *72*, 7066-7069.
- (40) Vedejs, E.; Daugulis, O.; Diver, S. T. Enantioselective acylations catalyzed by chiral phosphines. *J. Org. Chem.* **1996**, *61*, 430-431.
- (41) Vedejs, E.; Diver, S. T. Tributylphosphine - a remarkable acylation catalyst. *J. Am. Chem. Soc.* **1993**, *115*, 3358-3359.
- (42) Vedejs, E.; Daugulis, O. 2-aryl-4,4,8-trimethyl-2-phosphabicyclo[3.3.0]octanes: Reactive chiral phosphine catalysts for enantioselective acylation. *J. Am. Chem. Soc.* **1999**, *121*, 5813-5814.
- (43) Li, X. M.; Jiang, H.; Uffman, E. W.; Guo, L.; Zhang, Y. H.; Yang, X.; Birman, V. B. Kinetic resolution of secondary alcohols using amidine-based catalysts. *J. Org. Chem.* **2012**, *77*, 1722-1737.
- (44) Birman, V. B.; Uffman, E. W.; Hui, J.; Li, X. M.; Kilbane, C. J. 2,3-dihydroimidazo[1,2-a]pyridines: A new class of enantioselective acyl transfer catalysts and their use in kinetic resolution of alcohols. *J. Am. Chem. Soc.* **2004**, *126*, 12226-12227.
- (45) Birman, V. B.; Jiang, H. Kinetic resolution of alcohols using a 1,2-dihydroimidazo[1,2-a]quinoline enantioselective acylation catalyst. *Org. Lett.* **2005**, *7*, 3445-3447.
- (46) Birman, V. B.; Li, X. Benzotetramisole: a remarkably enantioselective acyl transfer catalyst. *Org. Lett.* **2006**, *8*, 1351-1354.
- (47) Birman, V. B.; Guo, L. Kinetic resolution of propargylic alcohols catalyzed by benzotetramisole. *Org. Lett.* **2006**, *8*, 4859-4861.
- (48) Birman, V. B.; Li, X. M. Homobenzotetramisole: An effective catalyst for kinetic resolution of aryl-cycloalkanols. *Org. Lett.* **2008**, *10*, 1115-1118.
- (49) Yang, X.; Birman, V. B. Homobenzotetramisole-catalyzed kinetic resolution of alpha-Aryl-, alpha-Aryloxy-, and alpha-Arylthioalkanoic acids. *Adv. Synth. Catal.* **2009**, *351*, 2301-2304.

- (50) Shiina, I.; Nakata, K. The first asymmetric esterification of free carboxylic acids with racemic alcohols using benzoic anhydrides and tetramisole derivatives: an application to the kinetic resolution of secondary benzylic alcohols. *Tetrahedron Lett.* **2007**, *48*, 8314-8317.
- (51) Shiina, I.; Nakata, K.; Sugimoto, M.; Onda, Y.; Iizumi, T.; Ono, K. 2,2-Disubstituted propionic anhydrides: Effective coupling reagents for the kinetic resolution of secondary benzylic alcohols using BTM. *Heterocycles* **2009**, *77*, 801-810.
- (52) Shiina, I.; Nakata, K.; Ono, K.; Sugimoto, M.; Sekiguchi, A. Kinetic resolution of the racemic 2-hydroxyalkanoates using the enantioselective mixed-anhydride method with pivalic anhydride and a chiral acyl-transfer catalyst. *Chem.—Eur. J.* **2010**, *16*, 167-172.
- (53) Nakata, K.; Gotoh, K.; Ono, K.; Futami, K.; Shiina, I. Kinetic resolution of racemic 2-hydroxy- γ -butyrolactones by asymmetric esterification using diphenylacetic acid with pivalic anhydride and a chiral acyl-transfer catalyst. *Org. Lett.* **2013**, *15*, 1170-1173.
- (54) Hu, B.; Meng, M.; Wang, Z.; Du, W. T.; Fossey, J. S.; Hu, X. Q.; Deng, W. P. A highly selective ferrocene-based planar chiral PIP (Fc-PIP) acyl transfer catalyst for the kinetic resolution of alcohols. *J. Am. Chem. Soc.* **2010**, *132*, 17041-17044.
- (55) Greene, T. W.; Wuts, P. G. M. *Protective groups in organic synthesis*; 3rd ed.; Wiley: New York, 1999.
- (56) Isobe, T.; Fukuda, K.; Araki, Y.; Ishikawa, T. Modified guanidines as chiral superbases: the first example of asymmetric silylation of secondary alcohols. *Chem. Commun.* **2001**, 243.
- (57) Zhao, Y.; Rodrigo, J.; Hoveyda, A. H.; Snapper, M. L. Enantioselective silyl protection of alcohols catalysed by an amino-acid-based small molecule. *Nature* **2006**, *443*, 67-70.
- (58) Zhao, Y.; Mitra, A. W.; Hoveyda, A. H.; Snapper, M. L. Kinetic resolution of 1,2-Diols through highly site- and enantioselective catalytic silylation. *Angew. Chem., Int. Ed.* **2007**, *46*, 8471-8474.
- (59) Rodrigo, J. M.; Zhao, Y.; Hoveyda, A. H.; Snapper, M. L. Regiodivergent reactions through catalytic enantioselective silylation of chiral diols. Synthesis of sapinofuranone A. *Org. Lett.* **2011**, *13*, 3778-3781.

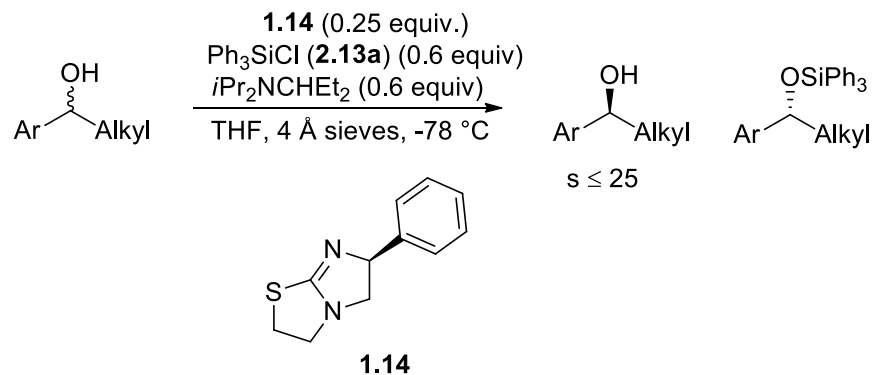
- (60) You, Z.; Hoveyda, A. H.; Snapper, M. L. Catalytic enantioselective silylation of acyclic and cyclic triols: Application to total syntheses of Cleroindicins D, F, and C. *Angew. Chem., Int. Ed.* **2009**, *48*, 547-550.
- (61) Manville, N.; Alite, H.; Haeffner, F.; Hoveyda, A. H.; Snapper, M. L. Enantioselective silyl protection of alcohols promoted by a combination of chiral and achiral Lewis basic catalysts. *Nat. Chem.* **2013**, *5*, 768-774.
- (62) Rendler, S.; Auer, G.; Oestreich, M. Kinetic resolution of chiral secondary alcohols by dehydrogenative coupling with recyclable silicon-stereogenic silanes. *Angew. Chem., Int. Ed.* **2005**, *44*, 7620-7624.
- (63) Klare, H. F. T.; Oestreich, M. Chiral recognition with silicon-stereogenic silanes: Remarkable selectivity factors in the kinetic resolution of donor-functionalized alcohols. *Angew. Chem., Int. Ed.* **2007**, *46*, 9335-9338.
- (64) Patel, S. G.; Wiskur, S. L. Mechanistic investigations of the Mukaiyama aldol reaction as a two part enantioselective reaction. *Tetrahedron Lett.* **2009**, *50*, 1164-1166.
- (65) Sheppard, C. I.; Taylor, J. L.; Wiskur, S. L. Silylation-based kinetic resolution of monofunctional secondary alcohols. *Org. Lett.* **2011**, *13*, 3794-3797.
- (66) Klauck, M. I.; Patel, S. G.; Wiskur, S. L. Obtaining enriched compounds via a tandem enantioselective reaction and kinetic resolution polishing sequence. *J. Org. Chem.* **2012**, *77*, 3570-3575.
- (67) Clark, R. W.; Deaton, T. M.; Zhang, Y.; Moore, M. I.; Wiskur, S. L. Silylation-based kinetic resolution of alpha-hydroxy lactones and lactams. *Org. Lett.* **2013**, *15*, 6132-6135.

CHAPTER 2

MECHANISTIC INVESTIGATION OF SILYLATION-BASED KINETIC RESOLUTION USING LINEAR FREE ENERGY RELATIONSHIPS AND RATE STUDY

2.1 Introduction

The silylation-based kinetic resolution methodology developed by the Wiskur group has shown a promise to become a highly selective and versatile method for the kinetic resolution of alcohols, as demonstrated in Chapter 1.¹ While the mechanism of acylation reactions in relationship to kinetic resolutions has been highly explored,²⁻⁵ there has been little work accomplished regarding the mechanism of silylation-based kinetic resolutions.⁶ Therefore, in order to efficiently improve upon the selectivity and expand the substrate class, a detailed understanding of the mechanism is crucial. In our system, triphenylsilyl chloride **2.13a** is used as a silicon source and (-)-tetramisole **1.14** as a nucleophilic catalyst (Scheme 2.1).



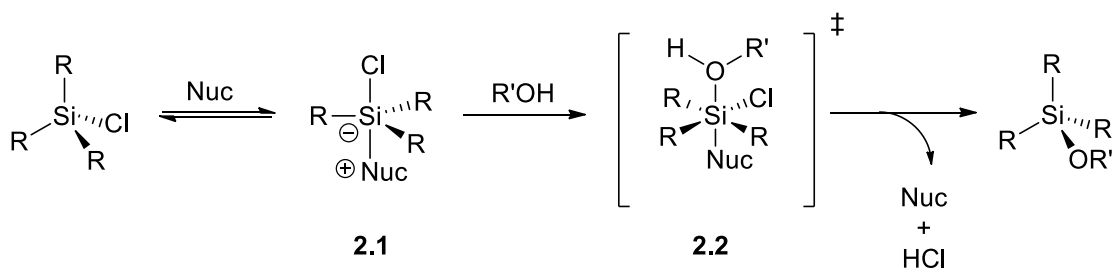
Scheme 2.1 Previously reported silylation-based kinetic resolution of monofunctional secondary alcohols

Based on literature reports, silyl chlorides can be activated through nucleophilic attack. In this regard, we believed that a complex could form between the catalyst and the triphenylsilyl chloride during the reaction. Therefore, we felt it was essential to understand involvement of triphenylsilyl chloride in our methodology, especially silyl chlorides role in chirality transfer and its role in the overall mechanism. To accomplish this goal, two different investigations were taken under consideration. First, a linear free energy relationship study was undertaken to understand the steric and electronic effects of substituted triphenylsilyl chlorides. Second, a ^{29}Si NMR study was performed to determine the coordination number of silicon in the potential activated intermediate. This chapter mainly focuses on the linear free energy relationship study towards understanding the mechanism and origin of selectivity in our silylation-based kinetic resolution, while the ^{29}Si NMR study will be discussed in following chapter 3.

2.2 Background: Nucleophilic assisted silylation and linear free energy relationships

2.2.1 Nucleophilic assisted silylation

The mechanistic work on nucleophilic assisted silylation that has been done in the past resulted in two proposed mechanisms. The first type of mechanism was proposed by Corriu.⁷ This mechanism proceeds through a pentavalent intermediate **2.1** when a nucleophile interacts with a silyl chloride (Scheme 2.2). The nucleophile and the chloride are in the axial positions on the silicon, and the reacting alcohol presumably approaches the silicon adjacent to the chloride to form a hexavalent transition state **2.2**, before extruding the nucleophile and chloride to form the silylated alcohol. To support this mechanism a kinetic study and a conductometric titration were performed.⁸ A negative entropy of activation ($\Delta S^\ddagger = -56$) was observed in the case of Ph_3SiCl and HMPT (hexamethylphosphortriamide) which suggested a highly organized transition state. This highly organized transition state was explained as a result of a reversible formation between the silicon and a nucleophile resulting in a hypervalent, pentacoordinated intermediate (**2.1**). The second step involves attack of the molecule being silylated, generating a hexavalent transition state (**2.2**) during the rate determining step. This hypothesis was further supported when low conductivity was observed in the case of Ph_3SiCl and HMPT, which provides evidence against formation of an ionic species.



Scheme 2.2 Nucleophilic assisted silylation mechanism proposed by Corriu

The second proposed mechanism by Chojnowski⁹, Bassindale^{10,11} and Frye¹² involves essentially two S_N2 reactions (Scheme 2.3). The activating nucleophile attacks the silyl chloride, kicking out the chloride and forming a reactive ionic tetravalent intermediate (**2.3**). The alcohol then does a backside attack on this intermediate to form the silylated alcohol, regenerating the nucleophilic catalyst. To support the tetravalent intermediate theory, Bassindale reported several ²⁹Si NMR chemical shifts of Me₃SiX (X = Br, Cl, I, OSO₂ and CF₃) reacted with DMF in *d*-dichloromethane and compared them with prepared pentacoordinated complexes (Figure 2.1).¹¹ Downfield ²⁹Si chemical shifts (10.6 to 44.0 ppm) were observed for all silyl chlorides reacted with DMF compared to the upfield frequency of ²⁹Si chemical shifts for the pentavalent complex (Figure 2.1) (-29.4 ppm).

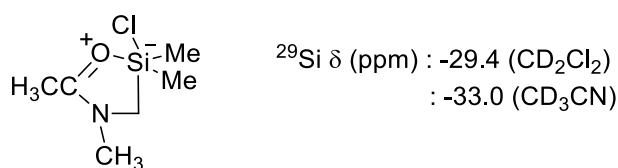
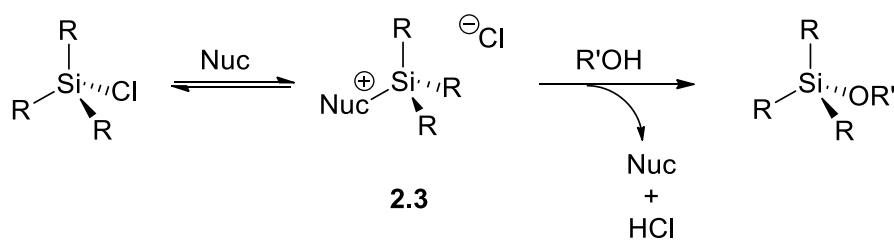


Figure 2.1 Five coordinated silicon species reported by Yoder¹³

This difference in ²⁹Si NMR frequency is a strong indication of a tetravalent complex over pentavalent. Ultimately, it has been stated that both mechanisms have been observed, and the path is affected by the nucleophile, leaving group, solvent, and substituents on silicon.¹⁴



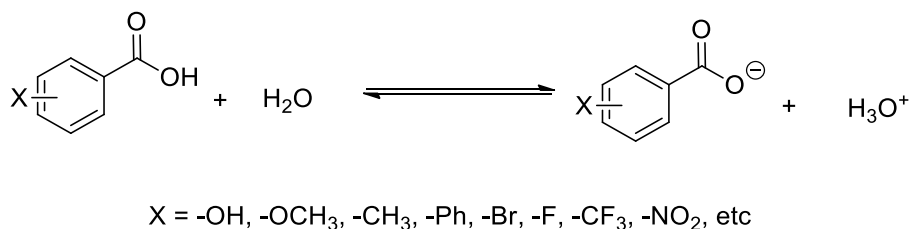
Scheme 2.3 Nucleophilic-assisted silylation mechanism proposed by Chojnowski, Bassindale, and Frye

2.2.2 Linear Free Energy Relationships (LFERs)

Linear free energy relationships^{15,16} are a very powerful empirical method in physical organic chemistry to systematically evaluate a relationship between a rate or equilibrium constant and the effect different substituents have on a reaction compared to a reference reaction. LFER has also been referred as a structure-reactivity relationship. It is a great way to gain insight into the mechanism of a reaction, particularly information regarding the transition state can be obtained. In a LFER study, a systematic change is made to one variable (for example: substrate or catalyst) while everything else remains constant. Therefore, the variable has to be the one which displays a substantial effect on the reaction and does not create any new interactions during the reaction. Electronic and steric effects are the most commonly studied substitution effects with LFERs. The original LFER analysis, which studied the electronic effect of substituents and is still widely employed today, was proposed by Hammett.¹⁵

2.2.2.1 Hammett Parameter (electronic effect parameter)

In 1930, Professor L. P. Hammett of Columbia University analyzed the electronic effect of substituents on the acidity of benzoic acid (Scheme 2.4).¹⁷



Scheme 2.4 Ionization of substituted benzoic acids in water at 25 °C

To test this, several *meta* and *para* substituted benzoic acids were prepared and compared to benzoic acid itself. *Ortho* substituents were avoided due to the steric hinderance to the carboxylic acid.

Hammett defined substituent parameters for each substituent as the difference between the acid dissociation constant of the substituted benzoic acid and benzoic acid, where the substituent parameter for hydrogen would be defined as $\sigma_H = 0$. The position of the substituent (*meta* or *para*) on the benzoic acid gives different sets of substituent parameters (σ_{meta} or σ_{para}). If the substituent is an EWG then the ionization of benzoic acid increases which results into the positive value of σ while an opposite effect can observed with EDG which make σ negative. In other word, a positive value of σ means the substituted benzoic acid is more acidic compared to benzoic acid, while a negative value of σ means the substituted benzoic acid is less acidic than benzoic acid.

Table 2.1 Hammett substituent constants¹⁸

substituent	Hammett value σ_p	substituent	Hammett value σ_m
H	0.00	H	0.00
Br	0.23	Br	0.39
Cl	0.22	Cl	0.37
F	0.06	F	0.34
CF ₃	0.54	CF ₃	0.43
OMe	-0.27	OMe	0.12
Me	-0.17	Me	-0.07
Et	-0.15	Et	-0.07
<i>i</i> Pr	-0.15	<i>i</i> Pr	-0.04
<i>t</i> Bu	-0.20	<i>t</i> Bu	-0.10
C ₆ H ₁₁	-0.15	C ₆ H ₁₁	-0.05
Ph	-0.01	Ph	0.06

Hammett used this scale of substituent parameters to correlate the substituent's effect on the acidity of benzoic acid. This acid/base reaction was then used as a reference reaction to compare the sensitivity of other reactions to the same substituents. The following table shows Hammett values for different substituents. (Table 2.1).

To analyze the substituent effect for other reactions the way benzoic acid does Hammett introduced an equation which is known as the Hammett equation.

$$\log (K_x/K_H) = \rho \sigma_x \quad \text{Eq. 2.1}$$

$$\log (k_x/k_H) = \rho \sigma_x \quad \text{Eq. 2.2}$$

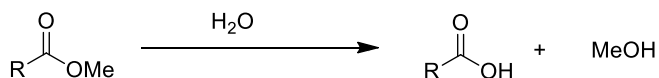
Where, K_x or k_x = Equilibrium constant or rate constant for the substituted benzoic acid and K_H or k_H = Equilibrium constant or rate constant for the Benzoic acid

In the above equation, rho (ρ) is a sensitivity constant for the reaction under study. In the ionization of benzoic acid rho was defined as one. Rho basically provides a magnitude of the substituent sensitivity of the reaction. The value of ρ provides a guideline to the amount and type of charge developing in the reaction being studied. If ρ is greater than 1, it suggests negative charge is building during the reaction. If ρ is between zero and 1, it suggests negative charge is still building during the reaction, but the reaction is less sensitive to the substituents than benzoic acid. If ρ is negative it suggests that positive charge is building during the reaction. Finally, if ρ is very close to zero or zero, it means the reaction shows no substituent effects.

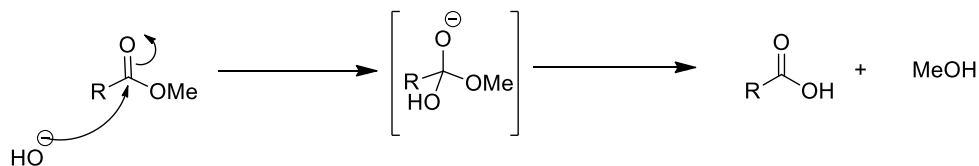
2.2.2.2 Steric Parameter

Another important effect that frequently affects the outcome of reactions is the steric effect, which can be investigated through a steric parameter. Steric effects in LFER can be mainly explained through Taft^{19,20} and Charton²¹⁻²³ type steric parameters. In order to investigate the effect of sterics, Taft measured a relative rate of a methyl ester hydrolysis (Figure 2.2). In the Taft parameter, reaction conditions played a vital role,¹⁵ especially in the base-catalyzed hydrolysis.

Methyl Ester Hydrolysis



Base Catalyzed Hydrolysis



Acid Catalyzed Hydrolysis

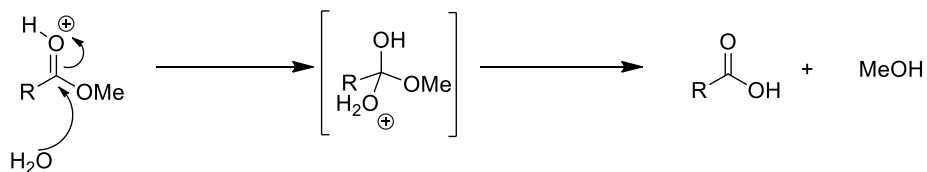


Figure 2.2 Taft's correlation for the development of steric parameter

In base catalyzed hydrolysis, the transition state was affected by both polar effects and steric effects due to the conversion of a neutral species into a negatively charged transition state. In the acid-catalyzed hydrolysis, a protonated reactant was converted into a protonated transition state, therefore it was assumed that substitution effects were purely steric effects.

Similar steric effects were observed for both the acid and base-catalyzed hydrolysis reactions, therefore the Taft steric parameter was mainly determined from the acid catalyzed hydrolysis. The Taft relationship for steric effects is shown in Eq. 2.3, which correlates the size of the substituent and the rate of hydrolysis.

$$\log \left(\frac{k_s}{k_{\text{CH}_3}} \right) = \delta E_s \quad \text{Eq. 2.3}$$

k_s / k_{CH_3} is the ratio of the rate of the substituted reaction over reference reaction

In this parameter, E_s is similar to σ in the Hammett equation and δ is the sensitivity constant similar to ρ in the Hammett equation. The steric parameter developed by Taft was the subject of debate during the 1960's and 70's due to the presence of the polar effect. To develop a parameter which is purely based on sterics and avoids the polar effect completely, Charton used the van der Waals radii of the substituents to form a parameter. Charton developed the relationship in Eq. 2.4, where v is an adjusted E_s value and ψ is the sensitivity constant similar to δ in Taft. If ψ is positive, then larger steric substituent increases the reaction rate and if ψ is negative then smaller steric substituent increase the reaction rate.

$$\log \left(\frac{k}{k_0} \right) = \psi v \quad \text{Eq. 2.4}$$

Table 2.2 Charton steric parameter for various substituents

Substituent	Charton Value ψ	Substituent	Charton Value ψ
H	0.00	Me	0.52
Br	0.65	Et	0.56
Cl	0.55	<i>i</i> Pr	0.76
F	0.27	<i>t</i> Bu	1.24
CF ₃	0.91	C ₆ H ₁₁	0.87
OMe	0.36	Ph	0.36

In above Table **2.2**, value of the all parameters are relative to H

2.2.2.3 Swain-Lupton parameter

Since electronic effects in many cases are a combination of inductive and resonance effects, isolation of these contribution from each other can provide a more detailed understanding of the transition state. In order to separate those effect from each other Swain and Lupton derived a separate parameter (Eq. 2.5) based on field effects and resonance effects with sensitivity constants f and r .²⁴ In this equation, $fF + rR$ is similar to the Hammett $\rho\sigma$, which gives us a power to separate the overall contribution of field effect form resonance effect

$$\log\left(\frac{k_x}{k_H}\right) = fF + rR \quad \text{Eq. 2.5}$$

Where F = field or inductive and R = Resonance, f & r = sensitivity factor

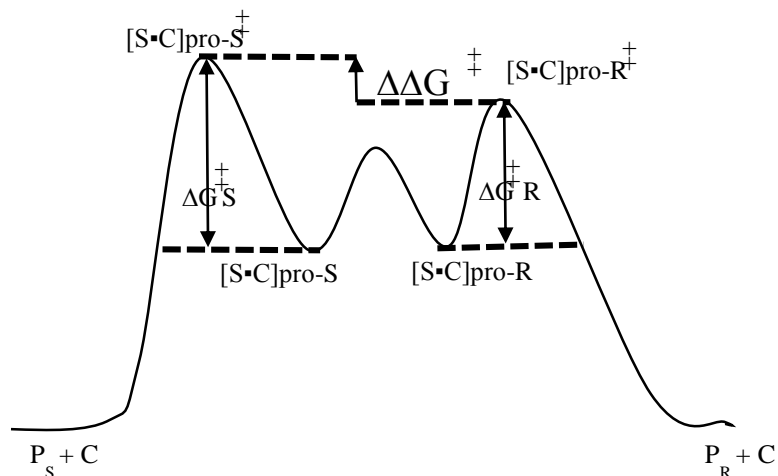
Following table shows Swain-Lupton parameter values for the different substituents (Table 2.3)

Table 2.3 Swain-Lupton parameter for various substituents

Substituent	<i>F</i>	<i>R</i>
H	0.03	0.00
Br	0.45	-0.22
Cl	0.42	-0.19
F	0.45	-0.39
CF ₃	0.38	0.16
OMe	0.29	-0.56
Me	0.01	-0.18
Et	0.00	-0.15
<i>i</i> Pr	0.04	-0.19
<i>t</i> Bu	-0.02	-0.18
C ₆ H ₁₁	0.03	-0.18
Ph	0.12	-0.13

2.3 LFER in asymmetric catalysis

In asymmetric catalysis, it has been reported that minor energy differences in a diastereomeric transition state could lead to high levels of enantioselectivity. Therefore, understanding asymmetric induction through a mechanistic point should allow for a systematic modification to catalyst or any other part of the reaction rather than spending a lot of time screening different catalyst or optimizing a reaction conditions to obtain high enantiomeric ratio. LFERs have shown great potential in asymmetric catalysis, by correlating observed enantioselectivity of a reaction with its catalyst or ligand substituent effect using variety of different substituent parameters, ultimately providing detailed mechanistic information regarding asymmetric induction.²⁵⁻³⁶



P_S and P_R = Product of S and R enantiomers respectively. $[S\bullet C]_{\text{pro-S/R}}$ = Diastereomeric substrate (S)/Catalyst (C) complexes. $[S\bullet C]_{\text{pro-S/R}}^\ddagger$ = Diastereomeric substrate (S)/Catalyst (C) complexes in transition state

Figure 2.3 Asymmetric catalysis explained through Curtin-Hammett principle

The correlation of enantioselectivity with different parameters was recently explained by the Sigman group using the Curtin-Hammett principle (Figure 2.3).²⁵ According to Curtin-Hammett principle, in a reaction where a product ratio is expected from two different interconverting forms or pathways, then the final product ratio is dependent on the energy difference between the diastereomeric transition states ($\Delta\Delta G^\ddagger$), not the energy of the intermediates. This principle, in relationship to asymmetric catalysis, is directly proportional to the final enantiomeric ratio of the asymmetric reaction. In an asymmetric reaction, the enantiomeric ratio is determined by $\Delta\Delta G^\ddagger = -RT \ln(k_{\text{rel}})$ where k_{rel} is the ratio of the fast reacting enantiomer rate over the slow reacting enantiomer rate. Therefore, when a series of catalysts or substrates are found to have a LFER the correlation

suggests that the the mechanism of the reaction is not altered, but the diastereomeric transition state energy is the only thing perturbed.

2.4 Example of LFER in asymmetric catalysis

Several asymmetric reactions have been studied over the years using LFERs involving different parameters. In 1991, Jacobsen and his co-workers reported a direct correlation of the enantioselectivity, of the epoxidations of *cis*-alkenes, with the electronic properties of a substituted (salen)Mn catalyst (Figure 2.4).³⁵ This report was one of the first examples of an asymmetric reaction mechanistic investigation using a LFER. To accomplished this goal, a variety of electronically different (salen)Mn complexes were synthesized from a diamine and different substituted salicyl aldehydes. This electronically modified catalyst was tested using three different substrates including 2,2-dimethylchromene (**2.5**), *cis*- β -methylstyrene (**2.6**) and dimethyl-3-hexene (**2.7**). For all three substrates examined, an increase in enantioselectivity was observed with electron donating groups on the catalyst while enantioselectivity decreased with electron withdrawing groups on the catalyst. To analyze this trend in enantioselectivity, a correlation was observed using Hammett σ_p parameters and enantiomeric ratio. All three substrates had similar linear correlations with a negative sensitivity constant (ρ). To explain this result, the Hammond postulate was invoked. When an electron donating group was introduced on the catalyst, it stabilized the Mn(V) oxo intermediate and generated a milder oxidant. Due to this milder oxidant, the transition states appears to be more product like (a late transition state) with significant involvement of the alkene with the catalyst. This provides a close catalyst/substrate interaction. This increased participation of the substrate with the catalyst leads to higher enantioselectivity. When electron withdrawing groups

were introduced on the catalyst, it destabilized the Mn(V) oxo intermediate and generated a reactive oxidant. Due to this reactive oxidant, involvement of alkene with catalyst occurs in an early transition state with little involvement of the alkene substrate. Due to the, limited involvement of substrate with catalyst leads to a decrease in enantioselectivity. To support this hypothesis, Jacobsen reported several other experiments including a kinetic isotope effect, a temperature profile of the epoxidation reaction using electronically different substituted catalysts, and an Eyring analysis. All of these experiments supported the Hammond postulate hypothesis.

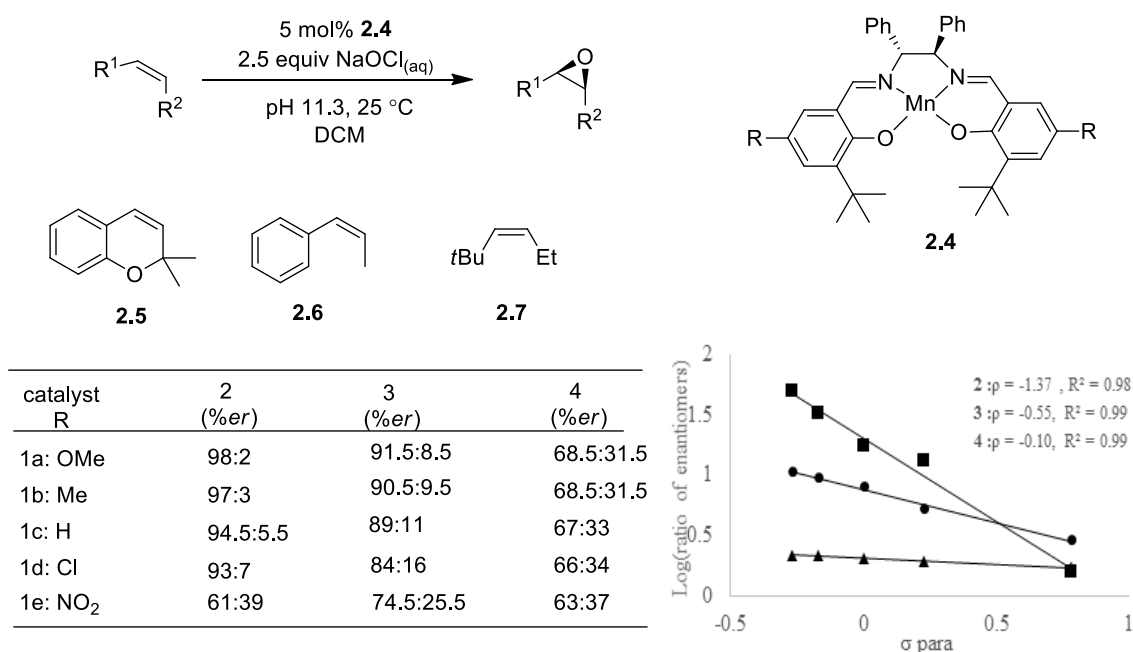
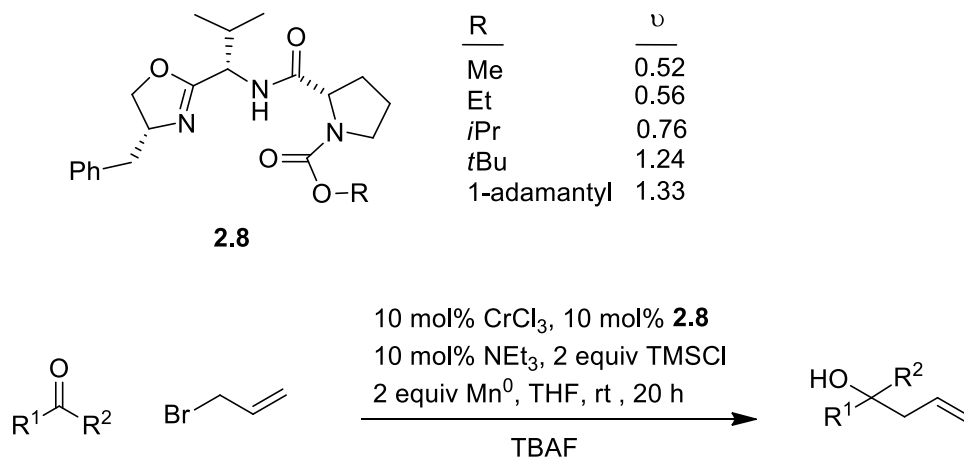


Figure 2.4 Correlation of electronic effect and enantioselectivity in Mn(III)-catalyzed epoxidation reaction.

More recently, the Sigman group reported a systematic evaluation of the steric effects on ligand substituent size and its correlation in asymmetric catalysis using LFERs.²⁷ The proline module of an oxazoline ligand (**2.8**) was modified and used in an

enantioselective Nozaki-Hiyama-Kishi reaction of allylic halides with both aldehydes and ketones (Figure 2.5). Different proline carbamates ligands (**2.8**) were synthesized by incorporating a small to large group as the carbamate substituent. Three different substrates, benzaldehyde, hydrocinnamaldehyde and acetophenone were investigated. In all three substrates, enantioselectivity increased with increase in ligand size. A linear free energy relationship was observed using Charton parameters. A positive slope in all three substrates indicated that the larger carbamate directly affected enantioselectivity (i.e. the diastereomeric transition state). The understanding of the steric effect of the ligand will direct future modifications of the system in a more efficient manner. This report is a great example of the evaluation of steric effects in asymmetric catalysis using a LFER.



entry	R	PhCHO e.r (R/S) ^a	PhCH ₂ CH ₂ CHO e.r (R/S) ^a	PhCOMe e.r (R/S) ^a
1	Me	1.5	1	0.3
2	Et	1.9	1.1	0.3
3	<i>i</i> Pr	3.5	1.3	0.6
4	<i>t</i> Bu	23	2.8	2.2
5	1-adamantyl	23	2.8	2.6

^a Enantiomeric ratio was determined by HPLC

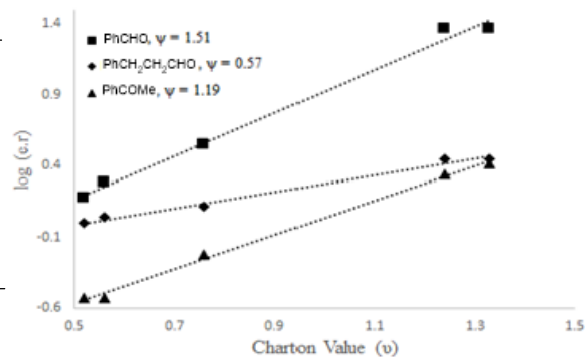


Figure 2.5 Correlation of the steric effect of the ligand and enantioselectivity in Nozaki-Hiyama-Kishi reaction of an allylic halide with both aldehydes and ketones.

In 2011, the Sigman group has also reported a simultaneous evaluation of steric (Charton) and electronic (Hammett) effects in a NHK propargylation of acetophenone (Scheme 2.6).³¹ In this reaction, ketone and propargyl bromide reacted enantioselectively in the presence of catalyst to form homopropargylic tertiary alcohol. The quinoline-proline based ligand was found to be the effective ligand to test both effects in a systematic way. Using different electronic and steric substituent combinations, a library of nine different ligand were created through synthesis and screened in the propargylation of acetophenone. One ligand was found to be the optimal ligand. Using this obtained $\Delta\Delta G^\ddagger$ value, an equation was developed to correlate experimentally measured enantioselectivity with the calculated value.

$$\Delta\Delta G^\ddagger = -1.20 + 1.22E + 2.84S - 0.85 S^2 - 3.79 ES + 1.25 ES^2 \quad \text{Eq. 2.6}$$

E = electronics and S = sterics

A good correlation was observed between the measured value and the predicated value of $\Delta\Delta G^\ddagger$. From this result, it was established which ligand would be the optimal

ligand. Various aryl and aliphatic ketones were employed in the propargylation reaction using the optimal ligand with modest to excellent enantioselectivity and yield.

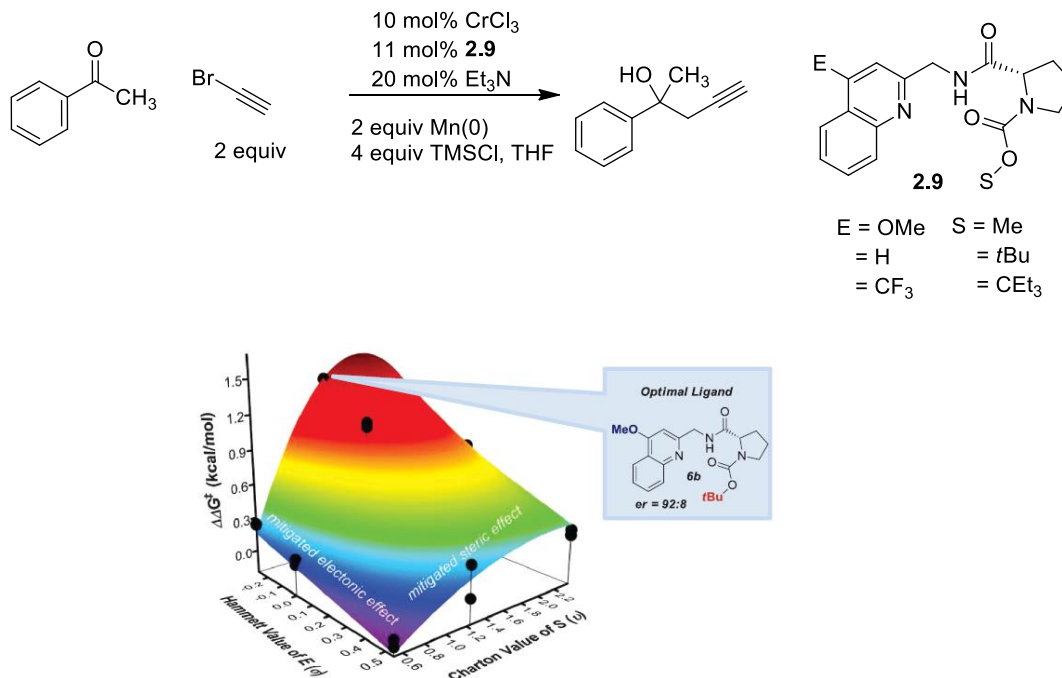


Figure 2.6 3D surface evaluation of steric and electronic effect vs measured enantioselectivity “From [Harper, K. C.; Sigman, M. S. Three-Dimensional Correlation of Steric and Electronic Free Energy Relationships Guides Asymmetric Propargylation. *Science*. **2011**, 333, 1875-1878.]. Reprinted with permission from AAAS.”

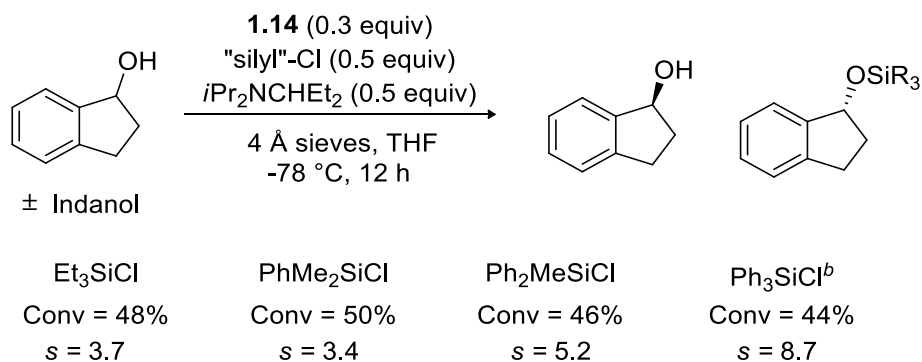
Inspired by the work done in LFERs and asymmetric catalysis, we decide to utilize this powerful tool in our system to study the mechanism of our silylation-based kinetic resolution.

2.5 Understanding the mechanism of our silylation-based kinetic resolution through linear free energy relationships using selectivity factors and a rate study³⁷

“Reprinted with permission from (Akhani, R. K.; Moore, M. I.; Pribyl, J. G.; Wiskur, S. L. Linear Free-Energy Relationship and Rate Study on a Silylation-Based Kinetic Resolution: Mechanistic Insights. *J. Org. Chem.*, **2014**, 79, 2384-2396). Copyright (2014) American Chemical Society.”

Previously we have shown that the selectivity of our kinetic resolution was dependent on the structure of the silyl chloride. Specifically, it was determined that three phenyl

groups were strategic in obtaining selectivity. For example, when diphenylmethyl and phenyldimethylsilyl chlorides were employed, the selectivity dramatically decreased as compared to triphenylsilyl chloride (Scheme 2.5). The same decrease in selectivity was obtained when all of the phenyl groups were replaced with alkyl groups (Scheme 2.5). This same effect on selectivity was seen with a second substrate class, α -hydroxy lactones with a much larger impact. Since the triphenylsilyl chloride is strategically involved in the enantio-discriminating step, it can be used as a valuable tool for exploring the mechanism. We therefore examined the steric and electronic effects on the silyl chloride to understand more about the reactivity of the silyl chloride and its role in enantioselective discrimination through the use of a linear free energy relationship (LFER). Ultimately, the knowledge gained from this study will be used to improve future resolutions and expand our substrate scope.

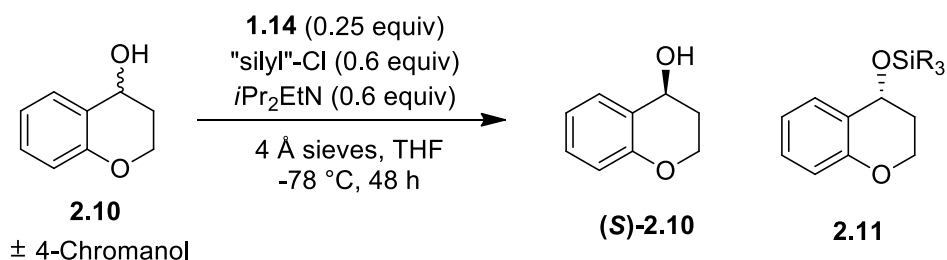


Scheme 2.5 Previously reported importance of triphenylsilyl chloride

Linear free energy relationship analysis is a powerful tool for investigating reaction mechanisms. As discussed earlier, there is an increase interest in employing this technique to evaluate asymmetric reactions. We wanted to use this tool to investigate the steric and electronic effects on the rate and selectivity of our silylation-based kinetic resolution in

Scheme 2.1. In triphenylsilyl chloride, three different positions (*ortho*, *meta* or *para*) could be utilized in the substitution study. In order to identify the effect of substituents in these three positions, three methyl substituted triphenylsilyl chlorides were used in the kinetic resolution of 4-chromanol (Table 2.4, Entries 1-3). As expected, no conversion was observed with the substitution (methyl group) on the *ortho* position of triphenylsilyl chloride (Table 2.4, Entry 1). This result suggests that substitution on the *ortho* position is too sterically hindered and therefore it is not a choice for our substitution study. Surprisingly, similar selectivity was observed with substitution on *para* position of triphenylsilyl chloride and *meta* position of triphenylsilyl chloride (Table 2.4, Entry 2 & 3). In the previous study (Scheme 2.5), a drop in the selectivity was observed by replacing one of the phenyl groups with a methyl group. In order to test the importance of the phenyl groups in our system, we exchanged the phenyl groups with benzyl groups and employed it in a kinetic resolution (Table 2.3, Entry 4). A racemic mixture was obtained which shows triphenylsilyl chloride is very important in obtaining selectivity. Since substituting the *para* position of triphenylsilyl chloride allows us to use a large substituent for our LFER study without any sterics hindrance, we decided to proceed with *para* position of triphenylsilyl chloride as our choice of substitution study.

Table 2.4 Effect of substitution on different position (*ortho*, *meta* and *para*) of triphenylsilyl chloride in kinetic resolution of 4-chromanol

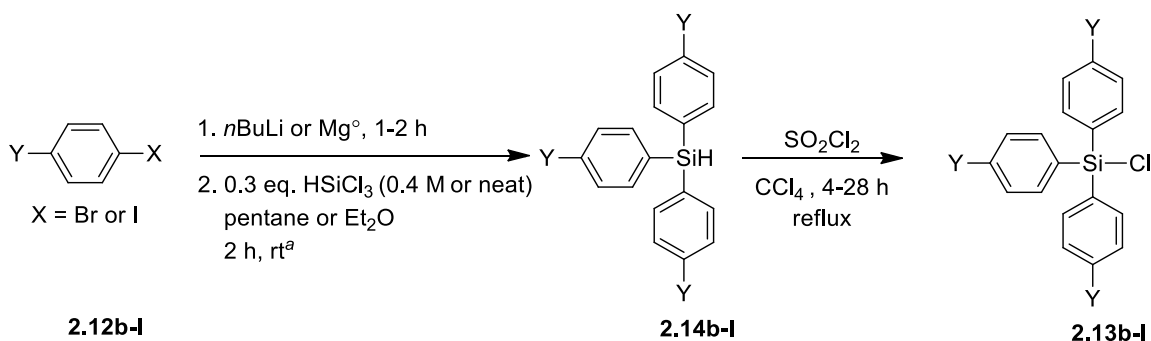


Entry	"Silyl"-Cl	%C	s
1		NR	NR
2		60	13
3		56	14
4		12	1.6

2.6 Synthesis of *p*-substituted triphenylsilyl chlorides

For this analysis, a series of *para* substituted triphenylsilyl chlorides (**2.13b-l**) (Scheme 2.6) were synthesized to employ in the kinetic resolution shown in Scheme 1. The substituents include halides (**2.13b-d**), trifluoromethyl (**2.13e**), methoxy (**2.13f**), various alkyl groups (**2.13g-k**), and phenyl (**2.13l**). The synthesis of the silyl chlorides was accomplished by a three-step process starting with a lithium halogen exchange³⁸ or Grignard formation³⁹ with *para* substituted phenyl bromides or iodides (**2.12b-l**). The resultant organometallic compound was reacted with trichlorosilane to make the triaryl

substituted silanes (**2.14b-l**). The silanes were then converted into the silyl chlorides (**2.13b-l**) by a radical chlorination with sulfuryl chloride.^{40,41} The silanes and silyl chlorides were prepared in moderate to good yields (see experimental).



Y = (b) Br, (c) Cl, (d) F, (e) CF₃, (f) OCH₃, (g) CH₃, (h) Et, (i) *i*Pr, (j) *t*Bu, (k) C₆H₁₁, (l) Ph

^a0 °C to rt was used for (**2.12e**), -40 °C for (**2.12h-j**) and -78 °C for (**2.12l**). See experimental for exact procedures and yields.

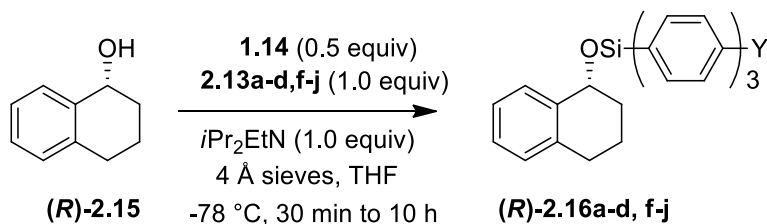
Scheme 2.6 Synthesis of *p*-Substituted triphenylsilyl chlorides

2.7 Rate study using fast reacting enantiomer with different para substituted triphenylsilyl chlorides

A rate study of the substituted silyl chlorides was done to explore the charge developing in the transition state and provide information on the mechanism of the reaction. Since kinetic resolutions consist of two substrates competitively reacting (the two enantiomers), the rate needed to be measured on one enantiomer at a time. Insitu IR was employed to measure the rate of silylation on the fast reacting (*R*) enantiomer of tetralol (**2.15**), employing silyl groups substituted with hydrogen, halides, methoxy, and alkyl groups (**2.13a-d,f-j**). The reaction conditions were nearly identical to the conditions in Scheme

2.1, except for the use of Hünig's base due to the lack of availability of the previously employed tertiary amine, diisopropyl-3-pentyl amine. The initial rate, up to 10% conversion (8 mmol), was observed in all cases, and the results are shown in Table 2.5. Silyl groups substituted with electron withdrawing groups (entries 2-4) were up to five times faster than triphenylsilyl chloride (entry 1) and electron donating groups (entries 5-9) significantly decreased the rate as much as two orders of magnitude versus **2.13a**.

Table 2.5 Rate study employing the fast reacting enantiomer (*R*) using different *para* substituted triphenylsilyl chlorides^a



Entry ^a	Y	Rate of (<i>R</i>)-2.16 ^b (mmol/min)
1	H	12
2	Br	66
3	Cl	68
4	F	32
5	OMe	0.09
6	Me	0.72
7	Et	0.36
8	<i>i</i> Pr	1.0
9	<i>t</i> Bu	0.29

^aReactions were carried out at a substrate concentration of 0.08 M on a 0.3 mmol scale.

Each entry is an average of two runs. ^bRate was obtained via in situ IR measurements. ¹H NMR conversion was used to monitor conversion of alcohol to silylated product.

The increase in rate when the silyl chloride is substituted with electron withdrawing groups is logical since those substituents would remove electron density from the silicon, making it more reactive. The same argument applies to electron donating groups increasing electron density on the silicon, slowing down the silylation.

A Hammett plot was generated from the log of the (**R**)-**2.15** rates in Table 1 versus σ_{para} substituent constants⁴² (Figure 2.7), which shows a linear relationship with a slope or sensitivity constant of $\rho = 5.8$ ($R^2 = 0.94$). The fact that a correlation exists signifies that the mechanism does not change upon altering the silyl chloride. The considerable magnitude of the slope (ρ) indicates that the silylation reaction is very sensitive to electron withdrawing and donating groups on the silyl chloride, signifying a significant redistribution of charges in the transition state. Finally, the positive slope is suggestive of a decrease in positive charge in the transition state.¹⁵ This decrease in positive charge and significant redistribution of charge is consistent with the silylation mechanism proposed by Chojnowski⁹, Bassindale^{10,11} and Frye,¹² while the mechanisms proposed by Corriu and Hoveyda and Snapper cannot be ruled out entirely. The mechanism is essentially two S_N2 reactions (Scheme 2.7), where the first S_N2 reaction involves the nucleophilic catalyst (**1** in our system) attacking the silyl chloride, displacing the chloride to form the reactive tetravalent intermediate **A**. An alcohol then does a backside attack on this intermediate to form the silylated alcohol, regenerating the nucleophilic catalyst. The proposed transition state for this last step is similar to the classical S_N2 transition state with the nucleophilic catalyst (**1**) departing as the alcohol is attacking. This involves a redistribution of the positive charge from a full positive charge on intermediate **A** to partial positive charges on the incoming alcohol oxygen and the departing catalyst **1.14**, displaying an overall decrease

in positive charge in the transition state. This proposed transition state can be employed in an effort to understand the origin of enantioselectivity.

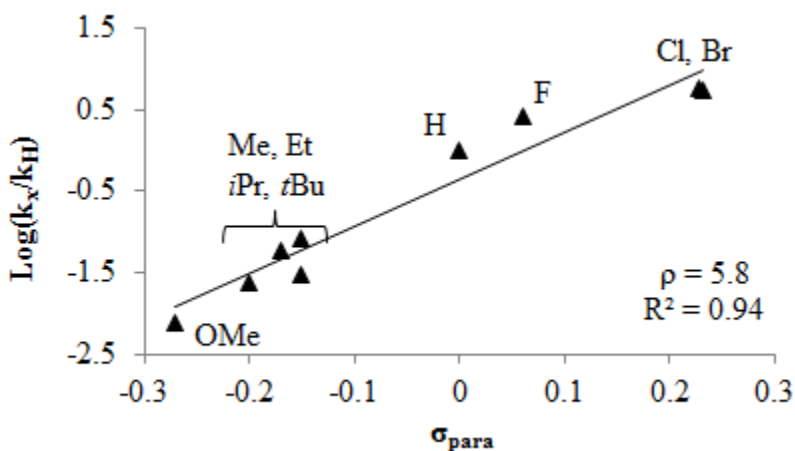
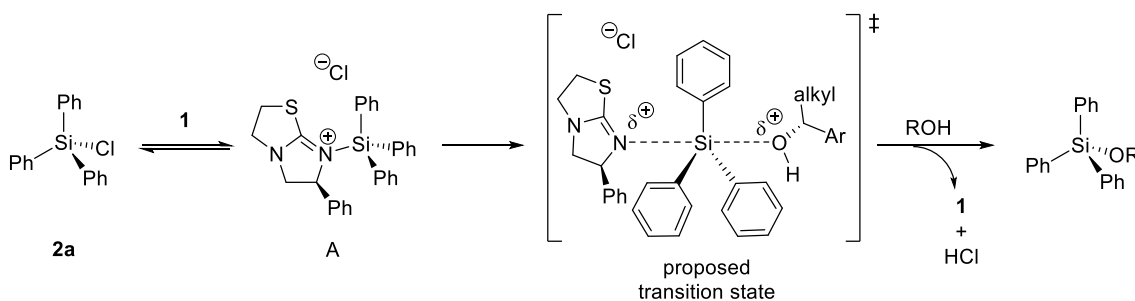


Figure 2.7 Hammett plot employing the parameter σ_{para} ¹⁸ versus the log of rates for the kinetic resolution of the fast reacting enantiomer (*R*) of alcohol **2.15** (average of two runs).



Scheme 2.7 Proposed mechanism of the silylation reaction

Since the σ_{para} parameter incorporates both inductive and resonance contributions, the linear correlation of the rate data indicates that the substituents in the *para* position can contribute to the reactivity of the silicon through some degree of resonance. The degree of inductive versus resonance contribution was determined using the Swain-Lupton dual parameter approach²⁴ (Eq. 2.5). The method separates the Hammett parameter into two

parameters, induction/field effects (F) and resonance (R), with sensitivity factors of r and f respectively. Employing F and R parameters recalculated by Hansch, the rate data from Table 1 was fit with a least squares regression analysis to solve for the two sensitivity constants. The similarity of f and r ($f = 5.4$, $r = 5.9$) indicates that induction and resonance contribute equally to the rate of the reaction. Figure 2.8 shows the good correlation between experimentally determined log of rate ratios versus those predicted by Eq. 2.5.

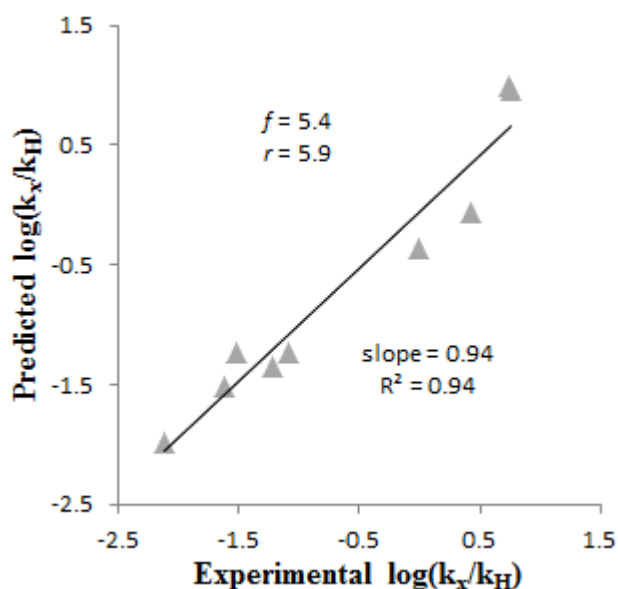


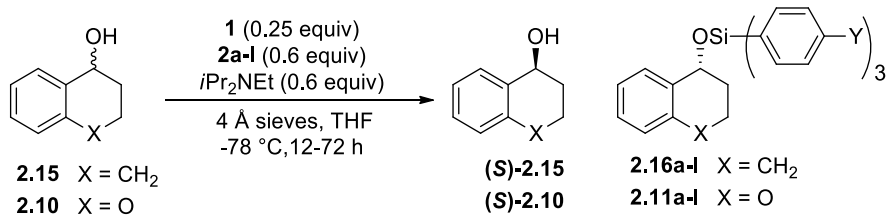
Figure 2.8 Comparison of the experimental $\log(k_x/k_H)$ using the rate data from Table 2.5 versus the predicted $\log(k_x/k_H)$ calculated from Eq. 2.5

As was stated earlier, LFERs have been employed to study asymmetric reactions, and provide information about the source of enantioselectivity. While these LFER studies mainly employ enantiomeric ratios as a way of measuring the change in the free energy of activation, traditionally, a ratio of pure rates is employed in the analysis as seen in the study above. Recently it was suggested that selectivity factors from kinetic resolutions could be employed in a LFER analysis⁴³ since selectivity factors are a ratio of rates.

2.8 Kinetic resolution of tetralol and chromanol using different *para* substituted triphenylsilyl chlorides

Two alcohols were chosen for the kinetic resolution reactions (Eq. 3) employing the *p*-substituted silyl chlorides: tetralol (**2.15**) and 4-chromanol (**2.10**). These alcohols were chosen since they displayed moderate selectivity under the reaction conditions, allowing us to see subtle differences in selectivity as the substituents are altered on the silyl chlorides. These subtle changes would be missed if highly selective substrates were employed. The same reaction conditions as the rate study were employed, and the selectivity factors for the reactions are shown in Table 2.5. Entry 1 and 13 show the small detrimental effect of switching the base from diisopropyl-3-pentyl amine to Hünig's base when we compare the originally published selectivity factors of 13 and 21 for **2.15** and **2.10**, respectively, versus the new selectivity factors of 11 and 15. Employing the silyl chlorides with substituents in the *para* position proved satisfactory at affecting the selectivity of the kinetic resolution reactions of **2.15** and **2.10**. The use of halide substituted silyl chlorides (**2.13b-d**) reduced the selectivity factors (entries 2-4, 14-16) for both alcohols. The selectivity of the kinetic resolution employing *para* bromide substituted silyl chloride (**2.13b**) was nearly half compared with the selectivity of employing **2.13a**. Both electron withdrawing and electron donating groups on the silyl chloride, trifluoromethyl (**2e**) (entry 5 & 17) and methoxy (**2.13f**) (entry 6 & 18) respectively, caused a reduction in selectivity when compared to **2.13a**. Silyl chlorides substituted with alkyl groups (**2.13g-k**) resulted in an increase in selectivity, with the bulkier groups resulting in the best selectivity (entries 7-11 & 19-23).

Table 2.6 Kinetic resolution using different *para* substituted triphenylsilyl chlorides^a



Entry	alcohol	Y	t(h)	conv (%) ^b	er of recovered alcohol	<i>s</i> ^b
1	2.15	H	24	50	85:15	11
2	2.15	Br	24	46	75:25	6.0
3	2.15	Cl	24	34	66:34	7.0
4	2.15	F	24	52	85:15	9.0
5	2.15	CF ₃	24	35	65:35	5.0
6	2.15	OMe	48	43	77:23	10
7	2.15	Me	48	49	86:14	14
8	2.15	Et	48	36	72:29	13
9	2.15	<i>i</i> Pr	48	51	88:12	14
10	2.15	<i>t</i> Bu	69	42	79:21	16
11	2.15	C ₆ H ₁₁	72	34	71:29	15
12	2.15	Ph	72	22	62:38	11
13	2.10	H	24	49	85:15	15
14	2.10	Br	24	41	73:27	8.0
15	2.10	Cl	24	50	86:14	11
16	2.10	F	24	48	85:15	13
17	2.10	CF ₃	24	21	60:40	7.0
18	2.10	OMe	48	46	81:19	11
19	2.10	Me	48	56	94:6	14
20	2.10	Et	48	45	83:17	17
21	2.10	<i>i</i> Pr	48	48	87:13	20
22	2.10	<i>t</i> Bu	69	47	88:12	28
23	2.10	C ₆ H ₁₁	72	44	83:17	21
24	2.10	Ph	72	17	59:41	13

^aReactions were carried out at a substrate concentration of 0.16 M on a 0.22 mmol scale.

^bSee ref ⁴⁹. %Conversion = $ee_s/(ee_s+ee_p) \times 100\%$ & $s = \ln[(1-C)(1-ee_s)]/\ln[(1-C)(1+ee_s)]$,

where ee_s = *ee* of recovered starting material and ee_p = *ee* of product

Hammett plots were generated (Figure 2.9) by plotting σ_{para} parameters versus the log of the selectivity factors from Table 2.6 for alcohols **2.15** and **2.10**. This explores the electronic contribution of silyl chlorides **2.13a-l** and how electronic effects affect selectivity. A correlation was observed with the silylation-based kinetic resolution showing that it is sensitive to the electronic effects of the triphenylsilyl chlorides. For both alcohols **2.15** and **2.10** the same trend was observed, a negative slope in both, suggesting a decrease in selectivity factors when electron withdrawing groups are employed. The selectivity improved when electron donating groups were employed, but only up to a point. When the strongest electron donating group in the series was used, methoxy, it did not follow the linear trend, and instead decreased in selectivity. The sensitivity for both substrates was nearly the same with $\rho = -0.73$ ($R^2 = 0.95$) and -0.68 ($R^2 = 0.80$) for **2.15** and **2.10** respectively not including methoxy.

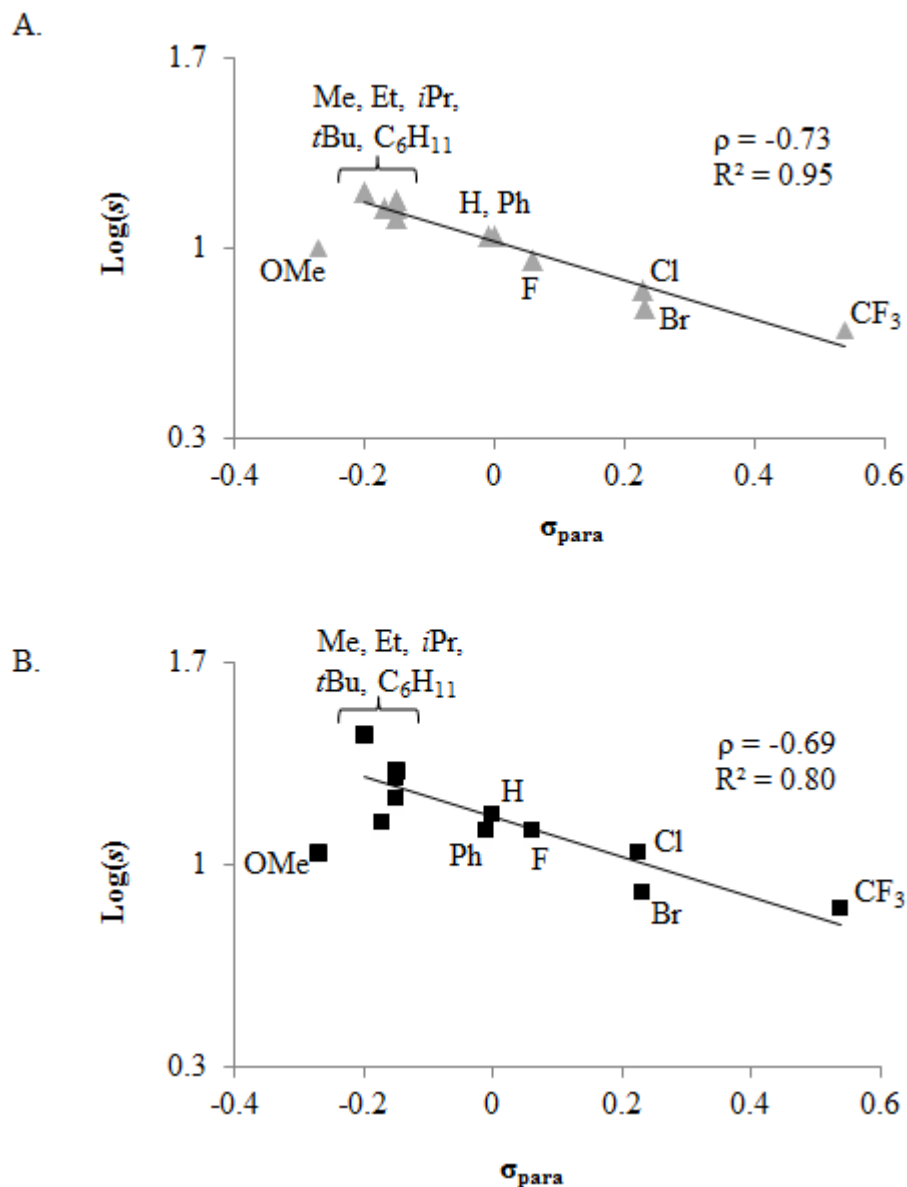


Figure 2.9 Hammett plots employing the parameter σ_{para} ¹⁸ versus the log of the selectivity factors for the kinetic resolution of alcohols (\blacktriangle) **2.15** and (\blacksquare) **2.10**. (σ_{para} values not listed in Figure 1. CF₃ = 0.54, Ph = -0.01, C₆H₁₁ = -0.15)

The sensitivity of the reaction to electronic changes on the silyl chloride can be explained by the Hammond postulate, proposed by Jacobsen in his own linear free energy relationship study.^{35,44} In our study, when electron withdrawing groups are on the silyl chloride (**2.13b-e**), the silyl chloride/catalyst intermediate is more reactive and higher in

energy versus a hydrogen substituent. Therefore the transition state would resemble the silyl chloride/catalyst intermediate with very little involvement of the attacking chiral alcohol (Figure 2.10A). With little alcohol participation in the transition state, the difference between the diastereomeric transition state energies for both enantiomers is small, therefore, the chiral catalyst intermediate cannot easily distinguish between the enantiomers, leading to low selectivity. When electron donating groups are employed, the transition state shifts to contain more product-like character with more participation of the attacking alcohol (Figure 2.10B). Therefore, there is a larger energy difference between the transition states of the two enantiomers, leading to higher selectivity.

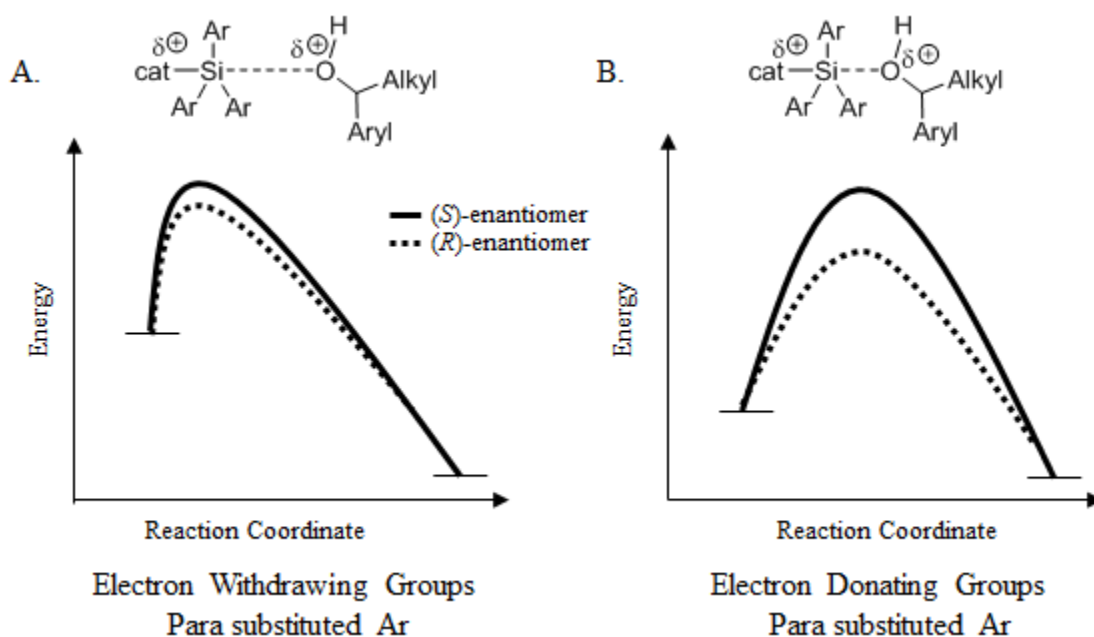


Figure 2.10 Hammond postulate diagram explaining electronic effect on selectivity factors. (A.) Early transition state with electron withdrawing substituents on silyl chloride. (B.) Late transition state with electron donating substituents on silyl chloride

Many asymmetric reactions have exhibited a relationship between enantioselectivity and steric effects on the catalyst or reactant.^{43,45} The sensitivity of the reaction presented herein to steric effects was investigated to establish if a correlation between steric effects

and selectivity exists, since selectivity factors for the kinetic resolution of **2.15** and **2.10** in Eq. 3 do increase as the alkyl substituents on **2.13** increase in size (entries 7-11 & 19-23). For example, by substituting a *t*-butyl group for a hydrogen, the selectivity factor increases from 16 to 28 when employing **7**. The log of the selectivity factors for all the silyl chlorides (**2.13a-l**) and the two alcohols were plotted against the Charton (ν) parameters (Figure 2.11 A & B). Charton values²¹⁻²³ are steric parameters that are based on the van der Waals radius of the substituent, and have been employed to show correlations between enantioselectivity and steric effects in a variety of asymmetric systems^{43,46-48}. When all of the substituents are plotted on the same graph, there is no observable correlation to the size of the substituent.

Upon removing the substituents that have a more pronounced electronic effect, and just alkyl substituents (methyl, ethyl, isopropyl, *t*-butyl, and cyclohexyl) are plotted (Figure 2.11C), there appears to be a small correlation to steric effects in the *para* position of triphenylsilyl chloride ($\psi = 0.13$ and 0.23 for **2.15** and **2.10**, respectively). The small magnitude of the slope suggests that the correlation is minor and the lack of a correlation when all of the substituents are plotted together (Figure 2.11A & 2.11B) indicate that electronic effects play a more significant role.

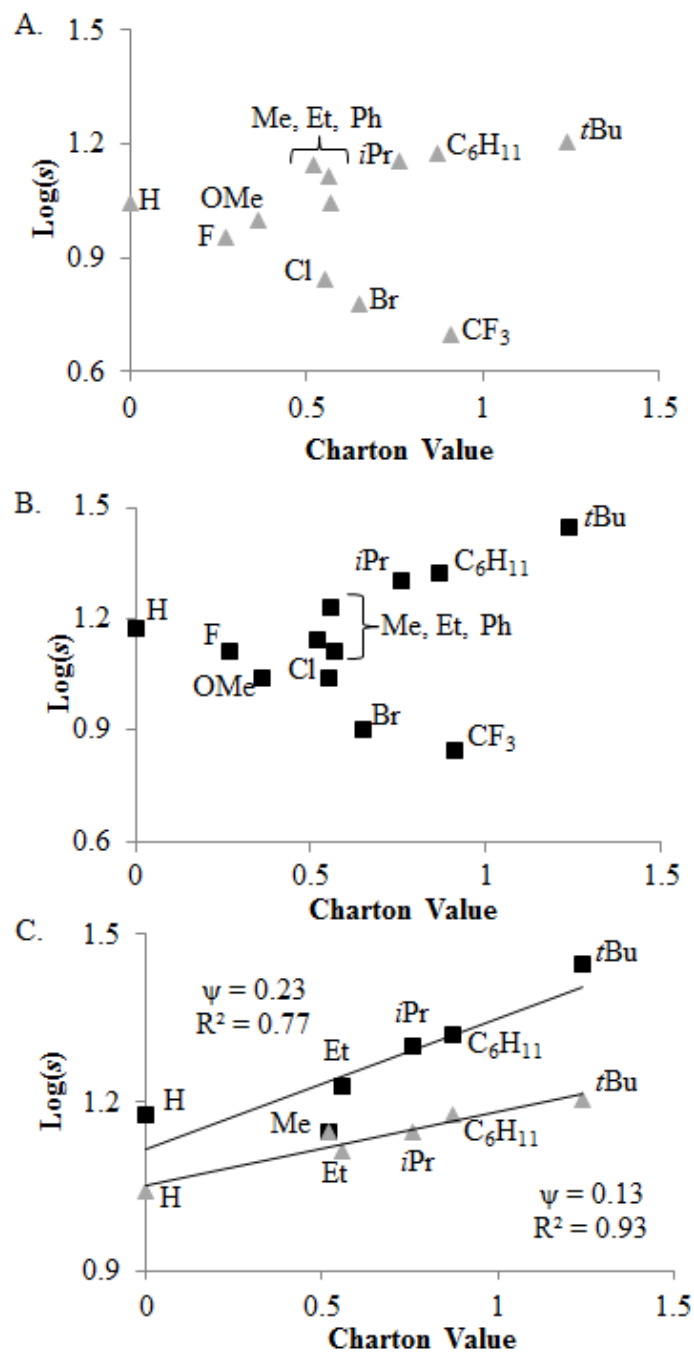


Figure 2.11 Charton analysis of alcohols (A.) **2.15** (\blacktriangle), (B.) **2.10** (\blacksquare), and (C.) selected alkyl substituted silyl chlorides (**2.13a-l**) in the silylation-based kinetic resolution

In order to determine the contribution of steric effects to the overall selectivity, a dual parameter approach was undertaken involving σ_{para} and Charton (ν) parameters. Least squares regression analysis was performed on Eq. 4 using the selectivity data for **2.15** (Table 2.6) to determine the sensitivity constants ρ and ψ , for the electronic and steric effect contributions respectively. The sensitivity constant related to electronic effects was an order of magnitude larger than the sensitivity constant for steric effects. This indicates that steric effects do not play a significant role in the selectivity of the reaction. Figure 2.12 shows the good correlation between the experimental $\log(s)$ versus that predicted by Eq. 2.7

$$\log(s) = \rho\sigma_{\text{para}} + \psi\nu \quad \text{Eq. 2.7}$$

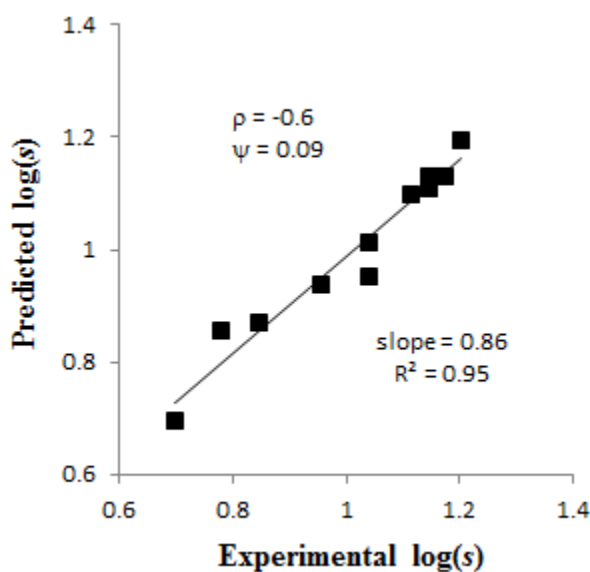
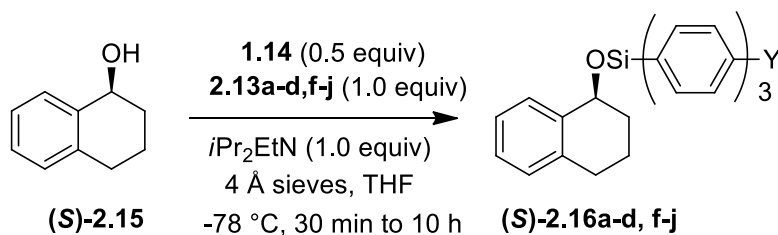


Figure 2.12 Comparison of the experimental $\log(s)$ using the selectivity data for **2.15** from Table 2.6 versus the predicted $\log(s)$ calculated from Eq. 2.6

With selectivity factors and the rate of the fast reacting enantiomer in hand for alcohol **2.15**, the rate of the slow reacting enantiomer ((*S*)-**2.15**) (Eq. 5) was calculated based on the selectivity factor definition.⁴⁹ These calculated rates are shown in Table 2.7. For three substituted silyl chlorides and **2.13a**, we also experimentally measured the rate of silylation of (*S*)-**2.16** to verify the calculated rates were correct. The experimental rates are shown in parentheses and show good correlation to the calculated rates. Electron donating groups again slow down the silylation (entries 5-9) while electron withdrawing groups speed up the silylation (entries 2-4) when compared to hydrogen in the para position (entry 1). The Hammett plot for the calculated rates is shown in Figure 2.15, again employing σ_{para} substituent constants. The calculated rates have a linear relationship, with a sensitivity constant (ρ) of 6.4, which is slightly higher than the sensitivity constant of the fast reacting enantiomer ($\rho = 5.8$). This shows that the substituted silyl chlorides essentially have the same effect on both the fast and slow reacting enantiomers (i.e. same sign of the slope therefore same transition state), with the sensitivity of the slow reacting enantiomer to the substituents being modestly higher. This suggests substituting the silyl chloride with electron donating groups improves the selectivity of the reaction by affecting the rate of the slow reacting enantiomer more than the fast reacting enantiomer since the selectivity factor is a ratio of these rates. Therefore, the slow reacting enantiomer is slightly more sensitive to changes in electronic effects.

Table 2.7 Rate of slow reacting enantiomer (*S*)-**2.15** for different *para* substituted triphenylsilyl chlorides



Entry	Y	Rate of (<i>S</i>)- 2.15 ^a (mmol/min)
1	H	1.1 (1.2)
2	Br	11 (9.5)
3	Cl	9.7
4	F	3.6
5	OMe	0.009 (0.02)
6	Me	0.05
7	Et	0.03
8	<i>i</i> Pr	0.07 (0.06)
9	<i>t</i> Bu	0.02

^aCalculated rate based on selectivity factor and fast reacting enantiomer. Rate in parenthesis was experimentally measured on a 0.3 mmol scale at 0.08 M. Each data point is a single run

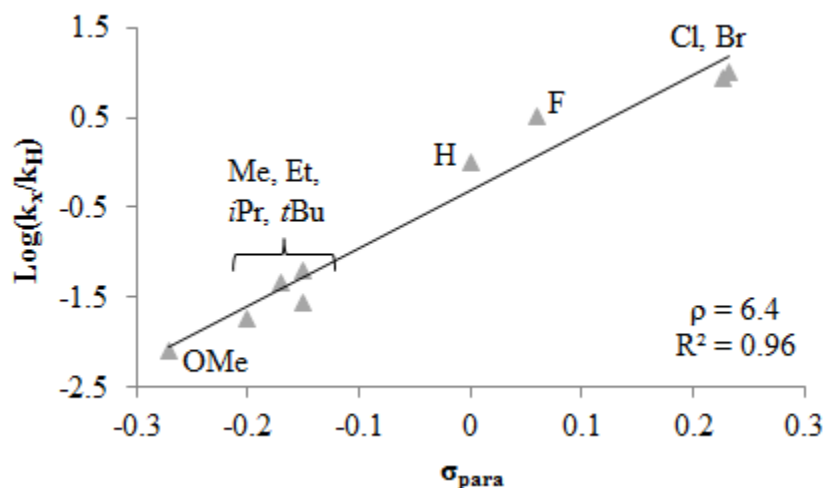


Figure 2.13 Hammett plot employing the parameter σ_{para} ¹⁸ versus the log of the calculated rates for the kinetic resolution of the slow reacting enantiomer (*S*)-2.15

2.9 Conclusions

In conclusion, we determined that mainly electronic effects around the triphenylsilyl chloride affect both the rate and the selectivity of the silylation-based kinetic resolution presented herein. Substituting the triphenylsilyl chlorides in the *para* position with a variety of electron withdrawing and donating groups allowed us to investigate the mechanism of our silylation-based kinetic resolution. The rates of the silylation reaction were measured employing the fast reacting enantiomer with different *para* substituted triphenylsilyl chlorides and a linear free energy relationship was discovered employing σ_{para} parameters. The sign and magnitude of the slope indicate that positive charge is decreasing in the transition state and there is a significant redistribution of the charge. From this data, we were able to postulate a pentavalent S_N2 like transition state with the tetramisole catalyst as the leaving group and the alcohol as the incoming nucleophile. By employing the substituted triphenylsilyl chlorides in kinetic resolutions, selectivity factors were obtained that indicate electronic effects on the silyl group play a more significant role

than steric effects in affecting the selectivity of the reaction. Ultimately, electron donating groups result in a late transition state according to the Hammond postulate, where the incoming alcohol is more involved in the rate determining step, and therefore the diastereomeric transition states between the two enantiomers have a larger energy difference as compared to electron withdrawing substituted triphenylsilyl chlorides. Ultimately, with this linear free energy relationship study we have been able to postulate the transition state and obtain some understanding on the enantioselective step, which can aid in future substrate expansion. Future studies will include employing a chiral silyl chloride for further evidence of a double inversion mechanism and an NMR and kinetic study to get a complete picture of the overall mechanism.

2.10 Experimental

General Information:

All kinetic resolution reactions and the synthesis of different silanes and silyl chlorides were carried out under a N₂ atmosphere using oven dried glassware. All solvents including THF, diethyl ether, and hexanes were dried by passing through a column of activated alumina before use and stored over molecular sieves. Pentane and carbon tetrachloride were distilled and stored over molecular sieves. CCl₄ was degassed before chlorination. Sulfuryl chloride was distilled prior to use. *n*-BuLi was titrated prior to use. All other chemicals were purchased from a commercial source and used without further purification. Molecular sieves were activated for 48 h at 130 °C in an oven. Flash column chromatography was performed with silica gel (32-63 μm). High resolution mass spectrometry (HRMS) was obtained using a magnetic sector mass spectrometer. IR data

(ν_{\max}) is reported in cm^{-1} . Rate data was collected using an FTIR spectrophotometer with a silicon probe. All enantiomeric ratios were determined by HPLC using the chiral stationary phase Chiralcel OD-H ($4.6 \times 250 \text{ mm} \times 5 \mu\text{m}$) column, and monitored using a photodiode array detector in comparison with authentic racemic materials. Melting points (mp) are uncorrected. Optical rotations were obtained using a polarimeter. Microwave assisted transformation were carried out using a chemical synthesis microwave. NMR spectra were obtained at room temperature using 400 MHz (^1H), 101 MHz (^{13}C), 80 MHz (^{29}Si), and 377 MHz (^{19}F). Chemical shifts for ^1H , ^{13}C , ^{19}F and ^{29}Si was recorded in part per million with either TMS (0.00 ppm), or CDCl_3 (7.26 ppm for ^1H or 77.0 ppm for ^{13}C) as a reference. TMS was used as a reference (0.00 ppm) to obtain ^{29}Si NMR. Data reported in ^1H NMR are as follows: Chemical shift, multiplicity (s = singlet, d = doublet, t = triplet, q = quartet, dd = doublet of doublet, dt = doublet of triplet, sept = septet, m = multiplet) and coupling constant (Hz).

General Procedure Making a *p*-Substituted Triphenyl Silane

General Procedure 1 (GP1):³⁸ (Written for a 10 mmol scale with regards to aryl bromide or iodide) *Important note regarding silane synthesis: Extreme caution should be undertaken while centrifuging and washing the lithium salts.*⁵⁰ *These salts are highly flammable and any contact with air or water should be avoided, especially when para substituted is an electron withdrawing group.* In an oven dried 250 ml three-neck round bottom flask, *p*-substituted bromo/iodo benzene (1 equiv) was dissolved using previously distilled pentane (28 mL) under nitrogen at room temperature. To the stirred solution, *n*-BuLi (1.025 equiv.) was added slowly at room temperature. After addition of *n*-BuLi, the resulting mixture formed a precipitate which was then allowed to stir for 1-1.5 h. After 1-

1.5 h, the white precipitate containing solution was carefully transferred to a test tube and centrifuged for 5 minutes (4 test tubes were used). The supernatant was carefully removed using a syringe (done under N₂ atmosphere). The white precipitate was washed 2-3 times using dry pentane and transferred to another three neck round bottom flask using approximately 22 mL of fresh pentane under nitrogen. A solution of HSiCl₃ (0.4 M in pentane, 0.3 equiv.) was added dropwise to the three neck flask (Caution: exothermic reaction). The reaction mixture was then allowed to stir for another 2 h. After 2 h, the resulting suspension (white precipitate) was centrifuged (4 test tubes were used). The supernatants were collected under nitrogen in a separate round bottom flask (liquid was collected using a syringe and transferred to another flask carefully). The remaining solid was washed 2-3 times with pentane, centrifuged and the supernatants were combined with the previously collected supernatants. Finally, the combined supernatants were quenched by chlorotrimethyl silane and the resulting solution was concentrated under vacuum to yield the crude triphenyl silane product. In most cases, purification of silane was done by recrystallization using an appropriate solvent.

General Procedure 2 (GP2): (Written for a 10 mmol scale with regards to aryl bromide or iodide) In an oven dried 250 mL three-neck round bottom flask, *p*-substituted bromo/iodo benzene (1 equiv) was dissolved using previously dried diethyl ether (30 mL) under nitrogen at room temperature. To the stirred solution, *n*-BuLi (1.025 equiv.) was added and the resulting mixture was allowed to stir for 1-1.5 h at room temp. The reaction was then cooled to -40 °C using a dry ice-acetonitrile bath. A solution of HSiCl₃ (0.4 M in ether, 0.3 equiv) was added dropwise to the three neck flask. The reaction mixture was allowed to stir for another 2 h at -40 °C, then the reaction was quenched using 10 mL of

water at -40 °C and allowed to warm to room temp. Extraction was done using diethyl ether. The organic layer was collected and dried over anhydrous sodium sulfate. The excess solvent was removed via a rotary evaporator and the crude was purified using recrystallization or a trituration method.

General Procedure Making a *p*-Substituted Triphenyl Silyl Chloride

General Procedure 3 (GP3): In an oven dried 25-50 mL three-neck round bottom flask was charged with *p*-substituted triphenylsilane and dissolved using dry degassed carbon tetrachloride (CCl₄) under a nitrogen atmosphere. The mixture was allowed to stir for 10-15 minutes. Sulfuryl chloride (SO₂Cl₂) (2-6 equiv) was then added to the flask. The resulting mixture was then allowed to reflux for 4-28 h (Conversion was monitored by disappearance of the silane peak using ¹H NMR). Hydrochloric acid generated during the reaction was removed from the reaction mixture via a bubbler. The excess solvent and other reagents were evaporated under vacuum (dry ice cooled cold trap). The final product was then recrystallized or triturated using an appropriate solvent under a N₂ atmosphere.

Synthesis of *p*-Substituted Triphenyl Silane and Silyl chlorides.

Tris(4-bromophenyl)silane (2.14b)³⁸

The product was synthesized employing 1-bromo-4-iodobenzene (98%) (2.88 g, 10 mmol) according to GP1. The final colorless solid product was obtained by recrystallization at -40 °C using pentane (1.16 g, yield = 78%). ¹H NMR: (400 MHz, CDCl₃): δ 7.54 (d, *J* = 8.0 Hz, 6 H), 7.39 (d, *J* = 8.0 Hz, 6 H), 5.39 (s, 1H). ¹³C NMR: (101 MHz, CDCl₃, 25 °C): δ 137.1, 131.5, 131.0, 125.4.

Tris(4-bromophenyl)chlorosilane (2.13b)³⁸

Chlorination was done employing **2.14b** (1.1 g, 2.21 mmol) according to GP3. Silane was dissolved using 12 mL degassed carbon tetrachloride followed by addition of sulfuryl chloride (895 μ L, 11 mmol) under nitrogen. The resulting mixture was allowed to reflux for 10-12 h. The final solid product was obtained by recrystallization using pentane at -40 °C. (430 mg, yield = 37%). ¹H NMR (400 MHz, CDCl₃): δ 7.58 (d, J = 8.2 Hz, 6H), 7.46 (d, J = 8.2 Hz, 6H). ¹³C NMR: (101 MHz, CDCl₃): δ 136.5, 131.6, 130.6, 126.4.

Tris(4-chlorophenyl)silane (2.14c)

The product was synthesized employing 1-chloro-4-iodobenzene (98%) (2.43 g, 10 mmol) according to GP1. The final product was obtained by recrystallization from pentane at -40 °C to yield colorless crystals (680 mg, yield = 62%). MP range = 74-76 °C. ¹H NMR (400 MHz, CDCl₃): δ 7.46 (d, J = 8.3 Hz, 6H), 7.38 (d, J = 8.3 Hz, 6H), 5.43 (s, 1H). ¹³C NMR (101 MHz, CDCl₃): δ 136.9, 136.8, 130.6, 128.6. ²⁹Si NMR (80 MHz, CDCl₃): δ -18.6. HRMS (EI) (M⁺) Calculated for (C₁₈H₁₃Cl₃Si⁺): 361.9846 Observed: 361.9858. IR (neat, cm⁻¹): 3042, 2142, 1578, 1481, 1380, 1080, 1013, 821, 798, 778, 740, 733, 698.

Chlorotris(4-chlorophenyl)silane (2.13c)

The product was obtained using **2.14c** (650 mg, 1.78 mmol) according to GP3. The silane was dissolved in 10 mL of degassed carbon tetrachloride under N₂. Excess sulfuryl chloride (750 μ L, 9.26 mmol) was added over the course of the reaction. The reaction took 28 h to go to completion, monitored by ¹H NMR. The crude was triturated with pentane at -78 °C using a dry ice/acetone bath to yield a colorless solid. (295 mg, yield = 40%). MP range = 58-60 °C. ¹H NMR (400 MHz, CDCl₃): δ 7.52 (d, J = 8.4 Hz, 6H), 7.41 (d, J = 8.4 Hz,

6H). ^{13}C NMR (101 MHz, CDCl_3): 137.8, 136.4, 130.3, 128.7. ^{29}Si NMR (80 MHz, CDCl_3): δ +1.1. HRMS (EI) (M^+) Calculated for $(\text{C}_{18}\text{H}_{12}\text{Cl}_4\text{Si}^+)$: 395.9456. Observed: 395.9460. IR (neat, cm^{-1}): 3041, 3020, 1915, 1575, 1482, 1381, 1186, 1119, 1083, 1014, 952, 813, 789, 735, 708.

Tris(4-fluorophenyl)silane (2.14d)⁵¹

Compound **2.14d** was synthesized using 1-fluoro-4-iodo benzene (2.22 g, 10 mmol) according to GP1. The product was obtained as an oily liquid. After leaving for almost two days in the freezer at $-20\text{ }^\circ\text{C}$, it became a colorless solid. The compound was used for the next step without any further purification. (730 mg, yield = 77%). ^1H NMR (400 MHz, CDCl_3): δ 7.56 – 7.47 (m, 6H), 7.15 – 7.05 (m, 6H), 5.46 (s, 1H). ^{13}C NMR (101 MHz, CDCl_3): δ 164.4 (d), 137.7 (d), 128.4 (d), 115.5 (d).

Chlorotris(4-fluorophenyl)silane(2.13d)⁵²

Chlorination was done using **2.14d** (1.3 g, 4.13 mmol) according to GP3. The silane was dissolved using 12 mL carbon tetrachloride under nitrogen. Sulfuryl chloride (670 μL , 9.90 mmol) was added to the reaction flask and allowed to reflux for 4 h resulting in an oil liquid after workup. Pentane was added to the oily liquid which solubilized the final product, while impurities remained undissolved. The pentane was carefully separated from impurities and transferred to another vial under nitrogen. The product was obtained through trituration at $-78\text{ }^\circ\text{C}$ using pentane to yield a colorless solid. (500 mg, yield = 35%). ^1H NMR (400 MHz, CDCl_3): δ 7.62 – 7.53 (m, 6H), 7.16 – 7.07 (m, 6H). ^{13}C NMR (101 MHz, CDCl_3): δ 164.8 (d), 137.4 (d), 128.1 (d), 115.6 (d).

Tris(4-(trifluoromethyl)phenyl)silane (2.14e)³⁹

The product was synthesized using a Grignard method on a 30 mmol scale. Magnesium metal was pre-activated by leaving it in the oven for 24 h before use. In a three-neck round bottom flask, 750 mg of magnesium metal was added and allowed to stir for 2 h under vacuum in order to activate. After 2 h, 1-iodo-4(trifluoromethyl)benzene (4.4 mL, 30 mmol) along with 4.4 mL of ether were added to the flask. The resulting mixture became a brown colored liquid which was allowed to stir for 10-15 min. After 15 minute, 25 mL of ether was added to the flask and the mixture was allowed to reflux for 30 minutes. After 30 minutes, the mixture was allowed to cool to 0 °C and HSiCl₃ (910 μ l, 9 mmol, neat) was added to the reaction mixture. The resulting mixture was allowed to stir for another 3 hr (first 30 min at 0 °C and then at room temp). After the reaction was complete, the mixture was poured into a beaker containing dry ice and dilute HCl. The reaction mixture was extracted with ether and dried over anhydrous sodium sulfate. Excess ether was removed under vacuum. A dark orange-brown colored oil was obtained. The final product was obtained by vacuum distillation at 175-178 °C and 3 mm Hg. A dark yellow liquid was obtained which was left under vacuum to yield a colorless solid as the final product. (1.1 g, yield = 26%). MP range = 74-76 °C. ¹H NMR (400 MHz, CDCl₃): δ 7.68 (s, 12H), 5.58 (s, 1H). ¹³C NMR (101 MHz, CDCl₃): δ 136.2, 136.0, 132.5 (q, J_{CF} = 33 Hz), 125 (q, J = 3.8 Hz), 123.9 (q, J_{CF} = 273 Hz). ¹⁹F NMR (377 MHz, CDCl₃): δ -111.9. ²⁹Si NMR (80 MHz): -18.7 HRMS (EI) (M-H)⁺ Calculated for (C₂₁H₁₂F₉Si)⁺: 463.0559 Observed: 463.0574. IR (neat, cm⁻¹): 2929, 2155, 1931, 1610, 1505, 1393, 1322, 1273, 1161, 1114, 1017, 844, 830, 793, 771, 722, 700.

Chlorotris(4-(trifluoromethyl)phenyl)silane (2.13e)

Chlorination was done employing **2.14e** (820 mg, 1.77 mmol) according to GP3. The silane was dissolved in 8 mL of carbon tetrachloride followed by addition of sulfuryl chloride (350 μ L, 4.32 mmol). After 4 h, only 20% conversion was observed from ^1H NMR. Excess sulfuryl chloride was added over the course of the reaction, but no further improvement in conversion was observed after 48 h. Finally, the reaction mixture was transferred to a microwave vessel equipped with a stir bar under an argon atmosphere. The reaction vessel was then purged with argon and sealed with a septa. The mixture was then microwaved for 40 minutes at 120 $^{\circ}\text{C}$ employing 70 W. The mixture was allowed to cool to ambient temperature and transferred to a 4 dram vial under an argon atmosphere. The crude was concentrated under vacuum. The final product was a yellowish solid (492 mg, yield = 56%), which was used directly without any purification for the kinetic resolution. No characterization was reported due to moisture sensitivity.

Tris(4-methoxyphenyl)silane (2.14f)⁵¹

The product was synthesized using 4-iodo anisole (98%) (2.34 g, 10 mmol) according to GP1. A colorless solid was obtained as the crude product. Silane was further purified by carefully washing crude 2 times with distilled pentane. (780 mg, yield = 74%). ^1H NMR (400 MHz, CDCl_3) δ 7.53 (d, J = 8.6 Hz, 6H), 6.96 (d, J = 8.4 Hz, 6H), 5.46 (s, 1H), 3.85 (s, 9H). ^{13}C NMR (101 MHz, CDCl_3): δ 160.9, 137.2, 124.8, 113.8, 55.0.

Chlorotris(4-methoxyphenyl)silane (2.13f)

Chlorination was done using **2.14f** (300 mg, 0.86 mmol) according to GP3. The silane was dissolved in 6 mL of carbon tetrachloride followed by addition of sulfuryl chloride (139

μL , 1.72 mmol). Complete conversion was achieved in 7-8 h. An oily liquid was obtained which became a light yellow solid after scratching for almost an hour under nitrogen. This solid was carefully washed with pentane to obtain the final product. (200 mg, yield = 60%). MP range = 67-69 °C ^1H NMR (400 MHz, CDCl_3): δ 7.57 (d, J = 8.7 Hz, 6H), 6.95 (d, J = 8.7 Hz, 6H), 3.84 (s, 9H). ^{13}C NMR (101 MHz, CDCl_3): δ 161.5, 136.8, 124.4, 113.8, 55.1. ^{29}Si NMR (80 MHz, CDCl_3): +1.2. HRMS (EI) (M^+) Calculated for ($\text{C}_{21}\text{H}_{21}\text{ClO}_3\text{Si}^+$): 384.0943. Observed: 384.0952. IR (neat, cm^{-1}): 3020, 2919, 2841, 1591, 1563, 1503, 1457, 1442, 1400, 1276, 1248, 1181, 1116, 1107, 1022, 817, 797, 659.

Tri-*p*-tolylsilane (2.15g)⁵¹

The product was synthesized using 4-iodotoluene (2.18 g, 10 mmol) according to GP1. A colorless solid was formed which was further recrystallized using pentane at -40 °C. (770 mg, yield = 85%). ^1H NMR (400 MHz, CDCl_3): δ 7.47 (d, J = 7.8 Hz, 6H), 7.18 (d, J = 7.6 Hz, 7H), 5.43 (s, 1H), 2.35 (s, 9H). ^{13}C NMR (101 MHz, CDCl_3): δ 139.6, 135.8, 130.1, 128.8, 21.5.

Chlorotri-*p*-tolylsilane (2.13g)

Chlorination was done using tri-*p*-tolylsilane (1.03 g, 3.4 mmol) according to GP3. The silane was dissolved in 17 mL of carbon tetrachloride followed by addition of sulfuryl chloride (550 μL , 6.8 mmol). It took 7-8 h to achieve complete conversion. The final product was obtained through recrystallization from hexanes at -40 °C to obtain a colorless solid. (590 mg, yield = 51%). MP range = 110 – 112 °C. ^1H NMR (400 MHz, CDCl_3): δ 7.52 (d, J = 7.6 Hz, 6H), 7.22 (d, J = 7.6 Hz, 6H), 2.38 (s, 9H). ^{13}C NMR (101 MHz, CDCl_3): δ 140.7, 135.2, 129.7, 128.9, 21.6. ^{29}Si NMR (80 MHz, CDCl_3): +1.8. HRMS (EI)

(M⁺) Calculated for (C₂₁H₂₁ClSi⁺): 336.1095 Observed: 336.1096. IR (neat, cm⁻¹): 3019, 2921, 2862, 1924, 1598, 1501, 1393, 1312, 1190, 1114, 1021, 712.

Tris(4-ethylphenyl)silane (2.14h)

Compound **2.14h** was synthesized using 1-ethyl-4-iodobenzene (98%) (1.48 mL, 10 mmol) according to GP2. After reaction completion, the solvent was removed under vacuum. The crude product was obtained as an oil. Further purification was done using column chromatography to yield an oil as the final product. (800 mg, yield = 77%). ¹H NMR (400 MHz, CDCl₃): δ 7.67 (d, *J* = 7.9 Hz, 6H), 7.36 (d, *J* = 7.7 Hz, 6H), 5.60 (s, 1H), 2.80 (q, *J* = 7.6 Hz, 6H), 1.39 (t, *J* = 7.6 Hz, 9H). ¹³C NMR (101 MHz, CDCl₃): δ 145.8, 135.9, 130.5, 127.6, 28.9, 15.4. ²⁹Si NMR (80 MHz, CDCl₃): -18.9. HRMS (EI) (M⁺) Calculated for (C₂₄H₂₈Si⁺): 344.1954 Observed: 344.1960. IR (neat, cm⁻¹): 3012, 2964, 2930, 2116, 1600, 1456, 1398, 1111, 1062, 967, 801, 772.

Chlorotris(4-ethylphenyl)silane (2.13h)

Chlorination was done using tris(4-ethylphenyl)silane (782 mg, 2.27 mmol) according to GP3. Excess sulfuryl chloride (550 μL, 6.78 mmol) was used to achieve full conversion in 4 h using 10 mL of carbon tetrachloride. The crude oily liquid was further purified by trituration with hexanes at -40 °C under a N₂ atmosphere which resulted in a yellowish solid. (455 mg, yield = 53%). MP range = 54-56 °C. ¹H NMR (400 MHz, CDCl₃): δ 7.56 (d, *J* = 8.1 Hz, 6H), 7.24 (d, *J* = 8.2 Hz, 6H), 2.67 (q, *J* = 7.6 Hz, 6H), 1.24 (t, *J* = 7.6 Hz, 9H). ¹³C NMR (101 MHz, CDCl₃): δ 146.9, 135.3, 130.0, 127.7, 28.9, 15.3. ²⁹Si NMR (80 MHz, CDCl₃): +1.6. HRMS (EI) (M⁺) Calculated for (C₂₄H₂₇ClSi⁺): 378.1565 Observed:

378.1573. IR (neat, cm^{-1}): 3012, 2967, 2933, 2873, 1600, 1456, 1397, 1272, 1190, 1115, 1062, 1020, 968, 796, 782.

Tris(4-isopropylphenyl)silane (2.14i)

Compound **2.14i** was synthesized using 4-bromo-isopropyl benzene(95%) (1.63 mL, 10 mmol) according to GP2. A colorless solid was obtained and purified further by trituration at $-40\text{ }^{\circ}\text{C}$ with hexanes under a N_2 atmosphere to get a colorless powder. (770 mg, yield = 66%). MP range = $58\text{--}60\text{ }^{\circ}\text{C}$ ^1H NMR (400 MHz, CDCl_3): δ 7.51 (d, $J = 8.0\text{ Hz}$, 6H), 7.23 (d, $J = 7.9\text{ Hz}$, 6H), 5.41 (s, 1H), 2.90 (m, 3H), 1.25 (d, $J = 6.9\text{ Hz}$, 18H). ^{13}C NMR (101 MHz, CDCl_3): δ 150.4, 135.9, 130.7, 126.2, 34.1, 23.8. ^{29}Si NMR (80 MHz, CDCl_3): -18.8. HRMS (EI) (M^+) Calculated for ($\text{C}_{27}\text{H}_{34}\text{Si}^+$): 386.2424 Observed: 386.2428. IR (neat, cm^{-1}): 2961, 2928, 2110, 1924, 1598, 1458, 1392, 1297, 1265, 1117, 1094, 1049, 1019, 822, 794, 760, 725.

Chlorotris(4-isopropylphenyl)silane (2.13i)⁵³

Chlorination was done by using tris(4-isopropylphenyl)silane (875 mg, 2.26 mmol) according to GP3. The silane was dissolved in 11 mL of carbon tetrachloride followed by addition of sulfuryl chloride (550 μL , 6.78 mmol) under a N_2 atmosphere. The resulting mixture was allowed to reflux for 4 h to achieve complete chlorination. After the reaction was complete, the excess reagents were removed under vacuum. The crude product was purified by trituration with hexanes at $-40\text{ }^{\circ}\text{C}$ under N_2 . A colorless solid product was obtained. (747 mg, yield = 78%). ^1H NMR (400 MHz, CDCl_3): δ 7.57 (d, $J = 8.1\text{ Hz}$, 6H), 7.27 (d, $J = 7.4\text{ Hz}$, 6H), 2.92 (septet, 3H), 1.26 (d, $J = 6.9\text{ Hz}$, 18H). ^{13}C NMR (101 MHz, CDCl_3): δ 151.4, 135.3, 130.2, 126.2, 34.2, 23.8.

Tris (4-(*tert*-butyl) phenyl)silane (2.14j)

Compound 2.14j was synthesized using 1-bromo-4-*tert*-butylbenzene (98%) (1.76 mL, 10 mmol) according to GP2. A colorless solid was obtained, after washing the crude solid with hexanes. (1.27 g, yield = 99%). MP range = 169-171 °C. ¹H NMR (400 MHz, CDCl₃): δ 7.54 (d, *J* = 8.2 Hz, 6H), 7.40 (d, *J* = 8.2 Hz, 6H), 5.42 (s, 1H), 1.32 (s, 27H). ¹³C NMR (101 MHz, CDCl₃): δ 152.6, 135.7, 130.2, 124.9, 34.7, 31.2. ²⁹Si NMR (80 MHz, CDCl₃): -18.9. HRMS (EI) (M⁺) Calculated for (C₃₀H₄₀Si⁺): 428.2893 Observed: 428.2894. IR (neat, cm⁻¹): 2960, 2868, 2108, 1596, 1463, 1387, 1362, 1267, 1137, 1085, 822, 788, 724.

Tris(4-(*tert*-butyl)phenyl)chlorosilane (2.13j)⁵³

Chlorination was done using tris(4-(*tert*-butyl)phenyl)silane (1.26 g, 2.93 mmol) according to GP3. The silane was dissolved in 12 mL of carbon tetrachloride followed by addition of sulfuryl chloride (710 μL, 8.79 mmol). The crude solid was purified by washing 2-3 times with hexanes to obtain a colorless solid. (850 mg, yield = 63%). ¹H NMR (400 MHz, CDCl₃): δ 7.59 (d, *J* = 8.3 Hz, 6H), 7.43 (d, *J* = 8.3 Hz, 6H), 1.32 (s, 27H). ¹³C NMR (101 MHz, CDCl₃): δ 153.6, 135.1, 129.8, 125.0, 34.8, 31.2.

Tris(4-cyclohexylphenyl)silane (2.14k)

Compound 2.14k was synthesized using 1-bromo-4-cyclohexylbenzene (98%) (1.89 mL, 10 mmol) according to GP2. The crude solid was recrystallized from pentane at -40 °C to yield a colorless solid (1.30 g, yield = 86%). MP range = 79-81 °C. ¹H NMR (400 MHz, CDCl₃): 7.52 (d, *J* = 8.0 Hz, 6H), 7.22 (d, *J* = 8.0 Hz, 6H), 5.41 (s, 1H), 2.53-2.47 (m, 3H), 1.91-1.82 (m, 12H), 1.77-1.73 (m, 3H), 1.45-1.34 (m, 12H), 1.31-1.24 (m, 3H). ¹³C NMR (101 MHz, CDCl₃): δ 149.6, 135.8, 130.7, 126.6, 44.6, 34.3, 26.9, 26.1. ²⁹Si NMR (80

MHz, CDCl₃): -18.8. HRMS (EI) (M⁺) Calculated for (C₃₆H₄₆Si⁺): 506.3363 Observed: 506.3352. IR (neat, cm⁻¹): 3011, 2922, 2850, 2122, 1598, 1447, 1400, 1263, 1111, 998, 891, 866, 772, 727, 687, 671.

Chlorotris(4-cyclohexylphenyl)silane (2.13k)

Chlorination was done using tris(4-cyclohexylphenyl)silane (1.26 g, 2.49 mmol) according to GP3. The silane was dissolved in 6 mL of carbon tetrachloride followed by the addition of sulfuryl chloride (602 μ L, 7.47 mmol). Product formation was complete in 4 h. The crude oil was triturated with pentane at -78 °C under N₂ resulting in a colorless solid. (500 mg, yield = 37%). MP range = 123-124 °C. ¹H NMR (400 MHz, CDCl₃): δ 7.57 (d, *J* = 8.2 Hz, 6H), 7.24 (d, *J* = 7.9 Hz, 6H), 2.53-2.51 (m, 3H), 1.90-1.83 (m, 12H), 1.77-1.73(m, 3H), 1.47-1.34(m, 12H), 1.30-1.23(m, 3H). ¹³C NMR (101 MHz, CDCl₃): δ 150.6, 135.3, 130.2, 126.6, 44.6, 34.2, 26.8, 26.1. ²⁹Si NMR (80 MHz, CDCl₃): +1.5. HRMS (EI) (M⁺) Calculated for (C₃₆H₄₅ClSi⁺): 540.2973. Observed: 540.2971. IR (neat, cm⁻¹): 3014, 2923, 2850, 1599, 1447, 1400, 1263, 1116, 998, 817, 673.

Tris([1,1'-biphenyl]-4-yl)silane (2.14l)

Compound **2.14l** was synthesized using 4-iodobiphenyl (97%) (2.89 g, mmol) according to GP2. Addition of SiHCl₃ after lithiation was done at -78 °C instead of -40 °C and allowed to stir for 2 h. The crude white solid was carefully filtered and used without further purification. (1.35 g, yield = 92 %). MP range = 192-193 °C ¹H NMR (400 MHz, CDCl₃): δ 7.73 (d, *J* = 8.3 Hz, 6H), 7.67 – 7.61 (m, 12H), 7.46 (t, *J* = 7.3 Hz, 6H), 7.37 (t, *J* = 7.4 Hz, 3H), 5.60 (s, 1H). ¹³C NMR (101 MHz, CDCl₃): δ 142.6, 140.9, 136.3, 132.0, 128.8, 127.6, 127.2, 126.9. ²⁹Si NMR (80 MHz, CDCl₃): -18.4. HRMS (EI) (M⁺) Calculated for

(C₃₆H₂₈Si⁺): 488.1954 Observed: 488.1959. IR (neat, cm⁻¹): 3011, 2106, 1595, 1542, 1481, 1384, 1182, 1115, 1007, 845, 835, 763, 755, 660.

Tris([1,1'- biphenyl]-4-yl)chlorosilane (2.13l)

Chlorination was done using tris([1,1'-biphenyl]4-yl)silane (**2.14l**) (1.43 g ,2.92 mmol) according to GP3. Carbon tetrachloride (14 mL) was added and the solution was heated in order to dissolve the compound. Sulfuryl chloride (708 μ L, 8.76 mmol) was added and refluxed for 4 h. The crude solid was washed with hexanes 2-3 times resulting in a light pink product. (800 mg, yield = 52%). MP range = 215-217 °C. ¹H NMR (400 MHz, CDCl₃): δ 7.79 (d, *J* = 8.3 Hz, 6H), 7.68 (d, *J* = 8.3 Hz, 6H), 7.63 (d, *J* = 8.2 Hz, 6H), 7.47 (t, *J* = 7.2 Hz, 6H), 7.40-7.36 (m, 3H). ¹³C NMR (101 MHz, CDCl₃): δ 143.5, 140.6, 135.7, 131.5, 128.9, 127.8, 127.2, 126.9. HRMS (EI) (M⁺) Calculated for (C₃₆H₂₇ClSi⁺): 522.1565 Observed: 522.1580.

General Procedure of Rate Study Using In Situ React IR: All reactions were carried out at 0.08 M concentration with regard to the alcohol. A three-neck 50 mL Schlenk tube with a 24/40 ground glass joint for probe insertion with two side arms was used as a reaction vessel. A probe was inserted into the Schlenk tube equipped with a stir bar under N₂ atmosphere. After calibrating the instrument an air background was taken first. THF (2.10 mL) was added to the Schlenk tube and the solvent was allowed to cool to -78 °C for approximately 20 minutes using a dry ice/acetone bath. The solvent background was recorded for each experiment at -78 °C, then IR data collection was started. A solution of (**R**)-**2.15** or (**S**)-**2.15** (55.3 mg), **1.14** (38 mg) and Hünig's base (64 μ L) was prepared in a 1 mL volumetric flask. From the above prepared solution, 810 μ L was carefully added to

the Schlenk tube via a syringe. The resulting mixture was allowed to stir for 10-15 minutes. Meanwhile a solution of **2.13** (0.357 M) was prepared using a volumetric flask, and 840 μL of this was added to the reaction mixture at $-78\text{ }^{\circ}\text{C}$. The time of the silyl chloride addition was recorded for reference and IR data was collected for 30 min -10 h. Rapid collect was used for data collection in the case of electron withdrawing *p*-substituted triphenylsilyl chloride rate experiments. The absorbance was obtained using ConcIRT. Reaction conversion was obtained at different time points by taking reaction aliquots at these time points, quenching them, and determining the conversion by ^1H NMR. The geminal proton of the product and the starting material were used for integration. The relationship between concentration and absorbance was constructed by calculating the product concentration from the NMR conversions and plotting it against the absorbance at each of those time points. Once the Beer's Law relationship was determined, the concentration at each data point was calculated from the absorbance and plotted against time to determine the rate. Initial rate was determined by using the data up to 10% conversion. The accuracy of the peak obtained from ConcIRT was confirmed by comparing the NMR conversion with the calculated conversion from the absorbance.

General Procedure for the Silylation-Based Kinetic Resolution of Secondary Alcohols and Desilylation of the Isolated Products.

An oven dried 1 dram vial was charged with 4 Å molecular sieves (10-15 mg) and a Teflon coated stir bar. The racemic alcohol (**2.10** or **2.15**) (0.22 mmol), catalyst **1.14** (11.2 mg, 0.055 mmol) and *N,N*-diisopropylethylamine (Hünig's Base) (23 μL , 0.132 mmol) were added to a vial and then quickly sealed under a nitrogen atmosphere. Dry THF (1.0 mL) was added and the reaction mixture was allowed to stir at $-78\text{ }^{\circ}\text{C}$ for 15-20 minutes.

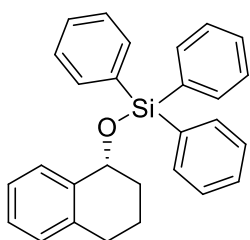
Meanwhile a solution of (*p*Y-Ph)₃SiCl (0.357 M) was prepared using a volumetric flask (under N₂). The solution of (*p*Y-Ph)₃SiCl **2.13** (370 μL, 0.6 mmol) was added to the reaction vial and the resulting mixture was allowed to react for the specified amount of time at -78 °C. The reaction mixture was then quenched using 300 μL of MeOH at -78 °C. The mixture was allowed to warm to room temperature followed by addition of 1.0 mL of saturated aqueous NH₄Cl. The reaction mixture was transferred to a 4 dram vial and extracted using diethyl ether (3 x 2 mL). The ether layer was then passed through a pad of silica gel. After filtration, it was concentrated and the crude mixture was purified using silica gel chromatography (100% CH₂Cl₂ followed by 2% MeOH in CH₂Cl₂). The analysis of the unreacted recovered alcohol was done by a chiral HPLC using a hexanes/*i*-PrOH solvent system. **Desilylation:** The silylated product was transferred to a 4 dram vial with a stir bar and dissolved in 3 mL of THF. The solution was treated with a 1M solution of TBAF in THF (500 μL - 1.0 mL) and allowed to stir for 3-10 h at room temperature (conversion was monitored by TLC). The reaction was quenched with brine and extracted with diethyl ether. The crude mixture was purified via silica gel column chromatography (CH₂Cl₂ to 2% MeOH in CH₂Cl₂). HPLC analysis was done for the desilylated product (alcohol). The absolute stereochemistry was confirmed by comparing the HPLC data with previously published data.¹

HPLC conditions for 1,2,3,4-tetrahydronaphthalen-1-ol (2.15)¹: Chiralpack OD-H column was used with 4% *i*PrOH in hexanes. Flow rate was 0.5 mL/min, 25 °C. *t*_R 25.2 min for (*S*)-enantiomer and *t*_R 28.7 min for (*R*)-enantiomer.

HPLC conditions for 4-Chromanol (2.10)¹: Chiralpack OD-H column was used with 2% *i*PrOH in hexanes. Flow rate was 1.3 mL/min, 25 °C. *t*_R 28.6 min for (*S*)-enantiomer and *t*_R 37.3 min for (*R*)-enantiomer.

1,2,3,4-tetrahydronaphthalen-1-ol (2.15): ¹H NMR (400 MHz, CDCl₃) δ ppm 7.44-7.23 (m, 1 H), 7.22-7.20 (m, 2 H), 7.12-7.10 (m, 1H) 4.79 (t, 5.0 Hz, 1H), 2.87-2.81 (m, 1 H), 2.77-2.69 (m, 1H), 2.01-1.88 (m, 3 H), 1.83-1.75(m, 2H). ¹³C NMR (101 MHz, CDCl₃) δ ppm 138.7, 137.1, 129.0, 128.6, 127.5, 126.1, 68.1, 32.2, 29.2, 18.7.

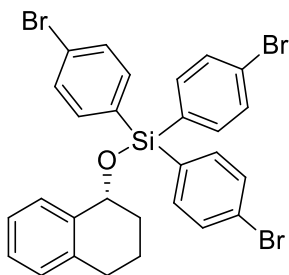
Triphenyl((1,2,3,4-tetrahydronaphthalen-1-yl)oxy)silane (2.16a)¹:



2.16a

33.5 mg (yield = 37%), White solid. ¹H NMR (400 MHz, CDCl₃): δ 7.68 (d, *J* = 6.0 Hz, 6H), 7.47-7.36 (m, 9H), 7.28(d, *J* = 6.8 Hz, 1H), 7.18-7.06 (m, 3H), 4.97 (t, *J* = 5.6 Hz, 1H), 2.88-2.81 (m, 1H), 2.72-2.64 (m, 1H), 2.10-2.03 (m, 1H), 1.96-1.82 (m, 2H), 1.72-1.63 (m, 1H). ¹³C NMR (101 MHz, CDCl₃): δ 138.9, 137.0, 135.6, 134.8, 129.9, 128.7, 128.6, 127.8, 127.1, 125.7, 70.2, 32.5, 29.0, 19.2.

(*R*)-tris(4-bromophenyl)((1,2,3,4-tetrahydronaphthalen-1-yl)oxy)silane (2.16b):

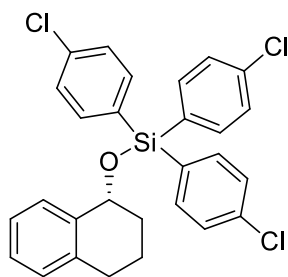


2.16b

55 mg (yield = 39%), white solid. MP range: 88-89 °C. ¹H NMR (400 MHz, CDCl₃) δ 7.54 (d, *J* = 8.2 Hz, 6H), 7.46 (d, *J* = 8.1 Hz, 6H), 7.21 – 7.14 (m, 2H), 7.13 – 7.06 (m, 2H), 4.94 (t, *J* = 5.0 Hz, 1H), 2.88-2.81 (m, 1H), 2.74-2.66 (m, 1H), 2.14 – 2.01 (m, 1H), 1.97 – 1.79 (m, 2H), 1.77 – 1.64 (m, 1H). ¹³C NMR (101 MHz, CDCl₃): δ 138.1, 137.1, 136.9, 132.6, 131.3, 128.9, 128.5, 127.5, 125.7, 125.5, 70.6, 32.5, 28.9, 18.9. Optical Rotation [α]_D²⁵ = + 19.0 (*c* = 0.75, CHCl₃). HRMS (EI) (*M*⁺) Calculated

for (C₂₈H₂₃Br₃OSi⁺): 641.9043. Observed: 641.9034. IR (neat, cm⁻¹): 3069, 2937, 2866, 1739, 1572, 1550, 1478, 1454, 1377, 1350, 1208, 1185, 1115, 1066, 1009, 988, 906, 807, 757.

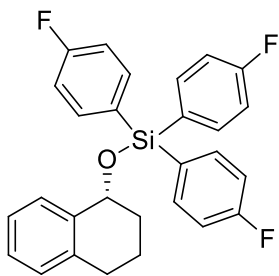
(R)-tris(4-chlorophenyl)((1,2,3,4-tetrahydronaphthalen-1-yl)oxy)silane (2.16c):



2.16c

34.9 mg (yield = 31%), colorless oil with minor amounts of tris(4-chlorophenyl)silanol present. ¹H NMR (400 MHz, CDCl₃) : δ 7.52 (d, *J* = 8.4 Hz, 6H), 7.38 (d, *J* = 8.4 Hz, 6H), 7.21 – 7.13 (m, 2H), 7.13 – 7.06 (m, 2H), 4.94 (m, 1H), 2.88-2.80 (m, 1H), 2.73-2.65(m, 1H), 2.12-2.02 (m, 1H), 1.95 – 1.78 (m, 2H), 1.75 – 1.65 (m, 1H). ¹³C NMR (101 MHz, CDCl₃) : δ 138.2, 137.1, 136.8, 136.7, 132.3, 128.9, 128.6, 128.4, 127.4, 125.7, 70.6, 32.5, 28.9, 18.9. Optical Rotation [α]_D²⁵ = + 22.6. (*c* = 0.88, CHCl₃). HRMS (EI) (M⁺) Calculated for (C₂₈H₂₃Cl₃OSi⁺): 508.0578. Observed: 508.0558. IR (neat, cm⁻¹): 3072, 2936, 1913, 1578, 1556, 1482, 1455, 1381, 1349, 1257, 1184, 1118, 1082, 1014, 989, 877, 812, 711.

(R)-tris(4-fluorophenyl)((1,2,3,4-tetrahydronaphthalen-1-yl)oxy)silane (2.16d):



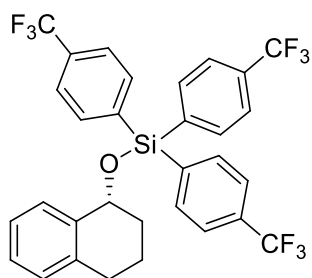
2.16d

38.0 mg (yield = 38%), colorless oil. ¹H NMR (400 MHz, CDCl₃) : δ 7.64 – 7.59 (m, 6H), 7.21 – 7.17 (m, 2H), 7.14 – 7.08 (m, 8H), 4.96 (t, *J* = 5.6 Hz, 1H), 2.89 – 2.82 (m, 1H), 2.74 - 2.67 (m, 1H), 2.14 - 2.04 (m, 1H), 1.96 – 1.81 (m, 2H), 1.76 – 1.66 (m, 1H). ¹³C NMR (101 MHz, CDCl₃): δ 165.6-163.1(d), 138.4, 137.6-137.5 (d), 137.1, 130.0(d), 128.9, 128.6, 127.4, 125.7, 115.4-115.2 (d), 70.4, 32.5, 28.9, 19.0. Optical Rotation [α]_D²⁵ = + 18.0 (*c* = 0.91, CHCl₃). HRMS (EI) (M⁺) Calculated for

(C₂₈H₂₃F₃OSi⁺): 460.1464. Observed: 460.1454. IR (neat, cm⁻¹): 3025, 2937, 1910, 1588, 1498, 1388, 1350, 1225, 1161, 1110, 1070, 1014, 989, 878, 755, 738, 715.

(R)-((1,2,3,4-tetrahydronaphthalen-1-yl)oxy)tris(4-(trifluoromethyl)phenyl)silane

(2.16e):

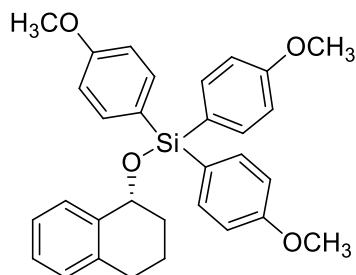


2.16e

33.1 mg (yield = 25%), colorless oil with minor amounts of tris(4-(trifluoromethyl)phenyl)silanol present. ¹H NMR (400 MHz, CDCl₃) : δ 7.73 (d, *J* = 8.2 Hz, 6H), 7.66 (d, *J* = 8.2 Hz, 6H), 7.21-7.17 (m, 1H), 7.14-7.08 (m, 3H), 5.00 (t, *J* = 5.1, 1H), 2.88-2.81 (m, 1H), 2.75-2.67 (m, 1H), 2.16-2.06 (m, 1H), 1.97-

1.83 (m, 2 H), 1.78-1.69 (m, 1H). ¹³C NMR (101 MHz, CDCl₃) : δ 138.1, 137.7, 137.2, 135.7, 132.5 (q, *J*_{CF} = 32.4 Hz), 129.1, 128.6, 127.7, 125.8, 124.8 (q, *J*_{CF} = 3.8 Hz), 124.0 (q, *J* = 272.5 Hz), 71.1, 32.5, 28.8, 18.8. ¹⁹F NMR (377 MHz, CDCl₃) : δ -63.1. Optical Rotation [α]_D²⁵ = + 9.7 (*c* = 0.67, CHCl₃). HRMS (EI) (M⁺) Calculated for:(C₃₁H₂₃F₉OSi⁺): 610.1368. Observed: 610.1372. IR (neat, cm⁻¹): 3031, 2939, 1610, 1393, 1318, 1164, 1121, 1017, 990, 829, 739, 704.

(R)-tris(4-methoxyphenyl)((1,2,3,4-tetrahydronaphthalen-1-yl)oxy)silane (2.16f):



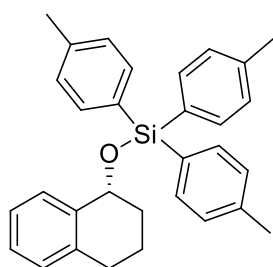
2.16f

21.3 mg (yield = 20%), colorless oil. ¹H NMR (400 MHz, CDCl₃) δ ¹H 7.58 (d, *J* = 8.7 Hz, 6H), 7.27 (m, 1H), 7.17 – 7.11 (m, 2H), 7.09 – 7.05 (m, 1H), 6.93(d, *J* = 8.7 Hz, 6H), 4.94 (t, *J* = 6.0 Hz, 1H), 3.83 (s, 9H), 2.87-2.80 (m, 1H), 2.71-2.64 (m, 1H), 2.09 – 2.01 (m, 1H), 1.92 – 1.82 (m, 2H),

1.71 – 1.62 (m, 1H). ¹³C NMR (101 MHz, CDCl₃) δ 160.9, 139.3, 137.1, 137.0, 128.7,

128.6, 127.0, 126.4, 125.6, 113.5, 69.9, 55.0, 32.6, 29.1, 19.3. Optical Rotation $[\alpha]^{25}_D = +13.1$ ($c = 0.95$, CHCl_3). HRMS (EI) (M^+) Calculated for ($\text{C}_{31}\text{H}_{32}\text{O}_4\text{Si}^+$): 496.2064. Observed: 496.2053. IR (neat, cm^{-1}): 3062, 2934, 2836, 1903, 1592, 1563, 1501, 1456, 1441, 1277, 1246, 1179, 1070, 1028, 987, 909, 814, 798, 733.

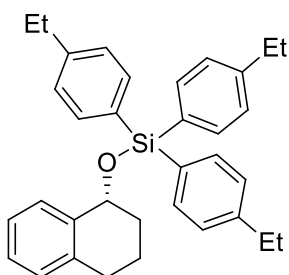
(R)-((1,2,3,4-tetrahydronaphthalen-1-yl)oxy)tri-*p*-tolylsilane (2.16g):



2.16g

43.4 mg (yield = 44%), colorless oil. ^1H NMR (400 MHz, CDCl_3) δ 7.55 (d, $J = 8.0$ Hz, 6H), 7.30 (d, $J = 8.5$ Hz, 1H), 7.18 (d, $J = 8.0$ Hz, 6H), 7.14 – 7.09 (m, 2H), 7.08 – 7.04 (m, 1H), 4.93 (t, $J = 5.6$ Hz, 1H), 2.85–2.79 (m, 1H), 2.69–2.62 (m, 1H), 2.35 (s, 9H), 2.08–1.99 (m, 1H), 1.92–1.82 (m, 2H), 1.69–1.60 (m, 1H). ^{13}C NMR (101 MHz, CDCl_3) δ 139.7, 139.3, 137.0, 135.6, 135.4, 131.6, 128.8, 128.6, 126.9, 125.6, 70.0, 32.6, 29.1, 21.6, 19.3. Optical Rotation $[\alpha]^{25}_D = +16.2$ ($c = 0.98$, CHCl_3). HRMS (EI) (M^+) Calculated for: 448.2216 ($\text{C}_{31}\text{H}_{32}\text{OSi}^+$). Observed: 448.2217. IR (neat, cm^{-1}): 3066, 2936, 2864, 1920, 1739, 1599, 1501, 1451, 1393, 1350, 1261, 1208, 1188, 1111, 1071, 1016, 988, 876, 738, 715.

(R)-tris(4-ethylphenyl)((1,2,3,4-tetrahydronaphthalen-1-yl)oxy)silane (2.16h):

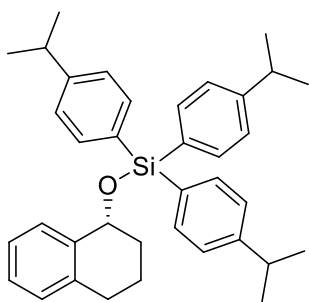


2.16h

33.3 mg (yield = 31%), colorless oil. ^1H NMR (400 MHz, CDCl_3) δ 7.59 (d, $J = 8.1$ Hz, 6H), 7.29 (d, $J = 7.4$ Hz, 1H), 7.20 (d, $J = 8.2$ Hz, 6H), 7.15 – 7.09 (m, 2H), 7.07 – 7.03 (m, 1H), 4.93 (t, $J = 6.1$ Hz, 1H), 2.86–2.79 (m, 1H), 2.63–2.70 (m, 7H), 2.09 – 2.00 (m, 1H), 1.94 – 1.81 (m, 2H), 1.70 – 1.60 (m, 1H), 1.24 (t, $J = 7.6$ Hz, 9H). ^{13}C NMR (101 MHz, CDCl_3) δ 145.9, 139.3, 137.0, 135.7, 132.0, 128.7, 128.6,

127.4, 126.9, 125.6, 70.0, 32.6, 29.1, 28.9, 19.3, 15.3. Optical Rotation $[\alpha]^{25}_{\text{D}} = +18.0$ ($c = 0.70$, CHCl_3). HRMS (EI) (M^+) Calculated for ($\text{C}_{34}\text{H}_{38}\text{OSi}^+$): 490.2686. Observed: 490.2691. IR (neat, cm^{-1}): 3066, 2964, 2932, 2872, 1601, 1553, 1455, 1398, 1190, 1072, 1039, 1017, 988, 821, 783, 739.

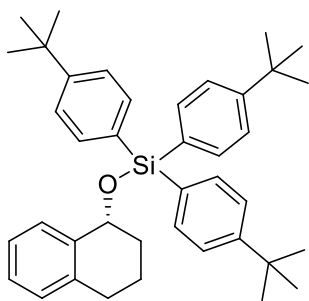
(R)-tris(4-isopropylphenyl)((1,2,3,4-tetrahydronaphthalen-1-yl)oxy)silane (2.16i):



2.16i

40.7 mg (yield = 35%), colorless oil. ^1H NMR (400 MHz, CDCl_3) δ 7.60 (d, $J = 8.2$ Hz, 6H), 7.28 (d, $J = 7.0$ Hz, 1H), 7.22 (d, $J = 7.8$ Hz, 6H), 7.15 – 7.08 (m, 2H), 7.05–7.03 (m, 1H), 4.93 (t, $J = 6.2$ Hz, 1H), 2.93 – 2.79 (m, 4H), 2.70–2.62 (m, 1H), 2.10–2.00 (m, 1H), 1.95 – 1.82 (m, 2H), 1.70 – 1.59 (m, 1H), 1.25 (d, $J = 8.0$ Hz, 18H). ^{13}C NMR (101 MHz, CDCl_3) δ 150.4, 139.3, 137.0, 135.7, 132.2, 128.7, 128.6, 126.9, 125.9, 125.6, 70.0, 34.1, 32.6, 29.1, 23.9, 19.3. Optical Rotation $[\alpha]^{25}_{\text{D}} = +16.8$ ($c = 0.95$, CHCl_3). HRMS (EI) (M^+) Calculated for ($\text{C}_{37}\text{H}_{44}\text{OSi}^+$): 532.3155. Observed: 532.3139. IR (neat, cm^{-1}): 3067, 2959, 2869, 1920, 1600, 1491, 1458, 1394, 1362, 1263, 1119, 1072, 1050, 1018, 988, 849, 769, 739, 710.

(R)-tris(4-(tert-butyl)phenyl)((1,2,3,4-tetrahydronaphthalen-1-yl)oxy)silane (2.16j):

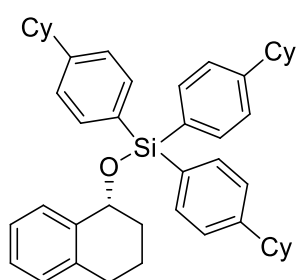


2.16j

48.5 mg (yield = 38%), white solid. MP range: 137–139 °C. ^1H NMR (400 MHz, CDCl_3) : δ 7.62 (d, $J = 8.4$ Hz, 6H), 7.39 (d, $J = 8.4$ Hz, 6H), 7.29 (d, $J = 7.4$ Hz, 1H), 7.17 – 7.10 (m, 2H), 7.08 – 7.05 (m, 1H), 4.95 (t, $J = 6.2$ Hz, 1H), 2.88 – 2.81 (m, 1H), 2.71 – 2.68 (m, 1H), 2.11–2.02 (m, 1H), 1.98 – 1.84 (m, 2H), 1.72 – 1.63 (m, 1H), 1.33 (s, 27H). ^{13}C NMR (101 MHz, CDCl_3) δ 152.6, 139.4, 137.0,

135.5, 131.7, 128.7, 128.6, 126.9, 125.6, 124.6, 69.9, 34.7, 32.6, 31.2, 29.1, 19.3. Optical Rotation $[\alpha]_D^{25} = +19.4$ ($c = 1.1$, CHCl_3). HRMS (EI) (M^+) Calculated for $(\text{C}_{40}\text{H}_{50}\text{OSi}^+)$: 574.3625 Observed: 574.3633. IR (neat, cm^{-1}): 2961, 2867, 1984, 1599, 1459, 1388, 1362, 1268, 1203, 1138, 1017, 988, 926, 876, 824, 750.4.

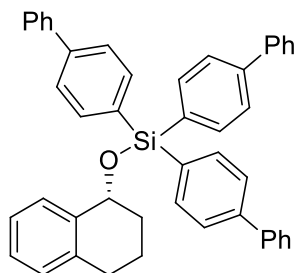
(*R*)-tris(4-cyclohexylphenyl)((1,2,3,4-tetrahydronaphthalen-1-yl)oxy)silane (2.16k):



2.16k

37.2 mg (yield = 26%), colorless oil. ^1H NMR (400 MHz, CDCl_3) : δ 7.58 (d, $J = 8.0$ Hz, 6H), 7.26 (d, $J = 7.5$ Hz, 1H), 7.19 (d, $J = 7.9$ Hz, 6H), 7.15-7.03 (m, 3H), 4.92 (t, $J = 6.0$ Hz, 1H), 2.86-2.78 (m, 1H), 2.69-2.62 (m, 1H), 2.52-2.46 (m, 3H), 2.09-1.99 (m, 1H), 1.93-1.81 (m, 14H), 1.75-1.72 (m, 3H), 1.69-1.63 (m, 1H), 1.51-1.33 (m, 12H), 1.28-1.20 (m, 3H). ^{13}C NMR (101 MHz, CDCl_3): δ 149.6, 139.4, 137.0, 135.7, 132.2, 128.7, 128.6, 126.9, 126.3, 125.6, 69.9, 44.6, 34.3, 32.6, 29.1, 26.9, 26.2, 19.3. Optical Rotation $[\alpha]_D^{25} = +14.3$ ($c = 1.04$, CHCl_3). HRMS (EI) (M^+) Calculated for $(\text{C}_{46}\text{H}_{56}\text{OSi}^+)$: 652.4094. Observed: 652.4094. IR (neat, cm^{-1}): 3066, 2923, 2851, 1923, 1600, 1448, 1397, 1350, 1263, 1115, 1072, 999, 1016, 988, 815, 755, 738, 668.

(*R*)-tri([1,1'-biphenyl]-4-yl)((1,2,3,4-tetrahydronaphthalen-1-yl)oxy)silane (2.16l):



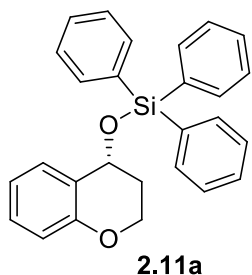
2.16l

27.2 mg (yield = 19%), white solid. MP range: 44-46 °C. ^1H NMR (400 MHz, CDCl_3) δ 7.81 (d, $J = 8.2$ Hz, 6H), 7.65 – 7.62 (m, 12H), 7.45 – 7.43 (m, 6H), 7.37 – 7.33 (m, 4H), 7.19 – 7.13 (m, 2H), 7.11-7.07 (m, 1H), 5.07 (t, $J = 6.2$ Hz, 1H), 2.91- 2.83 (m, 1H), 2.74 - 2.66 (m, 1H), 2.17- 2.07 (m, 1H), 2.04 – 1.88 (m, 2H), 1.76 – 1.65 (m, 1H). ^{13}C NMR (101 MHz, CDCl_3) δ 142.6, 140.9, 138.9, 137.1, 136.1,

135.9, 133.5, 128.9, 128.8, 128.7, 127.5, 127.2, 126.6, 125.7, 70.4, 32.6, 29.1, 19.2. Optical Rotation $[\alpha]_D^{25} = +23.3$ ($c = 0.94$, CHCl_3). HRMS (EI) (M^+) Calculated for ($\text{C}_{46}\text{H}_{38}\text{OSi}^+$): 634.2686 Observed: 634.2673. IR (neat, cm^{-1}): 3059, 3024, 2934, 1809, 1597, 1544, 1483, 1446, 1386, 1255, 1117, 1071, 1006, 988, 829, 756, 695.

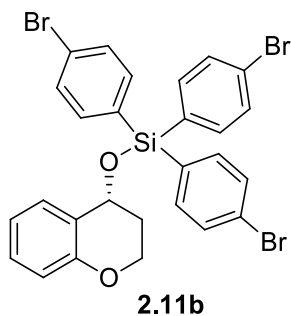
Chroman-4-ol (2.10): ^1H NMR (400 MHz, CDCl_3): δ 7.31(d, $J = 7.6$ Hz, 1H), 7.23-7.19 (m, 1H), 6.95-6.91 (m, 1H), 6.85 (d, $J = 8.2$ Hz, 1H), 4.79 (t, $J = 3.9$ Hz, 1H), 4.32-2.25 (m, 2H), 2.17-2.09 (m, 1H), 2.07-2.01 (m, 1H), 1.86 (s, 1H). ^{13}C NMR (101 MHz, CDCl_3): δ 154.5, 129.7, 129.6, 124.3, 120.6, 117.0, 63.2, 61.9, 30.8.

(chroman-4-yloxy)triphenylsilane (2.11a)¹:



White solid. 35.5 mg (yield = 40%). ^1H NMR (400 MHz, CDCl_3): δ 7.66 (d, $J = 6.5$ Hz, 6H), 7.48-7.37 (m, 9H), 7.18-7.14 (m, 1H), 6.99 (d, $J = 7.2$ Hz, 1H), 6.83-6.76 (m, 2H), 4.97 (t, $J = 4.0$ Hz, 1H), 4.51-4.45 (m, 1H), 4.24-4.19 (m, 1H), 2.02-1.96 (m, 2H). ^{13}C NMR (101 MHz, CDCl_3): δ 154.5, 135.5, 134.3, 130.1, 130.0, 129.2, 127.8, 124.2, 120.0, 116.7, 65.0, 62.2, 31.4.

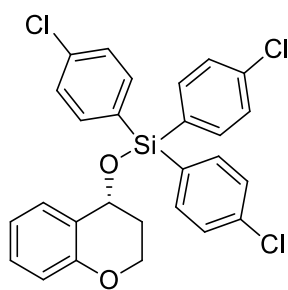
(R)-tris(4-bromophenyl)(chroman-4-yloxy)silane (2.11b):



49.3 mg (yield = 35%), white solid. MP range: 109-110 °C, ^1H NMR (400 MHz, CDCl_3): δ 7.52 (d, $J = 8.1$ Hz, 6H), 7.43 (d, $J = 8.2$ Hz, 6H), 7.20-7.16 (m, 1H), 6.89 (d, $J = 7.6$ Hz, 1H), 6.83-6.76 (m, 2H), 4.92 (t, $J = 4.0$ Hz, 1H), 4.47-4.40 (m, 1H), 4.26-4.21 (m, 1H), 2.01-1.97 (m, 2H). ^{13}C NMR (101 MHz, CDCl_3): δ 154.5, 136.8, 132.2, 131.4, 129.8, 129.6, 125.7, 123.3, 120.1, 116.9, 65.4, 61.9, 31.3.

Optical Rotation $[\alpha]^{25}_{\text{D}} = + 38.3$ ($c = 0.84$, CHCl_3). HRMS (EI) (M^+) Calculated for ($\text{C}_{27}\text{H}_{21}\text{Br}_3\text{O}_2\text{Si}^+$): 643.8836 Observed: 643.8859. IR (neat, cm^{-1}): 3071, 2926, 1915, 1610, 1572, 1478, 1377, 1224, 1116, 1063, 1008, 906, 806, 753.

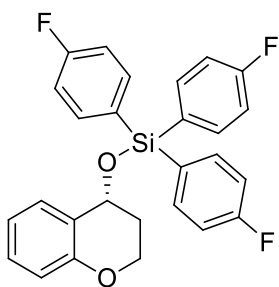
(*R*)-tris(4-chlorophenyl)(chroman-4-yloxy)silane (2.11c):



2.11c

46.6 mg (yield = 41%), yellowish color oil. ^1H NMR (400 MHz, CDCl_3): δ 7.51 (d, $J = 8.3$ Hz, 6H), 7.41 (d, $J = 8.3$ Hz, 6H), 7.20 – 7.16 (m, 1H), 6.91– 6.89 (m, 1H), 6.84 – 6.76 (m, 2H), 4.94 (t, $J = 4.4$ Hz, 1H), 4.48 – 4.42 (m, 1H), 4.27 – 4.22 (m, 1H), 2.01 – 1.97 (m, 2H). ^{13}C NMR (101 MHz, CDCl_3) δ 153.5, 136.1, 135.7, 130.9, 128.9, 128.6, 127.5, 122.4, 119.1, 116.0, 64.4, 60.9, 30.4. Optical Rotation $[\alpha]^{25}_{\text{D}} = + 49.9$ ($c = 1.17$, CHCl_3). HRMS (EI) (M^+) Calculated for ($\text{C}_{27}\text{H}_{21}\text{Cl}_3\text{O}_2\text{Si}^+$): 510.0370 Observed: 510.0363. IR (neat, cm^{-1}): 3072, 2927, 1912, 1609, 1578, 1482, 1381, 1224, 1118, 1082, 1014, 924, 809, 711.

(*R*)-(chroman-4-yloxy)tris(4-fluorophenyl)silane(2.11d):

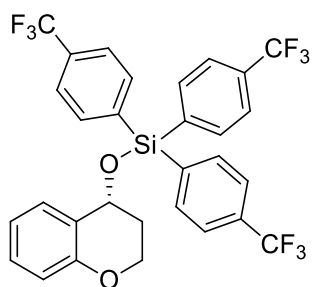


2.11d

37 mg (yield = 36%), colorless oil. ^1H NMR (400 MHz, CDCl_3) δ 7.60 – 7.56 (m, 6H), 7.20 – 7.15 (m, 1H), 7.13 – 7.08 (m, 6H), 6.89 (d, $J = 7.6$ Hz, 1H), 6.83 – 6.76 (m, 2H), 4.94 (t, $J = 4.0$ Hz, 1H), 4.49 – 4.42 (m, 1H), 4.27 – 4.21 (m, 1H), 2.01 – 1.97 (m, 2H). ^{13}C NMR (101 MHz, CDCl_3): δ 165.7–163.2 (d), 154.5, 137.5 (d), 129.8, 129.6(d), 129.5, 123.6, 120.0, 116.9, 115.5–115.3(d), 65.2, 62.0, 31.4. Optical Rotation $[\alpha]^{25}_{\text{D}} = + 47.4$ ($c = 0.98$, CHCl_3). HRMS (EI) (M^+) Calculated for

(C₂₇H₂₁F₃O₂Si⁺): 462.1257. Observed: 462.1266. IR (neat, cm⁻¹): 3065, 2928, 2888, 1909, 1610, 1498, 1489, 1388, 1269, 1223, 1161, 1110, 1092, 1064, 1003, 924, 821, 754, 715.

(R)-(chroman-4-yloxy)tris(4-(trifluoromethyl)phenyl)silane (2.11e):

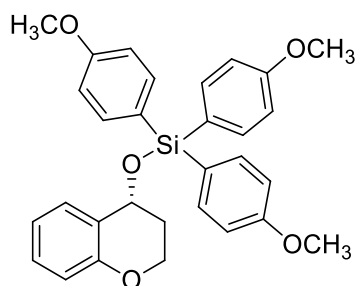


2.11e

22.8 mg (yield = 17%), colorless oil with minor amounts of tris(4-(trifluoromethyl)phenyl)silanol present. ¹H NMR (400 MHz, CDCl₃): δ 7.71 (d, *J* = 8.0 Hz, 6H), 7.66 (d, *J* = 8.1 Hz, 6H), 7.21-7.16 (m, 1H), 6.86-6.81 (m, 2H), 6.78-6.74 (m, 1H), 4.98 (t, *J* = 3.9 Hz, 1H), 4.50-4.44 (m, 1H), 4.30-4.25 (m, 1H),

2.05-2.02 (m, 2H). ¹³C NMR (101 MHz, CDCl₃): δ 154.5, 137.6, 135.6, 132.7 (q, *J*_{CF} = 32.3 Hz), 129.9, 129.8, 124.8 (q, *J*_{CF} = 3.71 Hz), 123.9 (q, *J*_{CF} = 272.5 Hz), 122.9, 120.1, 117.1, 65.9, 61.7, 31.3. ¹⁹F NMR (377 MHz, CDCl₃): δ -63.2. Optical Rotation [*α*]_D²⁵ = + 23.3 (*c* = 0.88, CHCl₃). HRMS (EI) (M⁺) Calculated for (C₃₀H₂₁F₉O₂Si⁺): 612.1161. Observed: 612.1171. IR (neat, cm⁻¹): 3034, 2929, 1611, 1585, 1490, 1393, 1318, 1269, 1164, 1120, 1017, 1005, 829, 755, 705.

(R)-(chroman-4-yloxy)tris(4-methoxyphenyl)silane (2.11f):



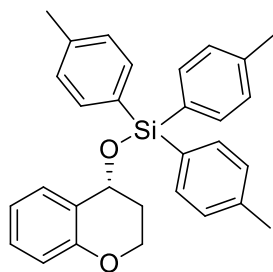
2.11f

25.1 mg (yield = 23%), colorless oil. ¹H NMR (400 MHz, CDCl₃): δ 7.57 (d, *J* = 8.2 Hz, 6H), 7.18- 7.13 (m, 1H), 7.02 (d, *J* = 7.7 Hz, 1H), 6.93 (d, *J* = 8.6 Hz, 6H), 6.82 – 6.78 (m, 2H), 4.94 (t, *J* = 4.3 Hz, 1H), 4.48 – 4.42 (m, 1H), 4.22 – 4.17 (m, 1H), 3.83 (s, 9H), 2.02 – 1.92 (m, 2H). ¹³C NMR

(101 MHz, CDCl₃): δ 161.1, 154.5, 137.1, 130.0, 129.1, 126.0, 124.5, 120.0, 116.6, 113.6, 64.7, 62.3, 55.0, 31.5. Optical Rotation [*α*]_D²⁵ = + 41.5 (*c* = 0.89, CHCl₃). HRMS (EI)

(M⁺) Calculated for (C₃₀H₃₀O₅Si⁺): 498.1857. Observed: 498.1869. IR (neat, cm⁻¹): 3018, 2837, 1902, 1592, 1501, 1489, 1276, 1179, 1090, 1065, 1001, 922, 810, 798, 753, 722.

(R)-(chroman-4-yloxy)tri-*p*-tolylsilane (2.11g):

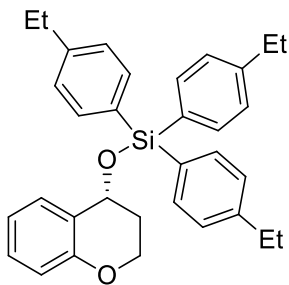


2.11g

30.4 mg (yield = 31%), colorless oil. ¹H NMR (400 MHz, CDCl₃): δ 7.53 (d, *J* = 7.8 Hz, 6H), 7.19 (d, *J* = 7.8 Hz, 6H), 7.15 – 7.11 (m, 1H), 7.03 – 7.01 (m, 1H), 6.80 – 6.75 (m, 2H), 4.93 (t, *J* = 4.2 Hz, 1H), 4.47 – 4.41 (m, 1H), 4.20 – 4.15 (m, 1H), 2.36 (s, 9H), 2.02 – 1.89 (m, 2H). ¹³C NMR (101 MHz, CDCl₃): δ 154.5, 139.9, 135.6,

131.2, 130.0, 129.1, 128.7, 124.5, 120.0, 116.6, 64.8, 62.3, 31.5, 21.6. Optical Rotation [α]_D²⁵ = +42.0 (*c* = 1.08, CHCl₃). HRMS (EI) (M⁺) Calculated for (C₃₀H₃₀O₂Si⁺): 450.2009. Observed: 450.2008. IR (neat, cm⁻¹): 3066, 2921, 1917, 1599, 1584, 1488, 1454, 1393, 1225, 1111, 1065, 1003, 922, 837, 753, 716.

(R)-(chroman-4-yloxy)tris(4-ethylphenyl)silane (2.11h):



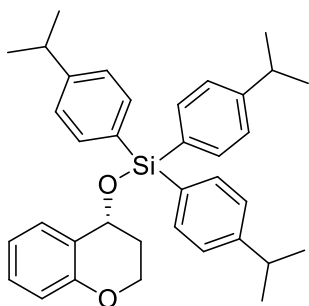
2.11h

39.2 mg (yield = 36%), colorless oil. ¹H NMR (400 MHz, CDCl₃): δ 7.59 (d, *J* = 8.0 Hz, 6H), 7.21 (d, *J* = 8.0 Hz, 6H), 7.15 – 7.11 (m, 1H), 7.01 – 6.99 (m, 1H), 6.80 – 6.75 (m, 2H), 4.93 (t, *J* = 4.0 Hz, 1H), 4.48 – 4.42 (m, 1H), 4.21 – 4.16 (m, 1H), 2.66 (q, *J* = 8.0 Hz, 6H), 2.04 – 1.90 (m, 2H), 1.24 (t, *J* = 8.0 Hz, 9H). ¹³C NMR

(101 MHz, CDCl₃): δ 154.5, 146.1, 135.6, 131.5, 130.0, 129.1, 127.5, 124.5, 120.0, 116.6, 64.8, 62.3, 31.5, 28.9, 15.3. Optical Rotation [α]_D²⁵ = +46.0 (*c* = 1.13, CHCl₃). HRMS (EI) (M⁺) Calculated for (C₃₃H₃₆O₂Si⁺): 492.2479. Observed: 492.2475. IR (neat, cm⁻¹): 3067,

2964, 2873, 1916, 1601, 1585, 1489, 1455, 1398, 1268, 1226, 1112, 1091, 1003, 922, 822, 809, 753, 719.

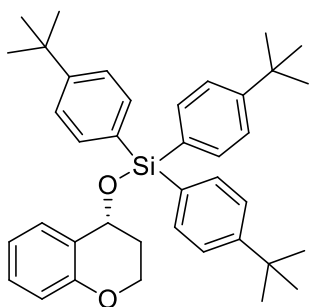
(R)-(chroman-4-yloxy)tris(4-isopropylphenyl)silane (2.11i):



2.11i

41.2 mg (yield = 35%), white solid. MP range: 90-92 °C. ¹H NMR (400 MHz, CDCl₃) : δ 7.58 (d, *J* = 7.8 Hz, 6H), 7.23 (d, *J* = 7.9 Hz, 6H), 7.13 (t, *J* = 8.1 Hz, 1H), 6.94 (d, *J* = 7.3 Hz, 1H), 6.79 – 6.73 (m, 2H), 4.93 (t, *J* = 4.2 Hz, 1H), 4.49 – 4.43 (m, 1H), 4.19 (dt, *J* = 6.3, 4.2 Hz, 1H), 2.91 (hept, *J* = 6.9 Hz, 3H), 2.05 – 1.90 (m, 2H), 1.25 (d, *J* = 6.9 Hz, 18H). ¹³C NMR (101 MHz, CDCl₃): δ 154.5, 150.6, 135.6, 131.7, 130.1, 129.0, 126.0, 124.5, 119.9, 116.6, 64.7, 62.3, 34.1, 31.5, 23.8. Optical Rotation [α]_D²⁵ = + 50.8 (*c* = 0.90, CHCl₃). HRMS (EI) (*M*⁺) Calculated for (C₃₆H₄₂O₂Si⁺): 534.2948. Observed: 534.2942. IR (neat, cm⁻¹): 3067, 2960, 2870, 1738, 1600, 1585, 1489, 1456, 1394, 1268, 1226, 1118, 1092, 1051, 1004, 922, 822, 809, 770, 754, 720.

(R)-tris(4-(tert-butyl)phenyl)(chroman-4-yloxy)silane (2.11j):

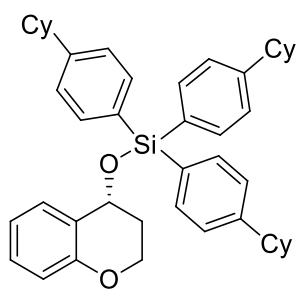


2.11j

47.5 mg (yield = 37%), white solid. MP range: 112-114 °C. ¹H NMR (400 MHz, CDCl₃): δ 7.60 (d, *J* = 8.1 Hz, 6H), 7.40 (d, *J* = 8.1 Hz, 6H), 7.14 (t, *J* = 7.6 Hz, 1H), 6.95 (d, *J* = 8.1 Hz, 1H), 6.81 – 6.74 (m, 2H), 4.94 (t, *J* = 4.0 Hz, 1H), 4.50 – 4.44 (m, 1H), 4.23 – 4.18 (m, 1H), 2.07 – 1.92 (m, 2H), 1.33 (s, 27H). ¹³C NMR (101 MHz, CDCl₃): δ 154.5, 152.8, 135.4, 131.3, 130.1, 129.0, 124.8, 124.6, 119.9, 116.6, 64.7, 62.3, 34.8, 31.5, 31.2. Optical Rotation [α]_D²⁵ = +49.5 (*c* = 1.13, CHCl₃).

HRMS (EI) (M^+) Calculated for ($C_{39}H_{48}O_2Si^+$): 576.3418. Observed: 576.3429. IR (neat, cm^{-1}): 3073, 2963, 2868, 1927, 1600, 1583, 1487, 1453, 1388, 1268, 1252, 1140, 1125, 1065, 1004, 918, 824, 809, 751.

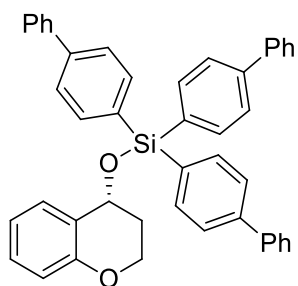
(*R*)-(chroman-4-yloxy)tris(4-cyclohexylphenyl)silane (2.11k)



2.11k

52.2 mg (yield = 36%), white solid. MP range: 47-49 °C, 1H NMR (400 MHz, $CDCl_3$): δ 7.57 (d, J = 8.0 Hz, 6H), 7.22 (d, J = 8.0 Hz, 6H), 7.15-7.11 (m, 1H), 6.95-9.92 (m, 1H), 6.80-6.73 (m, 2H), 4.92 (t, J = 4.3 Hz, 1 H), 4.49- 4.43 (m, 1 H), 4.22-4.17 (m, 1H), 2.53-2.48 (m, 3H), 2.05-1.93 (m, 2H), 1.90-1.48 (m, 12H), 1.76-1.73 (m, 3H), 1.48-1.34 (m, 12H), 1.30-1.23 (m, 3H). ^{13}C NMR (101 MHz, $CDCl_3$): δ 154.5, 149.8, 135.6, 131.7, 130.1, 129.0, 126.4, 124.5, 119.9, 116.5, 64.7, 62.3, 44.6, 34.2, 31.5, 26.9, 26.1. Optical Rotation $[\alpha]^{25}_D = +44.0$ (c = 0.94, $CHCl_3$). HRMS (EI) (M^+) Calculated for ($C_{45}H_{54}O_2Si^+$): 654.3887. Observed: 654.3884. IR (neat, cm^{-1}): 3067, 2922, 2850, 1968, 1600, 1585, 1489, 1448, 1348, 1268, 1253, 1192, 1115, 1091, 1067, 999, 922, 816, 752, 629.

(*R*)-tri([1,1'-biphenyl]-4-yl)(chroman-4-yloxy)silane (2.11l)



2.11l

26.5 mg (yield = 19%), white solid. MP range: 48-49 °C. 1H NMR (400 MHz, $CDCl_3$) δ 7.80 (d, J = 8.3 Hz, 6H), 7.69 - 7.64 (m, 12H), 7.49 - 7.45 (m, 8H), 7.40 - 7.36 (m, 3H), 7.21 - 7.17 (m, 1H), 7.11 - 7.09 (m, 1H), 6.85 - 6.80 (m, 2H), 5.08 (t, J = 4.2 Hz, 1H), 4.58 - 4.52 (m, 1H), 4.30 - 4.25 (m, 1H), 2.16 - 2.02 (m, 2H). ^{13}C NMR (101 MHz, $CDCl_3$): δ 154.5, 142.8, 140.8, 136.0, 133.1, 130.1, 129.3,

128.8, 127.6, 127.2, 126.7, 124.2, 120.1, 116.7, 65.1, 62.2, 31.5. Optical Rotation $[\alpha]^{25}_D = +49.7$ ($c = 0.58$, CHCl_3). HRMS (EI) (M^+) Calculated for $(\text{C}_{45}\text{H}_{36}\text{O}_2\text{Si}^+)$: 636.2479. Observed: 636.2485. IR (neat, cm^{-1}): 3025, 2882, 2056, 1597, 1484, 1455, 1386, 1268, 1252, 1225, 1117, 1065, 1005, 923, 830, 727, 695, 663.

HPLC data for Silylated Tetralol product

Kinetic Resolution for Table 2.6, Entry 1:

#	er _{SM} %	er _{PR} %	C%	<i>S</i>	<i>S</i> _{Avg}
1	85:15	15:85	50.1	11.9	11
2	91:9	19:81	57	10.9	

er_{PR}% is of deprotected and purified product.

Kinetic Resolution for Table 2.6, Entry 2:

#	er _{SM} %	er _{PR} %	C%	<i>S</i>	<i>S</i> _{Avg}
1	75:25	21:79	46.3	6.1	6.0
2	77:23	21:79	48	6.4	

er_{PR}% is of deprotected and purified product.

Kinetic Resolution for Table 2.6, Entry 3:

#	er _{SM} %	er _{PR} %	C%	<i>S</i>	<i>S</i> _{Avg}
1	66:34	18:82	33.7	6.4	7.0
2	67:33	16:84	32.3	8.1	

er_{PR}% is of deprotected and purified product.

Kinetic Resolution for Table 2.6, Entry 4:

#	er _{SM} %	er _{PR} %	C%	<i>S</i>	<i>S</i> _{Avg}
1	85:15	18:82	52.1	9.4	9.0
2	85:15	20:80	53.4	8.2	

er_{PR}% is of deprotected and purified product.

Kinetic Resolution for Table 2.6, Entry 5:

#	er _{SM} %	er _{PR} %	C%	<i>S</i>	<i>S</i> _{Avg}
1	65:35	22:78	35	4.8	5.0
2	56:44	18:82	14.9	5.1	

er_{PR}% is of deprotected and purified product.

Kinetic Resolution for Table 2.6, Entry 6:

#	er _{SM} %	er _{PR} %	C%	<i>S</i>	<i>S</i> _{Avg}
1	77:23	15:85	42.8	9.6	10
2	73:27	13:87	37.9	10.4	

er_{PR}% is of deprotected and purified product.

Kinetic Resolution for Table 2.6, Entry 7:

#	er _{SM} %	er _{PR} %	C%	<i>S</i>	<i>S</i> _{Avg}
1	86:14	13:87	49	14.1	14
2	84:16	13:87	47.7	13.4	

er_{PR}% is of deprotected and purified product.

Kinetic Resolution for Table 2.6, Entry 8:

#	er _{SM} %	er _{PR} %	C%	<i>S</i>	<i>S</i> _{Avg}
1	72:29	11:89	35.5	12.3	13
2	76:24	11:89	40.4	13.0	

er_{PR}% is of deprotected and purified product.

Kinetic Resolution for Table 2.6, Entry 9:

#	er _{SM} %	er _{PR} %	C%	<i>S</i>	<i>S</i> _{Avg}
1	88:12	14:86	50.9	14.1	14
2	84:16	12:88	47.5	14.3	

er_{PR}% is of deprotected and purified product.

Kinetic Resolution for Table 2.6, Entry 10:

#	er _{SM} %	er _{PR} %	C%	<i>S</i>	<i>S</i> _{Avg}
1	79:21	10:90	42.2	16.1	16
2	78:22	10:90	41.3	15.6	

er_{PR}% is of deprotected and purified product.

Kinetic Resolution for Table 2.6, Entry 11:

#	er _{SM} %	er _{PR} %	C%	<i>S</i>	<i>S</i> _{Avg}
1	71:29	9:91	34.1	15.6	15
2	70:30	9:91	32.8	15.2	

er_{PR}% is of deprotected and purified product.

Kinetic Resolution for Table 2.6, Entry 12:

#	er _{SM} %	er _{PR} %	C%	S	S _{Avg}
1	62:38	10:90	22.4	11	11
2	59:41	11:89	18.8	10	

er_{PR}% is of deprotected and purified product.

HPLC of Silylated 4-Chromanol product**Kinetic Resolution for Table 2.6, Entry 13:**

#	er _{SM} %	er _{PR} %	C%	S	S _{Avg}
1	85:15	13:87	48.6	14.2	15
2	89:11	12:88	50.5	16.6	

er_{PR}% is of deprotected and purified product.

Kinetic Resolution for Table 2.6, Entry 14:

#	er _{SM} %	er _{PR} %	C%	S	S _{Avg}
1	73:27	18:82	41.3	7.2	8.0
2	72:28	15.5:84.5	38.8	8.4	

er_{PR}% is of deprotected and purified product.

Kinetic Resolution for Table 2.6, Entry 15:

#	er _{SM} %	er _{PR} %	C%	<i>S</i>	<i>S</i> _{Avg}
1	86:14	14:86	49.9	12.6	11
2	73:27	15:85	39.7	8.8	

er_{PR}% is of deprotected and purified product.

Kinetic Resolution for Table 2.6, Entry 16:

#	er _{SM} %	er _{PR} %	C%	<i>S</i>	<i>S</i> _{Avg}
1	85:15	13:87	48.2	14	13
2	79:21	13:87	43.9	12.1	

er_{PR}% is of deprotected and purified product.

Kinetic Resolution for Table 2.6, Entry 17:

#	er _{SM} %	er _{PR} %	C%	<i>S</i>	<i>S</i> _{Avg}
1	59.5:40.5	15:85	21.4	6.8	7.0
2	59:41	14:86	19.6	7.1	

er_{PR}% is of deprotected and purified product.

Kinetic Resolution for Table 2.6, Entry 18:

#	er _{SM} %	er _{PR} %	C%	<i>S</i>	<i>S</i> _{Avg}
1	81:19	14:86	46.4	11.8	11
2*	80:20	16:84	47.4	9.3	

* 40 h reaction

er_{PR}% is of deprotected and purified product.

Kinetic Resolution for Table 2.6, Entry 19:

#	er _{SM} %	er _{PR} %	C%	<i>S</i>	<i>S</i> _{Avg}
1	94:6	16:84	56	14.8	14
2	77:23	11:89	40.9	14	

er_{PR}% is of deprotected and purified product.

Kinetic Resolution for Table 2.6, Entry 20:

#	er _{SM} %	er _{PR} %	C%	<i>S</i>	<i>S</i> _{Avg}
1	83:17	10:90	44.8	17.8	17
2	81:19	10:90	43.9	16.4	

er_{PR}% is of deprotected and purified product.

Kinetic Resolution for Table 2.6, Entry 21:

#	er _{SM} %	er _{PR} %	C%	<i>S</i>	<i>S</i> _{Avg}
1	87:13	10:90	48.1	19.9	20
2	87.5:12.5	10:90	48.4	19.7	

er_{PR}% is of deprotected and purified product.

Kinetic Resolution for Table 2.6, Entry 22:

#	er _{SM} %	er _{PR} %	C%	<i>S</i>	<i>S</i> _{Avg}
1	88:12	7:93	46.6	32.3	28
2	76:24	6:94	37.4	23.4	

er_{PR}% is of deprotected and purified product.

Kinetic Resolution for Table 2.6, Entry 23:

#	er _{SM} %	er _{PR} %	C%	<i>S</i>	<i>S</i> _{Avg}
1	83:17	8:92	43.7	22.4	21
2	78:22	8:92	40.3	20	

er_{PR}% is of deprotected and purified product.

Kinetic Resolution for Table 2.6, Entry 24:

#	er _{SM} %	er _{PR} %	C%	<i>S</i>	<i>S</i> _{Avg}
1	59:41	8:92	17	13.5	13
2	59:41	7:93	17.9	12.4	

er_{PR}% is of deprotected and purified product.

2.11 References

- (1) Sheppard, C. I.; Taylor, J. L.; Wiskur, S. L. Silylation-based kinetic resolution of monofunctional secondary alcohols. *Org. Lett.* **2011**, *13*, 3794-3797.
- (2) Shiina, I.; Nakata, K.; Ono, K.; Onda, Y. S.; Itagaki, M. Kinetic resolution of kanoic acids with achiral alcohols via the asymmetric esterification using carboxylic anhydrides and acyl-transfer catalysts. *J. Am. Chem. Soc.* **2010**, *132*, 11629-11641.
- (3) Shiina, I.; Nakata, K.; Ono, K.; Sugimoto, M.; Sekiguchi, A. Kinetic resolution of the racemic 2-hydroxyalkanoates using the enantioselective mixed-anhydride method with pivalic anhydride and a chiral acyl-transfer catalyst. *Chem.-Eur. J.* **2010**, *16*, 167-172.
- (4) Nakata, K.; Gotoh, K.; Ono, K.; Futami, K.; Shiina, I. Kinetic resolution of racemic 2-hydroxy- γ -butyrolactones by asymmetric esterification using diphenylacetic acid with pivalic anhydride and a chiral acyl-transfer catalyst. *Org. Lett.* **2013**, *15*, 1170-1173.
- (5) Li, X.; Jiang, H.; Uffman, E. W.; Guo, L.; Zhang, Y.; Yang, X.; Birman, V. B. Kinetic resolution of secondary alcohols using amidine-based catalysts. *J. Org. Chem.* **2012**, *77*, 1722-1737.
- (6) Manville, N.; Alite, H.; Haeffner, F.; Hoveyda, A. H.; Snapper, M. L. Enantioselective silyl protection of alcohols promoted by a combination of chiral and achiral Lewis basic catalysts. *Nat. Chem.* **2013**, *5*, 768-774.
- (7) Chuit, C.; Corriu, R. J. P.; Reye, C.; Young, J. C. Reactivity of pentacoordinate and hexacoordinate silicon-compounds and their role as reaction . *Chem. Rev.* **1993**, *93*, 1371-1448.
- (8) Corriu, R. J. P.; Dabosi, G.; Martineau, M. Nature of the interaction of nucleophiles such as hmpt, dmso, dmf and Ph₃PO with triorganohalo-silanes, triorganohalo-germanes, and triorganohalo-stannanes and organo-phosphorus compounds - Mechanism of nucleophile induced racemization and substitution at metal. *J. Organomet. Chem.* **1980**, *186*, 25-37.
- (9) Chojnowski, J.; Cypryk, M.; Michalski, J. The nature of the interaction between hexamethylphosphortriamide and trimethylhalosilanes; cations containing tetravalent silicon as possible intermediates in nucleophile-induced substitution of silicon halides. *J. Organomet. Chem.* **1978**, *161*, C31-C35.

- (10) Bassindale, A. R.; Lau, J. C. Y.; Taylor, P. G. Nucleophile-assisted racemisation of halosilanes; an alternative pathway involving halide exchange. *J. Organomet. Chem.* **1988**, *341*, 213-224.
- (11) Bassindale, A. R.; Stout, T. A. ^{29}Si , ^{13}C and ^1H NMR study of the interaction of various halotrimethylsilanes and trimethylsilyl triflate with dimethyl formamide and acetonitrile. A comment on the nucleophile induced racemisation of halosilanes. *J. Organomet. Chem.* **1982**, 238, C41-C45.
- (12) Chu, H. K.; Johnson, M. D.; Frye, C. L. Tertiary alcoholysis of chlorosilanes via tetracoordinate silylated quaternary ammonium intermediates. *J. Organomet. Chem.* **1984**, *271*, 327-336.
- (13) Yoder, C. H.; Ryan, C. M.; Martin, G. F.; Ho, P. S. Reactions of the ambidentate substrate chloromethyldimethylchlorosilane with amines and amides. *J. Organomet. Chem.* **1980**, *190*, 1-7.
- (14) Tandura, S. N.; Voronkov, M. G.; Alekseev, N. V. Molecular and electronic structure of penta- and hexacoordinate silicon compounds Structural Chemistry of Boron and Silicon. In Springer Berlin/Heidelberg: **1986**, *131*, pp 99-189.
- (15) Anslyn, E. V.; Dougherty, D. A. *Modern physical organic chemistry*; University Science: Sausalito, Calif., 2006.
- (16) Ramirez-Corredores, M. M.; Machin, I.; Grillo, M. E. A new concept for the application of linear free energy relationships in catalysis. *J. Mol. Catal. A: Chem.* **2000**, *151*, 271-278.
- (17) Hammett, L. P. The effect of structure upon the reactions of organic compounds benzene derivatives. *J. Am. Chem. Soc.* **1937**, *59*, 96-103.
- (18) Hansch, C.; Leo, A.; Taft, R. W. A survey of Hammett substituent constants and resonance and field parameters. *Chem. Rev.* **1991**, *91*, 165-195.
- (19) Taft, R. W. Linear free energy relationships from rates of esterification and hydrolysis of aliphatic and ortho-substituted benzoate esters. *J. Am. Chem. Soc.* **1952**, *74*, 2729-2732.
- (20) Taft, R. W. Linear steric energy relationships. *J. Am. Chem. Soc.* **1953**, *75*, 4538-4539.
- (21) Charton, M. Steric effects. I. esterification and acid-catalyzed hydrolysis of esters. *J. Am. Chem. Soc.* **1975**, *97*, 1552-1556.

- (22) Charton, M. Steric effects. 11. base-catalyzed ester hydrolysis. *J. Am. Chem. Soc.* **1975**, *97*, 3691-3693.
- (23) Charton, M. Steric effects. 111. Bimolecular nucleophilic substitution. *J. Am. Chem. Soc.* **1975**, *97*, 3694-3697.
- (24) Swain, C. G.; Lupton, E. C. Field and resonance components of substituent effects. *J. Am. Chem. Soc.* **1968**, *90*, 4328-4336.
- (25) Harper, K. C.; Sigman, M. S. Using physical organic parameters to correlate asymmetric catalyst performance. *J. Org. Chem.* **2013**, *78*, 2813-2818.
- (26) Jensen, K. H.; Sigman, M. S. Systematically probing the effect of catalyst acidity in a hydrogen-bond-catalyzed enantioselective reaction. *Angew. Chem., Int. Ed.* **2007**, *46*, 4748-4750.
- (27) Miller, J. J.; Sigman, M. S. Quantitatively correlating the effect of ligand-substituent size in asymmetric catalysis using linear free energy relationships. *Angew. Chem., Int. Ed.* **2008**, *47*, 771-774.
- (28) Gustafson, J. L.; Sigman, M. S.; Miller, S. J. Linear free-energy relationship analysis of a catalytic desymmetrization reaction of a diarylmethane-bis(phenol). *Org. Lett.* **2010**, *12*, 2794-2797.
- (29) Jensen, K. H.; Sigman, M. S. Evaluation of catalyst acidity and substrate electronic effects in a hydrogen bond-catalyzed enantioselective reaction. *J. Org. Chem.* **2010**, *75*, 7194-7201.
- (30) Jensen, K. H.; Webb, J. D.; Sigman, M. S. Advancing the mechanistic understanding of an enantioselective palladium-catalyzed alkene difunctionalization reaction. *J. Am. Chem. Soc.* **2010**, *132*, 17471-17482.
- (31) Harper, K. C.; Sigman, M. S. Three-dimensional correlation of steric and electronic free energy relationships guides asymmetric propargylation. *Science* **2011**, *333*, 1875-1878.
- (32) Harper, K. C.; Sigman, M. S. Predicting and optimizing asymmetric catalyst performance using the principles of experimental design and steric parameters. *Proc. Natl. Acad. Sci. U S A* **2011**, *108*, 2179-2183.
- (33) Rodriguez-Escrich, S.; Reddy, K. S.; Jimeno, C.; Colet, G.; Rodriguez-Escrich, C.; Sola, L.; Vidal-Ferran, A.; Pericas, M. A. Structural optimization of enantiopure 2-cyclialkylamino-2-aryl-1,1-diphenylethanol as catalytic ligands for enantioselective additions to aldehydes. *J. Org. Chem.* **2008**, *73*, 5340-5353.

- (34) Jacobsen, E. N.; Zhang, W.; Guler, M. L. Electronic tuning of asymmetric catalysis. *J. Am. Chem. Soc.* **1991**, *113*, 6703-6704.
- (35) Palucki, M.; Finney, N. S.; Pospisil, P. J.; Guler, M. L.; Ishida, T.; Jacobsen, E. N. The mechanistic basis for electronic effects on enantioselectivity in the (salen)Mn(III)-catalyzed epoxidation reaction. *J. Am. Chem. Soc.* **1998**, *120*, 948-954.
- (36) Li, X.; Deng, H.; Zhang, B.; Li, J. Y.; Zhang, L.; Luo, S. Z.; Cheng, J. P. Physical organic study of structure–activity–enantioselectivity relationships in asymmetric bifunctional thiourea catalysis: Hints for the design of new organocatalysts. *Chem.-Eur. J.* **2010**, *16*, 450-455.
- (37) Akhani, R. K.; Moore, M. I.; Pribyl, J. G.; Wiskur, S. L. Linear free-energy relationship and rate study on a silylation-based kinetic resolution: mechanistic insights. *J. Org. Chem.* **2014**, *79*, 2384-96.
- (38) Wander, M.; Hausoul, P. J. C.; Sliedregt, L. A. J. M.; van Steen, B. J.; van Koten, G.; Gebbink, R. J. M. K. Synthesis of polyaryl rigid-core carbosilane dendrimers for supported organic synthesis. *Organometallics* **2009**, *28*, 4406-4415.
- (39) Benkeser, R. A.; Riel, F. J. The reactions of some triarylsilanes with methyllithium and phenylisopropylpotassium. *J. Am. Chem. Soc.* **1951**, *73*, 3472-3473.
- (40) Arai, M. Chlorination by sulfonyl chloride. III.1) The reactivities of the C-H bond to sulfonyl chloride. *Bull. Chem. Soc. Jpn.* **1964**, *37*, 1280-1283.
- (41) Lee, K. H. Directive effects in benzylic hydrogen atom abstraction .2. radical chlorination by sulphonyl chloride. *Tetrahedron* **1969**, *25*, 4363-4369.
- (42) Hansch, C.; Leo, A.; Taft, R. W. A survey of hammett substituent constants and resonance and field parameters *Chem. Rev.* **1991**, *91*, 165-195.
- (43) Sigman, M. S.; Miller, J. J. Examination of the role of Taft-type steric parameters in asymmetric catalysis. *J. Org. Chem.* **2009**, *74*, 7633-7643.
- (44) Jacobsen, E. N.; Zhang, W.; Guler, M. L. Electronic tuning of asymmetric catalysis. *J. Am. Chem. Soc.* **1991**, *113*, 6703-6704.
- (45) Jacobsen, E. N.; Pfaltz, A.; Yamamoto, H. *Eds. comprehensive asymmetric catalysis I-III*; Springer Verlag: New York, 1999; Vol. 1-3.

- (46) Wu, J. H.; Zhang, G. R.; Porter, N. A. Substrate steric effects in enantioselective Lewis acid promoted free radical reactions. *Tetrahedron Lett.* **1997**, 38, 2067-2070.
- (47) Mantilli, L.; Gerard, D.; Torche, S.; Besnard, C.; Mazet, C. Improved catalysts for the iridium-catalyzed asymmetric isomerization of primary allylic alcohols based on Charton analysis. *Chem.-Eur. J.* **2010**, 16, 12736-12745.
- (48) Huang, H.; Zong, H.; Bian, G.; Song, L. Constructing a quantitative correlation between N-substituent sizes of chiral ligands and enantioselectivities in asymmetric addition reactions of diethylzinc with benzaldehyde. *J. Org. Chem.* **2012**, 77, 10427-10434.
- (49) Selectivity factor (s) = (rate of fast reacting enantiomer)/(rate of slow reacting enantiomer). Selectivity factor (s) = (rate of fast reacting enantiomer)/(rate of slow reacting enantiomer).
- (50) Alnajjar, M.; Quigley, D.; Kuntamukkula, M.; Simmons, F.; Freshwater, D.; Bigger, S. Methods for the safe storage; handling; and disposal of pyrophoric liquids and solids in the laboratory J. Chem. Health Safe. 2011, 18, 5-10.
- (51) Prince, P. D.; Bearpark, M. J.; McGrady, G. S.; Steed, J. W. Hypervalent hydridosilicates: synthesis, structure and hydride bridging. *Dalton Trans.* **2008**, 271-282.
- (52) Beyer, C.; Bohme, U.; Pietzsch, C.; Roewer, G. Preparation, characterization and properties of dipolar 1,2-N,N-dimethylaminomethylferrocenylsilanes. *J. Organomet. Chem.* **2002**, 654, 187-201.
- (53) Liew, S. K.; Al-Rafia, S. M. I.; Goettel, J. T.; Lummis, P. A.; McDonald, S. M.; Miedema, L. J.; Ferguson, M. J.; McDonald, R.; Rivard, E. Expanding the steric coverage offered by bis(amidosilyl) chelates: Isolation of low-coordinate N-heterocyclic germylene complexes. *Inorg. Chem.* **2012**, 51, 5471-5480.

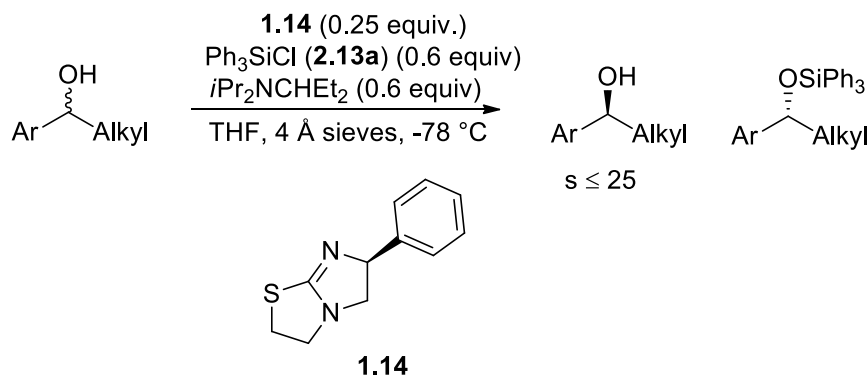
CHAPTER 3

COMPLEX FORMATION STUDY OF TRIPHENYLSILYL CHLORIDE AND (-)-TETRAMISOLE USING $^1\text{H}/^{29}\text{Si}$ NMR FOR THE ENANTIOSELECTIVE Silylation REACTION

3.1 Introduction

One of the main goals of the Wiskur lab is to understand the mechanism of our silylation-based kinetic resolution system (Scheme 3.1).¹⁻³ Several silylation methodologies that have been reported in the literature displays the nucleophilic activation of silicon.⁴⁻¹⁰ As explained in chapter 2 (section 2.2.1.), a two fundamental mechanism was proposed and in both mechanism, a different mechanistic pathway was discussed. Ultimately, it has been stated that both mechanisms have been observed, and the path is affected by the nucleophile, leaving group, solvent, and substituents on silicon. Therefore, in order to efficiently expand our system to other substrate classes, an understanding of our mechanism is necessary. In past several years, various methodology have been developed on enantioselective silylations, but none of them have reported detailed mechanistic investigation.¹¹⁻¹⁶

Therefore, understanding the mechanism of our system would not only allow us to understand our mechanism but also contribute significantly to the field of enantioselective silylation.



Scheme 3.1 Previously reported silylation-based kinetic resolution by the Wiskur lab

Over past couple years, our lab has taken different approaches to gain insight about the mechanism of our silylation reaction through a linear free energy relationship study and a rate study. In our mechanism, **1.14** serves as the catalyst. Traditionally, tetramisole¹⁷ has been used as a nucleophilic catalyst in other types of reactions, therefore we hypothesized that tetramisole nucleophilically activates the Ph_3SiCl in our system followed by attack of the substrate. From our recent linear free energy relationship study (Chapter 2)¹⁸ we found a good correlation between the absolute rate of the silylation and Hammett parameters¹⁹ for different *para* substituted Ph_3SiCl . This slope was positive, which indicates the buildup of a negative charge or a decrease in positive charge at the transition state.²⁰ Using this information from the LFER study and the two previously proposed mechanism by Chojnowski⁷, Bassindale^{6,21} and Frye⁵ as well as by Corriu⁴, a mechanism was proposed for our silylation reaction (Figure 3.1). In both pathways presented in Figure 3.1 (A and B), tetramisole is presumed to activate Ph_3SiCl followed by nucleophilic attack of the

alcohol. In one possibility, the catalyst and silyl source may form a pentavalent intermediate for the alcohol to attack (**A**, Figure 3.1), while the second possibility is that they may form a tetravalent intermediate (**B**, Figure 3.1). Therefore, to test our hypothesis of a complex formation (pentavalent vs tetravalent) and identify the coordination number of silicon, many proton and silicon NMR experiments were carried out. Various attempt to form a complex between **1.14** and Ph_3SiCl chlorides followed by the determination of coordination number of silicon in our mechanism will be discussed. This report represents our efforts in the Wiskur lab to study the silylation mechanism through ^1H - ^{29}Si NMR and its overall outcome including future directions.

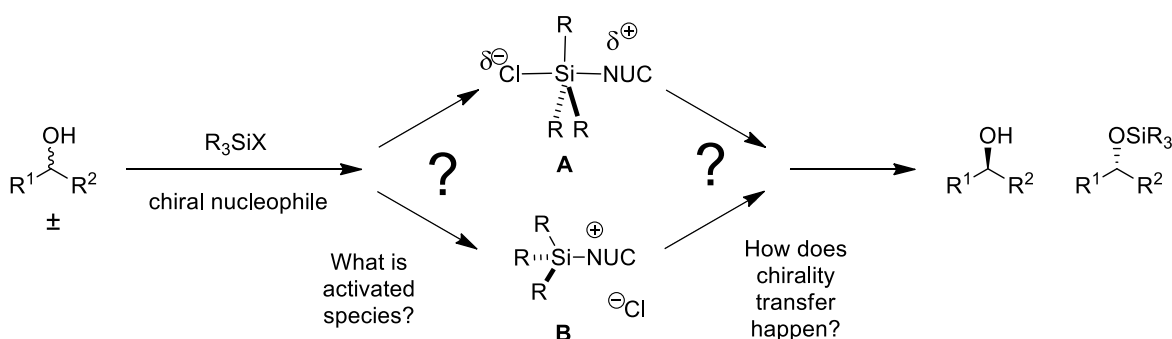
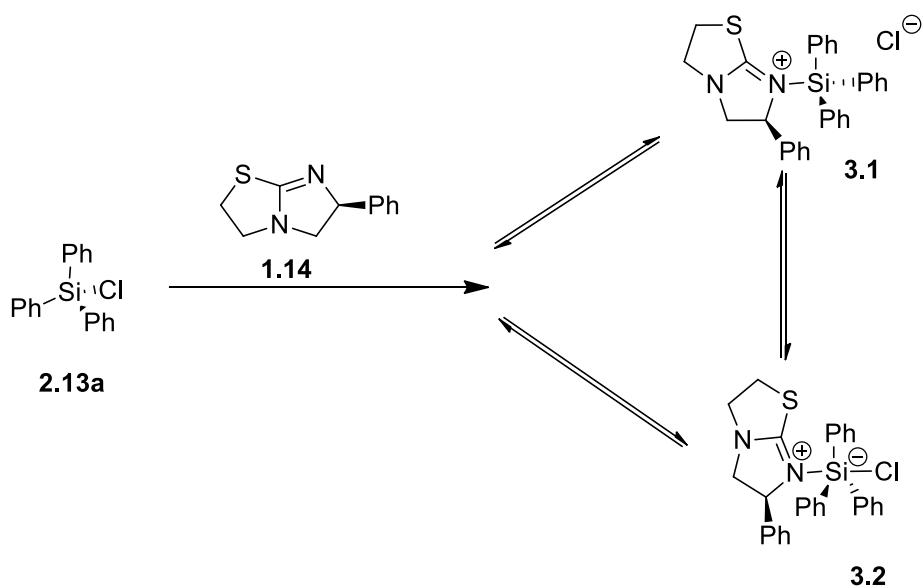


Figure 3.1 Two possible mechanistic pathways for our enantioselective silylation

3.2 Background:

3.2.1 Summary of the previous study of a complex formation in the Wiskur lab

In the past couple of years, the Wiskur group has used several different approaches to form the complex between Ph_3SiCl (**2.13a**) and (-)-tetramisole (**1.14**). This section is a review of our past work that has been done in our lab to form a complex and the conclusions that were made from that data.²²



Scheme 3.2 Plausible tetravalent or pentavalent silicon complex formations between (-)-tetramisole and Ph_3SiCl in our enantioselective silylation

Scheme 3.2 shows the possibility of two different intermediates, a tetravalent silicon (**3.1**) versus a pentavalent silicon (**3.2**). To identify the actual intermediate (**3.1** or **3.2**), several NMR experiments were carried out. To synthesize the intermediate a 1:1 mixture of both catalyst (**1.14**) and Ph_3SiCl (**2.13a**) were mixed together in a glovebox. A 1 M solution of Ph_3SiCl in dry THF was made and added to 1.0 equivalent of (-)-tetramisole (**1.14**). A white precipitate formed instantaneously. Since the precipitate was soluble in dichloromethane, the solvent was removed from the solution under vacuum to leave the dried precipitate, and then dissolved in CD_2Cl_2 to obtain ^{29}Si and ^1H NMR spectra. From the ^1H NMR spectra (Figure 3.2) of the mixture, a downfield shift was observed compared to **1.14** itself, and no unreacted Ph_3SiCl and **1.14** was observed. These results displayed potential of a complex formation between $\text{Ph}_3\text{SiCl}/\mathbf{1.14}$.

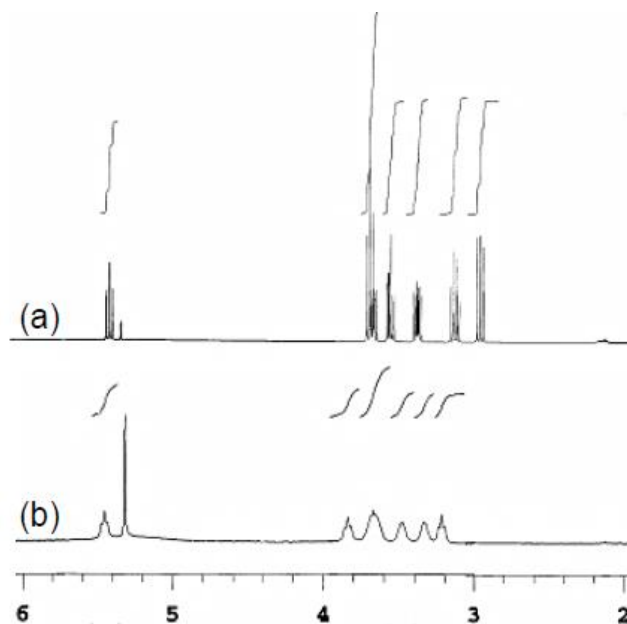


Figure 3.2 Comparison of the bicyclic ring protons of the catalyst and the precipitate which formed from **1.14** and **2.13a** (Spectra was taken directly from Cody Sheppard's dissertation)

To get further evidence of complex formation between $\text{Ph}_3\text{SiCl}/\mathbf{1.14}$, a 1D NOE (Nuclear Overhauser Effect)-experiment was also performed. A methine proton of (-)-tetramisole was irradiated and a positive nOe was observed (Figure 3.3) between an *ortho* ring proton of Ph_3SiCl (H_a) and the methine proton (H_b) of **1.14**. This suggests that the *ortho* proton on the phenyl ring of Ph_3SiCl was very close to the methine proton on **1.14**. From these experiments, a silicon-catalyst complex formation was concluded to be occurring.

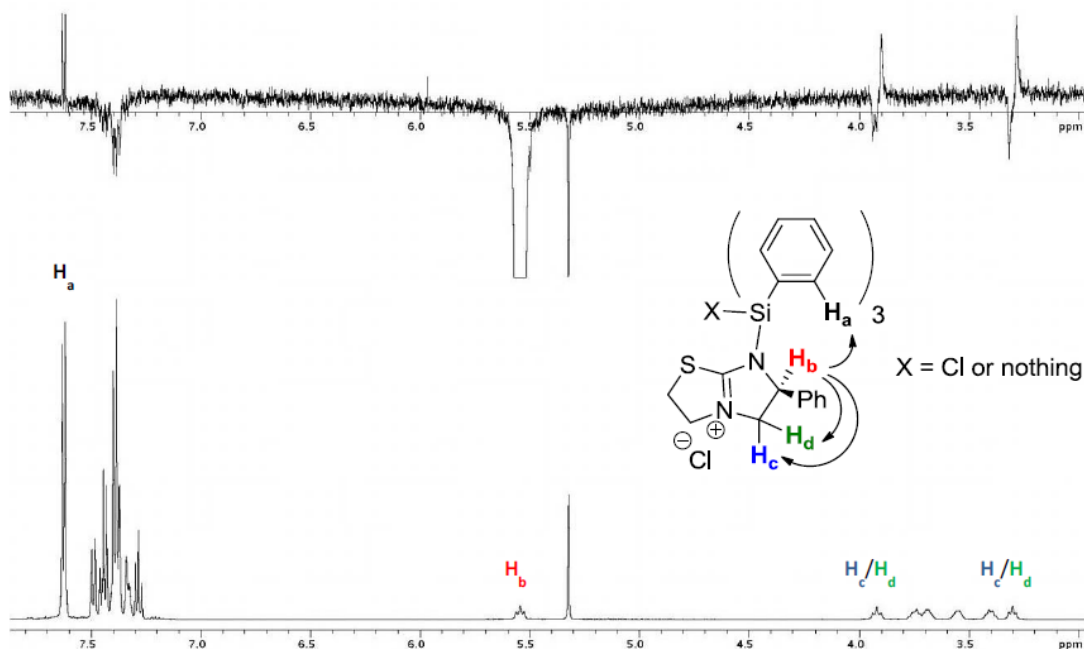


Figure 3.3: An nOe-difference experiment spectrum of precipitate obtained from **1.14** and Ph_3SiCl in THF (Spectra was directly taken from Cody Sheppard's dissertation)

After confirmation of a complex formation, the silicon coordination number was determined through experiment to identify if the intermediate was tetravalent (**3.1**) or pentavalent (**3.2**). Solid-state ^{29}Si NMR was used to determine the coordination number of silicon in the mixture of **1.14** and Ph_3SiCl . A single peak at -16.6 ppm was observed compared to unbound Ph_3SiCl (+2.5 ppm). A ^{29}Si NMR was also taken of the hydrolyzed products triphenylsilanol (Ph_3SiOH) and hexaphenyl-di-siloxane (HPDS). The triphenylsilanol showed a peak at -11 ppm, while HPDS was at -18.5 ppm. To identify the valency, these results were compared to the report published by the Wagler group²³ (Figure 3.4) where a pentavalent species (^{29}Si) was obtained for a pseudo isothioureia/TMSCl complex formation at -34.7 ppm SSNMR) (TMSCl = +31.0 ppm, Which results the Si NMR difference of an overall upfield shift of 60 ppm).

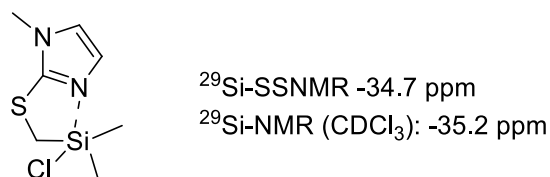


Figure 3.4. Pentavalent silicon reported by the Wagler group

These results suggested the absence of a hypervalent silicon intermediate. Therefore, we concluded that our system was more likely to form the tetravalent intermediate. To support this tetravalent intermediate theory we wanted to observe its presence in solution. For this ^1H - ^{29}Si gradient heteronuclear multiple quantum coherence spectroscopy (gHSQC) was utilized. The main advantage of this technique is that the proton nuclei which are 2-3 bonds away from ^{29}Si nuclei will be also observable instead of simply looking at proton nuclei directly attached to ^{29}Si . This means that using this method, additional information is obtained such as the ^1H NMR spectra which can help to identify other side products. Also, this technique has higher resolution than using the traditional method of multiple bond correlation HMBC. To compare results, several pentavalent silicon compounds were found from the literature as listed below (Figure 3.5).

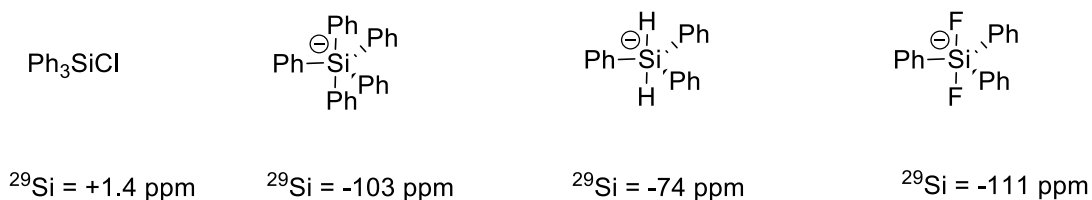


Figure 3.5 Pentavalent silicon reported in the literature²⁴⁻²⁶

In all the pentavalent species, the ^{29}Si peak was higher upfield than any of the tetravalent peaks. The complex was formed in the same way as mentioned earlier and the experiment was done at $-78\text{ }^\circ\text{C}$ using gHSQC ^1H - ^{29}Si NMR. Similar results to the solid

state NMR were observed (Table 3.1). In this technique, associated error in terms of ^{29}Si was reported around +1.5 ppm. Unfortunately, in the ^{29}Si NMR the silanol peak (-13.4 ppm)(Table 3.1, Entry 5) was observed very close to the complex peak (-11.3 ppm) (Table 3.1, Entry 1), but in ^1H spectra the signal had almost a 0.4 ppm upfield difference that was seen compared to complex. Based on the differences in the ^1H NMR spectra, a peak obtained very close to Ph_3SiOH was identified as the complex peak. In this experiment HPDS ($\text{Ph}_3\text{Si-O-Ph}_3\text{Si}$) was found at -20.1 ppm. The same experiment was also performed with excess catalyst but similar results were found. Finally, the experiment was also repeated at room temperature (Table 3.1, Entry 3) in which two peaks at -13.9 and -18.8 ppm were reported. Both peaks were found in very close proximity to Ph_3SiOH and HPDS. The only difference was seen in the ^1H NMR. Based on all the data reported above, enantioselective silylation was assumed to be going through a tetravalent intermediate rather than a pentavalent intermediate.

Table 3.1 Previous data of ^1H - ^{29}Si gHSQC NMR of complex **1.14**/ Ph_3SiX

Entry	$\text{Ph}_3\text{SiX}/\mathbf{1.14}$	δ_{Si} (ppm)	δ_{H} (ppm)
1 ^a	$\text{Ph}_3\text{SiCl}/\mathbf{1.14}$	-11.3	7.61; 7.45
2 ^b	$\text{Ph}_3\text{SiCl}/\mathbf{1.14}$	-11.0 -19.2	7.60 7.52
3 ^c	$\text{Ph}_3\text{SiCl}/\mathbf{1.14}$	-13.9 -18.8	7.61 7.50
4	Ph_3SiCl	+1.9	7.64
5	Ph_3SiOH	-13.4	7.20
6	$\text{Ph}_3\text{Si-O-SiPh}_3$	-20.1	7.53

^a Performed at -78 °C

^b 3.0 equiv. of **1.14** at -78 °C

^c Performed at room temp

3.3 Re-examination of complex formation

From the above data, we can see that all the ^{29}Si peaks mentioned in Table 3.1 are very close to the ^{29}Si peaks for the hydrolyzed products (TPSOH and HPDS) with very minor differences in the ^1H NMR. Therefore, we thought more definitive data was required to claim the intermediate was tetravalent. In this regard, we decided to rerun the complex formation experiment using a different approach and try to avoid possible hydrolyzed products, to confirm the peak is from the complex formation. The integration of a complex (^1H NMR) was also a problem in the previous study, therefore we begin our study by repeating the same complex formation experiment. In the previous studies, complex formation was confirmed based on two experiments (i.e. ^1H NMR study of complex $\text{Ph}_3\text{SiCl}/\mathbf{1.14}$ and nOe experiment). To our surprise, when we repeated these experiments, very different results were obtained. No complex formation was seen as reported previously and no nOe was observed. These experiments were repeated several times but we were unable to reproduce the earlier results. One of the reasons may include the moisture sensitivity of complex. To avoid this issue, we also tried forming the complex in a glove box but still no successful results were obtained. We therefore decided to use a more systematic approach.

3.3.1 Analysis of $\mathbf{1.14}/\text{Ph}_3\text{SiCl}$ complex at different concentration

In the previous study, the concentration of the complex was not accurately measured. Therefore, we thought it could be a concentration issue. We decided to try forming the complex at different concentrations, specifically higher concentrations, which might favor complex formation. In the previous study, Ph_3SiCl and $\mathbf{1.14}$ were initially mixed in THF and once a precipitate formed, precipitate was then dried on the vacuum

pump and dissolved in CD_2Cl_2 to take the NMR. Therefore, to use the vacuum pump, the compound had to be taken out of the glove box which could be another possible reasons for hydrolysis. One way to avoid any hydrolyzed products was to eliminate the use of the vacuum pump. With this in our mind, a variety of different concentration based complexes were made in a glove box by just mixing solids of **1.14** and Ph_3SiCl in 1:1 ratio followed by the addition of CD_2Cl_2 . Several different concentration based solutions were formed (1.0 M, 0.8 M, 0.55 M, 0.5 M, 0.275 M). ^1H NMR spectra were taken of these different solutions. Surprisingly, there was negligible change in the bicyclic ring proton region (2.85 ppm to 3.85 ppm) for the catalyst (Figure 3.6), and we were unable to achieve the previously reported results.

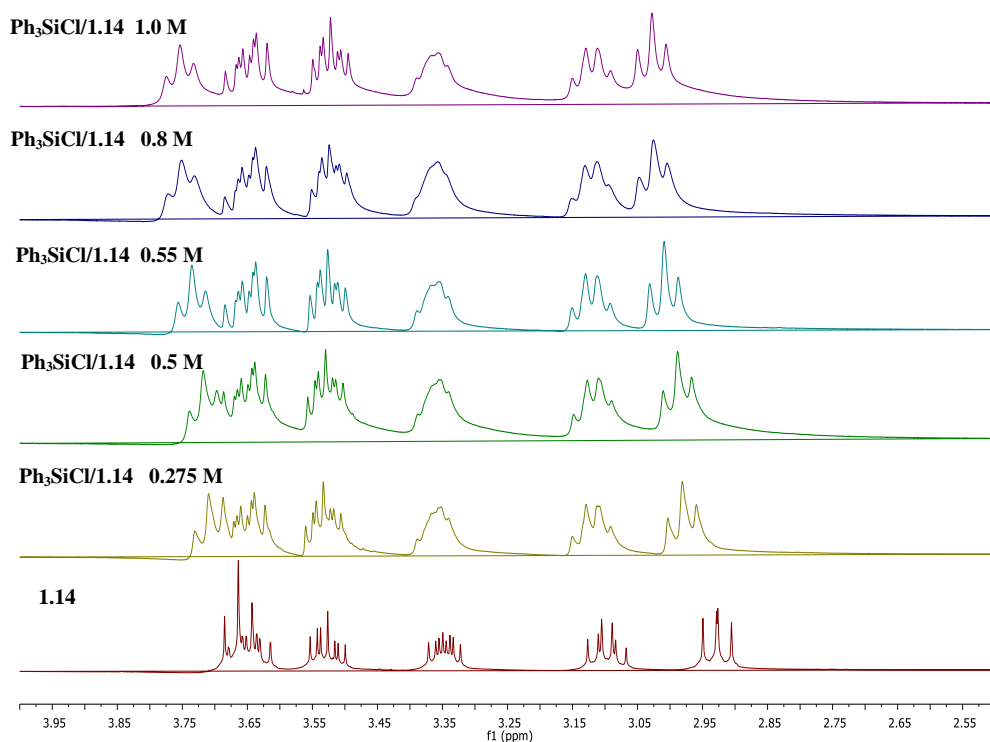


Figure 3.6 ^1H NMR of a solution of **1.14** and Ph_3SiCl (1:1 ratio) at different concentrations

Now forming the complex became the main challenge for us before moving further in this study. We thought, one possible issue for not forming the complex could be the way we were undertaking the previous experiment, was the way we were preparing the samples. In our experiment, two solids were mixed together, then dissolved in a solvent which results in an instantaneous precipitate formation. As a result, there was always a solid at the end of this experiment, and we could not tell if it was a precipitate from the two reagents interacting or undissolved reagents. To avoid this problem, we decided to repeat the same experiment but with a new method. Instead of mixing **1.14** and Ph_3SiCl (as a solid) directly followed by CD_2Cl_2 addition, we made separate known molar solutions of both **1.14** as well as Ph_3SiCl using CD_2Cl_2 and then mixed the two at different concentrations. As expected, no precipitate formed when **1.14** and Ph_3SiCl were mixed together, and the solution remained clear. Several samples with different concentrations were made (0.05 M, 0.066 M, 0.076 M, 0.083 M, 0.1 M, 0.125 M, 0.25 M and 0.5 M) and the ^1H NMR data collected. We started the ^1H NMR study from a 0.5 M concentration of each reagent followed by dilution using CD_2Cl_2 to make 0.25 M, 0.125 M and the other mentioned concentrations down to a 0.05 M solution. A noticeable change in the ^1H NMR of the bicyclic region of the catalyst **1.14** was observed, resulting in a down field shift in the ^1H NMR (Figure 3.7), when the sample was more concentrated (0.5 M and 0.25 M). There was not a significant change when the sample was diluted more, especially going from 0.125 M to 0.05 M. This experiment suggested that some sort of change was happening when the sample concentration was high. To investigate, ^1H NMR shifting in detail, a sample with 0.5 M concentration was prepared. ^1H - ^{29}Si gHSQC analysis was performed, to study the resulting silicon peak. To our surprise, only one peak at -18.5 ppm (^{29}Si) was

observed, which is very close to the ^{29}Si NMR peak of HPDS (-20 ppm). Since the gHSQC experiment has an error of ± 1.5 ppm, we could not assume the peak was a new silicon peak. The corresponding ^1H signal in gHSQC was also found < 0.3 ppm upfield which made it difficult for us to claim it as a possible complex peak. Since higher concentrations seemed promising (0.5 M, as discussed above), we attempted to make a 1.5 M solution of the two reagents (made separate 1.5 M solutions first using CD_2Cl_2 and then mixed), but unfortunately precipitation was seen after a couple minutes. Finally we decided to use 0.8 M concentration for our study. A sample was prepared similar way as mentioned earlier, by mixing a **1.14**/ Ph_3SiCl and ^1H - ^{29}Si gHSQC was taken. Similar results as seen for 0.5 M were obtained but this time unreacted Ph_3SiCl was also observed (+1.4 ppm) along with -18.5 ppm peak, unable to make any conclusion.

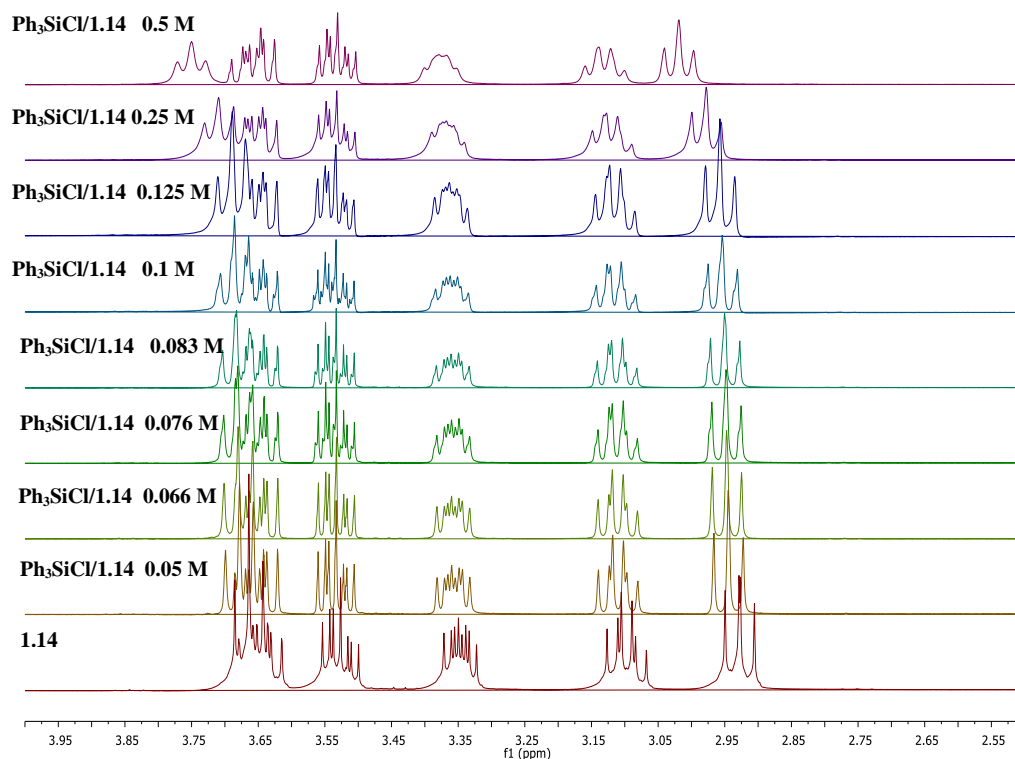


Figure 3.7 ^1H NMR study of **1.14**/ Ph_3SiCl at different concentrations

3.3.2 ^1H NMR titration and ^1H - ^{29}Si gHSQC experiments

From the above data, it was still unclear whether the observed ^{29}Si peak in the previous studies could be assigned as the complex, therefore, a more detailed investigation was needed. We thought it would be interesting to see proton shift changes in the ^1H NMR spectra, if we used one of the species in excess in an attempt to make the complex. A ^1H NMR titration was employed for further analysis. Using this technique, we can potentially force the complex to form with excess Ph_3SiCl or **1.14**, by shifting the equilibrium towards complex formation. Using an excess amount of one of the species either Ph_3SiCl or **1.14**, we would not miss any possible silicon peaks in ^1H - ^{29}Si NMR through gHSQC.

Table 3.2 ^1H - ^{29}Si gHSQC NMR analysis after saturation of ^1H NMR titration of Ph_3SiCl /**1.14** complex

Entry	Ph_3SiCl -tetramisole titration	NMR taken at equiv	δ_{Si} (ppm)	δ_{H} (ppm)
1	0.0015 M Ph_3SiCl titrated using excess 1.7 M 1.14	500	-18.5	7.30
2	0.0015 M 1.14 titrated using excess 1.7 M TPSCI	200	-18.5 -13.0	7.25, 7.45 7.30, 7.60
3	0.0015 M Ph_3SiCl titrated using excess 0.85 M 1.14	10	-16.8	7.30, 7.55
4	0.015 M Ph_3SiCl titrated using excess 0.85 M 1.14	1	-13.0 +1.2	7.40, 7.70 7.45, 7.65

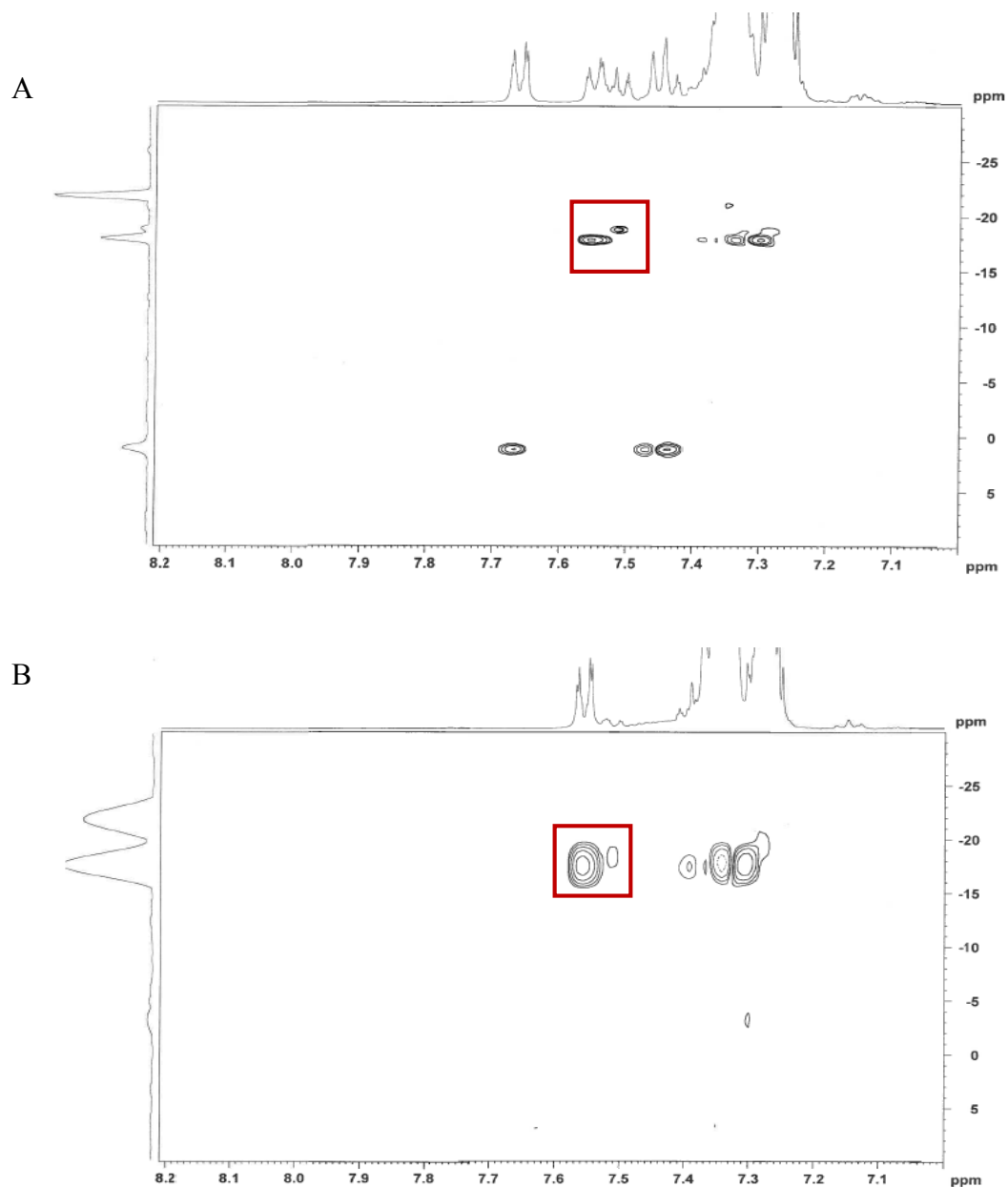
The ^1H NMR titration was carried out by keeping one of the species (either **1.14** or Ph_3SiCl) at really low concentrations while the other was at a very high concentration. The titrations were carried out using two separate approaches (Table 3.2, Entries 1 & 2). In the first approach, a higher concentration of 1.7 M catalyst (**1.14**) in CD_2Cl_2 was titrated into a much solution of Ph_3SiCl (0.0015 M in CD_2Cl_2) at a much lower concentration. In the

second approach it was just the opposite, Ph_3SiCl was at a higher concentration and was titrated into the lower concentration solution containing **1.14** (0.0015 M in CD_2Cl_2). In both cases, similar results were obtained. When excess catalyst (**1.14**) was titrated into Ph_3SiCl , after 500 equivalents, a saturation (no further proton shifting) in the ^1H NMR was observed (no further shifting of peak, Entry 1, Table 3.2). At this point a ^1H - ^{29}Si NMR (gHSQC) was taken and only one ^{29}Si peak at -18.5 ppm was observed. With excess Ph_3SiCl , after 200 equivalent, a saturation in ^1H NMR was observed (no further shifting of peak) and two different ^1H - ^{29}Si peaks were observed, one at -18.5 and a second at -13.0 ppm (Table 3.2, Entry 2). The peak at -13.0 ppm seems to be the Ph_3SiOH peak. Since the -18.5 ppm was a common ^{29}Si peak in both titrations, we decided to investigate that peak further.

To identify if we are forming the complex and if so, how many equivalents of Ph_3SiCl and **1.14** were needed to form a complex, we wanted to investigate the ^1H - ^{29}Si gHSQC NMR early in the titration (to observe at what equivalent ^{29}Si peak (-18.5) appears). Two different experiments were set up. Using excess Ph_3SiCl , there is a higher chance of forming hydrolyzed product (as we saw in the previous experiment, Table 3.2, Entry 2), therefore to avoid this we used an excess of **1.14** for the titration instead of Ph_3SiCl . In the first experiment, we stopped our titration after adding 10 equivalents of **1.14** into a solution of Ph_3SiCl (0.015 M). A ^1H - ^{29}Si gHSQC NMR was taken and a ^{29}Si peak at -16.8 ppm was observed (Table 3.2, Entry 3). This result was really exciting because it showed a peak similar to what we had observed previously in section 3.2.1, which was thought to be a complex peak. To claim this peak as a complex peak, we decided to do a control experiment by adding water into the same NMR sample. If the silicon NMR

peak is a result of the $\text{Ph}_3\text{SiCl}/\mathbf{1.14}$ complex then after adding water that peak should disappear. Unfortunately, the peak remained the same with no observable change in the ^1H - ^{29}Si NMR. With this result, we became suspicious that our peak at $-16.8 (\pm 1.5 \text{ ppm})$ and all previously reported peaks at -18 ppm were not originating from the complex. In another experiment, we stopped adding $\mathbf{1.14}$ (0.85 M) into a solution of Ph_3SiCl (0.015 M) after 1 equivalent. Two peaks were observed, one at -13.0 ppm and one at $+1.2 \text{ ppm}$ instead of one at -16.8 ppm . The two peaks, -13.0 and $+1.2 \text{ ppm}$, belong to Ph_3SiOH and Ph_3SiCl , respectively, showing that somehow water was introduced into our sample.

We decided to repeat both experiments, again with more caution to avoid the hydrolysis of the silyl chloride. All solvents and reagents were carefully distilled and dried before the experiment. A similar titration as discussed earlier were carried out using 0.85 M $\mathbf{1.14}$ and adding in to 0.015 M Ph_3SiCl . After adding 36 equivalents of $\mathbf{1.14}$, the ^1H - ^{29}Si HSQC NMR was taken. Two different ^{29}Si peaks were observed at -18.0 ppm and a very small one at -18.5 ppm . To confirm the complex peak, water was added to the sample. Surprisingly, the small silicon peak at -18.5 ppm disappeared while the peak at -18.0 ppm remained (shown in Figure 3.8). It is difficult for us to confirm if the small peak at -18.5 was real or not. No peak at -18.5 ppm was observed when a repetition of the above experiment using the same stock solutions was done. From the above experiment, it seems complex formation is very difficult at least at room temperature and even if it is forming, it seems highly unstable and difficult to capture.”



(A) ^1H - ^{29}Si gHSQC after adding 36 equiv of **1.14** in 0.015 M Ph_3SiCl at -18.5 ppm (B) ^1H - ^{29}Si gHSQC after adding water to see disappearance of ^{29}Si peak at -18.5 ppm

Figure 3.8 ^1H - ^{29}Si gHSQC possible complex formation at -18.5 ppm

As our data always showed a peak at -18.0 ppm, very similar to the HPDS and therefore to identify that peak, we synthesized HPDS. ^{29}Si NMR for HPDS was taken and showed a peak at -18.0 ppm as well, however we observed different in corresponding ^1H NMR peak. it is a very difficult to come to any conclusion regarding the peak observed in

past at -18 ppm (± 1.5 ppm). As we have seen -13 ppm peak (Ph_3SiOH) in our early titration study (table 3.2, Entry 4), which makes us skeptical about our peak at -18 ppm. We took commercially available Ph_3SiOH and did NMR titration using **1.14**. To our surprise, a similar shift in ^1H NMR was observed as we saw when titration was carried out using Ph_3SiCl and **1.14**. Also, to our surprise, the same ^{29}Si peak at -17.6 ppm was observed from gHSQC experiment. We thought, this shift in ^1H NMR (Figure 3.9) could be the result of hydrogen bonding of Ph_3SiOH to **1.14**. This result suggests that as we do not have any evidence regarding the complex formation mechanism between **1.14**/ Ph_3SiCl and therefore other mechanisms need to be taken under consideration. As we saw, a similar results in both a ^1H NMR as well as in ^{29}Si peak (^1H - ^{29}Si gHSQC) of Ph_3SiCl /**1.14** and Ph_3SiOH /**1.14**, therefore we thought, looking into a mechanism involving some kind of hydrogen bonding also needs to be consider at this point. In other word, one cannot rule out, the general base catalysis mechanism, as it could be one of the possibility in our system. In general base catalysis, base should involve during the rate determining step.

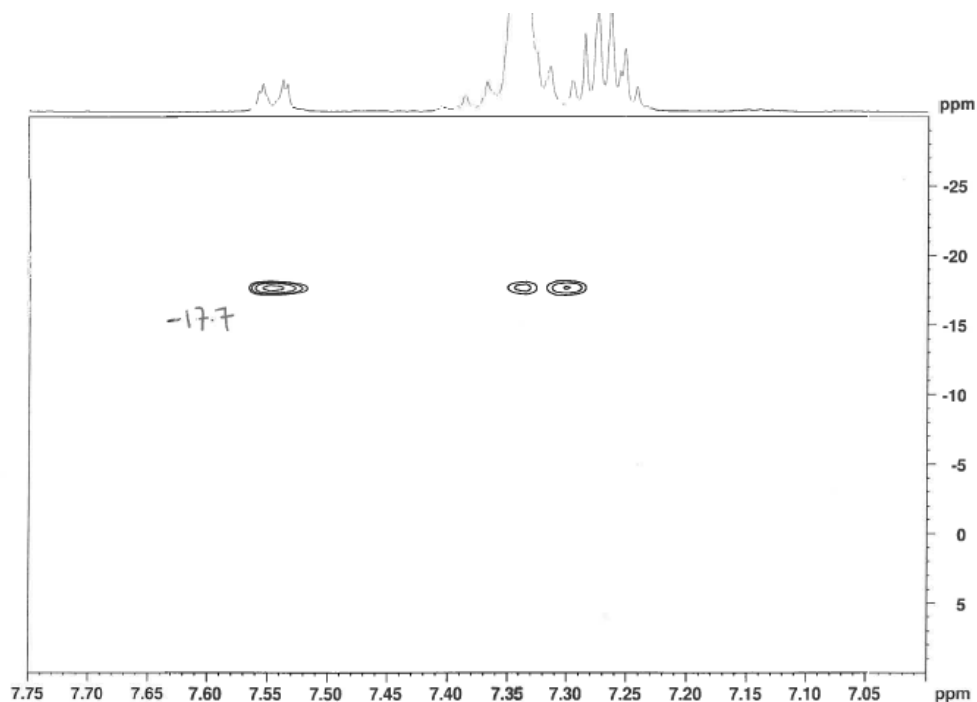
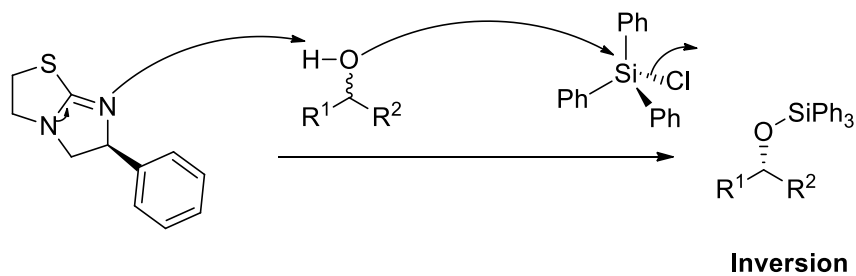


Figure 3.9 ^1H - ^{29}Si HSQC NMR of Ph_3SiOH -**1.14** at room temperature

A peak shifting was reported in ^1H NMR with **1.14**/ Ph_3SiOH . Therefore, in our system, one possible general catalysis mechanism could be the involvement of **1.14** as a Brønsted base. Hypothesis of general base catalysis is shown in Scheme 3.3. In this mechanism, catalyst (as a Brønsted base) will pull the proton from racemic alcohol (substrate) followed by attack on Ph_3SiCl .

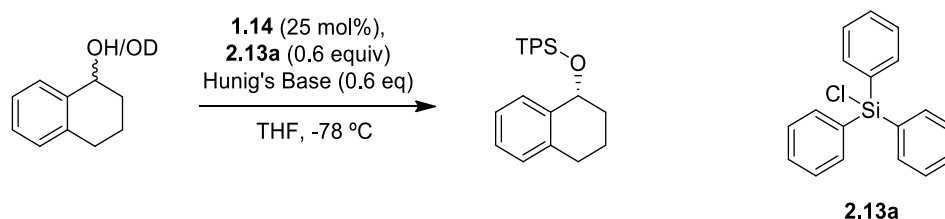
Hydrogen bonding:



Scheme 3.3 Plausible general base catalysis mechanism in our silylation-based methodology

Therefore to test a possibility of the general base catalysis mechanism in our system, we decided to perform the rate study. In general base catalysis, base should participate during the rate determining step and therefore, if our mechanism is going through general base catalysis path then using deuterated substrate should have a great impact on a rate compare to regular alcohol substrate.

Table 3.3 Rate study comparison of deuterated versus non-deuterated tetralol



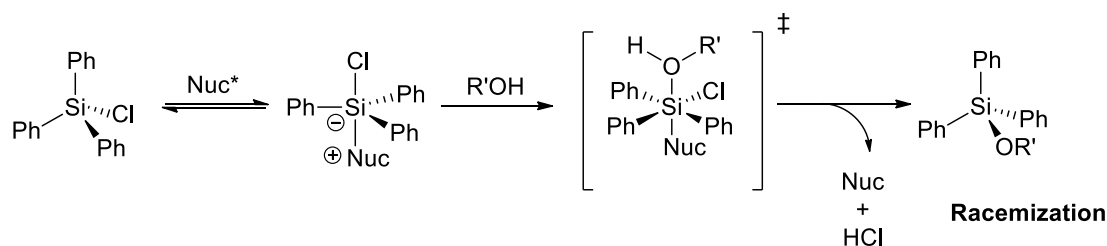
Entry	Time (min)	% Conv. ¹ H NMR -OH	% Conv. ¹ H NMR -OD
1	2	5.60	5.79
2	4	10.52	9.70
3	8	15.51	14.39
4	16	19.72	17.37
5	32	19.19	18.36
6	60	26.88	19.03

Making deuterated tetralol was found to be difficult for us. Deuterated tetralol (racemic) was synthesized using deuterated methanol through azeotrope. Due to the sensitivity of deuterium being exchanged back to the proton, the compound was directly used for study without any characterization. Using React IR, rate study was performed and rate was compared between the deuterated tetralol and regular substrate (racemic). A similar

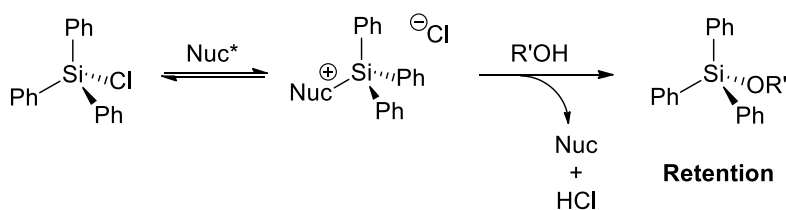
rate was observed compare to tetralol (Table 3.3).which makes really complicated to conclude any mechanism at this point.

After unsatisfactory results from all the presented studies, we looked back into our earlier discussed LFER data. A large slope was reported using the Hammett plot employing the parameter σ_{para} ²⁷ versus the log of rates for the kinetic resolution of the fast reacting enantiomer (*R*) of alcohol **2.15**. This suggested a strong negative charge or decrease in positive charge in the transition state. In all mechanisms mentioned above, we have either an increase in negative charge or decrease in positive charge. Therefore, a careful investigation is required to distinguish the operative mechanism from the three possible mechanisms (Scheme 3.4). Making a chiral silane and using that in our silylation reaction will give us more definitive answer to our actual mechanism for our silylation-based kinetic resolution. One way to quickly test our mechanism to separate complex formation (tetravalent and pentavalent) as well as the general base catalysis mechanism is to use chiral silane in our experiment (Scheme 3.4). If the mechanism involves a complex formation between **1.14**/ Ph_3SiCl , then two pathways are possible via either through a pentavalent intermediate which can give a racemization at the end or a tetravalent intermediate which could give a retention of stereochemistry. If the mechanism is proceeding through general base catalysis then, inversion will be expected in chiral silane.

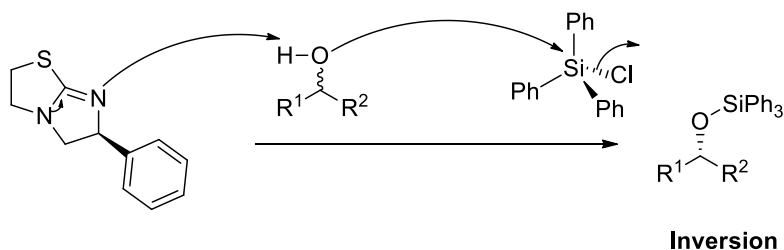
Pentavalent:



Tetravalent:



Hydrogen bonding:



Scheme 3.4 Three potential mechanisms for our silylation-based kinetic resolution

3.4 Conclusions

A mechanistic study to identify reactive intermediate was presented. In our silylation, a complex formation between **1.14** and Ph_3SiCl was anticipated based on literature reports. Two separate pathway was proposed from previous mechanistic data, tetravalent intermediate (**3.1**) and pentavalent intermediate (**3.2**). Data from the previous NMR study, shows a complex formation between **1.14** and Ph_3SiCl based on ^1H NMR shift between **1.14**/ Ph_3SiCl and **1.14**. Finally, NOE experiment was performed to further confirm complex formation between **1.14**/ Ph_3SiCl . With the help of ^1H - ^{29}Si gHSQC experiment,

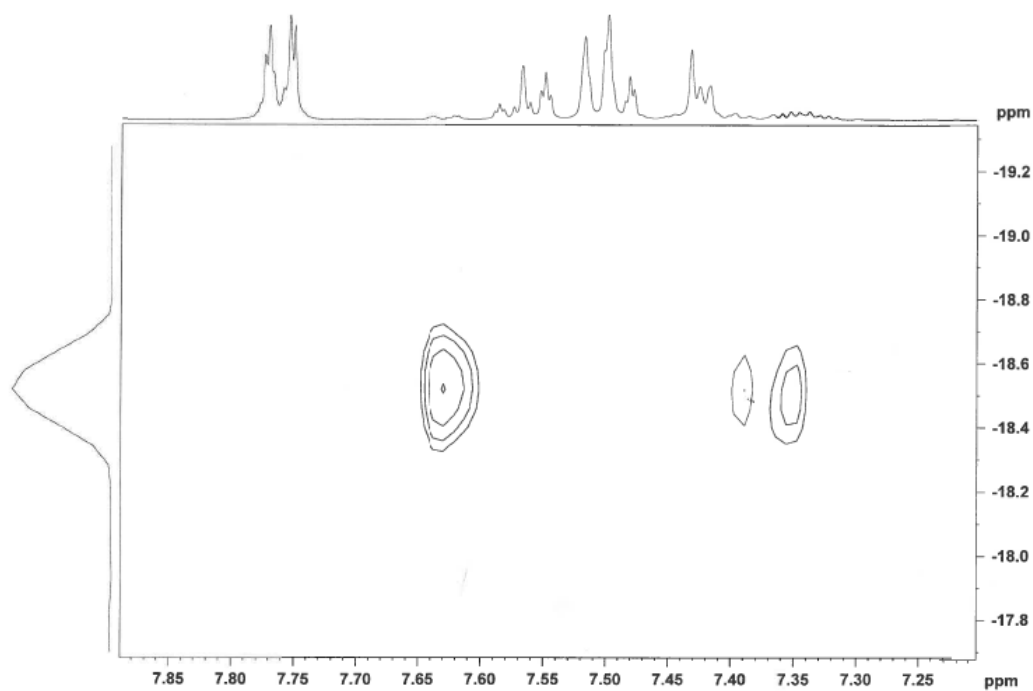
upfield shift was observed. To identify the intermediate, the observed ^{29}Si was compared to literature data. Finally, the valency of our reactive intermediate was concluded to be the tetravalent rather than pentavalent. Unfortunately, a result reported in previous study had an integration issue (complex formation through ^1H NMR) and also ^{29}Si NMR peak was very close to the hydrolyzed product (Ph_3SiOH and HPDS). To get a better integration and to avoid any hydrolyzed ^{29}Si peak from our complex. A complex formation study was repeated. Surprisingly, a completely different result was obtained and we were unable to reproduce previously reported data. Numerous attempts were made to reproduce previous data but no successful results were obtained. Further analysis was then taken under investigation. Various method were used to form a complex and then analyzed using ^1H and ^1H - ^{29}Si gHSQC. We begin to troubleshoot our experiments by avoiding any contact with moisture (moisture sensitivity of complex). The instantaneous precipitate formation after adding **1.14** into the 1 M Ph_3SiCl makes difficult to judge two reagent interaction. Therefore, a different approach was used where **1.14**/ Ph_3SiCl samples at different concentrations were directly prepared in CD_2Cl_2 using separately made stock solution of Ph_3SiCl and **1.14**. Minor change in ^1H NMR at higher concentration (0.25 M and 0.5 M) was observed while other sample has same ^1H NMR spectra as **1.14**. We thought, complex might be forming in small quantities and therefore ^1H NMR titration was used for further investigation. Excess **1.14** (higher concentration) was found to be the useful for the titration and titrated in Ph_3SiCl (lower concentration). ^1H NMR was recorded at different equivalences of **1.14** added. At saturation, ^1H - ^{29}Si gHSQC was recorded with ^{29}Si peak observed at -18.5 ppm. Repetition of same experiment was done (cautiously made sample) with different concentration of **1.14** and ^1H - ^{29}Si gHSQC was taken after adding 10 equiv

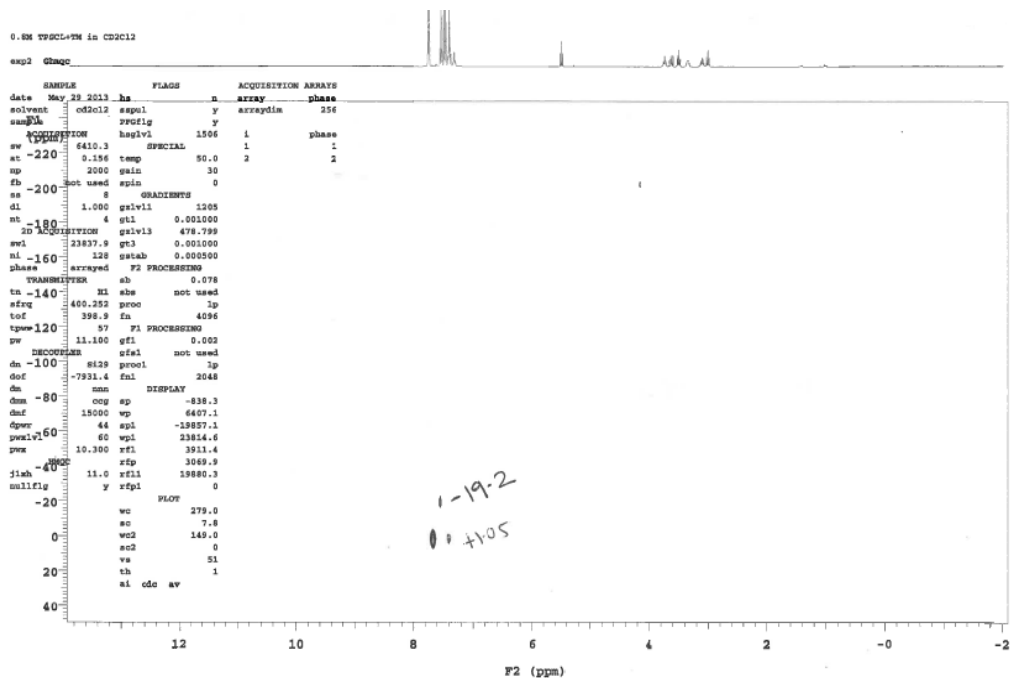
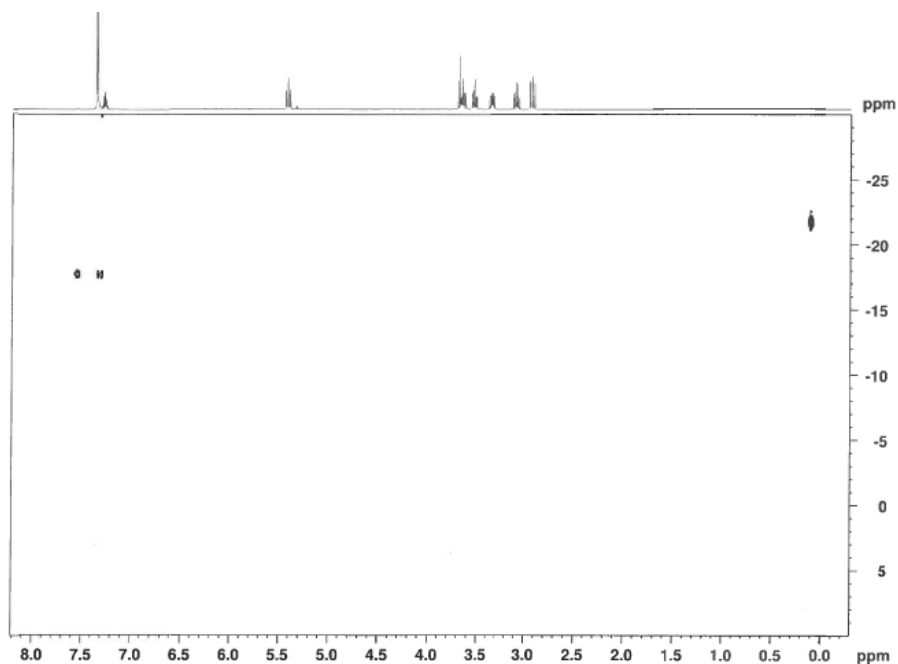
and 1 equiv of **1.14** to 0.015 M of Ph_3SiCl . With 10 equiv. of **1.14** only one ^{29}Si peak at -16.8 ppm was observed. This peak seems very promising to us as a complex peak as it was very close to claim as a complex peak in our earlier study. To further confirm, water was introduced to our sample as complex is very moisture sensitive and disappearance of peak was expected. Surprisingly, peak didn't disappear and remained as it is. Also with 1 equiv. two different ^{29}Si peak -13.0 and +1.2 ppm was observed, a very similar to Ph_3SiOH and Ph_3SiCl . It was assumed that compound was hydrolyzed somehow during sample preparation. Same experiment was repeated with extra caution. ^{29}Si peak at -18.5, -18.0 ppm and +1.2 ppm were observed. To confirm complex formation, water was introduced to our sample and peak at -18.5 disappeared. It appears peak at -18.5 could be the complex peak and but very close to the HPDS peak. However, we were unable to reproduce the result. As in all experiments, hydrolyzed product was found to be the major problem in our complex formation. To further address this problem, we simply titrated **1.14** in Ph_3SiOH and ^1H - ^{29}Si gHSQC were recorded. A ^1H NMR peak shifting was observed in **1.14** region of spectra. Also, from gHSQC, ^{29}Si peak at -17.6 ppm was observed. This data was very confusing due to the similar silicon peak as complex. Other mechanism like general base catalysis was taken under consideration where **1.14** was assumed to be acting as Brønsted base to substrate followed by attack on Ph_3SiCl . To test this hypothesis, an absolute rate study of deuterated substrate was done and compared to regular substrate. Almost no difference in rate was observed. From all this data, we were unable to come to any conclusion at this point and therefor in future, further investigation is required. This study still provides very useful information which needs to be consider for future analysis which include sensitivity of complex formation, use of different approach to make sample

of **1.14**/ Ph_3SiCl (specially solvent and ^1H NMR titration) and possibility of other mechanism which would have been missed without this investigation.

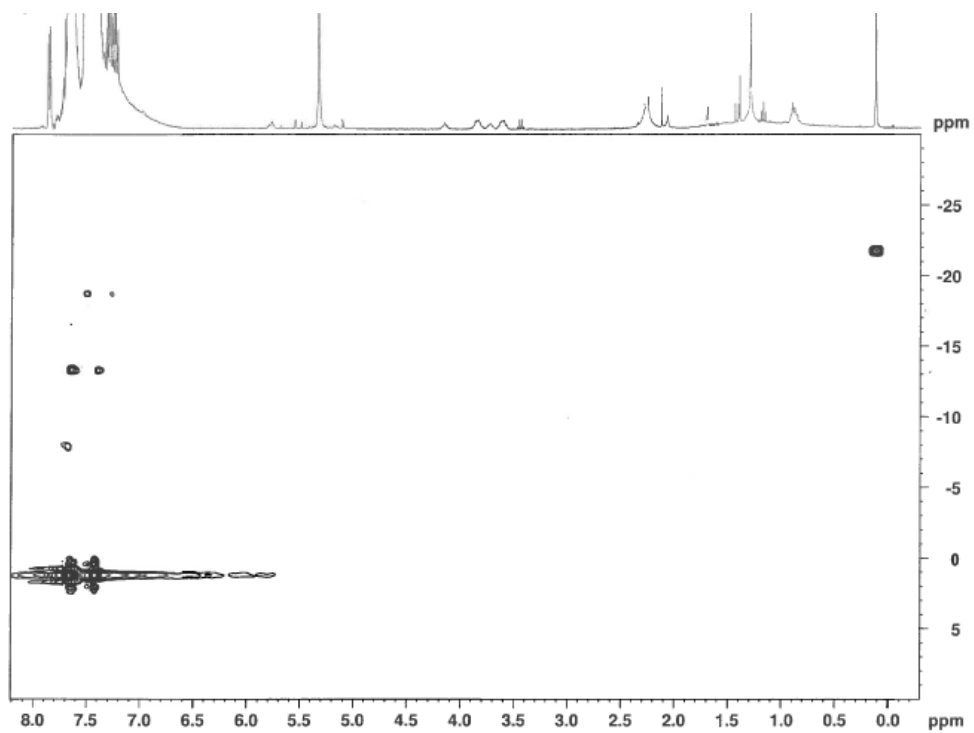
3.5 Experimental

NMR Spectra: ^1H - ^{29}Si gHSQC NMR at 0.5 M 1:1 Ph_3SiCl /**1.14**

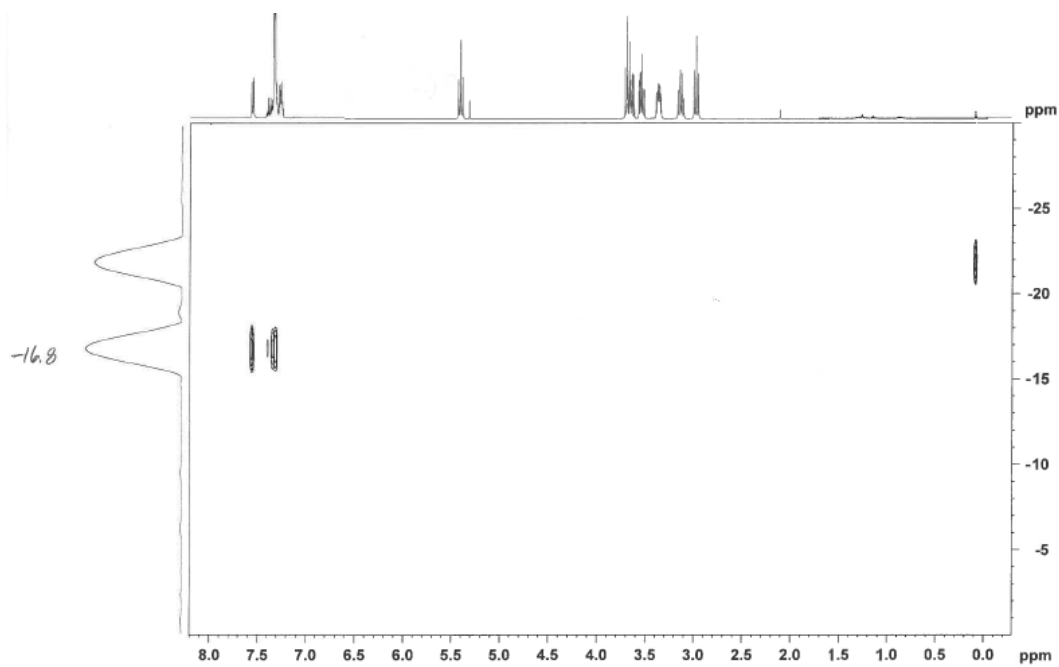


¹H-²⁹Si gHSQC NMR at 0.8 M 1:1 Ph₃SiCl/**1.14**¹H-²⁹Si gHSQC 500 eq. of excess **1.14** (1.7 M) in 0.015 M Ph₃SiCl (Table 3.2, Entry 1)

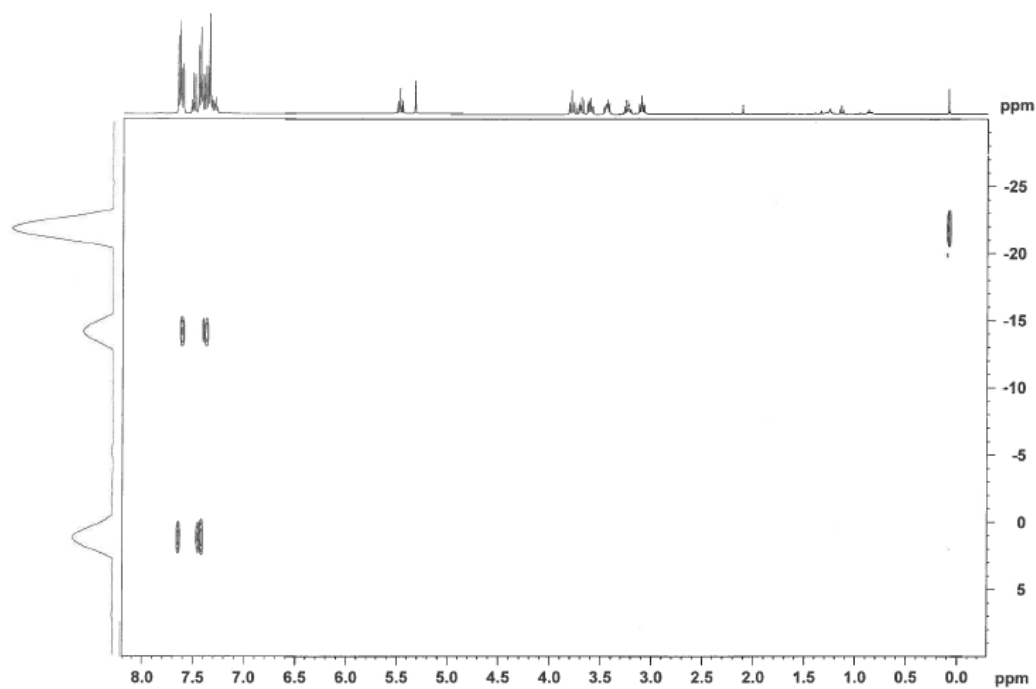
^1H - ^{29}Si gHSQC 200 eq. of excess Ph_3SiCl (1.7 M) in 0.015 M **1.14** (Table 3.2, Entry 2)



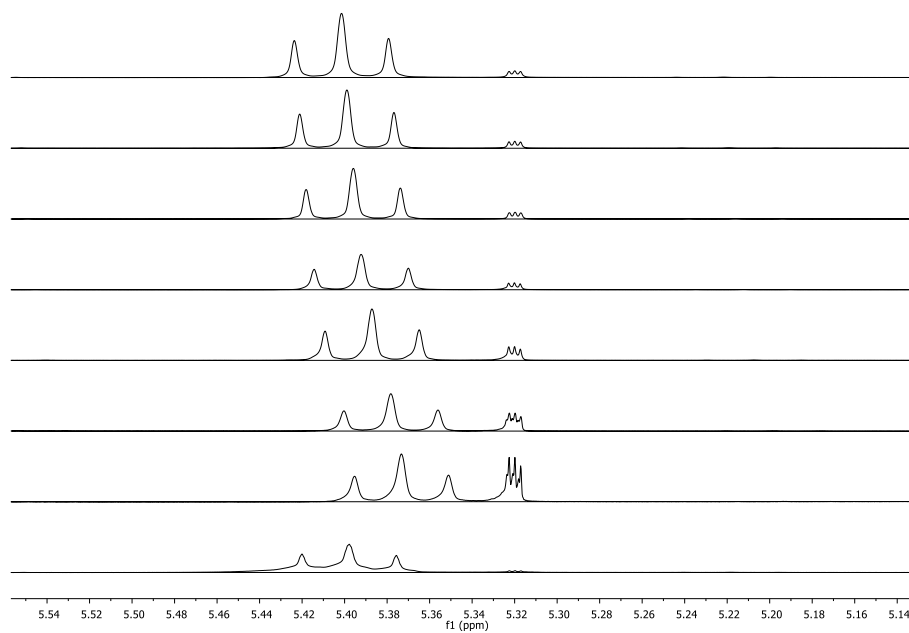
^1H - ^{29}Si gHSQC 10 equiv. of excess **1.14** (0.85 M) in 0.015 M Ph_3SiCl



^1H - ^{29}Si gHSQC 1 equiv. of **1.14** (0.85 M) in 0.015 M Ph_3SiCl



^1H NMR titration of $\text{Ph}_3\text{SiOH}/\mathbf{1.14}$ (germinal proton shifting of catalyst)



3.6 References

- (1) Clark, R. W.; Deaton, T. M.; Zhang, Y.; Moore, M. I.; Wiskur, S. L. Silylation-based kinetic resolution of alpha-hydroxy lactones and lactams. *Org. Lett.* **2013**, *15*, 6132-6135.
- (2) Sheppard, C. I.; Taylor, J. L.; Wiskur, S. L. Silylation-based kinetic resolution of monofunctional secondary alcohols. *Org. Lett.* **2011**, *13*, 3794-3797.
- (3) Klauck, M. I.; Patel, S. G.; Wiskur, S. L. Obtaining enriched compounds via a Tandem enantioselective reaction and kinetic resolution polishing sequence. *J. Org. Chem.* **2012**, *77*, 3570-3575.
- (4) Chuit, C.; Corriu, R. J. P.; Reye, C.; Young, J. C. Reactivity of pentacoordinate and hexacoordinate silicon-Compounds and their role as reaction intermediates. *Chem. Rev.* **1993**, *93*, 1371-1448.
- (5) Chu, H. K.; Johnson, M. D.; Frye, C. L. Tertiary alcoholysis of chlorosilanes via tetracoordinate silylated quaternary ammonium intermediates. *J. Organomet. Chem.* **1984**, *271*, 327-336.
- (6) Bassindale, A. R.; Stout, T. A Si-29, C-13 and H-1-NMR study of the Interaction of various halotrimethylsilanes and trimethylsilyl triflate with dimethyl formamide and acetonitrile - A comment on the nucleophile induced racemization of halosilanes. *J. Organomet. Chem.* **1982**, *238*, C41-C45.
- (7) Chojnowski, J.; Cypryk, M.; Michalski, J. Nature of interaction between hexamethyl-phosphortriamide and trimethylhalosilanes - Cations containing tetravalent silicon as possible intermediates in nucleophile-induced substitution of silicon halides. *J. Organomet. Chem.* **1978**, *161*, C31-C35.
- (8) Rendler, S.; Oestreich, M. Hypervalent silicon as a reactive site in selective bond-forming processes. *Synthesis-Stuttgart* **2005**, 1727-1747.
- (9) Marciniak, B.; Chojnowski, J. Progress in organosilicon chemistry., 1st ed.; Gordon and Breach: Amsterdam, 1995.
- (10) Patai, S.; Apeloig, Y. The chemistry of organic silicon compounds. . John Wiley & Sons Ltd: Chichester, 2001; Vol. 3.
- (11) Weickgenannt, A.; Mewald, M.; Oestreich, M. Asymmetric Si-O coupling of alcohols. *Org. Biomol. Chem.* **2010**, *8*, 1497-1504.

- (12) Rodrigo, J. M.; Zhao, Y.; Hoveyda, A. H.; Snapper, M. L. Regiodivergent reactions through catalytic enantioselective silylation of chiral Diols. synthesis of sapinofuranone A. *Org. Lett.* **2011**, *13*, 3778-3781.
- (13) Manville, N.; Alite, H.; Haeffner, F.; Hoveyda, A. H.; Snapper, M. L. Enantioselective silyl protection of alcohols promoted by a combination of chiral and achiral Lewis basic catalysts. *Nat. Chem.* **2013**, *5*, 768-774.
- (14) Isobe, T.; Fukuda, K.; Araki, Y.; Ishikawa, T. Modified guanidines as chiral superbases: the first example of asymmetric silylation of secondary alcohols. *Chem. Commun.* **2001**, 243.
- (15) Sun, X.; Worthy, A. D.; Tan, K. L. Scaffolding catalysts: Highly enantioselective desymmetrization reactions. *Angew. Chem., Int. Ed.* **2011**, *50*, 8167-8171.
- (16) Sun, X.; Worthy, A. D.; Tan, K. L. Resolution of terminal 1,2-Diols via silyl transfer. *J. Org. Chem.* **2013**, *78*, 10494-10499.
- (17) Birman, V. B.; Li, X. M. Benzotetramisole: A remarkably enantioselective acyl transfer catalyst. *Org. Lett.* **2006**, *8*, 1351-1354.
- (18) Akhiani, R. K.; Moore, M. I.; Pribyl, J. G.; Wiskur, S. L. Linear free-energy relationship and rate study on a silylation-based kinetic resolution: mechanistic insights. *J. Org. Chem.* **2014**, *79*, 2384-2396.
- (19) Hansch, C.; Leo, A.; Taft, R. W. A survey of hammett substituent constants and resonance and field parameters. *Chem. Rev.* **1991**, *91*, 165-195.
- (20) Anslyn, E. V.; Dougherty, D. A. *Modern physical organic chemistry*; University Science: Sausalito, Calif., 2006.
- (21) Bassindale, A. R.; Stout, T. A ^{29}Si , ^{13}C and ^1H NMR study of the interaction of various halotrimethylsilanes and trimethylsilyl triflate with dimethyl formamide and acetonitrile. A comment on the nucleophile induced recamisation of halosilanes. *J. Organomet. Chem.* **1982**, *238*, C41-C45.
- (22) Cody Sheppard dissertation Chapter 3.
- (23) Brendler, E.; Heine, T.; Hill, A. F.; Wagler, J. A Pentacoordinate Chlorotrimethylsilane Derivative: A very Polar Snapshot of a Nucleophilic Substitution and its Influence on Si-29 Solid State NMR Properties. *Z. Anorg. Allg. Chem.* **2009**, *635*, 1300-1305.
- (24) Bearpark, M. J.; McGrady, G. S.; Prince, P. D.; Steed, J. W. The first structurally characterized hypervalent silicon hydride: Unexpected

molecular geometry and Si-H center dot center dot center dot K interactions. *J. Am. Chem. Soc.* **2001**, *123*, 7736-7737.

- (25) Rot, N.; Nijbacker, T.; Kroon, R.; de Kanter, F. J. J.; Bickelhaupt, F.; Lutz, M.; Spek, A. L. Introduction of bulky substituents at the bridgehead position of a 9-silatriptycene: Pentacoordinate hydridoorganylsilicates as intermediates. *Organometallics* **2000**, *19*, 1319-1324.
- (26) Bassindale, A. R.; Stout, T. The preparation and observation by Si-29 NMR-Spectroscopy of simple, acyclic, 5-Co-ordinate silicon salts. *J Chem Soc Chem Comm* **1984**, 1387-1389.
- (27) Hansch, C.; Leo, A.; Taft, R. W. A survey of hammett substituent constants and resonance and field parameters *Chem. Rev.* **1991**, *91*, 165-195.

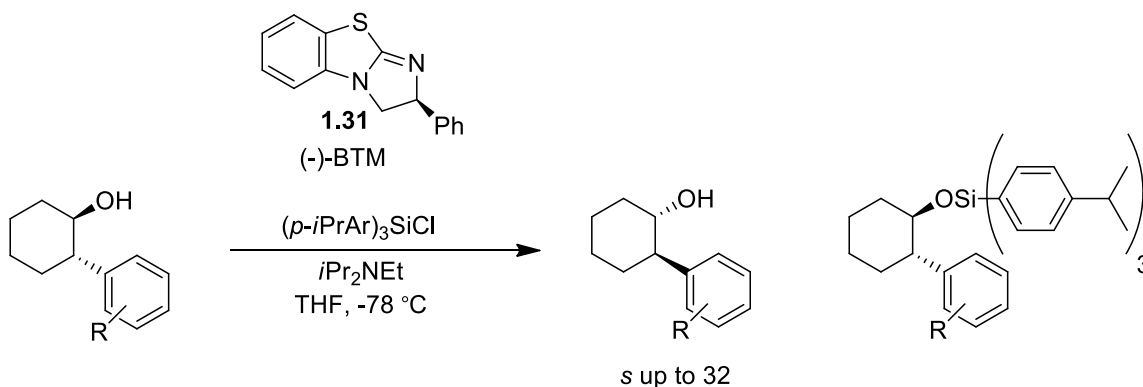
CHAPTER 4

SUBSTRATE EXPANSION: KINETIC RESOLUTION OF ALLYLIC ALCOHOLS, HOMO ALLYLIC ALCOHOLS AND 2-ARYLCYCLOHEXANOLS USING OUR Silylation BASED METHODOLOGY

4.1 Introduction

As discussed in chapter 1, a silylation based kinetic resolution methodology developed in the Wiskur lab was successfully applied to monofunctional secondary alcohols.¹ To apply this methodology for further expansion of the substrate class, several allylic alcohols and homoallylic alcohols were analyzed. Unfortunately no selectivity was observed with allylic alcohols except with one substrate ((-)-carveol). Meanwhile, α -hydroxyl lactones and lactams were found to be the selective substrate class by other graduate student in the Wiskur lab.² After careful analysis of the selective substrates, a common structural pattern was discovered. Using this information, a new substrate class, 2-substituted cycloalkanols, was found to be the most logical substrate class to explore. Commercially available (\pm)-*trans*-2-phenylcyclohexanol was used for the preliminary investigation. Similar reaction conditions to previous kinetic resolutions were employed. Moderate levels of selectivity ($s = 5.9$) were observed using Ph_3SiCl and (-)-BTM (**1.31**) as the catalyst.

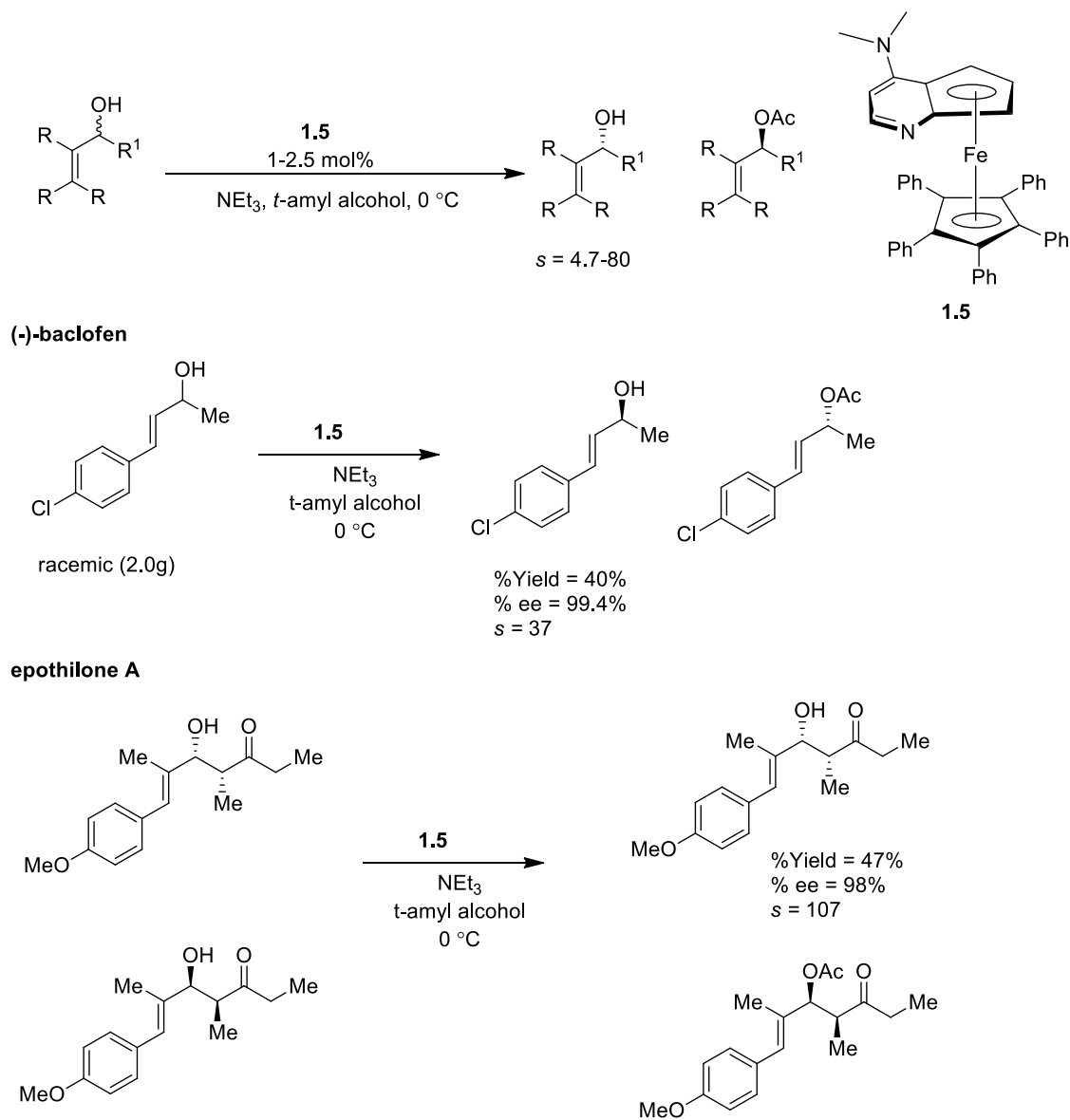
To further improve the selectivity, the information obtained from our previous mechanistic study (as discussed in chapter 2) was utilized.³ Electron donating *para* substituted tris(4-isopropylphenyl)silyl chloride was employed as the silyl source in the kinetic resolution of (\pm)-*trans*-2-phenylcyclohexanol with (-)-BTM as the catalyst. The selectivity factor improved from 5.9 to 10. This chapter will highlight our preliminary efforts to identify a new substrate class, the reaction optimization to improve the selectivity, and the substrate synthesis.



4.2 Background

The silylation based kinetic resolution developed in the Wiskur lab was successfully applied to the monofunctional secondary alcohols.¹ To extend this methodology to other substrate classes, allylic alcohols were taken under investigation due to their biological importance.^{4,5,6} The most discussed non enzymatic kinetic resolution of allylic alcohol was reported by Barry Sharpless (Discussed in Chapter 1).⁷ In this system, various allylic alcohols were reported with selectivity factors⁸ ranging from 15 to 140. The major drawback of this methodology is the long reaction times. In some cases a reaction was required to run for 4-12 days, which can limit its practicality. With regards to organocatalyzed kinetic resolutions of allylic alcohols there are only limited examples

reported in the literature.⁹⁻¹¹ In 2000, the Fu group reported a method to successfully resolve allylic alcohols.¹⁰ In this reaction, a derivative of the planar chiral DMAP (**1.5**) was used as a catalyst.

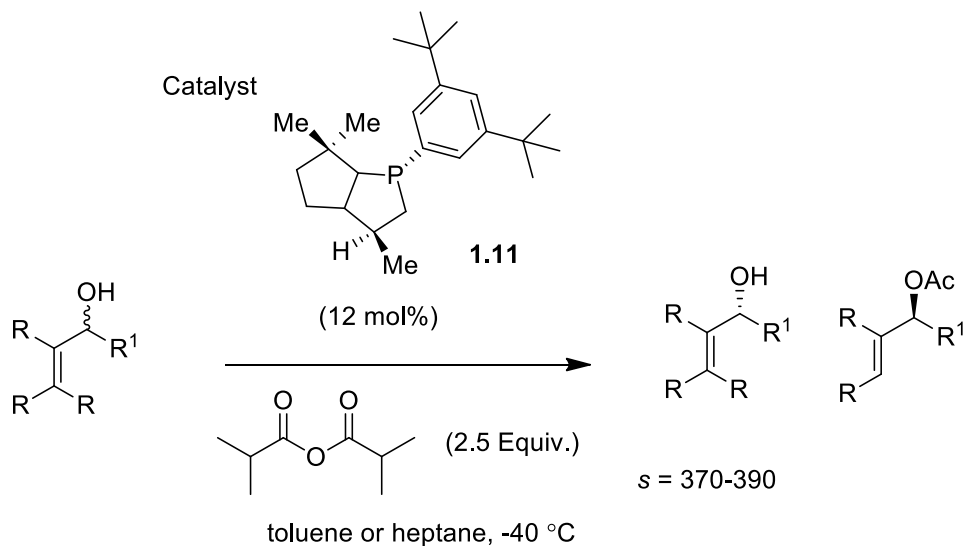


Scheme 4.1 Kinetic resolution of allylic alcohols developed by the Fu group and its application to the synthesis of (-) baclofen and epothilone A

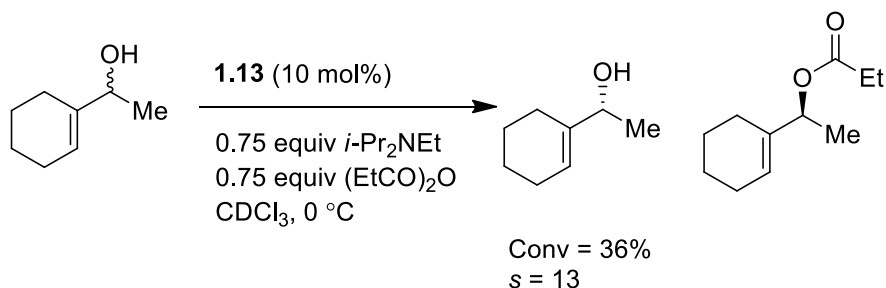
Several structurally diverse allylic alcohols were resolved using this methodology with selectivity factors ranging 5-80. To demonstrate the applicability of this system, Fu showed the kinetic resolution of two allylic alcohols which are key intermediates for the synthesis of (-) baclofen¹² and epothilone A¹³ (Scheme 4.1).

In 2001, the Vedejs group also reported the kinetic resolution of allylic alcohols using a chiral phosphine as a catalyst (**1.11**).⁹ In this methodology, a reaction was performed at -40 °C using 2.5 equivalents of isobutyric anhydride in toluene with selectivities ranging from 25-82 (Scheme 4.2 (A)). More recently, the Birman group has also used an amidine based catalyst (ABC) to resolve various allylic alcohols with moderate to good (2-22) selectivity (Scheme 4.2 (B)).¹¹ All of the examples discussed above employ acylation as a means of derivatization. Since silyl groups are one of the most common protecting groups in organic chemistry, it makes sense to employ them as a means of separating enantiomers in kinetic resolutions. The advantages of silyl groups include tunable reactivity, orthogonality to other protecting groups, and tolerance of many other functional groups.¹⁴ To the best of our knowledge, not a single report published in the literature for the kinetic resolution of allylic alcohols that employs silylation. In this regards, we decided to investigate several allylic alcohols as shown in Table 4.1.

A. Kinetic resolution reported by Vedejs Group



B. Kinetic resolution reported by Birman Group



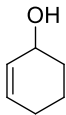
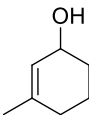
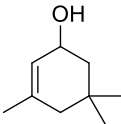
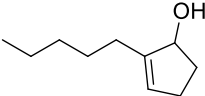
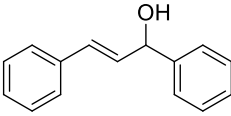
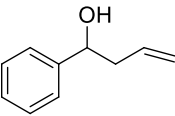
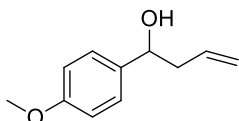
Scheme 4.2 Kinetic resolution of allylic alcohols reported by the Vedejs group and the Birman group

4.3 Silylation based kinetic resolution of allylic and homoallylic alcohols

Several commercially available allylic alcohols were purchased. Similar reaction conditions were employed in the kinetic resolution of allylic alcohols as utilized for previous substrates (monofunctional secondary alcohols).¹ Commercially available (-)-tetramisole (**1.14**) was used as the catalyst and triphenylsilyl chloride as the silicon source.

THF was used as a solvent and all reactions were carried out at -78 °C. We began our kinetic resolution reaction study using 2-cyclohexen-1-ol as a substrate. To our surprise, the recovered starting material was racemic after 24 h with a 32% conversion. To improve the selectivity factor and to understand this substrate class, we turned our attention towards various structurally modified 2-cyclohexen-1-ol (Table 4.1, entry 2-4). A similar result was obtained when the substrate containing a methyl group at the C3 position was investigated. To make the substrate more sterically hindered both C3 and C5 substituted 2-cyclohexene-1-ol was used in the kinetic resolution (entry 3). No improvement in selectivity factor was observed. Finally a slight improvement in the selectivity factor was observed when the C2 position of cyclohex-2-enol was substituted with a pentyl group (entry 4). Due to the lack of significant change in the selectivity factors for the allylic alcohols, we next tried homoallylic alcohols. Various homoallylic alcohols were investigated but no successful selectivity was observed (Table 4.1, entry 5-7). It was really surprising for us that none of the allylic alcohols as well as homoallylic alcohols were selective.

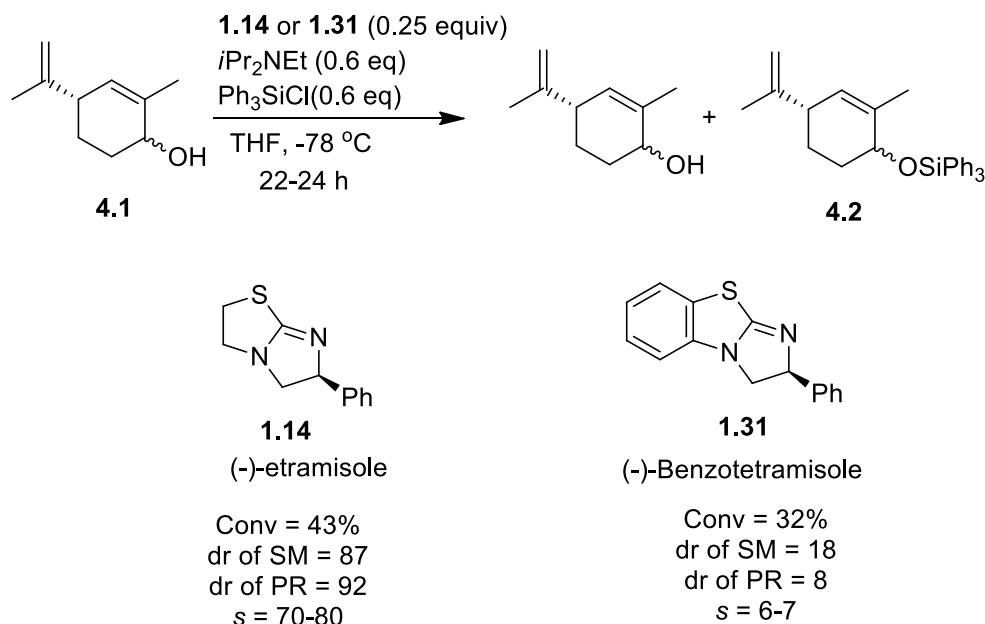
Table 4.1. Kinetic resolution of structurally different allylic & homoallylic alcohols

entry	substrate	t(h)	%C ^a	er of recovered SM	s ^b
1 ^c		24	32	52:48	1.2
2 ^c		18	41	51:49	1.1
3 ^c		18	41	≤5%	1.2
		24 ^d	42	9.4	1.4
4		15	46	68:32	3.4
5		15	46	58:42	1.7
		15 ^d	50	35:65	2.4
6		16	40	51:49	1.1
7		16	52	55:45	1.3

^a Conv corresponds to single run. ^b Selectivity factor is an average of two run ^c Conv is based on ¹H NMR

^d Kinetic resolution was done using **1.31** as a catalyst. Due to the chromophore issue, HPLC traces for Entry 1-4 needs to be repeated before publication using benzylation for accurate data.

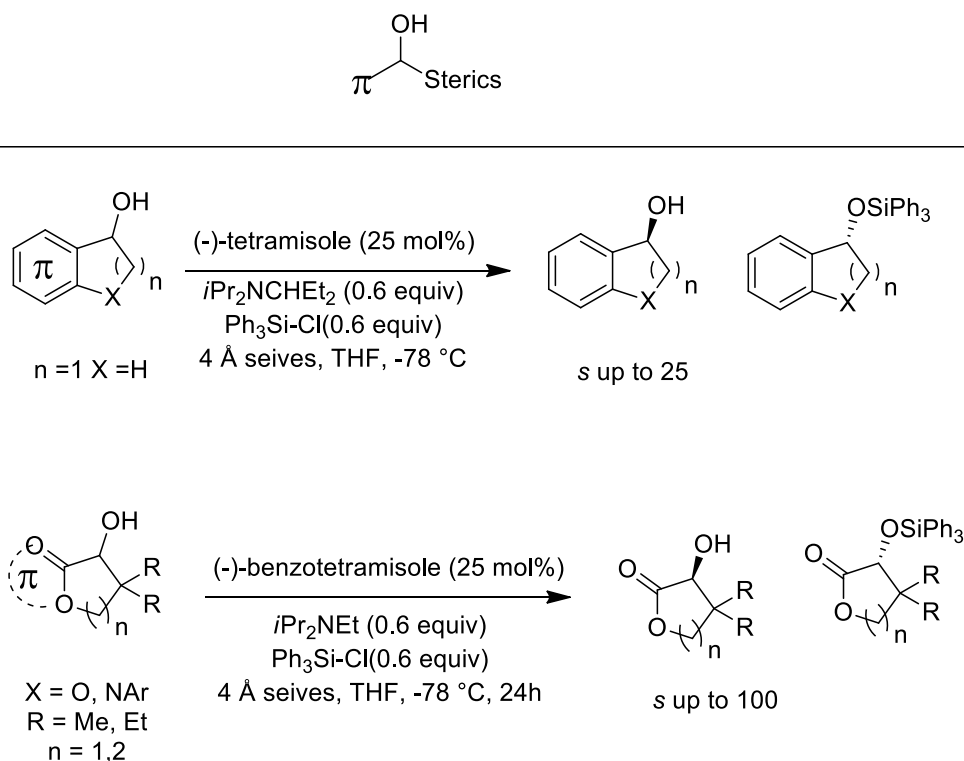
From the Table 4.1 data only one result (entry 4) showed some level of selectivity. Therefore, we thought using the structurally similar and available (-)-carveol (**4.1**) (monocyclic monoterpenoid) would be interesting for our kinetic resolution reaction.¹⁵ Moreover, carveol has a wide range of applications in organic synthesis as a chiral template.¹⁶⁻¹⁸ A kinetic resolution was done using a diastereomeric mixture (55:45) of **4.1**. Therefore, after kinetic resolution of (-)-carveol, selectivity factor was calculated using diastereomeric ratio of the product and starting material. Both catalyst **1.14** and **1.31** were tested. In the case of (-)-tetramisole, a selectivity factor greater than 70 was obtained while surprisingly (-)-benzotetramisole gave a selectivity factor of 6-7 (Scheme 4.3). There is a huge difference in selectivity factors between (-)-carveol (**4.1**) and the previously screened allylic alcohol (Table 4.1, entry 4). A major difference between two structures is the extra stereocenters, which could be the reason for the higher selectivity factor in (-)-carveol. The higher selectivity in (-)-carveol seems to be very promising for further expansion of similar substrates containing set mixture of diastereomers. In future various structurally similar to (-)-carveol type diastereomeric mixture will be tested, as it promise better selectivity factor. At this point, the goal for us was to find a substrate without any set stereocenter (purely based on enantiomers) and therefore we carried our further search of an appropriate substrate class.



Scheme 4.3 Silylation based kinetic resolution of (-)-carveol

Since most of the allylic alcohols were not selective, we decided move to another substrate class. During the same time, other members of the Wiskur group reported α -hydroxy lactones as selective substrates (another biologically important substrate)¹⁹⁻²² using our silylation based methodology with a slight modification in the catalyst compared to the monofunctional secondary alcohols. In this substrate, (-)-BTM (**1.31**) was found to be the most selective catalyst compared to **1.14**, along with triphenylsilyl chloride as a silicon source. Several structurally modified α -hydroxyl lactones were found to be the selective with *s* up to 100.² With this information in hand, we thought it would be very important for us to identify common structural features of selective substrates before screening any other substrate classes. Interestingly, we found both substrate classes, monofunctional secondary alcohols and α -hydroxyl lactones, have the same types of topology (as shown in Scheme 4.4) To achieve a better selectivity factor, two fundamental structural feature were found common in both substrate class, a π system adjacent to the

chiral center and sterics on the opposite side of the π system. In both substrate classes, we observed that the removal of either sterics or the π system dramatically diminished the selectivity.^{1,2}



Scheme 4.4 Common structural topology in previously studied kinetic resolutions

Since the combination of the π -system and the sterics were promising in our previously investigated substrates, we decided to explore a substrate class containing a similar topology. The goal was to find a substrate class which will be either simple to synthesize or commercially available. Fortunately, commercially available 2-arylcyclohexanols were found to align closely with the above mentioned substrate requirements. This substrate has a very similar topology, except the π system is one carbon further away from the alcohol instead of adjacent to it. We thought this would be a good way to check the role of the π system when it is a one carbon away. Besides topology,

another reason we became interested in this particular substrate class was the presence of this moiety in many biologically important compounds (Figure 4.1) which includes lycorine,^{23,24} (+)-catechin, PF-998,425²⁵ and several other compounds.²⁶

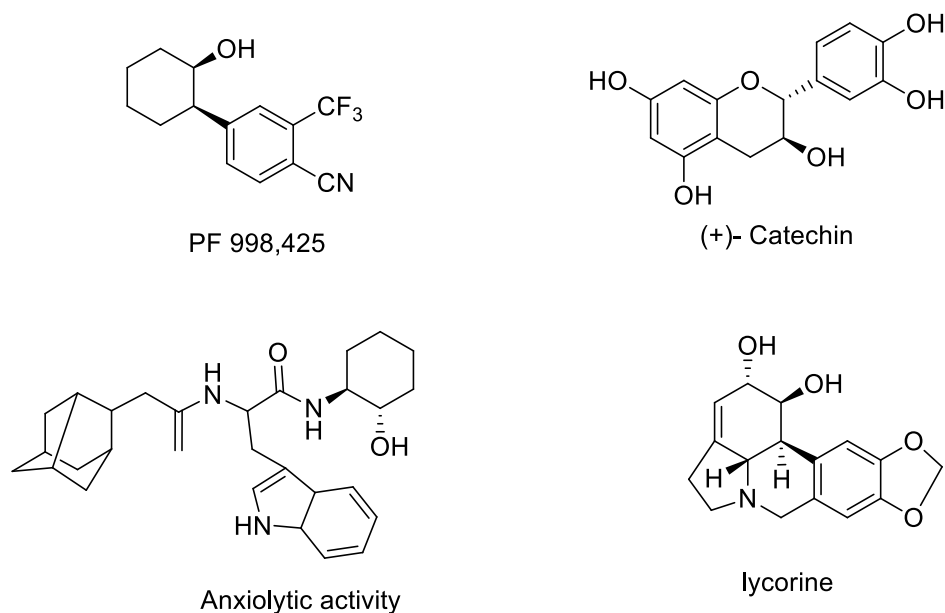
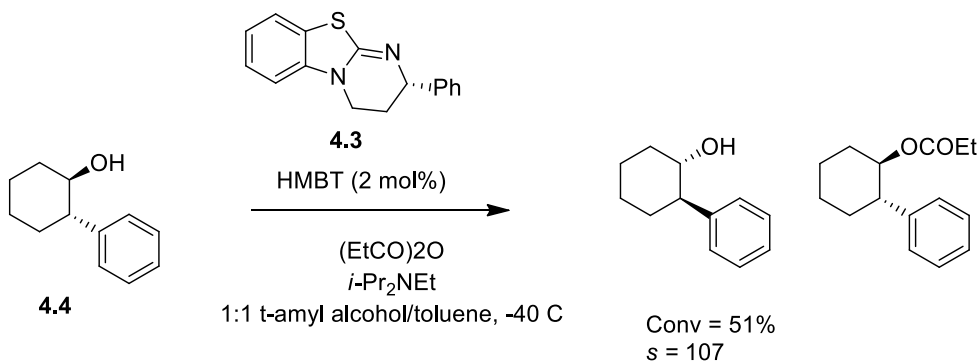


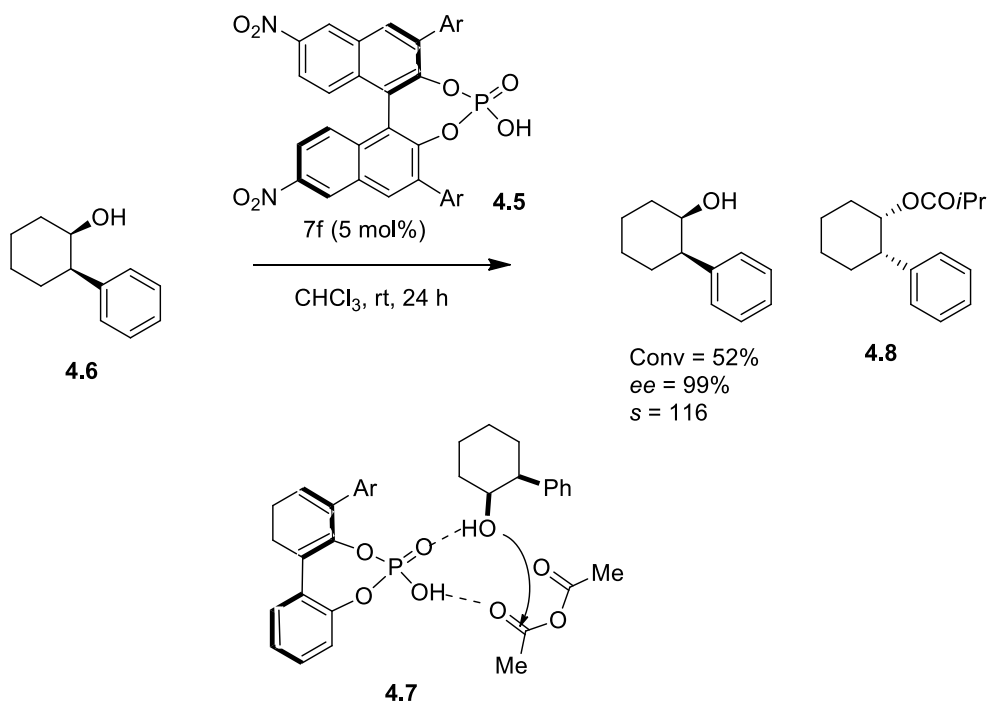
Figure 4.1 2-Arylcycloalkanols moiety in bioactive compounds

There are limited examples of non-enzymatic kinetic resolutions of 2-arylcycloalkanols that have been reported in the literature.²⁷⁻²⁹ In 2009, the Birman group successfully resolved this substrate class **4.4** ((±)trans 2-arylcycloalkanols) using homobenzotetramisole (**4.3**) as a catalyst through acylation.³⁰ Several structurally different 2-arylcycloalkanols including trans-aryl and hetero-aryl groups at the C2 position of cyclohexanols were found to be very selective. The highest selectivity factor was achieved at -40 °C using *t*-amyl alcohol as the solvent. This methodology reports selectivity factors ranging from 3-107 (Scheme 4.5). Scheme 4.2 shows the kinetic resolution of **4.4** using (**4.3**) as a catalyst with a selectivity factor of 107.

Birman:



Yamada & Takasu:

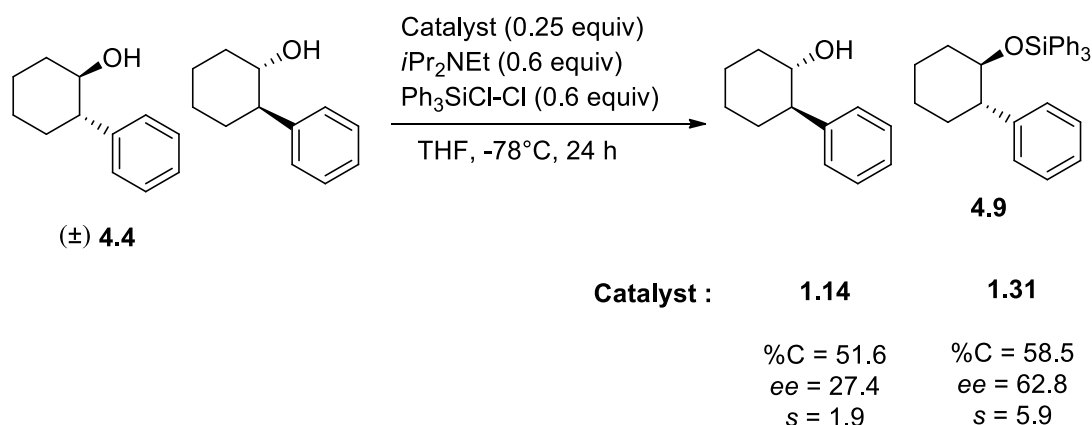


Scheme 4.5 Non-enzymatic kinetic resolutions reported in literature for 2-arylcyloalkanols

More recently, the Yamada and Takasu groups have also reported a non-enzymatic kinetic resolution with a similar substrate class using a Brønsted acid activated acylation.³¹ In contrast to the Birman report, this methodology has resolved various (\pm)-*cis*- 2-arylcyloalkanols (**4.6**) with selectivity factors up to 215. In this report, a chiral Brønsted

acid was used to activate the acylating reagent. Chiral phosphoric acid (**4.5**) was used as a catalyst and isobutyric anhydride as an acylating reagent. The transition state **4.7** was proposed using B3LYP/6-31G** molecular modeling. Hydrogen bonding of the catalyst to the alcohol and the anhydride was found as a source of chirality determination (Scheme 4.5).

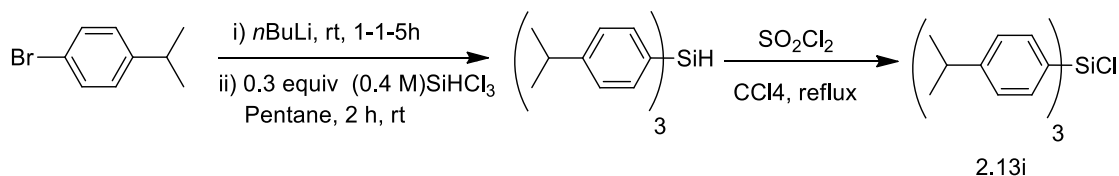
Due to this limited literature report and the interesting application of 2-arylcycloalkanols class, we (including graduate student Li Wang and undergraduate student Julia Pribyl in the Wiskur group) started to investigate this substrate class using our silylation based kinetic resolution methodology. To begin our investigating, commercially available (\pm)-*trans*-2-phenylcyclohexanol was purchased. Since the reaction conditions were very similar between our previous substrates, the same reaction conditions were used for the investigating of this substrate. In the previous substrate classes, switching the catalysts from (-)-TM (**1.14**) to (-)-BTM (**1.31**) had shown a dramatic effect on the selectivity factor. Specifically, **1.14** was found to be more selective in the case of monofunctional secondary alcohols, while **1.31** was more selective with α -hydroxyl lactones. In this regard, we decided to test both **1.14** as well as **1.31** as our catalyst with triphenylsilyl chloride as the silicon source. To test both catalysts, reactions were run for 24 h using substrate **4.4** at a concentration of 0.42 M. Almost racemic mixture of recovered starting material was obtained when **1.14** was used as the catalyst, while **1.31** produced a moderate level of selectivity (5.9)³² (Scheme 4.6). This difference between selectivity factors shows that **1.31** is the better catalyst compared to **1.14** in this substrate class. This moderate selectivity factor was still promising for us to do a further investigation.



Scheme 4.6 Investigation of a catalyst using (±)-*trans*-2-phenylcyclohexanol

Next, we turned our attention towards improvement of the selectivity factor. We decided to test our silyl source. Since we had observed an effect on selectivity in substituting the triphenylsilyl chloride in the *para* position in a silylation based kinetic resolution (as discussed in Chapter 2),³ we thought this would be interesting to apply to our reaction to improve the selectivity of our newly discovered substrate ((±)-*trans*-2-phenylcyclohexanol). One of the major advantages for examining *para* substituted triphenylsilyl chloride is that we have a good understanding on how these reagents affect the selectivity. In the previous mechanistic study using a LFER, the selectivity factor was found to be improved by using a sterically hindered electron donating group (EDG) at the *p*-position of triphenylsilyl chlorides. Therefore, using a sterically hindered EDG at the *p*-position of triphenylsilyl chloride was used in the kinetic resolution of **4.4**. In the past, we reported a better selectivity factor with chlorotris(4-*tert*butylphenyl)silane, but this silyl chloride was quite insoluble. Since these reactions were being to run at much higher concentrations, we decided not to employ chlorotris(4-*tert*butylphenyl)silane since the solubility of silyl chloride was big concern for our study. To get a better solubility of our

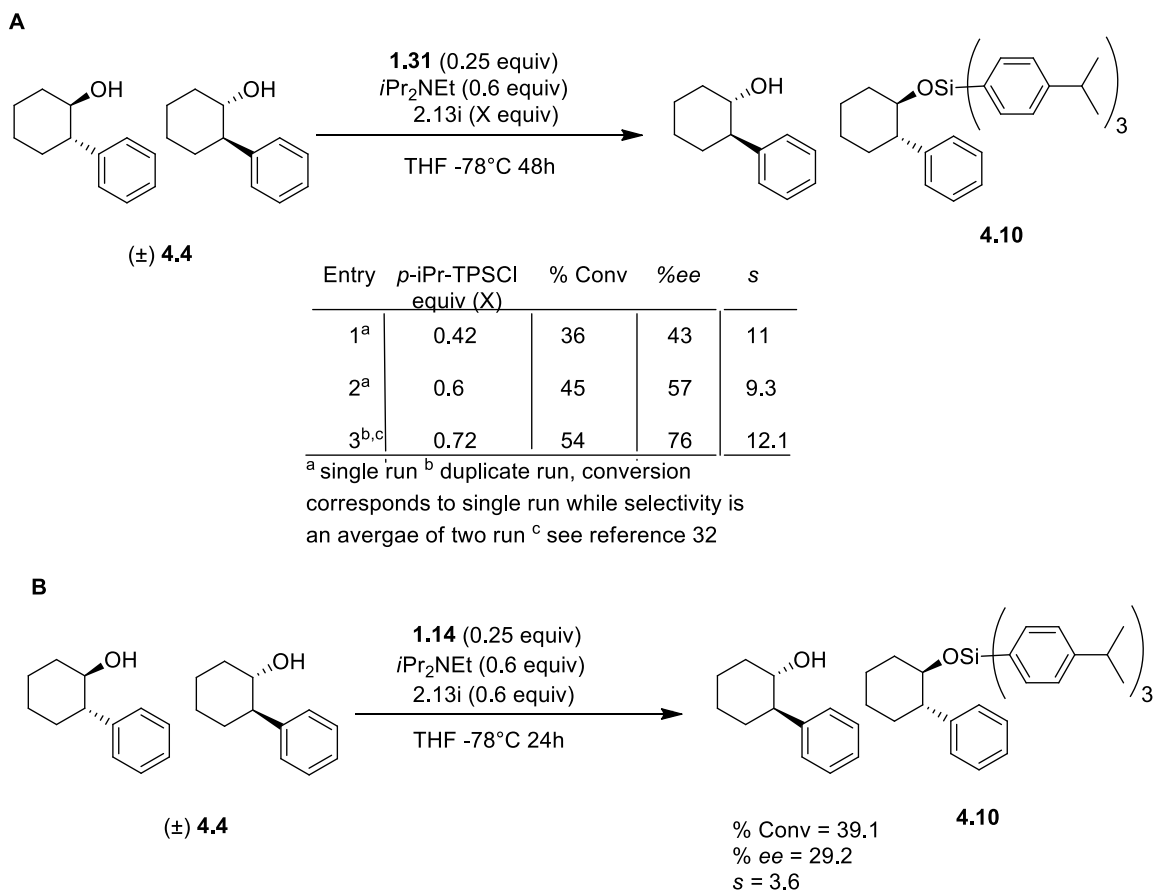
silyl chloride and also to get an improved selectivity factor, a very similar chlorotris(4-isopropylphenyl)silane (**2.13i**) was synthesized (**Scheme 4.7**) (discussed in chapter 2).



Scheme 4.7 Synthesis of chlorotris(4-isopropylphenyl)silane

Using the same reaction conditions as α -hydroxyl lactone, chlorotris(4-isopropylphenyl)silane was used in the kinetic resolution of **4.4**. To our surprise, a jump in selectivity from 5.9 to 11 (Scheme 4.5 (A), entry 1) was observed by switching the silyl source from triphenylsilyl chloride to chlorotris(4-isopropylphenyl)silane. It is important to note that in the previous mechanistic study, only 20% improvement in the selectivity factor was observed when tetralol and 4-chromanol were subjected to chlorotris(4-isopropylphenyl)silane (**2.13i**) compared to triphenylsilyl chloride. However, in this substrate class, the selectivity factor is almost doubled. Conversion was found to be little low after 48 h (Scheme 4.8). To improve conversion, a little excess (0.72 equiv instead of 0.6 equiv) of *p*-iPr-TPSCl (**2.13i**) were decided to used. Almost 54% conversion was achieved after 48h with selectivity factor **12.1**. The selectivity factor was found to be changing slightly in all three entry, the difference in selectivity arises due to conversion. At higher conversion, selectivity factor is more accurate.³³ This improvement in selectivity factor shows that an electron donating substituent at the *para* position of triphenylsilyl chloride has significant effect in chirality determination. One of the possibilities is the back

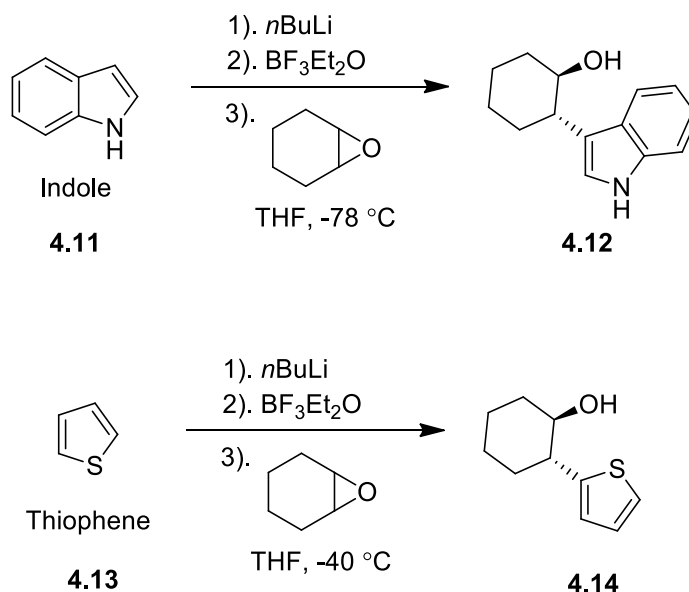
side attack of alcohol on *para* substituted triphenylsilyl chloride, as discussed in our previous mechanistic study.³ Kinetic resolution reaction was also performed using **1.14** as a catalyst with chlorotris(4-isopropylphenyl)silane. A drop in selectivity factor from 12.1 to 3.6 was reported (Scheme 4.8 (B)). This is the same selectivity difference between **1.14** and **1.31**, as observed with triphenylsilyl chloride. Finally from these results, it shows that an extended π system of the catalyst plays a key role in selectivity determination.



Scheme 4.8 Kinetic resolution reaction using **1.31** and **1.14** catalysts with chlorotris(4-isopropylphenyl)silane

As results presented in Scheme 4.8 (A) shows good selectivity factor and therefore no further optimization was done. Next, we turned our attention to substrate expansion.

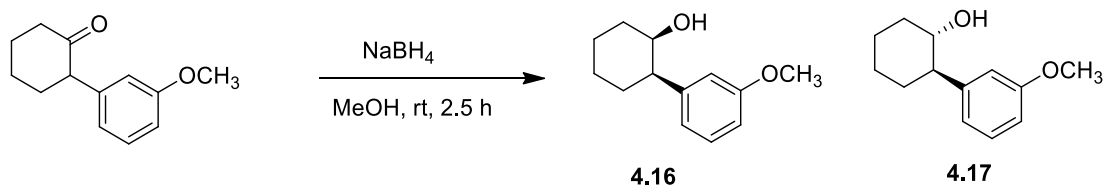
The major problem with this substrate class was that the commercially available substrates were very expensive and had a limited commercial availability. Therefore, we turn our attention towards the synthesis of structurally different 2-arylcycloalkanols. To accomplish the main goal of this project, a quick literature search was carried out on available synthesis reports of 2-arylcyclohexanols. Fortunately, a synthesis of *trans*-2-(1H-indol-3-yl)-cyclohexanol (**4.12**) was found in the literature (reported by Birman group), and the same procedure was adopted for synthesis (Scheme 4.9).³⁰ In this synthesis, *n*BuLi was added to the solution of commercially available indole (**4.11**) in THF at -78 °C under N₂ atmosphere followed by boron trifluoride etherate and cyclohexene oxide. After the workup, the crude mixture was purified using column chromatography. Unfortunately, only 16% yield was obtained. HPLC for this substrate was run using the published separation method and nice HPLC separation was achieved using OD-H column. It was difficult for us to identify the problem of the lower yield. We found unreacted indole along with other side products in our crude TLC. As we have been using all old reagents, all new reagents were ordered to avoid any yield problems. Even after repeating the reaction with new materials, the same problem of low yield was encountered. Currently, we are trying to optimize reaction condition of this substrate.



Scheme 4.9 Synthesis of 2-arylcycloalkanols

Meanwhile, another substrate (*trans*-2-(2-thienyl)-cyclohexanol) (**4.14**) was also synthesized using same procedure but instead of using the indole, a thiophene was used. This substrate was found to be very difficult to separate using column chromatography. Various solvent systems were used for separation but coelution of the desired product with few unidentified side product was observed.

Finally, successful synthesis of substrate was done when electron rich, 3-methoxyphenyl containing cyclohexanol (**4.15**) at the C2 position was synthesized by simple reduction using NaBH_4 in CH_3OH from the commercially available 2-(3-methoxyphenyl)cyclohexanon (Scheme 4.10).³¹ This procedure was adopted from the literature and it resulted into two separate substrates (**4.16 & 4.17**); *cis* and *trans*-2-(3-methoxyphenyl)cyclohexanol. Both were prepared in good yield and separated using column chromatography.



Scheme 4.10 NaBH₄ reduction of 2-(3-methoxyphenyl)cyclohexanone

The kinetic resolution reaction was run using both substrates. Interestingly, no conversion was seen in the case of (±)-*cis*-2-(3-methoxy)cyclohexanol (**4.16**). With (±)-*trans*-2-(3-methoxy)cyclohexanol (**4.17**) an average selectivity factor of 53 was measured (Figure 4.2). This is the highest reported selectivity factor so far using silylation based kinetic resolution of 2-arylcycloalkanols. This difference in reactivity and selectivity of both *cis* and *trans* prompted us analyze system in more detailed.

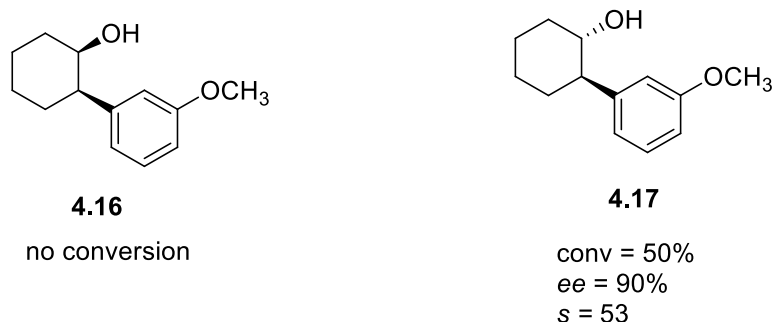


Figure 4.2 Data from kinetic resolution of *cis* and *trans* (±)-2-(3-methoxy)cyclohexanol
See reference 32

To understand system in detail, (±)-*cis*-2-phenylcyclohexanol was synthesized and used in the kinetic resolution reaction. Similar results (no conversion) were obtained compared to the previous run. This result excite us to look in a new direction for this project where mixture of *cis* and *trans* can be used in kinetic resolution reaction to separate one enantiomer out of four. After all this interesting results, Wiskur group is trying to build a project where several *cis*, *trans* and mixture of both can be analyzed using our optimized

silylation based kinetic resolutions. Due to the lack of commercially available substrates, a synthesis of several 2-arylcycloalkanols will be our next goal. After a great selectivity factor was reported for 2-(3-methoxyphenyl)cyclohexanol, we became interested to test *ortho* and *para* position of 2-(2 or 4-methoxyphenyl). Following two substrate will be synthesized/purchased (if commercially available) for our preliminary screening (Figure 4.3). Once we obtain the selectivity factor for those two substrates, then we will get idea which position on the “aryl ring” can be beneficial for us to test different substrate to achieve highest possible selectivity.

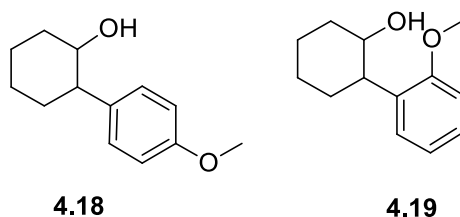
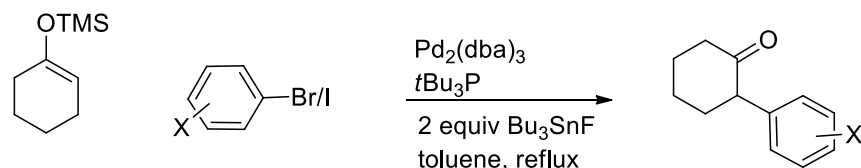


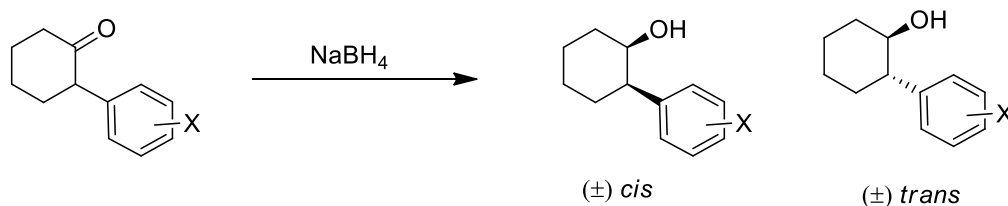
Figure 4.3 Commercially available 2-arylcycloalkanols

After literature search, we found a way to synthesize various 2-arylcycloalkanone (Scheme 4.11).^{34,35} In this experiment, all reagent are commercially available including the TMS protected silyl enol ether, $\text{Pd}_2(\text{dba})_3$, Bu_3SnF and $t\text{-PBu}_3$ and aryl bromide.

Step 1:



Step 2:



Scheme 4.11 Two-step synthesis of 2-aryl cycloalkanols

To perform this reaction all reagents excluding $t\text{-PBu}_3$ will be dissolved in toluene. A solution of $t\text{-Bu}_3\text{P}$ (1.0 M in toluene) will be added under N_2 atmosphere at room temperature. The resulting mixture then will be allowed to reflux for 24 h. After 24 h, mixture will be allowed to cool at room temperature followed by addition of ether to precipitate tin. This precipitate will be removed and mixture will be washed with 1 N aqueous NaOH and then brine. Dry over sodium sulfate and solution will be concentrated. The crude mixture can be purified using column chromatography. After getting 2-aryl cycloalkanone, next step can be reduction which could be achieved the same way as shown previously using NaBH_4 . Finally after reduction both *cis* and *trans* can be separated by column chromatography.

4.4 Conclusion

A silylation based methodology was applied to several allylic as well as homoallylic alcohols. Almost all substrate had selectivity factor between 1-3.4.

Surprisingly, a big jump in selectivity factor was observed when commercially available (*-*)-carveol were subjected to our silylation based kinetic resolution. After careful analysis of all previously screened (including monofunctional secondary alcohols and α -hydroxyl lactone) selective substrate, common structural topology was discovered. In this regard, commercially available 2-arylcycloaryl alcohols was chosen for further investigation. Initial screening was done by using *trans*-2-phenylcyclohexanol. Kinetic resolution was done using both **1.14** and **1.31** as a catalyst and triphenylsilyl chloride as a silicon source. Selectivity factor of 5.9 was observed with **1.31** while almost racemic mixture was obtained with **1.14**. To improve this selectivity factor, further optimization was taken under consideration. Using previous mechanistic data, triphenylsilyl chloride was replaced with electron donating *para* substituted triphenylsilyl chloride. Almost, double selectivity factor ($s = 11$ vs 5.9) was observed when chlorotris(4-isopropylphenyl)silane used in kinetic resolution. For further expansion, several substrate synthesis were carried out. After successful synthesis of both (\pm)-*cis*-2-(3-methoxy)cyclohexanol and (\pm)-*trans*-2-(3-methoxy)cyclohexanol, kinetic resolution reaction were done using optimized reaction condition. To our surprise, no conversion was observed with (\pm)-*cis*-2-(3-methoxy)cyclohexanol while selectivity factor 53 was observed (\pm)-*trans*-2-(3-methoxy)cyclohexanol. Similar result (no conversion) was obtained with (\pm)-*cis*-2-phenylcyclohexanol. With this result, we became interested to screen mixture of *cis* and *trans* isomer and selectively separate one enantiomer. With this goal in our mind, we are currently synthesizing several *cis*, *trans* and mixture of 2-arylcycloalcohols. In near future, several substrate will be prepare and analyzed using our silylation based system. This work highlights our contribution towards our intial goal of substrate expansion.

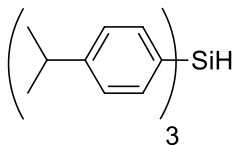
4.5 Experimental

General procedure for the kinetic resolution of allylic & homoallylic alcohols (Table 1.31) :

An oven dried 1 dram vial was charged with 4 Å molecular sieves (10-15 mg) and a Teflon coated stir bar. The racemic allylic or homoallylic alcohol (0.22 mmol), catalyst **1.14** or **1.31** (11.2 mg, 0.055 mmol) and *N,N*-diisopropylethylamine (Hünig's Base) (23 µL, 0.132 mmol) were added to a vial and then quickly sealed under a nitrogen atmosphere. Dry THF (1.0 mL) was added and the reaction mixture was allowed to stir at -78 °C for 15-20 minutes. Meanwhile a solution of Ph₃SiCl (0.357 M) was prepared using a volumetric flask (under N₂). The solution of Ph₃SiCl (370 µL, 0.6 mmol) was added to the reaction vial and the resulting mixture was allowed to react for the specified amount of time at -78 °C. The reaction mixture was then quenched using 300 µL of MeOH at -78 °C. The mixture was allowed to warm to room temperature followed by addition of 1.0 mL of saturated aqueous NH₄Cl. The reaction mixture was transferred to a 4 dram vial and extracted using diethyl ether (3 x 2 mL). The ether layer was then passed through a pad of silica gel. After filtration, it was concentrated and the crude mixture was purified using silica gel chromatography (100% CH₂Cl₂ followed by 2% MeOH in CH₂Cl₂). The analysis of the unreacted recovered alcohol was done by a chiral HPLC using a hexanes/*i*-PrOH solvent system. **Desilylation:** The silylated product was transferred to a 4 dram vial with a stir bar and dissolved in 3 mL of THF. The solution was treated with a 1M solution of TBAF in THF (500 µL - 1.0 mL) and allowed to stir for 3-10 h at room temperature (conversion was monitored by TLC). The reaction was quenched with brine and extracted with diethyl ether. The crude mixture was purified via silica gel column chromatography (CH₂Cl₂ to

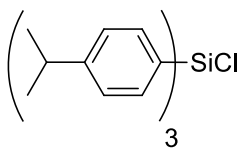
2% MeOH in CH₂Cl₂). HPLC analysis was done for the desilylated product (alcohol). The absolute stereochemistry was confirmed by comparing the HPLC data with previously published data.

Procedure to make Tris(4-isopropylphenyl)silane



In an oven dried 250 mL three-neck round bottom flask, 4-bromo-isopropyl benzene(95%) (1.63 mL, 10 mmol) was dissolved using previously dried diethyl ether (30 mL) under nitrogen at room temperature. To the stirred solution, *n*-BuLi (1.025 equiv.) was added and the resulting mixture was allowed to stir for 1-1.5 h at room temp. The reaction was then cooled to -40 °C using a dry ice-acetonitrile bath. A solution of HSiCl₃ (0.4 M in ether, 0.3 equiv) was added dropwise to the three neck flask. The reaction mixture was allowed to stir for another 2 h at -40 °C, then the reaction was quenched using 10 mL of water at -40 °C and allowed to warm to room temp. Extraction was done using diethyl ether. The organic layer was collected and dried over anhydrous sodium sulfate. The excess solvent was removed via a rotary evaporator and the crude was purified using recrystallization or a trituration method. MP range = 58-60 °C ¹H NMR (400 MHz, CDCl₃): δ 7.51 (d, *J* = 8.0 Hz, 6H), 7.23 (d, *J* = 7.9 Hz, 6H), 5.41 (s, 1H), 2.90 (m, 3H), 1.25 (d, *J* = 6.9 Hz, 18H). ¹³C NMR (101 MHz, CDCl₃): δ 150.4, 135.9, 130.7, 126.2, 34.1, 23.8. ²⁹Si NMR (80 MHz, CDCl₃): -18.8. HRMS (EI) (M⁺) Calculated for (C₂₇H₃₄Si⁺): 386.2424 Observed: 386.2428. IR (neat, cm⁻¹): 2961, 2928, 2110, 1924, 1598, 1458, 1392, 1297, 1265, 1117, 1094, 1049, 1019, 822, 794, 760, 725.

Procedure making a Chlorotris(4-isopropylphenyl)silane (2.13i)



In an oven dried 25-50 mL three-neck round bottom flask was charged with *p*-substituted triphenylsilane and dissolved using dry degassed carbon tetrachloride (CCl₄) under a nitrogen atmosphere. The mixture was allowed to stir for 10-15 minutes. Sulfuryl chloride (SO₂Cl₂) (2-6 equiv) was then added to the flask. The resulting mixture was then allowed to reflux for 4-28 h (Conversion was monitored by disappearance of the silane peak using ¹H NMR). Hydrochloric acid generated during the reaction was removed from the reaction mixture via a bubbler. The excess solvent and other reagents were evaporated under vacuum (dry ice cooled cold trap). The final product was then recrystallized or triturated using an appropriate solvent under a N₂ atmosphere. ¹H NMR (400 MHz, CDCl₃): δ 7.57 (d, *J* = 8.1 Hz, 6H), 7.27 (d, *J* = 7.4 Hz, 6H), 2.92 (septet, 3H), 1.26 (d, *J* = 6.9 Hz, 18H). ¹³C NMR (101 MHz, CDCl₃): δ 151.4, 135.3, 130.2, 126.2, 34.2, 23.8.

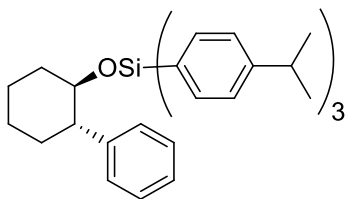
General procedure for the kinetic Resolution of 2-cycloalkanol (Scheme 4.6 & Scheme

4.8): An oven dried 1 dram vial was charged with 4 Å molecular sieves (10-15 mg) and a Teflon coated stir bar. The racemic alcohol (0.4 mmol), catalyst **1.14**/**1.31** (0.1 mmol) and *N,N*-diisopropylethylamine (Hünig's Base) (41.8 µL, 0.24 mmol) were added to a vial and then quickly sealed under a nitrogen atmosphere. Dry THF (1.0 mL) was added and the reaction mixture was allowed to stir at -78 °C for 15-20 minutes. Meanwhile a solution of (*pi*Pr-Ph)₃SiCl (0.65 M) was prepared using a volumetric flask (under N₂). The solution of (*pi*Pr-Ph)₃SiCl **4.9** (400 µL, 0.26 mmol, 0.65 equiv or as mentioned equiv) was added

to the reaction vial and the resulting mixture was allowed to react for the specified amount of time at -78 °C. The reaction mixture was then quenched using 300 μ L of MeOH at -78 °C. The mixture was allowed to warm to room temperature followed by addition of 1.0 mL of saturated aqueous NH_4Cl . The reaction mixture was transferred to a 4 dram vial and extracted using diethyl ether (3 x 2 mL). The ether layer was then passed through a pad of silica gel. After filtration, it was concentrated and the crude mixture was purified using silica gel chromatography (5-25% EtOAc/Hexane). The analysis of the unreacted recovered alcohol was done by a chiral HPLC using a hexanes/*i*-PrOH solvent system.

Desilylation: The silylated product was transferred to a 4 dram vial with a stir bar and dissolved in 3 mL of THF. The solution was treated with a 1M solution of TBAF in THF (500 μ L - 1.0 mL) and allowed to stir for 3-10 h at room temperature (conversion was monitored by TLC). The reaction was quenched with brine and extracted with diethyl ether. The crude mixture was purified via silica gel column chromatography (5-25% EtOAc/Hexane). HPLC analysis was done for the desilylated product (alcohol). The absolute stereochemistry was confirmed by comparing the HPLC data with previously published data.

Tris(4-isopropylphenyl)((1R,2S)-2-phenylcyclohexyl)oxy)silane:



4.10

^1H NMR (400 MHz, CDCl_3): δ 7.55 (d, J = 8.0 Hz, 2 H), 7.24-7.18 (m, 7 H), 7.10 (d, J = 8.0 Hz, 6 H), 7.05-7.03 (m, 2 H), 3.85-3.79 (m, 1 H), 2.93-2.83 (hept, 3 H), 2.69-2.63 (m, 1 H), 2.00-1.36 (m, 8 H), 1.23 (d, J = 6.8 Hz, 18H) ^{13}C NMR

(101 MHz, CDCl₃) δ 150.6, 150.0, 145.0, 135.7, 135.6, 132.1, 128.2, 126.0, 125.9, 125.6, 76.0, 53.2, 36.5, 34.2, 34.1, 26.0, 25.1, 23.9.

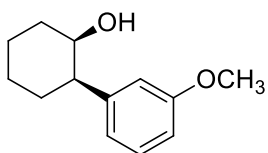
Synthesis of *trans*-2-(1H-indol-3-yl)-cyclohexanol (4.12): In 50 ml, three neck round bottom flask was charged with 352 mg indol (3 mmol) in 5 ml THF under N₂ atmosphere. Reaction mixture was cooled to -78 °C using dry ice/acetone bath. *n*BuLi (3.2 ml, 1.26 M, 4.05 mmol)) was added drop wise to the solution. Resulting mixture was allow to stir for 30 minutes at -78 °C. Solution of BF₃OEt₂ (500 μ l ,4.05 mmol) was added to the mixture and stir for another 15 minutes. Finally, cyclohexene oxide (364 , 3.6 mmol) was slowly added to the reaction mixture and reaction was allowed to stir for 2.5-3 h. Reaction was quenched with NH₄Cl. Extraction was done using diethyl ether and organic layer dried over MgSO₄. Reaction mixture was concentrated using rotary vapor. Crude was purified using column chromatograpohy using (30% EtOAc in hexane).

Yield = 16% (105 mg). ¹H NMR (400 MHz, CDCl₃) : δ 8.08 (br, 1H), 7.73 (d, J =8.0 Hz, 1H), 7.38 (d, J = 8.0 Hz, 1H), 7.21 (t, J = 7.2 Hz , 1H), 7.14-7.09 (m, 2H), 3.81-3.75 (m, 1H), 2.79-2.73 (m, 1H), 2.18-1.66 (m, 7H), 1.47-1.39 (m, 1H). ¹³C NMR (101 MHz, CDCl₃) δ 135.0, 127.0, 122.3, 121.3, 119.6, 119.5, 111.3, 74.7, 44.5, 34.2, 32.6, 26.3, 25.1.

Synthesis of *trans*-2-(2-thienyl)-cyclohexanol (4.14): In 50 ml, three neck round bottom flask was charged with 474 μ L thiophene (6 mmol) in 10 ml THF under N₂ atmosphere. Reaction mixture was cooled to -78 °C using dry ice/acetone bath. *n*BuLi (6.4 ml, 1.26 M, 8.1 mmol)) was added drop wise to the solution. Resulting mixture was allow to stir for 30 minutes at -78 °C. Solution of BF₃OEt₂ (1.00 ml, 8.1 mmol) was added to the mixture and stir for another 15 minutes. Finally, cyclohexene oxide (728 μ L , 7.2 mmol) was slowly added to the reaction mixture and reaction was allowed to stir for 2.5-3 h. Reaction was

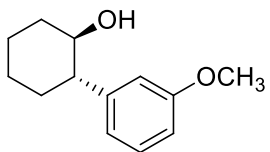
quenched with NH_4Cl . Extraction was done using diethyl ether and organic layer dried over MgSO_4 . Reaction mixture was concentrated using rotary vapor. Crude was purified using column chromatography using (30% EtOAc in hexane). Co-elution was observed along with product and it was very difficult to separate impurities. Several solvent systems were tried to separate product but no successful separation was achieved. In future, prep TLC will be performed to separate product.

Synthesis of *cis* & *trans* 2-(3-methoxyphenyl)cyclohexanol : To an oven dried 100 mL round bottom flask, 2-(3-methoxyphenyl)cyclohexanone (900 mg, 4.4 mmol) was dissolved using 20 mL of MeOH. Color of the solution became light orange to yellowish after stirring for 5 minutes. 454 mg of NaBH_4 (12 mmol) was added to the stirred solution in small portions. Resulting mixture was allowed to stir for 1-1.5 h. After 1-1.5 h, work up was done using water (10 mL) and toluene (30 mL). Extraction was done using 10% HCl, water and sodium bicarbonate. Finally, organic layer was separated and dried over Na_2SO_4 . Solution was concentrated and column chromatography was performed (5% to 15% EtOAc in Hexane). Colorless oil product was obtained.



4.16

Yield = 20% (178 mg). ^1H NMR (400 MHz, CDCl_3) : δ 7.25-7.22 (m, 1H), 6.85 (d, $J = 7.6$ Hz, 1H), 6.81 (s, 1H), 6.78-6.75 (m, 1H), 4.01 (m, 1H), 3.80 (s, 3H), 2.74-2.69 (m, 1H), 2.08-1.95 (m, 2H), 1.90-1.85 (m, 1H), 1.67-1.35 (m, 5H). ^{13}C NMR (101 MHz, CDCl_3) δ 159.7, 145.6, 129.5, 120.0, 113.6, 111.6, 70.5, 55.1, 48.0, 32.8, 26.1, 24.3, 19.5.



4.17

Yield = 27% (248 mg). ^1H NMR (400 MHz, CDCl_3): δ 7.26-7.22 (m, 1H), 6.84 (d, $J = 7.6$ Hz, 1H), 6.80-6.76 (m, 2H), 3.80 (s, 3H), 3.63 (m, 1 H), 2.42-2.36 (m, 1H), 2.15-2.08 (m, 1H), 2.11-1.27 (m, 8H). ^{13}C NMR (101 MHz, CDCl_3) δ 159.8, 144.9, 129.7, 120.1, 113.7, 111.9, 74.3, 55.1, 53.2, 34.3, 33.2, 26.0, 25.0

4.6 References

- (1) Sheppard, C. I.; Taylor, J. L.; Wiskur, S. L.: Silylation-based kinetic resolution of monofunctional secondary alcohols. *Org. Lett.* **2011**, *13*, 3794-3797.
- (2) Clark, R. W.; Deaton, T. M.; Zhang, Y.; Moore, M. I.; Wiskur, S. L.: Silylation-based kinetic resolution of alpha-hydroxy lactones and lactams. *Org. Lett.* **2013**, *15*, 6132-6135.
- (3) Akhani, R. K.; Moore, M. I.; Pribyl, J. G.; Wiskur, S. L.: Linear free-energy relationship and rate study on a silylation-based kinetic resolution: mechanistic insights. *J. Org. Chem.* **2014**, *79*, 2384-2396.
- (4) Johnson, R. A.; Sharpless, K. B. In *Comprehensive Organic Synthesis*; Trost, B. M., Ed.; Pergamon: Oxford, 1991; Vol. 7, p 389
- (5) Johnson, R. A.; Sharpless, K. B. In *Catalytic Asymmetric Synthesis*; Ojima, I., Ed.; VCH: New York, 1993; Chapter 4
- (6) Heck, R. F. *Palladium Reagents in Organic Synthesis*; Academic: London, 1985, Chapter 5
- (7) Martin, V. S.; Woodard, S. S.; Katsuki, T.; Yamada, Y.; Ikeda, M.; Sharpless, K. B.: Kinetic resolution of racemic allylic alcohols by enantioselective epoxidation - A route to substances of absolute enantiomeric purity. *J. Am. Chem. Soc.* **1981**, *103*, 6237-6240.
- (8) Kagan, H. B.; Fiaud, J. C.: Kinetic resolution. *Top. Stereochem.* **1988**, *18*, 249-330.
- (9) Vedejs, E.; MacKay, J. A.: Kinetic resolution of allylic alcohols using a chiral phosphine catalyst. *Org. Lett.* **2001**, *3*, 535-536.
- (10) Bellemin-Lapponnaz, S.; Tweddell, J.; Ruble, J. C.; Breitling, F. M.; Fu, G. C.: The kinetic resolution of allylic alcohols by a non-enzymatic acylation catalyst; application to natural product synthesis. *Chem. Commun.* **2000**, 1009-1010.
- (11) Li, X. M.; Jiang, H.; Uffman, E. W.; Guo, L.; Zhang, Y. H.; Yang, X.; Birman, V. B.: Kinetic resolution of secondary alcohols using amidine-based catalysts. *J. Org. Chem.* **2012**, *77*, 1722-1737.
- (12) Brenna, E.; Caraccia, N.; Fuganti, C.; Fuganti, D.; Grasselli, P.: Enantioselective synthesis of beta-substituted butyric acid derivatives via orthoester Claisen rearrangement of enzymatically resolved allylic

alcohols: application to the synthesis of (R)-(-)-baclofen. *Tetrahedron-Asymmetr* **1997**, 8, 3801-3805.

- (13) Sinha, S. C.; Barbas, C. F.; Lerner, R. A.: The antibody catalysis route to the total synthesis of epothilones. *Proc. Natl. Acad. Sci. U.S.A.* **1998**, 95, 14603-14608.
- (14) Greene, T. W.; Wuts, P. G. M.: *Protective groups in organic synthesis*; 3rd ed.; Wiley: New York, 1999.
- (15) Valeev, R. F.; Vostrikov, N. S.; Miftakhov, M. S.: Synthesis and some transformations of (-)-carveol. *Russ. J. Org. Chem.* **2009**, 45, 810-814.
- (16) Srikrishna, A.; Reddy, T. J.; Kumar, P. P.: Synthesis of taxanes - The carveone approach; A simple, efficient stereo- and enantio-selective synthesis of the functionalised A ring. *Chem. Commun.* **1996**, 1369-1370.
- (17) Mehta, G.; Karmakar, S.; Chattopadhyay, S. K.: Grob-type fragmentation of a carveone derived beta-hydroxymesylate: application to the synthesis of chiral lavandulol derivatives. *Tetrahedron* **2004**, 60, 5013-5017.
- (18) Jiang, C. H.; Bhattacharyya, A.; Sha, C. K.: Enantiospecific total synthesis of (-)-bakkenolide III and formal total synthesis of (-)-bakkenolides B, C, H, L, V, and X. *Org. Lett.* **2007**, 9, 3241-3.
- (19) Winterbottom, R.; Clapp, J. W.; Miller, W. H.; English, J. P.; Roblin, R. O.: Studies in chemotherapy .15. amides of pantoyletaurine. *J. Am. Chem. Soc* **1947**, 69, 1393-1401.
- (20) King, T. E.; Stewart, C. J.; Cheldelin, V. H.: Beta-aletheine and pantetheine. *J. Am. Chem. Soc.* **1953**, 75, 1290-1292.
- (21) Dolle, R. E.; Nicolaou, K. C.: Total synthesis of elfamycins - aurodox and efrotomycin .1. strategy and construction of key intermediates. *J. Am. Chem. Soc.* **1985**, 107, 1691-1694.
- (22) Fischer, G. C.; Turakhia, R. H.; Morrow, C. J.: Irreducible analogs of mevaldic acid coenzyme a hemithioacetal as potential inhibitors of hmg-coa reductase - synthesis of a carbon sulfur interchanged analog of mevaldic acid pantetheine hemithioacetal. *J. Org. Chem.* **1985**, 50, 2011-2019.
- (23) Liu, J.; Li, Y.; Tang, L. J.; Zhang, G. P.; Hu, W. X.: Treatment of lycorine on SCID mice model with human APL cells. *Biomed Pharmacother* **2007**, 61, 229-234.

- (24) Liu, J.; Hu, W. X.; He, L. F.; Ye, M.; Li, Y.: Effects of lycorine on HL-60 cells via arresting cell cycle and inducing apoptosis. *FEBS Lett.* **2004**, 578, 245-250.
- (25) Li, J. J.; Iula, D. M.; Nguyen, M. N.; Hu, L. Y.; Dettling, D.; Johnson, T. R.; Du, D. Y.; Shanmugasundaram, V.; Van Camp, J. A.; Wang, Z.; Harter, W. G.; Yue, W. S.; Boys, M. L.; Wade, K. J.; Drummond, E. M.; Samas, B. M.; Lefker, B. A.; Hoge, G. S.; Lovdahl, M. J.; Asbill, J.; Carroll, M.; Meade, M. A.; Ciotti, S. M.; Krieger-Burke, T.: Rational design and synthesis of 4-((1R,2R)-2-hydroxycyclohexyl)-2(trifluoromethyl)benzonitrile (PF-998425), a novel, nonsteroidal androgen receptor antagonist devoid of phototoxicity for dermatological indications. *J. Med. Chem.* **2008**, 51, 7010-7014.
- (26) Rouf, A.; Gupta, P.; Aga, M. A.; Kumar, B.; Parshad, R.; Taneja, S. C.: Cyclic trans-beta-amino alcohols: preparation and enzymatic kinetic resolution. *Tetrahedron-Asymmetr* **2011**, 22, 2134-2143.
- (27) Oriyama, T.; Hori, Y.; Imai, K.; Sasaki, R.: Nonenzymatic enantioselective acylation of racemic secondary alcohols catalyzed by a SnX(2)-chiral diamine complex. *Tetrahedron Lett.* **1996**, 37, 8543-8546.
- (28) Copeland, G. T.; Miller, S. J.: Selection of enantioselective acyl transfer catalysts from a pooled peptide library through a fluorescence-based activity assay: An approach to kinetic resolution of secondary alcohols of broad structural scope. *J. Am. Chem. Soc.* **2001**, 123, 6496-6502.
- (29) Jeong, K. S.; Kim, S. H.; Park, H. J.; Chang, K. J.; Kim, K. S.: A new nucleophilic catalyst for kinetic resolution of racemic sec-alcohols. *Chem. Lett.* **2002**, 1114-1115.
- (30) Birman, V. B.; Li, X. M.: Homobenzotetramisole: An effective catalyst for kinetic resolution of aryl-cycloalkanols. *Org. Lett.* **2008**, 10, 1115-1118.
- (31) Harada, S.; Kuwano, S.; Yamaoka, Y.; Yamada, K.; Takasu, K.: Kinetic resolution of secondary alcohols catalyzed by chiral phosphoric acids. *Angew. Chem., Int. Ed.* **2013**, 52, 10227-10230.
- (32) Reaction was done by Li Wang
- (33) Keith, J. M.; Larrow, J. F.; Jacobsen, E. N.: Practical considerations in kinetic resolution reactions. *Adv. Synth. Catal.* **2001**, 343, 5.
- (34) Iwama, T.; Rawal, V. H.: Palladium-catalyzed regiocontrolled alpha-arylation of trimethylsilyl enol ethers with aryl halides. *Org. Lett.* **2006**, 8, 5725-5728.

- (35) Cheon, C. H.; Kanno, O.; Toste, F. D.: Chiral bronsted acid from a cationic gold(I) complex: Catalytic enantioselective protonation of silyl enol ethers of ketones. *J. Am. Chem. Soc.* **2011**, *133*, 13248-13251.

CHAPTER 5

A SILYLATION BASED KINETIC RESOLUTION OF SECONDARY ALCOHOLS USING POLYMER SUPPORTED TRIPHENYLSILYL CHLORIDE

5.1 Introduction

Our previous mechanistic study of a silylation based kinetic resolution of a monofunctional secondary alcohols (Chapter 2) demonstrated that substitution at the *para* position of triphenylsilyl chloride affected the selectivity factor of our substrates in a dramatic way.¹ The selectivity factor improved with EDGs at the *para* position of triphenylsilyl chloride while it decreased with EWGs. The kinetic resolution of 2-arylcyclohexanols is a good example to demonstrate the practicality of enhanced selectivity from the *para* substitution of triphenylsilyl chloride. A big improvement in the selectivity factor was obtained when triphenylsilyl chloride was simply replaced by chlorotris(4-isopropylphenyl)silane (Chapter 4). This kinetic resolution of 2-arylcyclohexanol further confirmed the importance of substitution at the *para* position of triphenylsilyl chloride in our kinetic resolution system. With respect to this, we thought that it would be very interesting if we could take further advantage of the *para* position of triphenylsilyl chloride by incorporating a polymer at the *para* position instead of a substituent. The main goal of any kinetic resolution system is the ease of enantiomeric separation. In our kinetic resolution system, one enantiomer was silylated while the other remained unreacted.²

Therefore, having a polymer attached to tetrakis(triphenylsilyl) chloride in our system would allow us to use a “crash out method” for separation. In this way, one enantiomer will remain in the solution while the other enantiomer crashes out with polymer supported triphenylsilyl chlorides (Figure 5.1). In our system, a reaction is quenched using methanol and therefore designing a polymer in such a way that it can crash it out by methanol after the reaction is completed. These would allow us to take advantage of the crash out method of enantiomers. Using simple filtration, both enantiomers can be separated. With this in our mind, we decided to start working toward the development of our system. In this chapter, our research design, preliminary results and future direction of this new project is discussed.

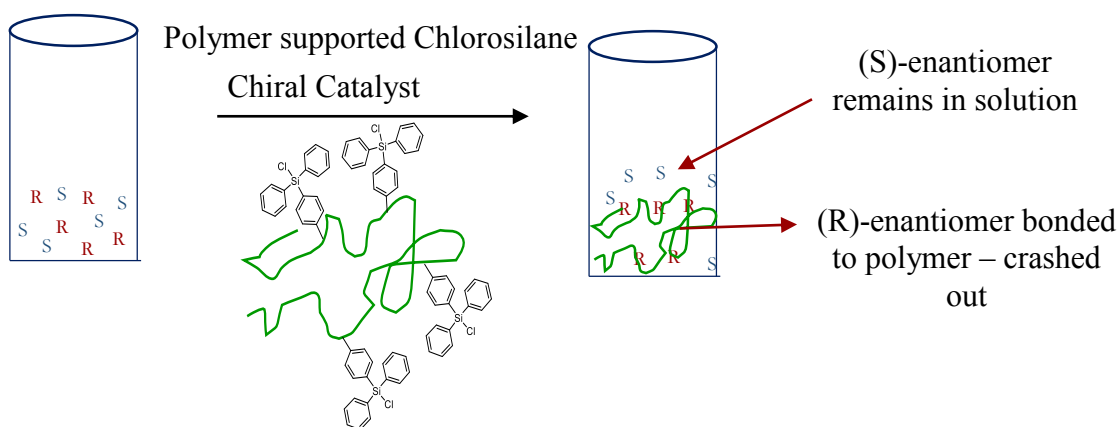


Figure 5.1 Graphical presentation of the kinetic resolution using polymer supported chlorosilane

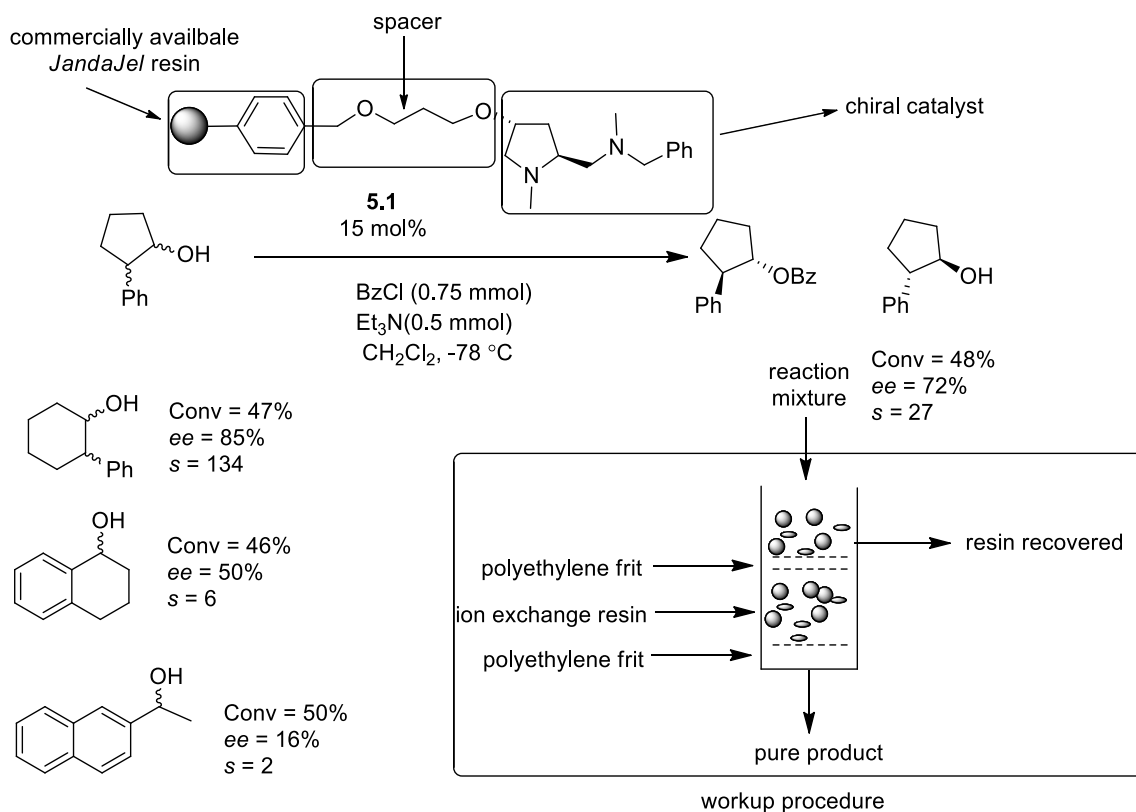
5.2 Background

Polymers have been known to have a great role in organic reactions to manipulate reaction conditions and product isolation.³ Particularly in asymmetric catalysis, polymers have shown tremendous level of applications in catalyst recovery. Use of solid support system in kinetic resolutions/asymmetric catalysis often comes with advantages and

disadvantages.⁴ The main advantages of solid supported systems include, ease of workup, ease of separation, and solid supported reagent recovery. While on the other hand, disadvantages of solid supported systems include longer reaction times compared to their homogenous counterpart, involvement of a multistep synthesis to attach reagent to a solid support and tuning of reaction conditions to achieve compatible results with a homogeneous system. Therefore, in order to perform a kinetic resolution using a solid supported system, one should always consider the above mentioned issues. Several examples have been reported in the literature using polymer supported catalysts or chiral auxiliaries to perform asymmetric reactions⁵⁻¹² as well as kinetic resolutions.¹³⁻²¹ The main goal of this dissertation is to develop an efficient non-enzymatic kinetic resolution system and therefore only examples of polymer supported kinetic resolutions will be discussed.

In 2001, Janda et al. carried out a kinetic resolution of secondary alcohols using a polymer supported proline-based diamine catalyst (Scheme 5.1).²² In this system, the catalyst (**5.1**) was attached to the resin (*JandaJel*) using trans-4-hydroxyproline. A short spacer was introduced between the diamine chiral catalyst and the resin. Using this polymer, the reaction conditions were optimized. To make the work up simple and efficient, and to isolate the products free from any byproduct, a workup procedure was also developed (as shown in Scheme 5.1). In this method, after the reaction, the resulting mixture was filtered from a small cartridge which was made using ion-exchange resin in a plastic syringe. This plastic syringe was then fitted with polyethylene frit and an additional frit on top of it. Using this procedure, the polymer supported catalyst was separated from the reaction and the resulting mixture was purified by column chromatography. Various secondary alcohols were analyzed using this polymer supported chiral catalyst with

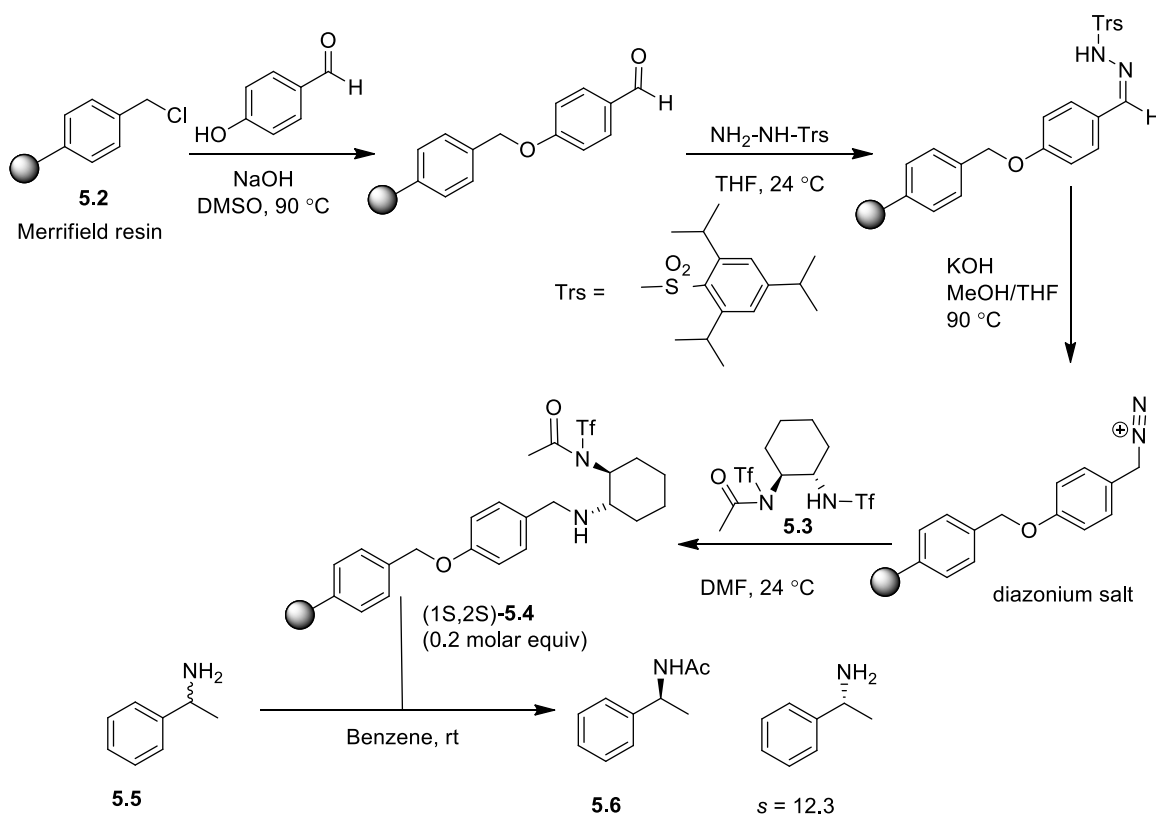
selectivities ranging from 1-200. Very similar selectivity factors were observed compared to the solution based system. In this system, the polymer supported catalyst was reported to be recycled and reused up to five times without losing catalytic activity and selectivity.



Scheme 5.1 Kinetic resolution of secondary alcohols using a polymer supported proline-based catalyst by Janda et al.

In 2005, the Wagner and Mioskowski group published a report where the kinetic resolution of racemic amines was achieved at room temperature using a polymer supported chiral acetylating reagent **5.4** (Scheme 5.2).²³ To prepare the polymer supported reagent, a four step synthesis was carried out using commercially available Merrifield resin (**5.2**) and catalyst (**5.3**). Finally, a Catalyst (**5.3**) was reacted with preformed diazonium salt to get the desired polymer (**5.4**). Using this polymer at 0.2 molar equiv, a solvent study was carried out through the kinetic resolution of (±)-1-phenylethylamine (**5.5**). Benzene was reported as the optimal solvent to achieve high enantioselectivity. Finally, using this

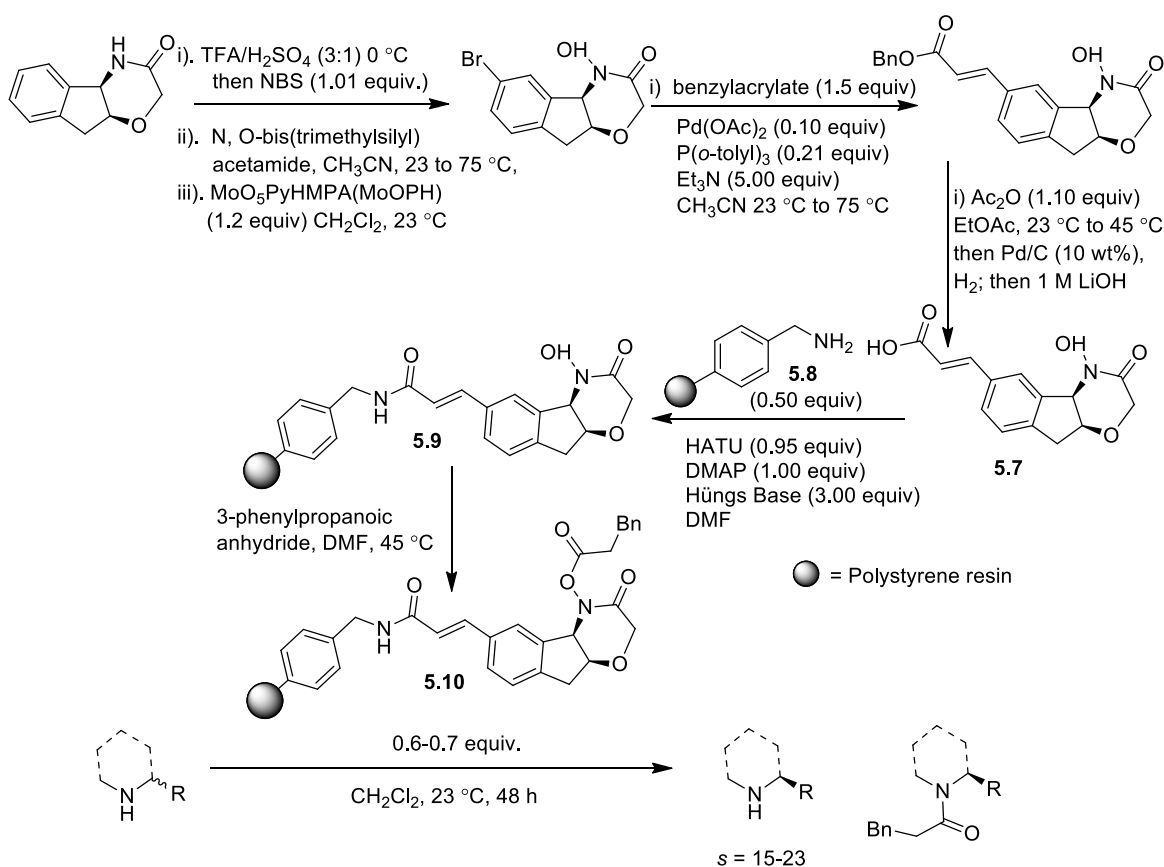
polymer four different substrates were screened. A moderate to good selectivity factors ranging from 6.4-12.3 were reported. The recyclability of this polymer supported reagent was tested. Up to four times, the polymer was found to be recycled without any noticeable loss of selectivity. Moreover, in this report, a better selectivity was observed with the polymer supported chiral acetylating reagent compared to the catalyst used in solution phase.



Scheme 5.2 Kinetic resolution of amines using a polymer supported enantioselective *N*-acetylation

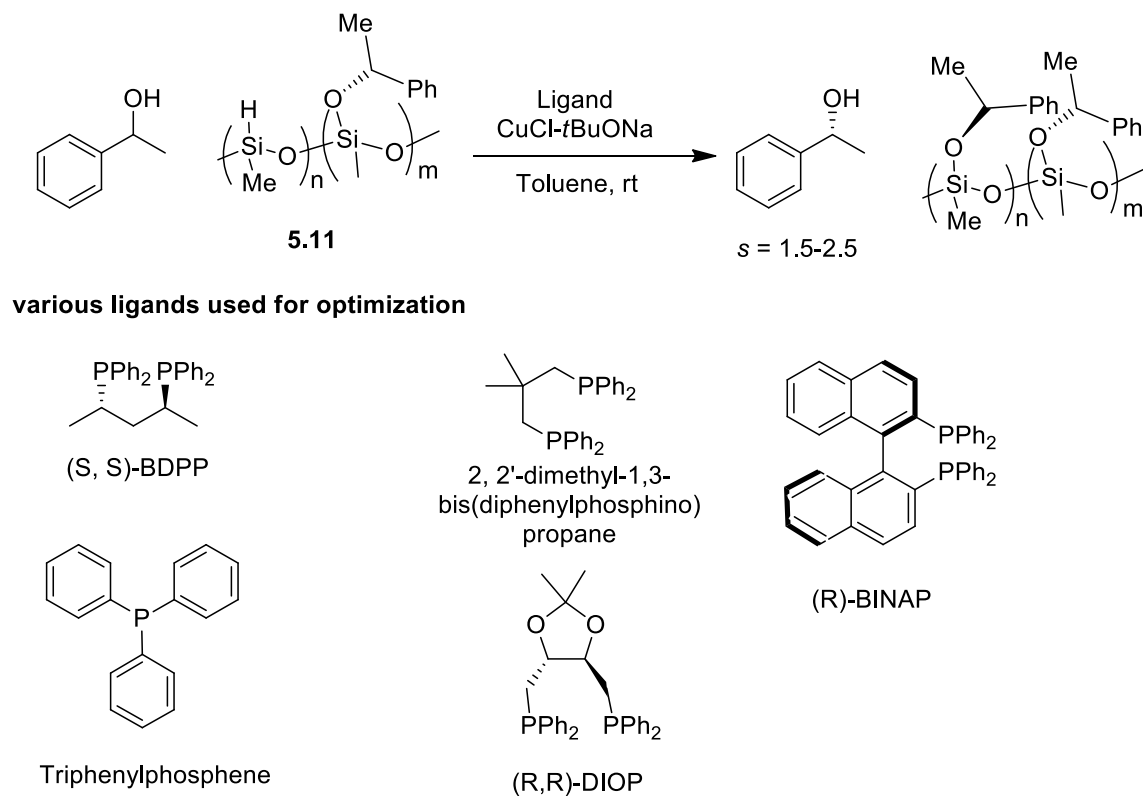
Bode and his group used a polymer supported enantioselective acylating reagent for the kinetic resolution of *N*-heterocycles.²⁴ In this system, chiral *O*-acyl hydroxamic

acid (**5.7**) was attached to the reusable amino methyl polystyrene (**5.8**) to get the desired polymer (**5.10**) and was used in the kinetic resolution of racemic amines (**Scheme 5.3**). The product can be simply separated from the unreacted amine through an aqueous workup or column chromatography. After the reaction, using a simple filtration method, the precursor of the polymer supported acylating reagent was recovered and (**5.9**) regenerated by treatment with 3-phenylpropionic anhydride. The polymeric supported acylating reagent (**5.10**) was reused several times without any compromise in the selectivity. Various structurally diverse *N*-heterocycles were resolved with high selectivity using this solid supported kinetic resolution system which including derivatives like piperidines, piperazines, morpholines, tetrahydroisoquinolines and diazaenones.



Scheme 5.3 Polymer supported kinetic resolution of *N*-heterocycles reported by the Bode group

Most recently, Dagorne and Laponnaz developed a kinetic resolution of secondary alcohols based on a polymeric silane (Scheme 5.4).²⁵ In this system, to show the practical approach of the kinetic resolution a system similar to Oestreich's²⁶⁻³⁰ was taken under investigation. The kinetic resolution was carried out using a CuCl/NaOtBu/chiral phosphine catalytic system and a chiral polymethylhydrosiloxane (**5.11**, PMHS) polymer as a hydride source to perform a dehydrogenative silylation coupling reaction. Various phosphine based ligands were screened in this system using chiral PMHS with selectivity factors between 1.5-2.5. Even with moderate to low selectivity, this method shows the potential of silicon based polymers (PMHS) to perform the kinetic resolution of secondary alcohols.



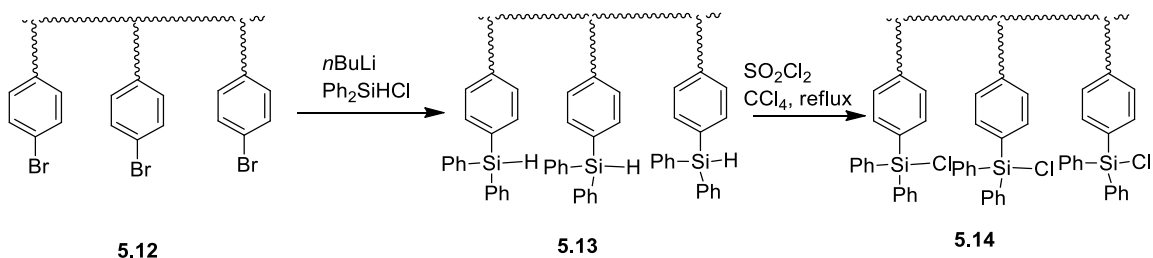
Scheme 5.4 Kinetic resolution of secondary alcohols using polymeric silane

Inspired from the above polymer-based kinetic resolutions and particularly the one with PMHS (Scheme 5.4) where silicon can be utilized to do the kinetic resolution, we thought it would be interesting if we could attach our silicon source to a polymer to create a solid supported kinetic resolution system. A silyl group is one of the most common protecting groups with several advantages like tunable reactivity, orthogonality to other protecting groups and tolerance of many other functional groups.³¹ To the best of our knowledge, no other examples have been reported in the literature where silylation-based kinetic resolutions was achieved through a solid support system.

5.3 Research Design

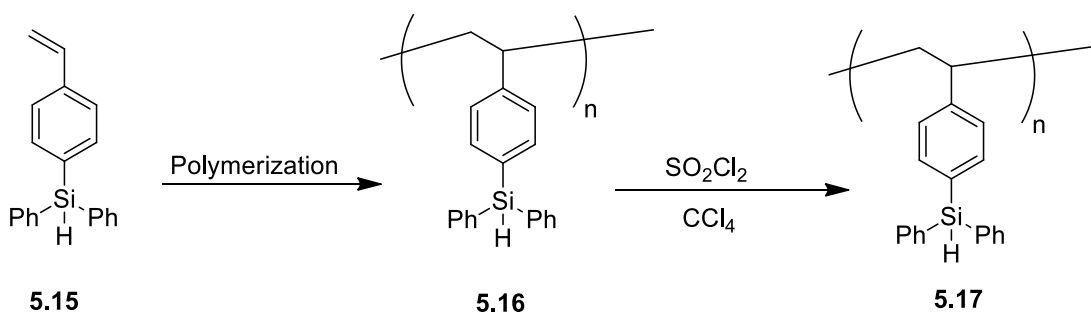
The focus of this project is to make the separation of enantiomers easy and more efficient. We are interested in crashing out one enantiomer with a polymer while the other remains in solution. To accomplish this goal, a careful synthesis of polymer supported silyl chloride is required. In our previous study, we showed that the selectivity of our kinetic resolution was dependent on the structure of the silyl chloride. Specifically, it was determined that three phenyl groups were strategic in obtaining selectivity. Therefore, the final polymer supported silyl chloride should possess three phenyl groups to get optimal selectivity. Also, the final polymer needs to be soluble in THF during the reaction and crash out upon addition of methanol after the reaction for its recovery. Two separate approaches are possible for polymer synthesis. In the first approach (**Approach 1**), a styrene based pendant type polymer (**5.12**) can be synthesized from the monomer 4-bromostyrene (**Scheme 5.5**). This polymer can be functionalized, a halogen source in polymer will allow us to do a lithium halogen exchange followed by the addition of a commercially available diphenylchlorosilane to achieve the polymer supported triphenyl

silane (**5.13**). This silane based polymer can then be converted into the chlorosilane (**5.14**) using SO_2Cl_2 in CCl_4 .



Scheme 5.5 Synthesis of polymer supported triphenylsilyl chloride from pendant type polymer

In the second approach (**Approach 2**), polymerization can be directly done using a silane monomer (**5.15**). In the first step, a monomer of interest will be synthesized and then polymerized to get **5.16**. In the second step it will be converted into a chlorosilane polymer (**5.17**) using sulfuryl chloride in CCl_4 (**Scheme 5.6**). The only limitation in this approach is that a special monomer is needed and if the monomer is not commercially available than it needs to be synthesized.



Scheme 5.6 Synthesis of polymer supported triphenylsilyl chloride using a silane monomer polymerization

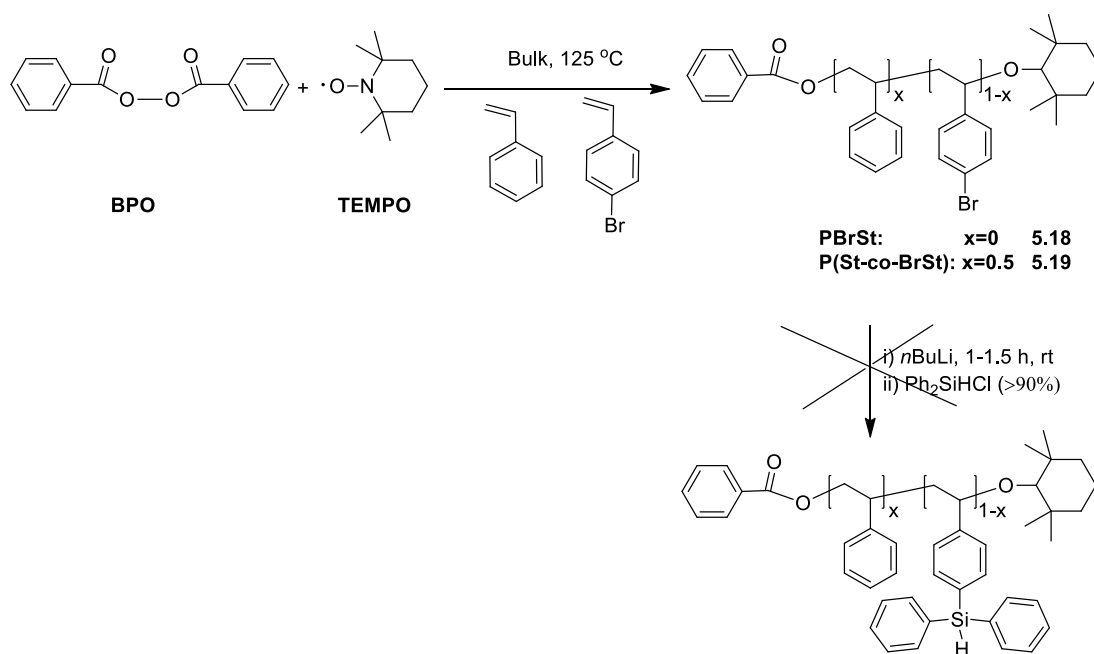
Overall using either method, a polymer supported chlorosilane can be achieved. Once we have a polymer supported chlorosilane, optimization of the kinetic resolution

reaction can be done using various modified versions of polymer in terms of their molecular weight and grafting patterns. After identifying the right polymer supported chlorosilane, several kinetic resolutions can be accomplished to resolve various substrates.

5.4 Result and discussion

In the beginning of our study, the polymer functionalization approach (approach 1) seemed to be a very promising way to attach the silane to the polymer. We begin our study with the synthesis of the polymer. To synthesize the polymers, a collaboration was undertaken with Dr. Tang's research group at the University of South Carolina. Liang Yuan, a graduate student in Dr. Tang's lab synthesized two different polymers, one a homopolymer and the other a random copolymer. In both polymers, 4-bromostyrene was used as the starting material to provide an attachment site for the silane through a lithium halogen exchange. Homo-polymer and random copolymer were synthesized using 4-bromostyrene and styrene (Scheme 5.7). A controlled radical polymerization was used to synthesis both homo and random polymers. A TEMPO (2,2,6,6-Tetramethylpiperidin-1-yl)oxy, BPO (benzoyl peroxide), 4-bromostyrene and styrene (in the case of random copolymer) were mixed together in a schlenk tube. The sealed system was degassed with three freeze-pump-thaw cycles and refilled with N₂. The flask was then put into an oil bath at 125°C and stirred for 20 h. After the polymerization, the cooled product was dissolved in CH₂Cl₂ and precipitated from cold methanol. The product was filtrated and dried under vacuum overnight. To analyze the molecular weight of the homopolymer and the random copolymer, GPC was used. For the homopolymer a Mw of 10.5 k was found with a PDI of 1.1, while for the random copolymer a Mw of 9.3 k was found with a PDI of 1.1. The functionalization of both polymers was attempted by performing the lithium halogen

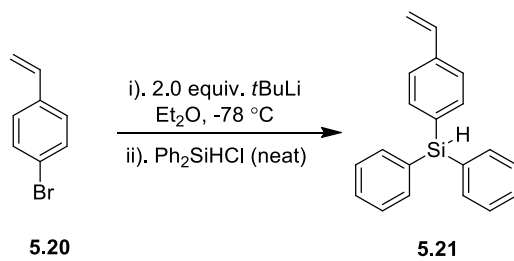
exchange using *n*BuLi followed by the addition of commercially available diphenylsilyl chloride (Ph₂SiHCl) for the silane formation. Unfortunately, in both polymers, a solid crude was obtained after each reaction which was found to be extremely difficult to solubilize in any solvent. We were unable to characterize the compounds through ¹H NMR due to solubility issues. (One possible problem could be the cross linking of the polymer after adding *n*BuLi, which resulted in the high molecular weight polymer, making it difficult to dissolve the crude product. To characterize the polymer product and make the polymer soluble, different techniques were tried where diphenylsilyl chloride was added first along with the polymer before adding *n*BuLi. A similar problem was encountered and therefore we decided to use another approach towards polymer supported silane synthesis.



Scheme 5.7 Attempted synthesis of triphenylsilane based polymer from homo and random co-polymer

In this approach (**Approach 2**), a monomer containing silane was synthesized first followed by the polymerization. During the synthesis of monomer, three key features were

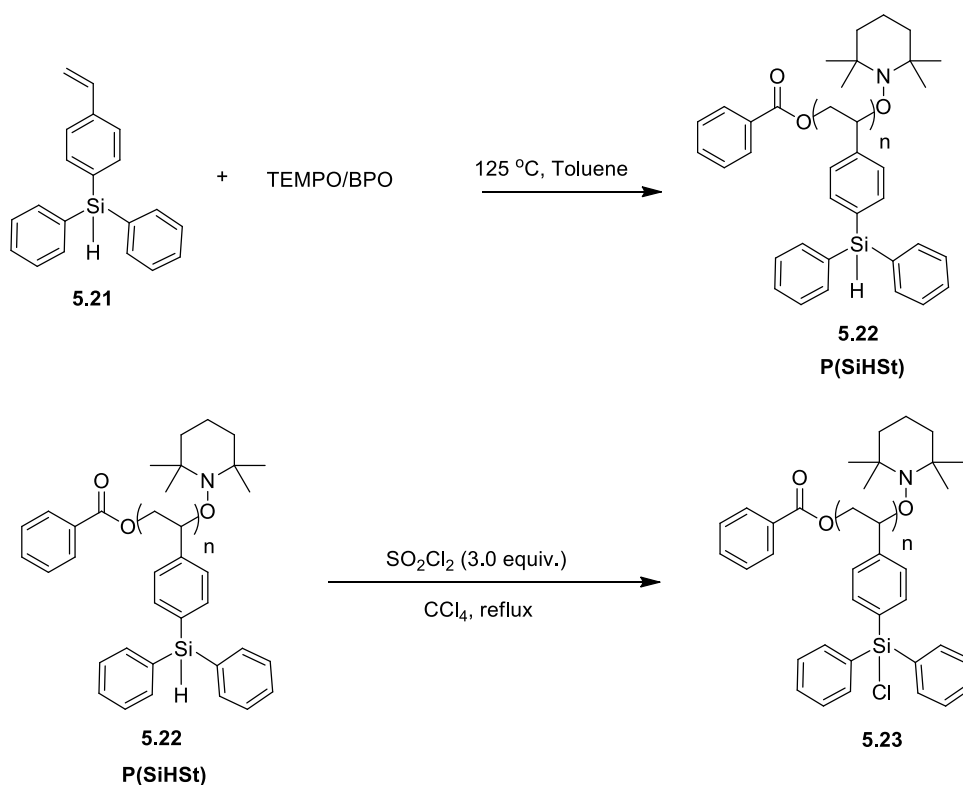
taken under consideration. In our system, the phenyl rings play a key role for selectivity and therefore the monomer must contain three phenyl rings. Second, the monomer should have an active site to carry out polymerization (double bond like styrene group). Third, the monomer should not react with other reagents during polymerization. With these three things in mind, we envisioned compound (**5.21**) as our choice of monomer. A Scifinder search was done to find any literature precedence. Fortunately, we found a synthesis of the compound in the literature³², which was very close to our requirement. Using the literature procedure, the monomer was synthesized (**Scheme 5.8**).



Scheme 5.8 Synthesis of *p*-Diphenylsilane styrene as a monomer

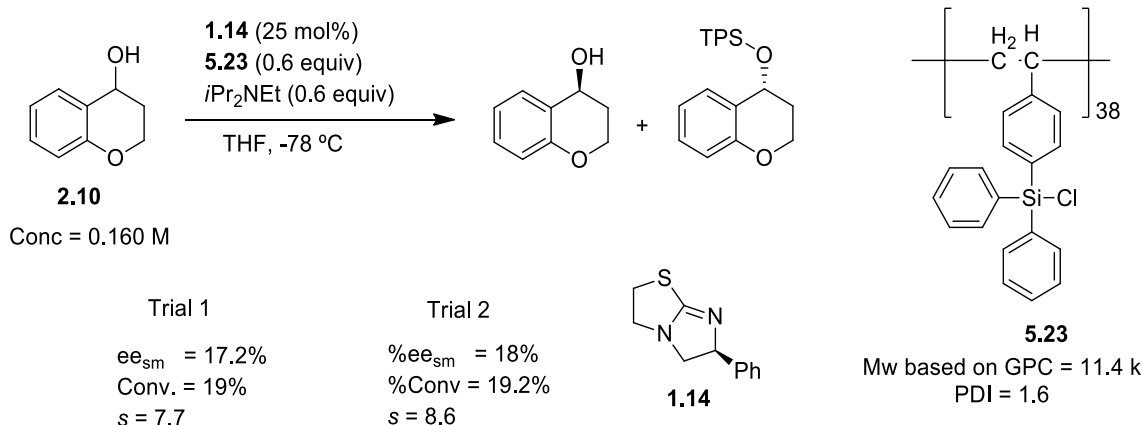
In this synthesis, a commercially available 4-bromostyrene (**5.20**) was purchased and dissolved in diethyl ether at -78 °C. Lithiation was done using 2 equivalent of *t*BuLi. After lithiation, one equivalent of diphenylchlorosilane was added at -78 °C and the resulting mixture was allowed to warm slowly to room temperature. The reaction was kept at room temperature for two hours before quenching. The monomer was purified using column chromatography with hexane as the eluent and utilized for the polymerization. The polymerization was carried out using the monomer and a successful polymer synthesis was achieved (**Scheme 5.9**). As mentioned earlier, Liang a graduate student from Dr. Chuanbing Tang lab synthesized the polymer similar way as mentioned in Scheme 5.7. GPC was used to find the molecular weight of the polymer and it was found to be 11.4 k

with a PDI of 1.6. After, getting polymer **5.22** from Dr. Tang's lab, it was converted into the chlorosilane polymer (**5.23**) using sulfuryl chloride in CCl₄. A colorless solid was obtained as a final product. To use this polymer in our kinetic resolution system, two key features were tested. First, the solubility of the polymer in THF and second whether it would crash out upon addition of methanol. Both solubility and recovery of polymer in THF as well as in methanol worked well.



Scheme 5.9 Synthesis of polymer supported triphenylsilyl chloride using monomer polymerization method

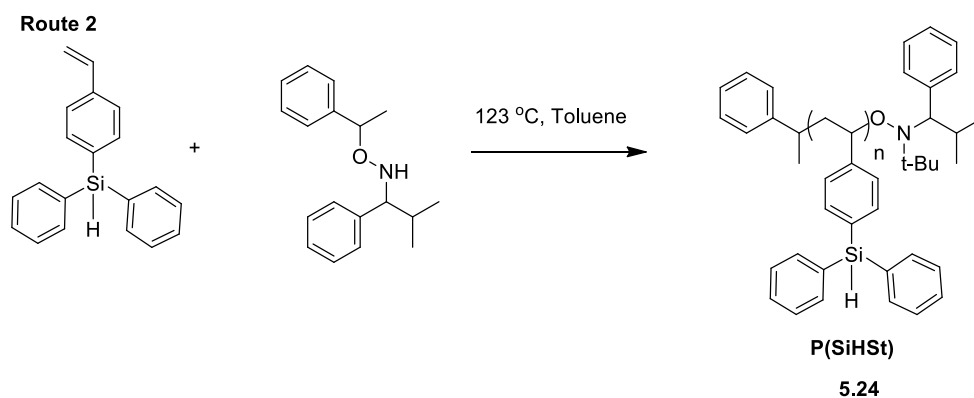
With this polymer in our hand, we started our preliminary investigation (**Scheme 5.10**). Similar reaction conditions were used as the solution based system. Due to the high selectivity in the solution based system, commercial availability, 4-chromanol (**2.10**) was used as the substrate of choice for kinetic resolution.



Scheme 5.10 Preliminary study using polymer supported chlorosilane in the kinetic resolution reaction

Duplicate reactions were set up using the polymer **5.23**. Similar reaction conditions were kept, as it was used in the solution based system for the silylation based kinetic resolution of monofunctional secondary alcohols. Nice solubility of the polymer was observed when a 0.357 M solution of **5.23** was prepared for the kinetic resolution. After 48 h, reaction was quenched with methanol and the polymer crashed out of the reaction. As expected one enantiomer covalently linked with the polymer and it was obtained simply by filtration while everything else remained in solution. Purification of the remaining enantiomer was done using column chromatography. To obtain the other enantiomer, the recovered polymer **5.23** was reacted with TBAF to desilylate the other alcohol enantiomer. Using chiral HPLC, the enantiomeric excess of both enantiomers were recorded. In both runs, similar conversions and selectivity factors were obtained. The average selectivity factor of 8.0 was obtained for 4-chroman-2-ol with conversion below 20% using the polymer supported silyl chloride. This selectivity factor was almost half that of the solution based system. To get a more accurate selectivity factor, higher conversion is required and therefore we decided to repeat the reaction with a slight modification to the reaction

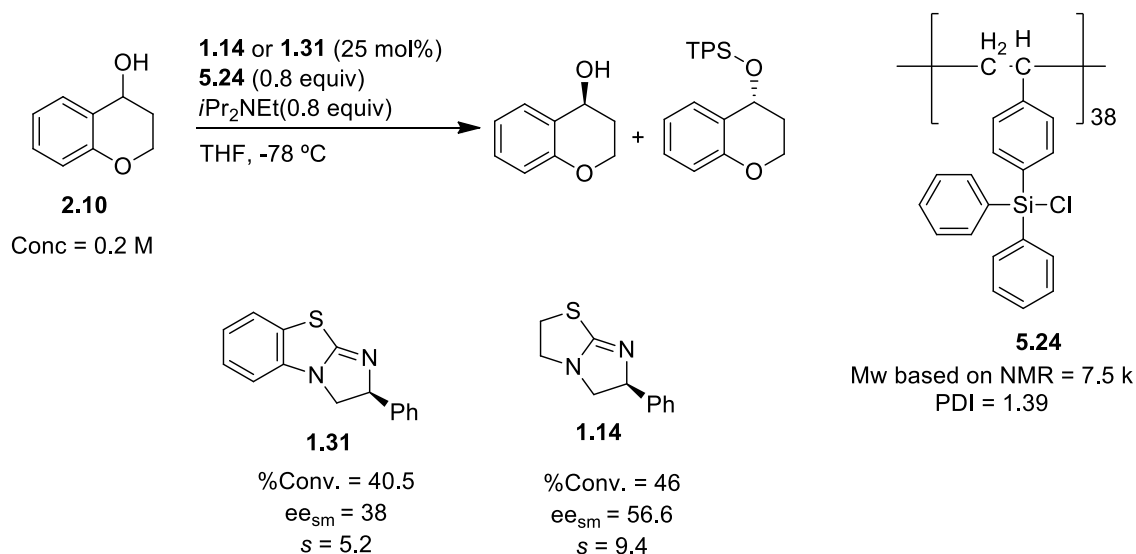
conditions. Another batch of **5.23** was synthesized and used in the kinetic resolution of 4-chromanol. Surprisingly, instead of getting a similar selectivity factor, a big drop in the selectivity factor was observed from 8 to 3. Also from the crude TLC, a lot of side products could be seen. To analyze this difference in selectivity factor, we looked back at our polymer. In both polymers, we found similar molecular weights but the only difference was the PDI. The previous polymer had a molecular weight of 11.4 k with a PDI of 1.61 while the second one had a molecular weight of 12.6 k with a PDI of 1.75. We thought, this higher PDI could be the major issue for the drop in selectivity factor and therefore we looked for a different method to synthesize the triphenylsilane based polymer to achieve a better PDI.



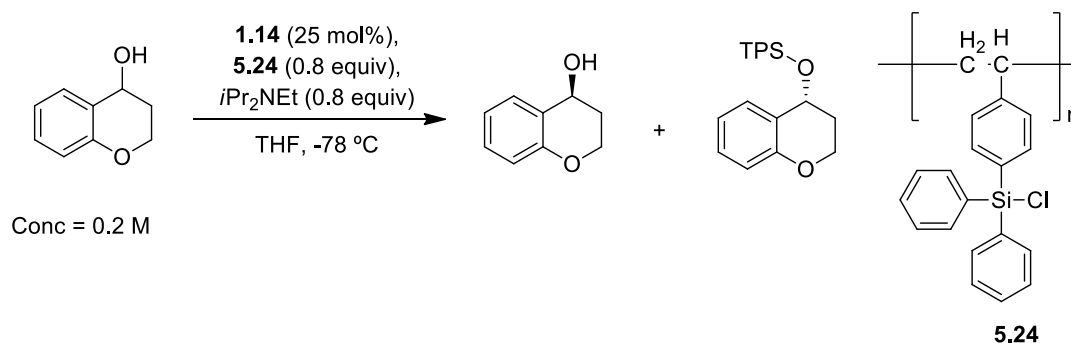
Scheme 5.11 Synthesis of polymer supported chlorosilane using different method

A lower molecular weight silane based polymer with a better PDI was synthesized (**Scheme 5.11**) using previously mentioned method but with using different initiator. A series of P(SiHSt) were prepared through this method and converted into the chlorosilane. The monomer and calculated amount of initiator were charged into a 10 ml Schlenk flask and dissolved using 2.0 mL dry toluene. The sealed system was degassed with three freeze-pump-thaw cycles and refilled with N₂. The flask was then put into an oil bath at 123 °C

and stirred for 24 h. After the polymerization, the cooled product was dissolved in CH₂Cl₂ and precipitated from cold methanol. The product was filtrated and dried under vacuum overnight. For all the polymerizations here, the conversion were driven to 100% as checked by ¹H NMR. The main difference between this methods of polymer synthesis form previous method Scheme 5.9 is the initiator. A better PDI was obtained due to the change in initiator. Since lower conversion was the major issue (Scheme 5.10) with polymer **5.23**, the overall reaction concentration was changed from 0.16 M to 0.2 M with excess polymer supported triphenylsilyl chloride (**5.24**) and Hünig's base (0.6 equiv. to 0.8 equiv.) being added to force the reaction to achieve higher conversion. Since both (-)-tetramisole (**1.14**) and (-)-benzotetramisole (**1.31**) have shown dramatic effects on the selectivity factors in our solution based systems, both were used in the kinetic resolution of 4-chromanol. Using these reaction conditions, the kinetic resolution was set up using both **1.14** and **1.31** to see which catalyst will work better with this system (Scheme 5.12). Better conversion was observed in both cases as compared to the previous system. A selectivity factor of 5.2 was observed with **1.31** while a selectivity factor of 9.4 was observed with **1.14**. In this regard, (-)-tetramisole was used as the catalyst in further reactions



Scheme 5.12 Screening of catalyst in the polymer supported kinetic resolution of 4-chromanol³³



Entry	Polymer Mw (Si-H)	n	PDI	%C	%e.r SM	s
1	7575	25	1.33	46	79:21	9.4
2	6125	20	1.24	44	73:27	5.5
3	3950	12.5	1.18	40	72:28	7.5

i) All reactions were carried out at a substrate concentration of 0.2 M on a 0.22 mmol scale. ii) %Conversion = $ees/(ees+eep) \times 100\%$ & $s = \ln[(1-C)(1-ees)]/\ln[(1-C)(1+ees)]$, where ees = ee of recovered starting material and eep = ee of product

Scheme 5.13 Screening of different molecular weight polymers in the kinetic resolution of 4-chromanol¹⁸

Now, we have our system working and therefore we turn our attention towards whether the molecular weight of the polymer affects the selectivity of the reaction. To test this, three different molecular weight polymers (**5.24**) were synthesized ranging from 3950-7575 and used in the kinetic resolution (Scheme 5.13). An average selectivity factor of 9.4 with conversion around 46% was obtained when higher molecular weight polymer supported triphenylchloro silane were used in our kinetic resolution of 4-chromanol (entry 1, Scheme 5.13). Two lower molecular weight polymer were also screened in our kinetic resolution system (entry 2 & 3, Scheme 5.13) but a very similar selectivity factor was observed with both polymers. From all three different molecular weight polymer, it is clear that change in molecular weight of polymer supported triphenylchloro silane have negligible effect on the selectivity factor. From the above result, polymer supported silylation based kinetic resolution systems have a promising future. A lot of work has been already done in this project. The next step for this project is to test several substrates to show the applicability towards various substrate classes using the best polymer from the above preliminary studies. Also, in a polymer supported system, the recyclability of the polymer is always a key concern. To show this, a large scale polymer supported kinetic resolution will be set up and after quenching each reaction, the polymer will be reused using a DIBAL-H (diisobutylaluminum hydride) reduction followed by the chlorination for multiple times to check selectivity factor.

5.5 Future Direction

Several modifications can be done to improve the selectivity factor in the future for the polymer supported silylation based kinetic resolution. A one important change can be the introduction of a spacer between the polymer or the attachment of Ph_3SiCl to a polymer

resin. Several commercially available resins can be used to attach Ph_3SiCl through a linker. A spacer between the polymer and Ph_3SiCl may allow us to improve the selectivity factor. Several examples have been reported where the introduction of a spacer improves both reactivity and selectivity.

Another important modification can be done through the catalyst. As catalyst recovery is a big concern in asymmetric reactions, incorporation of the catalyst on the polymer instead of the silyl source would allow to recover catalyst. Also, catalyst and Ph_3SiCl can be incorporated on a separate polymer to create a biphasic system where using one solvent, the catalyst can be crashed out while using another solvent would cause the silylated polymer to crash out. Using this dual approach, both catalyst and silyl chloride can be recovered and recycle.

5.6 Conclusions

In conclusion, substituents at the *para* position of Ph_3SiCl have shown promising effects in the selectivity improvement of monofunctional secondary alcohols during the mechanistic investigation through a LFER. The more definitive evidence of the selectivity improvement using substituent at *para* position of Ph_3SiCl was seen in the kinetic resolution of 2-arylcyclohexanol (Chapter 4). Therefore, to take the advantage of this *para* position and to develop a more practical kinetic resolution system, polymer was incorporated to the Ph_3SiCl in our system. The advantage of using polymer supported Ph_3SiCl would include the easy separation of enantiomer and recovery of polymer for further recyclability. A synthesis of polymer supported Ph_3SiCl was the major challenge in our project and to achieve that two separate approach was envisioned. In first approach, using a 4-bromostyrene polymer was synthesized followed by Ph_2SiHCl grafting to it.

Unfortunately, no desired polymer product was obtained due to crosslinking of polymer. Finally, using a second approach a successful synthesis of polymer supported Ph_3SiCl was achieved through pre-synthesized monomer and using it for polymerization. To achieve polymer supported Ph_3SiCl , chlorination was done using SO_2Cl_2 in CCl_4 . Using a similar reaction condition as reported in a solution based kinetic resolution reaction, duplicate reaction was set up. A selectivity factor of 8.0 was obtained for 4-chromanol with conversion lower than 20%. To achieve, higher conversion and test the various polymer molecular weight effect on selectivity factor, three different molecular weight containing polymer supported Ph_3SiCl was synthesized using better polymerization technique followed by chlorination. Using this polymers, kinetic resolution of 4-chromanol was carried out. Very similar selectivity factor was observed in all three cases. In future, one higher molecular weight Ph_3SiCl base polymer will be tested. Using the best result, best molecular weight polymer will be utilized for substrate screening. Finally to show practicality of our system, large scale polymer supported kinetic resolution will be set up and polymer recyclability will be tested.

5.7 Experimental

General Information

All kinetic resolution reactions and the synthesis of different silanes and silyl chloride based polymers including monomer were carried out under a N_2 atmosphere using oven dried glassware. THF and diethyl ether were dried by passing through a column of activated alumina before use and stored over molecular sieves. Carbon tetrachloride were distilled and stored over molecular sieves. CCl_4 was degassed before chlorination. Sulfuryl chloride was distilled prior to use. All other chemicals were purchased from a commercial source

and used without further purification. Molecular sieves were activated for 48 h at 130 °C in an oven. Flash column chromatography was performed with silica gel (32-63 μm). All enantiomeric ratios were determined by HPLC using the chiral stationary phase Chiralcel OD-H (4.6 \times 250 mm \times 5 μm) column, and monitored using a photodiode array detector in comparison with authentic racemic materials. NMR spectra were obtained at room temperature using 400 MHz (^1H), 101 MHz (^{13}C), 80 MHz (^{29}Si), and 377 MHz (^{19}F). Chemical shifts for ^1H , ^{13}C , ^{19}F and ^{29}Si was recorded in part per million with either TMS (0.00 ppm), or CDCl_3 (7.26 ppm for ^1H or 77.0 ppm for ^{13}C) as a reference. TMS was used as a reference (0.00 ppm) to obtain ^{29}Si NMR. Data reported in ^1H NMR are as follows: Chemical shift, multiplicity (s = singlet, d = doublet, t = triplet, q = quartet, dd = doublet of doublet, dt = doublet of triplet, sept = septet, m = multiplet) and coupling constant (Hz).

General Procedure for the polymer supported Silylation-Based Kinetic Resolution of Secondary Alcohols and Desilylation of the Isolated Products.

An oven dried 1 dram vial was charged with 4 Å molecular sieves (10-15 mg) and a Teflon coated stir bar. The racemic alcohol (**2.10**) (0.22 mmol), catalyst **1.14** or **1.31** (11.2 mg, 0.055 mmol) and *N,N*-diisopropylethylamine (Hünig's Base) (31 μL , 0.176 mmol) were added to a vial and then quickly sealed under a nitrogen atmosphere. Dry THF (1.0 mL) was added and the reaction mixture was allowed to stir at -78 °C for 15-20 minutes. Meanwhile a solution of (*Poly-Ph*) $_3\text{SiCl}$ (0.5 M) was prepared using a volumetric flask (under N_2). The solution of (*Poly-Ph*) $_3\text{SiCl}$ **5.24** (352 μL , 0.8 mmol) was added to the reaction vial and the resulting mixture was allowed to react for the specified amount of time at -78 °C. The reaction mixture was then quenched using 300 μL of MeOH at -78 °C. The mixture was allowed to warm to room temperature. The reaction mixture was

transferred to a 4 dram vial and excess methanol was added. One enantiomer with polymer crash out in solution. Mixture was filtered and filtrate was rotavap it down. Filtrate was washed 2-3 times to avoid any polymer ppt. Filtrate was collected into separate vial. While solid collected during filtration was transfer to another vial. Column chromatography was performed on filtrate collected vial, as it's a unreacted enantiomer. (5% EtOAc in hexane to 25% EtOAc in hexane). The analysis of the unreacted recovered alcohol was done by a chiral HPLC using a hexanes/*i*-PrOH solvent system.

Desilylation: The silylated product (solid collected in vial) was added a stir bar and dissolved in 3 mL of THF. The solution was treated with a 1M solution of TBAF in THF (500 μ L - 1.0 mL) and allowed to stir for 10-12 h at room temperature (conversion was monitored by TLC). The reaction was quenched with brine and extracted with diethyl ether. The crude mixture was purified via silica gel column chromatography (CH₂Cl₂ to 2% MeOH in CH₂Cl₂). HPLC analysis was done for the desilylated product (alcohol). The absolute stereochemistry was confirmed by comparing the HPLC data with previously published data.

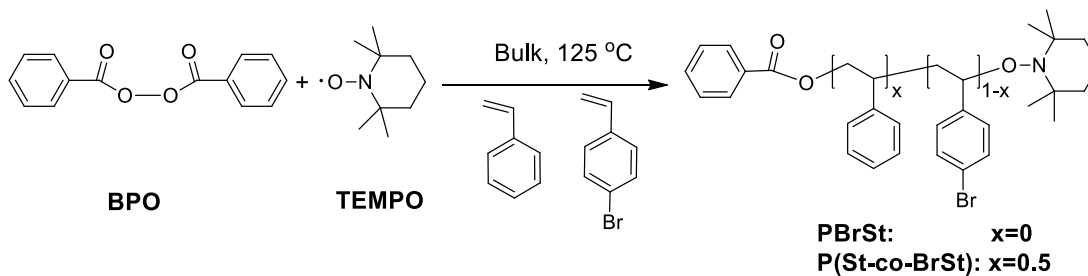
Synthesis of Monomer (*p*-Diphenylsilane styrene) (5.21):

In an oven dry three neck 250 mL rbf was charged with stir bar und N₂. 70 mL diethyl ether was added to the flask at room temperature under N₂ and allow to cool at -78 °C. After 15-20 minutes later, 17.6 ml (1.7 M, 30 mmol) tBuLi was added to the flask and allow to stir for 5-10 minutes. 4-bromostyrene (1.96 ml ,15 mmol) was added slowly to reaction flask. A color change from light yellow to dark red to deep orange was observed. A reaction was allow to stir for 30 minutes at -78 °C. Finally, after 30 minute, diphenylchloro silane (3.24 mL, 15 mmol) was added drop wise and bath was removed from -78 °C. Resulting mixture

was allowed to stir at room temp for 2 h. After 2 h, reaction mixture was quenched using 15 mL of water. Extraction was done using hexane and washed with brine. Reaction mixture was concentrated using vacuum and column chromatography was performed using hexane as a solvent. Colorless liquid was obtained as a final product. (2.6 g, 9.1 mmol, Yield = 61%). ^1H NMR (300 MHz, CDCl_3) : 7.57 (m, 6H), 7.39 (m, 8H), 6.75 (m, 1H), 5.79 (d, $J = 18$ Hz, 1H), 5.47 (s, 1 H), 5.28 (d, $J = 9$ Hz, 1 H). ^{13}C NMR (75 MHz, CDCl_3): 139.0, 136.8, 136.1, 135.8, 133.3, 132.9, 129.9, 128.1, 125.9, 114.8.

Materials for polymer synthesis: Styrene (Alfa Aesar) was passed through a basic Al_2O_3 column before use. TEMPO (Alfa Aesar), 4-Bromostyrene (Alfa Aesar), BPO (Fisher Scientific), and N-tert-Butyl-N-(2-methyl-1-phenylpropyl)-O-(1-phenylethyl) hydroxylamine (NMP universal initiator, Sigma Aldrich) were purchased and used as received.

Schemes 5.7: Synthesis of 4-bromostyrene containing polymers (5.18 & 5.19).



Synthesis of homopolymer from 4-bromostyrene (PBrSt)

TEMPO 15.6 mg (0.1 mmol), BPO 12.1 mg (0.05 mmol) and 4-bromostyrene 1.83 g (10.0 mmol) were charged into a 10 ml Schlenk flask. The sealed system was degassed with three freeze-pump-thaw cycles and refilled with N_2 . The flask was then put into an oil bath at 125°C and stirred for 20 h. After the polymerization, the cooled product was dissolved in

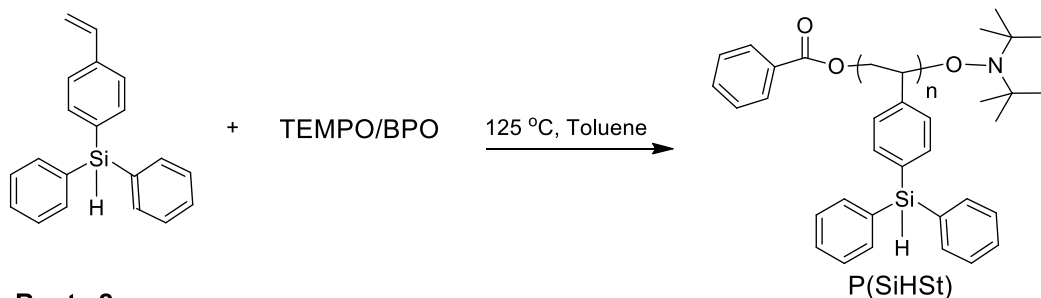
CH₂Cl₂ and precipitated from cold methanol. The product was filtrated and dried under vacuum overnight.

Synthesis of random copolymer P(St-co-BrSt) (5.19):

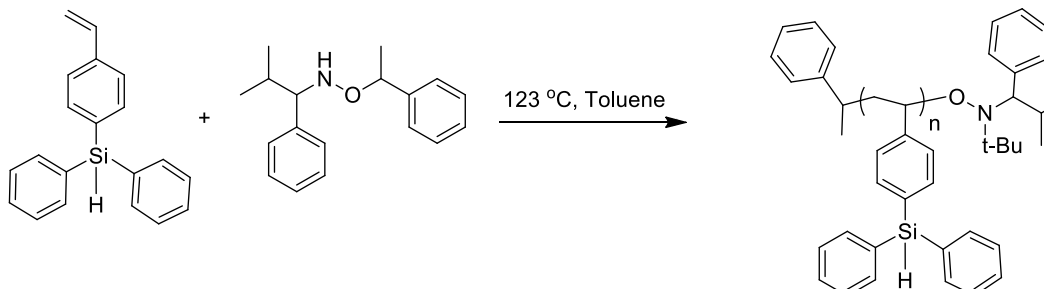
TEMPO 31.2 mg (0.2 mmol), BPO 24.2 mg (0.1 mmol), styrene 1.04 g (10.0 mmol) and 4-bromostyrene 1.83 g (10.0 mmol) were charged into a 10 ml Schlenk flask. The sealed system was degassed with three freeze-pump-thaw cycles and refilled with N₂. The flask was then put into an oil bath at 125°C and stirred for 20 h. After the polymerization, the cooled product was dissolved in CH₂Cl₂ and precipitated from cold methanol. The product was filtrated and dried under vacuum overnight.

Synthesis of homopolymers of 4-diphenylhydrosilylstyrene (PSiHSt) (5.23)

Route 1



Route 2



Synthesis of P(SiHSt) by BPO/TEMPO (Route 1):

TEMPO 9.15 mg (0.05 mmol), BPO 6.05 mg (0.025 mmol), and SiHSt 0.58 g (2.0 mmol) were charged into a 10 ml Schlenk flask and dissolved 2.0 mL dry toluene. The sealed system was degassed with three freeze-pump-thaw cycles and refilled with N₂. The flask was then put into an oil bath at 125°C and stirred for 24 h. After the polymerization, the cooled product was dissolved in CH₂Cl₂ and precipitated from cold methanol. The product was filtrated and dried under vacuum overnight.

Synthesis of P(SiHSt) by NMP universal initiator (5.24)(Route 2):

A series of P(SiHSt) were prepared through this method. The monomer and calculated amount of initiator were charged into a 10 ml Schlenk flask and dissolved 2.0 mL dry toluene. The sealed system was degassed with three freeze-pump-thaw cycles and refilled with N₂. The flask was then put into an oil bath at 123°C and stirred for 24 h. After the polymerization, the cooled product was dissolved in CH₂Cl₂ and precipitated from cold methanol. The product was filtrated and dried under vacuum overnight. For all the polymerizations here, the conversion were driven to 100% as checked by ¹H NMR.

HPLC data for Silylated Chromanol product**Kinetic Resolution for Scheme 5.13, Entry 1:**

#	er _{SM} %	er _{PR} %	C%	S	S _{Avg}
1	78:22	15:85	44.9	9.70	9.4
2	79:21	16:84	46	9.03	

er_{PR}% is of deprotected and purified product.

Kinetic Resolution for Scheme 5.13, Entry 2:

#	er _{SM} %	er _{PR} %	C%	<i>S</i>	<i>S</i> _{Avg}
1	73:27	21:79	44.2	5.91	5.5
2	71:29	23:77	44	5.00	

er_{PR}% is of deprotected and purified product.

Kinetic Resolution for Scheme 5.13, Entry 3:

#	er _{SM} %	er _{PR} %	C%	<i>S</i>	<i>S</i> _{Avg}
1	72:28	16:84	39.8	7.91	7.5
2	73:27	18:82	42.1	7.07	

er_{PR}% is of deprotected and purified product

5.8 References

- (1) Akhani, R. K.; Moore, M. I.; Pribyl, J. G.; Wiskur, S. L.: Linear free-energy relationship and rate study on a silylation-based kinetic resolution: mechanistic insights. *J. Org. Chem.* **2014**, *79*, 2384-2396.
- (2) Sheppard, C. I.; Taylor, J. L.; Wiskur, S. L.: Silylation-based kinetic resolution of monofunctional secondary alcohols. *Org. Lett.* **2011**, *13*, 3794-3797.
- (3) Clapham, B.; Reger, T. S.; Janda, K. D.: Polymer-supported catalysis in synthetic organic chemistry. *Tetrahedron* **2001**, *57*, 4637-4662.
- (4) Bhalay, G.; Dunstan, A.; Glen, A.: Supported reagents: Opportunities and limitations. *Synlett* **2000**, 1846-1859.
- (5) De, B. B.; Lohray, B. B.; Sivaram, S.; Dhal, P. K.: Enantioselective Epoxidation of Olefins Catalyzed by Polymer-Bound Optically-Active Mn(III)-Salen Complex. *Tetrahedron-Asymmetr* **1995**, *6*, 2105-2108.
- (6) De, B. B.; Lohray, B. B.; Sivaram, S.; Dhal, P. K.: Polymeric catalysts for chemo- and enantioselective epoxidation of olefins: New crosslinked chiral transition metal complexing polymers. *J. Polym. Sci., Part A: Polym. Chem.* **1997**, *35*, 1809-1818.
- (7) Minutolo, F.; Pini, D.; Petri, A.; Salvadori, P.: Heterogeneous asymmetric epoxidation of unfunctionalized olefins catalyzed by polymer-bound (salen)manganese complexes. *Tetrahedron-Asymmetr* **1996**, *7*, 2293-2302.
- (8) Minutolo, F.; Pini, D.; Salvadori, P.: Polymer-bound chiral (salen)Mn(III) complex as heterogeneous catalyst in rapid and clean enantioselective epoxidation of unfunctionalised olefins. *Tetrahedron Lett.* **1996**, *37*, 3375-3378.
- (9) Song, C. E.; Roh, E. J.; Yu, B. M.; Chi, D. Y.; Kim, S. C.; Lee, K. J.: Heterogeneous asymmetric epoxidation of alkenes catalysed by a polymer-bound (pyrrolidine salen)manganese(III) complex. *Chem. Commun.* **2000**, 615-616.
- (10) Sellner, H.; Seebach, D.: Dendritically cross-linking chiral ligands: High stability of a polystyrene-bound Ti-TADDOLate catalyst with diffusion control. *Angew. Chem., Int. Ed.* **1999**, *38*, 1918-1920.
- (11) Kamahori, K.; Ito, K.; Itsuno, S.: Asymmetric Diels-Alder reaction of methacrolein with cyclopentadiene using polymer-supported catalysts: Design of highly enantioselective polymeric catalysts. *J. Org. Chem.* **1996**, *61*, 8321-8324.

- (12) Glos, M.; Reiser, O.: Aza-bis(oxazolines): New chiral ligands for asymmetric catalysis. *Org. Lett.* **2000**, 2, 2045-2048.
- (13) Zheng, X. L.; Jones, C. W.; Weck, M.: Poly(styrene)-supported co-salen complexes as efficient recyclable catalysts for the hydrolytic kinetic resolution of epichlorohydrin. *Chem.-Eur. J.* **2006**, 12, 576-583.
- (14) Kumar, M.; Kureshy, R. I.; Shah, A. K.; Das, A.; Khan, N. U.; Abdi, S. H. R.; Bajaj, H. C.: Asymmetric Aminolytic Kinetic Resolution of Racemic Epoxides Using Recyclable Chiral Polymeric Co(III)-Salen Complexes: A Protocol for Total Utilization of Racemic Epoxide in the Synthesis of (R)-Naftopidil and (S)-Propranolol. *J. Org. Chem.* **2013**, 78, 9076-9084.
- (15) Shamoto, K.; Miyazaki, A.; Matsukura, M.; Kobayashi, Y.; Shioiri, T.; Matsugi, M.: A Nonenzymatic Kinetic Resolution of (+/-)-trans-2-Arylcyclohexanols via Esterification Using Polymer-Supported DCC, DMAP, and 3 beta-Acetoxyetienic Acid. *Synth. Commun.* **2013**, 43, 1425-1431.
- (16) Annis, D. A.; Jacobsen, E. N.: Polymer-supported chiral Co(salen) complexes: Synthetic applications and mechanistic investigations in the hydrolytic kinetic resolution of terminal epoxides. *J. Am. Chem. Soc.* **1999**, 121, 4147-4154.
- (17) Matkiewicz, K.; Bukowska, A.; Bukowski, W.: Novel highly active polymer supported chiral Co(III)-salen catalysts for hydrolytic kinetic resolution of epichlorohydrin. *J. Mol. Catal. A.: Chem.* **2013**, 368, 43-52.
- (18) Okudomi, M.; Shimojo, M.; Nogawa, M.; Hamanaka, A.; Taketa, N.; Matsumoto, K.: Easy separation of optically active products by enzymatic hydrolysis of soluble polymer-supported substrates. *Tetrahedron Lett.* **2007**, 48, 8540-8543.
- (19) Okudomi, M.; Nogawa, M.; Chihara, N.; Kaneko, M.; Matsumoto, K.: Enzyme-mediated enantioselective hydrolysis of soluble polymer-supported dendritic carbonates. *Tetrahedron Lett.* **2008**, 49, 6642-6645.
- (20) Whalen, L. J.; Morrow, C. J.: Resolution of a chiral alcohol through lipase-catalyzed transesterification of its mixed carbonate by poly(ethylene glycol) in organic media. *Tetrahedron-Asymmetr* **2000**, 11, 1279-1288.
- (21) Wallace, J. S.; Reda, K. B.; Williams, M. E.; Morrow, C. J.: Resolution of a Chiral Ester by Lipase-Catalyzed Transesterification with Poly(Ethylene Glycol) in Organic Media. *J. Org. Chem.* **1990**, 55, 3544-3546.

- (22) Clapham, B.; Cho, C. W.; Janda, K. D.: A polymer-supported proline-based diamine catalyst for the kinetic resolution of racemic secondary alcohols. *J. Org. Chem.* **2001**, *66*, 868-873.
- (23) Arseniyadis, S.; Subhash, P. V.; Valleix, A.; Wagner, A.; Mioskowski, C.: Unprecedented, fully recyclable, solid-supported reagent for the kinetic resolution of racemic amines through enantioselective N-acetylation. *Chem. Commun.* **2005**, 3310-3312.
- (24) Kreituss, I.; Murakami, Y.; Binanzer, M.; Bode, J. W.: Kinetic Resolution of Nitrogen Heterocycles with a Reusable Polymer-Supported Reagent. *angew. Chem., Int. Ed.* **2012**, *51*, 10660-10663.
- (25) Issenhuth, J. T.; Dagorne, S.; Bellemin-Laponnaz, S.: A practical concept for the kinetic resolution of a chiral secondary alcohol based on a polymeric silane. *J. Mol. Catal. A.: Chem.* **2008**, *286*, 6-10.
- (26) Rendler, S.; Auer, G.; Oestreich, M.: Kinetic resolution of chiral secondary alcohols by dehydrogenative coupling with recyclable silicon-stereogenic silanes. *Angew. Chem., Int. Ed.* **2005**, *44*, 7620-7624.
- (27) Rendler, S.; Auer, G.; Keller, M.; Oestreich, M.: Preparation of a privileged silicon-stereogenic silane: Classical versus kinetic resolution. *Adv. Synth. Catal.* **2006**, *348*, 1171-1182.
- (28) Rendler, S.; Oestreich, M.: Conformational rigidity of silicon-stereogenic silanes in asymmetric catalysis: A comparative study. *Beilstein J Org Chem* **2007**, *3*.
- (29) Rendler, S.; Oestreich, M.: Polishing a diamond in the rough: "Cu-H" catalysis with silanes. *Angew. Chem., Int. Ed.* **2007**, *46*, 498-504.
- (30) Klare, H. F. T.; Oestreich, M.: Chiral recognition with silicon-stereogenic silanes: Remarkable selectivity factors in the kinetic resolution of donor-functionalized alcohols. *Angew. Chem., Int. Ed.* **2007**, *46*, 9335-9338.
- (31) Greene, T. W.; Wuts, P. G. M.: *Protective Groups in Organic Synthesis*; 3rd ed.; Wiley: New York, 1999.
- (32) Lindsley, C. W.; Hodges, J. C.; Filzen, G. F.; Watson, B. M.; Geyer, A. G.: Rasta silanes: New silyl resins with novel macromolecular architecture via living free radical polymerization. *J. Comb. Chem.* **2000**, *2*, 550-559.
- (33) Conversion and selectivity factors were calculated from the ee of the product and the ee of the left over starting material. Selectivity factors are an average of two runs. Conversion and er correspond to a single run.

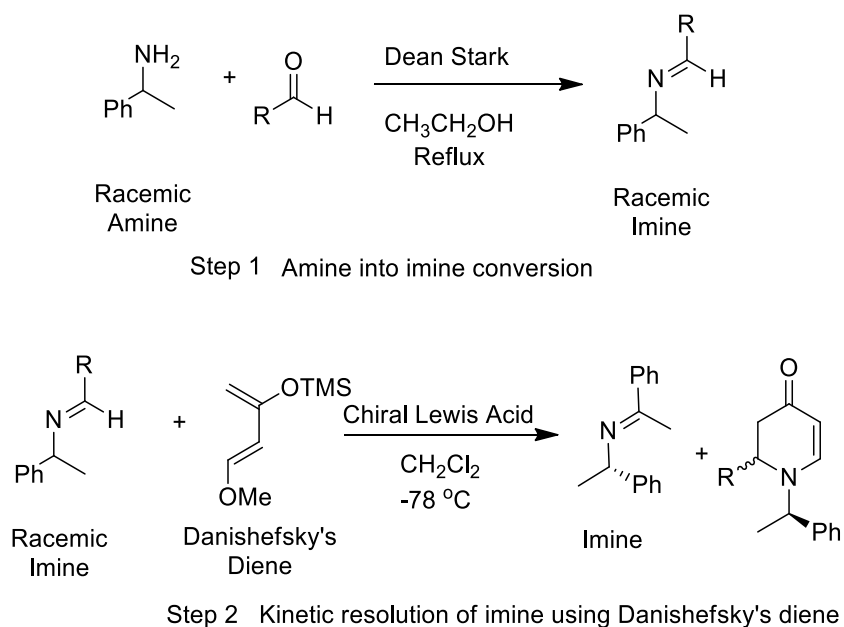
CHAPTER 6

KINETIC RESOLUTIONS OF AMINES VIA IMINES USING AN AZA DIELS-ALDER REACTION

6.1 Introduction

The aim of this project was to develop a method to enantioselectively resolve chiral amines. The resolution of amines is an important task in organic methodology due to frequent use as building blocks in the pharmaceutical industry. In this project, the main challenge to overcome was how to circumvent the inherent nucleophilicity of amines. In order to achieve this, amines were converted into imines where a chiral aza-Diels-Alder reaction can be utilized to achieve the resolution of amines via imines. By converting amines into imines it provides a different mechanism for resolving amines, circumventing the problem of the amines intrinsic nucleophilicity and provides an efficient route for the preparation of enantiomerically pure amines. Additionally, the kinetic resolution provides the optically active piperidine heterocycles, itself a useful building block. In this research, we present our attempt to develop the successful kinetic resolution of amines by means of a chiral Lewis acid. The recovered imine was simply hydrolyzed to recover amine starting material (Scheme 6.1).

Here, the imine acts as a dienophile towards Danishefsky's diene to facilitate the reaction. Several chiral Lewis acid were tested to achieve better selectivity factor. Unfortunately, no meaningful selectivity was observed in any cases. This work represents our initial efforts towards the kinetic resolution of amines via imines.



Scheme 6.1 Basic protocol for the kinetic resolution of amines via imines

6.2 Background

Enantiomerically enriched chiral amines are the most valuable building blocks due to their use as resolving agents, chiral auxiliaries and synthetic building blocks for pharmaceuticals as well as agrochemicals.¹ Chiral amines play a key role in pharmaceuticals due to its hydrogen bonding ability. Figure 6.1 displays a few examples of the use of chiral amines in drugs and therefore the importance of their enantiomeric synthesis in the pharmaceutical industry.²

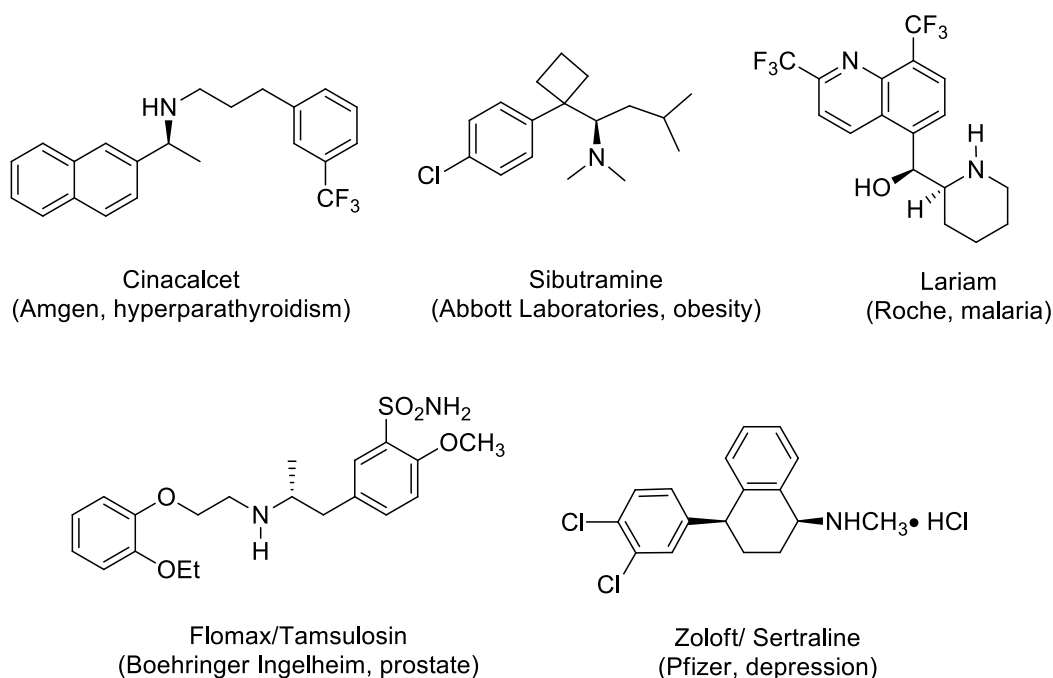


Figure 6.1 Chiral amines in pharmaceutical drugs

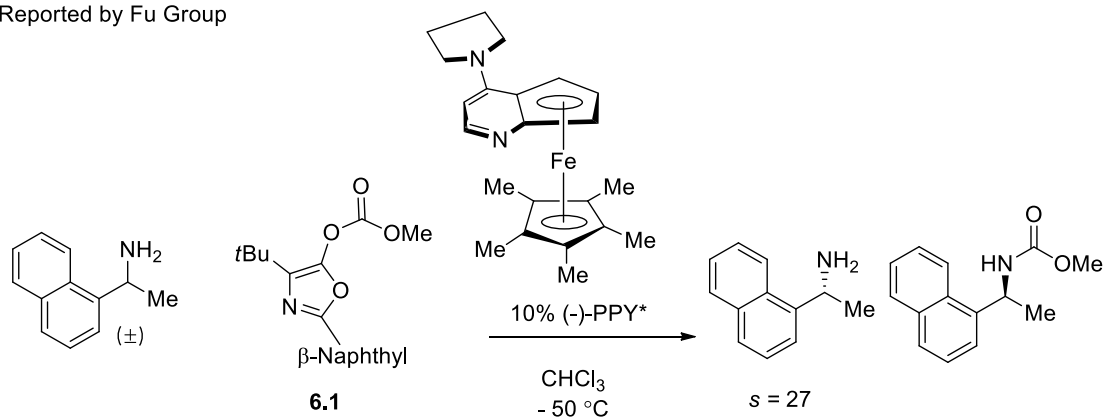
A variety of methodologies have been proposed for the generation of enantiomerically pure amines, but we wanted to obtain them enantiomerically pure through kinetic resolutions.³ As discussed in chapter 1, kinetic resolutions have several advantages associated with it, including cheap starting material (racemic mixture) and control over conversion to achieve highest enantiomeric ratio even with lower selectivity factor. Several enzymatic kinetic resolutions have been reported in the past to resolve amines.^{4,5} However, enzymes can have a limited substrate scope and might only work under certain reaction conditions. Alternatively, non-enzymatic kinetic resolutions (in which our group is interested) can be more widely applicable with regards to conditions and substrates. Several small molecule catalyzed kinetic resolutions were reported in the past to resolve amines. Most examples of non-enzymatic kinetic resolutions of amines employ a stoichiometric chiral acylating reagent.⁶⁻¹¹

In 2000, the Fu group reported the first successful non enzymatic kinetic resolution of amines.⁸ Several acylating reagents were examined in this methodology using the catalyst (-)-PPY* with no selectivity. Interestingly, bulky O-acylated azalactone **6.1** (Scheme 6.2 (A)) was found to be an effective acylating reagent. Numerous benzylic amines were resolved with good selectivity ranging from 11-27.^{12,13}

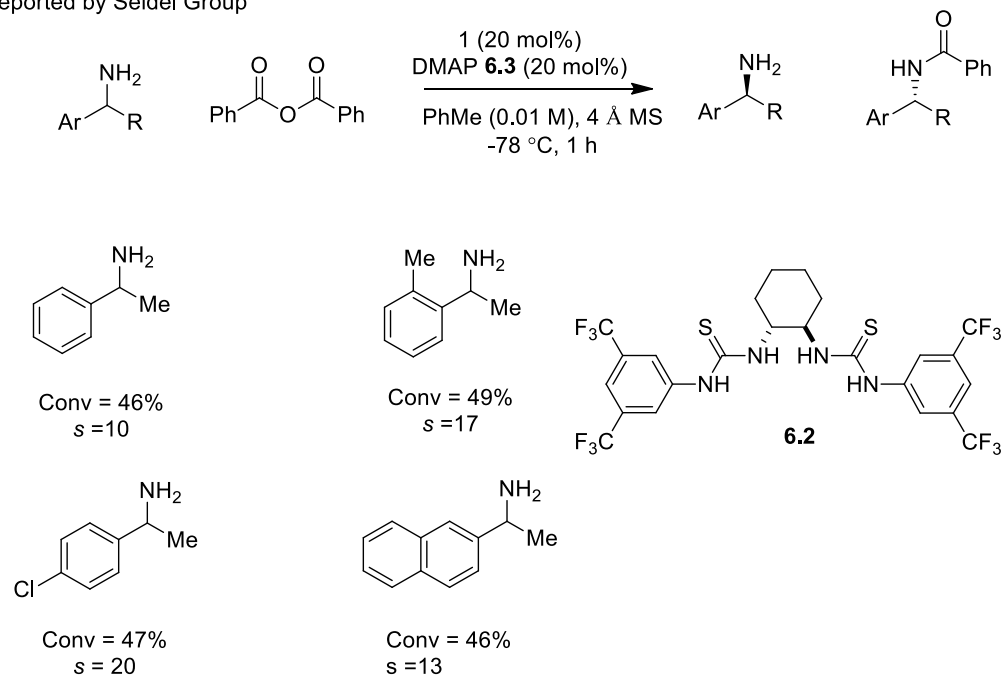
In 2009, the Seidel group reported a dual catalysis approach¹⁴ to selectively resolve racemic amines using a chiral hydrogen-bond donor catalyst along with an achiral nucleophilic cocatalyst.¹⁵ In this methodology, bistiourea **6.2** (Scheme 6.2 (B)) was used as a chiral catalyst and DMAP (**6.3**) (Scheme 6.2) as a cocatalyst. Using an equimolar mixture of chiral catalyst and cocatalyst, benzylic amines were resolved with selectivity factors ranging from 7.1 to 24.^{15,16} Using the same dual catalyst principal, this methodology was further extended to other classes of amines including the kinetic resolution of propargylic amines ($s = 12$ to 56),¹⁷ allylic amines ($s = 3.5$ - 20)¹⁸, and 1,2-diarylethane-1,2-diamines ($s = 4$ - 30).¹⁹

More recently, Bode and his group reported a kinetic resolution reaction of secondary amines (Scheme 6.2 (C)).^{20,21} A dual-catalysis redox approach was used to resolve several structurally modified amines. The major reason for the limited progress of catalytic kinetic resolutions of amines could be the nucleophilicity of amines. In most cases, amines can become acylated without the aid of a catalyst. It is for this reason that the kinetic resolution of amines remains under explored.

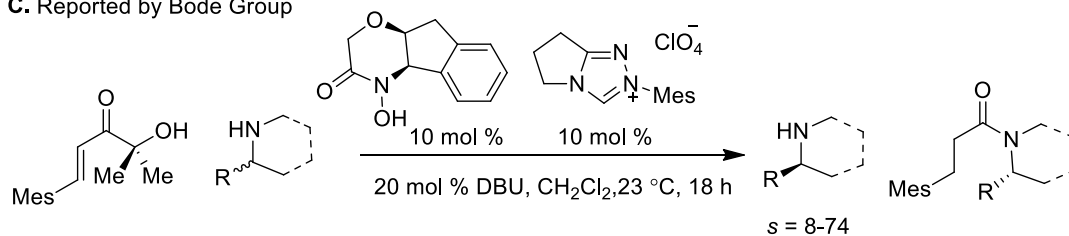
A. Reported by Fu Group



B. Reported by Seidel Group



C. Reported by Bode Group



Scheme 6.2 Catalytic non-enzymatic kinetic resolution of amines

Birman Work:

er Work:

6.7

6.5

2 (5 mol%)

Boc₂O **6.6** (0.6 equiv)

CHCl₃, 4 Å MS,
25 °C, 15 h

6.8

F₃CCOOH
CH₂Cl₂
NaOH, MeOH

6.9

Yield = 82%

s = 170

Conv = 51%
ee = 73%
s = 12.8

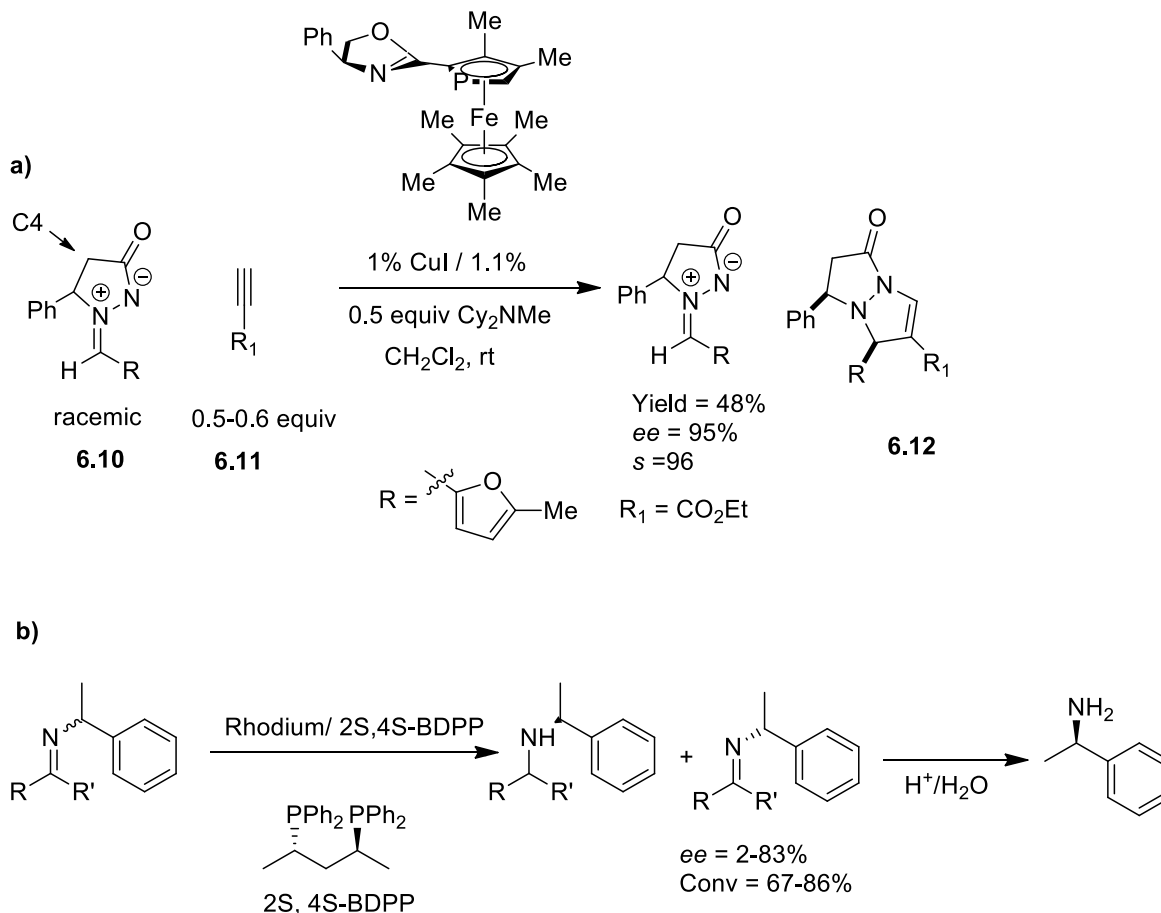
In 2006, the Birman group reported the kinetic resolution of 2-oxazolidinones (**6.4**) (Scheme 6.3), where the best selectivity factor (up to 520) was reported using benzotetramisole (BTM, **1.15**) as the catalyst and isobutyric anhydride as the acylating

reagent.²² The Miller group has also reported the kinetic resolution of formamides and thioformamides as a way to avoid the background reaction caused by amine nucleophilicity.²³ In this system, the kinetic resolution of thioformamide (**6.7**) was performed at room temperature using the peptide based catalyst **6.5** (Scheme 6.3) along with di-*tert*-butyldicarbonate (**6.6**) (Scheme 6.3) as the acylating reagent. Selectivity factors ranging from 6-44 were reported for various thioformamides. Finally, enantiomerically enriched amine derivative such as formamide **6.9** can be achieved by oxidative hydrolysis of the newly resolved boc-protected thioformamides **6.8** (Scheme 6.3).

Even with all the progress made to achieve kinetic resolution of amines, one major challenge still remains which is substrate limitation. Developing a methodology for the kinetic resolution of amines would allow us to provide a valuable contribution to the field of organic chemistry. We proposed a way to solve the nucleophilicity issue was to convert chiral amines into imines and resolve the imine functionality. After the kinetic resolution, the enantioenriched imine can be simply converted back into the amine. To date, only a few scattered examples of the kinetic resolution of imines has been reported.

An example of the kinetic resolution of imines, reported by Fu and his coworker, is based on a copper catalyzed [3+2] cycloaddition (Scheme 6.4a) of an azomethine imine (**6.10**) with an alkyne (**6.11**).²⁴ The product of this reaction is the bicyclic pyrazolidinone derivative **6.12**, a biologically important compound. With this system, they achieved up to 99% ee and selectivity factors ranging from 15-96 for various azomethine imines. The highest selectivity factor was reported using electron withdrawing alkynes. Some disadvantages include the imines need to be azomethine imines, and C4-substituted azomethine imines like cyclohexyl do not undergo the kinetic resolution, which limits their

access to certain substrates. Another example reported by Lensink and Vries is based on a rhodium/diphosphine catalyst (Scheme 6.4b), where the kinetic resolution of amines is achieved by hydrogenation of one enantiomer of the corresponding imine.²⁵ However, most of the selectivity factors ranged between 1.1-5.7, with their highest selectivity factor 8 with only one substrate.



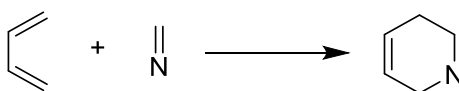
Scheme 6.4 (a) Copper catalyzed [3+2] kinetic resolution of imines (b) Kinetic resolution of Imines using Rhodium/diphosphine catalyzed hydrogenation

Other report of kinetic resolution of imines includes Buchwald, asymmetric hydrosilylation of imines of 3-substituted indanones and 4-substituted tetralones²⁶ as well as more recently

reported kinetic resolution of azomethine imines using N-heterocyclic carbene by the Chi group have.²⁷

6.3 Research Design

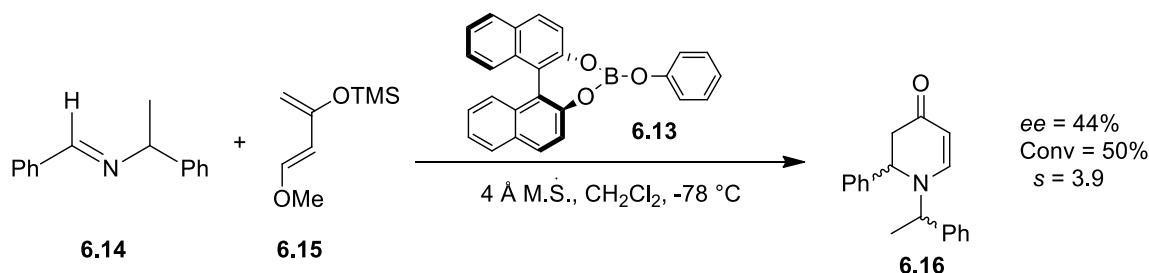
Our approach to the kinetic resolution of amines is to perform an enantioselective aza-Diels-Alder reaction between a chiral imine and a diene. As mentioned in the beginning, resolving amines will be first reacted with an appropriate aldehyde and converted into the imines using the Dean Stark apparatus. Once amines will be converted into the imines then the aza-Diels-Alder reaction can be performed to accomplish the kinetic resolution reaction. In, the aza-Diels-Alder reaction, the diene reacts with the one enantiomer of imine (racemic) functionality of the substrate to provide a functionalized piperidine product (as shown in Scheme 6.5)^{28,29} While other enantiomer remains as imine. Enantiomerically enriched, recovered imine will be then converted back into amine through hydrolysis (Scheme 6.1). The use of the imine in a Diels-Alder reaction avoids the issues associated with the nucleophilicity of amines.



Scheme 6.5 Aza-Diels-Alder reaction

The use of electron rich dienes in the reaction will help to facilitate the reaction even with less electrophilic imines. So far there has been only one report in the literature (Scheme 6.6) by the Yamamoto group where the kinetic resolution of imines was accomplished by using a Diels-Alder reaction.^{30,31} In this account, a stoichiometric amount of a boron-based BINOL catalyst **6.13** was used to facilitate the reaction between a racemic imine **6.14** and Danishefsky's diene **6.15** (Scheme 6.6). They only reported one reaction

where they obtained 50% conversion with an *ee* of 44% in the product **6.16**. This works out to a selectivity factor of four.

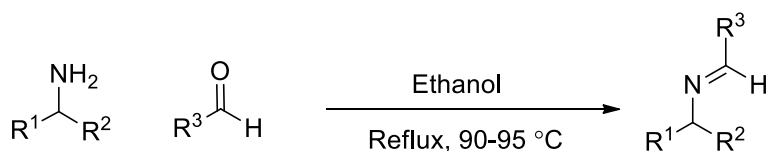


Scheme 6.6 Kinetic Resolution of an Imine using an aza-Diels-Alder reaction reported by Yamamoto and his co-worker

Thus the original problem of finding an efficient chiral system for the kinetic resolution of amines via an aza-Diels-Alder reaction of imines still persists. Further research is required to develop a catalyst system that will distinguish between two enantiomers. In this research plan, a method was proposed for the kinetic resolution of amines by using an aza-Diels -Alder reaction of imines with commercially available Danishefsky's diene. We began our study by screening different chiral Lewis acid systems with the aza-Diels-Alder reaction. Different metal and boron compounds with BINOL as a Boron/Metal-BINOL complex will try for activation of imines. Also other commercially available chiral catalysts including MeCBS and (+)-Ipc₂B(allyl)borane will be screened. Once an efficient chiral catalyst has been found, the next step will involve the future study of using different imines, dienes, solvent, and temperature to see what role, if any, these have on the reaction. Once these conditions are optimized, mechanistic studies will be performed for detailed understanding of the reaction.

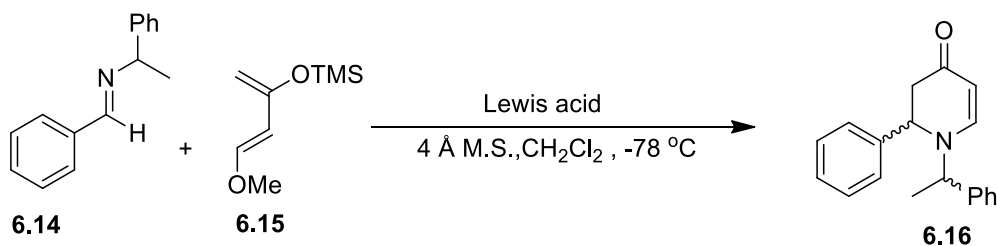
6.4 Result and Discussion

In order to develop a system for the kinetic resolution of amines, our initial focused was to convert the amines into imines. The imines were prepared by mixing (1:1) racemic amines and aldehydes in ethanol, and water was removed using a Dean Stark apparatus for 8-9 h. This was used as a general procedure for the conversion of amines into imines. We chose to start our studies with imine **6.14** made from 1-phenylethylamine and benzaldehyde because of the literature precedence of Yamamoto's work.¹⁶ Danishefsky's diene **6.15** was selected due to its high electron density, its commercially availability and again the precedence mentioned above. We began our study by reacting imine **6.14** with Danishefsky' diene (**6.15**) in dichloromethane at room temperature for 3-4 hours in the presence of different Lewis acids like ZnCl₂, BF₃OEt₂ and B(OPh)₃ to understand the nature of the reaction in more detail (Table 6.1). Low conversion was found with ZnCl₂ (Table 1, entry 1), conversion was improved when B(OPh)₃ used as a Lewis acid (Table 6.1, entry 3). A control reaction was also run without a Lewis acid present where no reaction took place. A lack of product indicates that the activation of the imine is required in order to initiate the reaction.



Scheme 6.7 Imine formation from amines using a Dean-Stark procedure

Table 6.1 Reaction of phenyl imine and Danishefsky's Diene in the presence of different Lewis acids



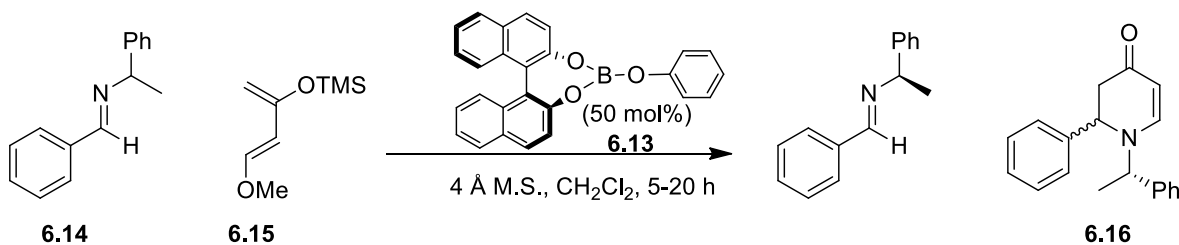
No.	Lewis Acid	Time	%Conv ^b
1	ZnCl ₂	22	14
2	BF ₃ OEt ₂	15	28
3	B(OPh) ₃	18	43
4 ^c	B(OH) ₂ Ph	18	35

a. 1.5 equiv Lewis acid and 1.2 equiv Danishefsky's diene was used. b. Conversion is calculated from ¹H NMR c. Reaction was done at 0 °C

After, making sure that the reaction was working with different Lewis acids, particularly with boron, we turned our attention to finding a chiral Lewis acid system for the kinetic resolution process. A variety of different chiral Lewis acids were examined as probable catalysts. The initial conditions involve a stoichiometric amount of the chiral Lewis acid and excess Danishefsky's diene using dichloromethane as the solvent at -78 °C. Since the product contained two stereocenters, there was a potential to form four different products, two diastereomers and their enantiomers. The enantiomeric excess of the imine and the product was determined using chiral HPLC. The stereochemistry was assigned by forming each individual imine enantiomer and the four products with Danishefsky's diene and determining their elution times on the HPLC. The selectivity factor was calculated by using the *ee* of the recovered starting material and the conversion. Separation of all four products was very difficult using various chiral HPLC columns and therefore conversion

was reported from the crude ^1H NMR. We started our investigation of the chiral Lewis acids by using the published literature procedure from the Yamamoto group, where a $\text{B}(\text{OPh})_3$ and (*S*)-BINOL complex was used as the chiral Lewis acid.

Table 6.2 (*s*)-BINOL- $\text{B}(\text{OPh})_3$ at different temperatures



No.	T (°C)	Conv ^a	ee of SM (%)	s
1	-78	38	4	1.2
2	-40	38	5	1.2
3	0	48	2	1.1
4	25	49	4	1.1
5 ^c	-78	46	2	1.1

a. conversion is calculated from ^1H NMR spectra.

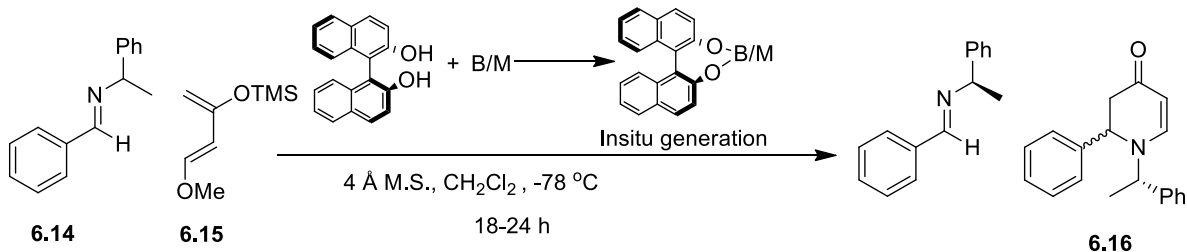
b. Selectivity factors are based on the ee of the recovered starting materials and products.

c. (*S*)-BINOL-boron (2:1)

The chiral Lewis acid complex was prepared in situ by mixing a 1:1 ratio of $\text{B}(\text{OPh})_3$ and (*S*)-BINOL in dichloromethane at room temperature for 1 h. When we tried to replicate the same reaction performed in the Yamamoto paper (dichloromethane, -78 °C), we were unable to reproduce the reported selectivity factor of 4.1 (Table 6.2, entry 1). A repetition of the same experiment was done several times but the highest selectivity factor we could achieve was 1.2. The same reaction was repeated at 0, -40, and 25 °C but a successful result was not obtained (entries 2-4). Even when we used 2 equivalents of (*S*)-BINOL with $\text{B}(\text{OPh})_3$, we did not observe a change in the selectivity factor (Table 6.2, entry 5).

Even though we could not reproduce the literature results, we started to explore conditions that would result in a successful kinetic resolution. The first change we decided to make to our system was the use of different Lewis acids which included different boron starting materials and metals with (*S*)-BINOL (Table 6.3). We employed a number of metals with (*S*)-BINOL including ZnCl₂, Eu(NO₃)₃, Sc(OTf)₃ and CoCl₂ (entries 1-4), but there was no selectivity generated. After experimenting with these metal sources we started to explore different boron compounds with (*S*)-BINOL. As shown in Table 6.2, a selectivity factor of 1.5 was achieved when phenyl boronic acid (Table 6.3, entry 5) was used as a boron source. Substituted boronic acids like 2-tolylboronic acid and 3-tolylboronic acid (Table 6.3, entries 6 & 7) were also tried which gave no selectivity for either chiral system. Boronic acid containing electron withdrawing groups still resulted in no selectivity (entries 8 & 9). The sterically hindered compound 2,4,6 trimethyl phenylboronic (entry 10) did not help with the selectivity (*s*= 1.1) but the anthracenylboronic acid catalyst gave a little bit of selectivity with a selectivity factor of 1.5 (entry 11).

Table 6.3 Reaction of phenyl imine with different (*S*)-BINOL-boron/metal complex



No.	Boron/Metal compound	Conv ^a	ee of SM (%)	<i>s</i> ^b
1	ZnCl ₂	37	2	1.1
2	Eu(NO ₃) ₃	45	1	1.1
3	CoCl ₂	24	1	1.1
4 ^c	Sc(OTf) ₃	34	1	1.0
5	Phenyl boronic Acid	44	12	1.5
6	2-Tolylboronic Acid	47	1	1.0
7	3-Tolylboronic Acid	45	1	1.0
8	(3-(trifluoromethyl)-phenyl)boronic acid	46	2	1.1
9	(2,4,6-trifluorophenyl)boronic acid	23	2	1.2
10	(2,4,6-trimethylphenyl)boronic acid	23	1	1.1
11	Anthracen-9-ylboronic acid	38	10	1.5

a. conversion is calculated from ¹H NMR spectra.

b. Selectivity is determined by using conversion and *ee* of the recovered starting material.

c. Reaction was done using PMP as base. Chiral complex was made by using azeotrope in reaction 5-11

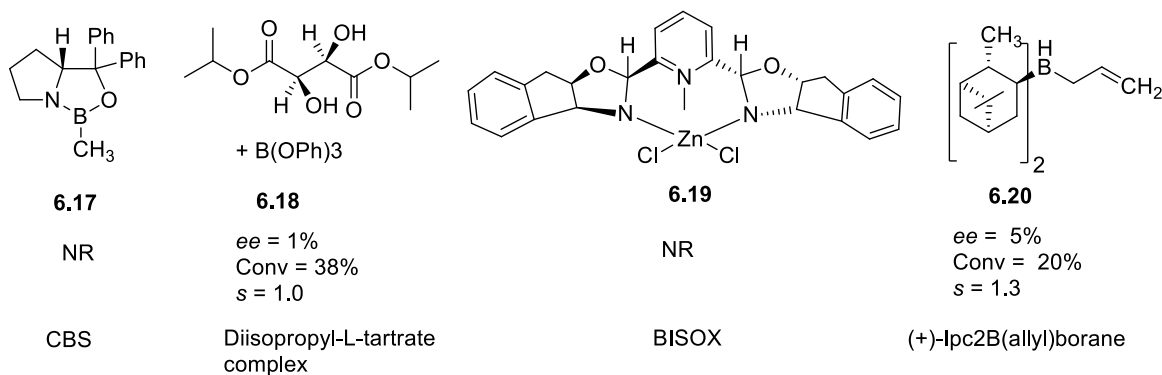
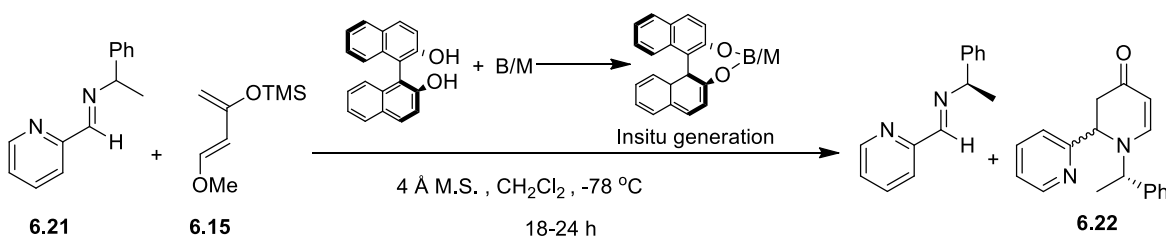


Figure 6.2 Other chiral Lewis acid catalysts

Other chiral ligands were also screened as either boron or other Lewis acid based catalysts (Figure 6.2). Diisopropyl-L-tartrate **6.18** with B(OPh)₃ was investigated, but it

gave no selectivity ($s = 1$). Catalysts like MeCBS **6.17** and the BISOX-Zn **6.19** complex gave no conversion. Surprisingly the commercially available catalyst, (+)-Ipc₂B(allyl)borane (**6.20**, 1 M solution in dioxane) gave a selectivity factor of 1.3 but only 20% conversion was achieved even after 78-80 h.

Table 6.4 Reaction of imine **6.21** with Danishefsky's diene in the presence of different chiral Lewis acids



No.	Boron/Metal compound	Conv ^a	ee of the recovered SM (%) ^{s^b}	
1	B(OPh) ₃	27	4	1.3
2	Eu(NO ₃) ₃	32	2	1.1
3 ^c	ZnCl ₂	NR	-	-
4 ^c	CoCl ₂	NR	-	-

a. conversion is calculated from ee of starting material and product.

b. Selectivity is determined by using conversion and ee of the recovered starting material.

c. No reaction.

Lacking a successful selectivity factor from imine **6.15**, we decided to change our substrate to the imine (**6.21**, a two point binding sites substrate), synthesized from 1-phenylethylamine and 2-formylpyridine. Imine **6.21** was selected as a substrate due to improved separation of both the imine and the four diastereomeric products on HPLC. This allowed us to more readily measure enantiomeric excess of the product **6.22**, which allowed us to calculate a more accurate conversion. It was also chosen since it had two Lewis basic binding sites in which to interact with the Lewis acid. We wanted to investigate whether this would aid in improving selectivity. A similar experiment to Table 6.2, Entry 1 was

performed by taking (*S*)-BINOL and B(OPh)₃ using imine **6.22** as the substrate, but disappointingly produced similar selectivity factors to imine **6.14** (*s* = 1.3) (Table 6.4, Entry 1). To our surprise, metals like ZnCl₂, and CoCl₂ did not give any product formation even after 22-24 h. This indicated a strong binding of the metal between the two nitrogens on the imine which prevented further reactivity with Danishefsky's diene. We have also tried catalysts with hydrogen bonding capabilities, such as the two thioureas catalysts shown in Figure 6.3, but the highest selectivity factor achieved was 1.1. Diisopropyl-L-tartrate was also tried but it gave almost no selectivity.

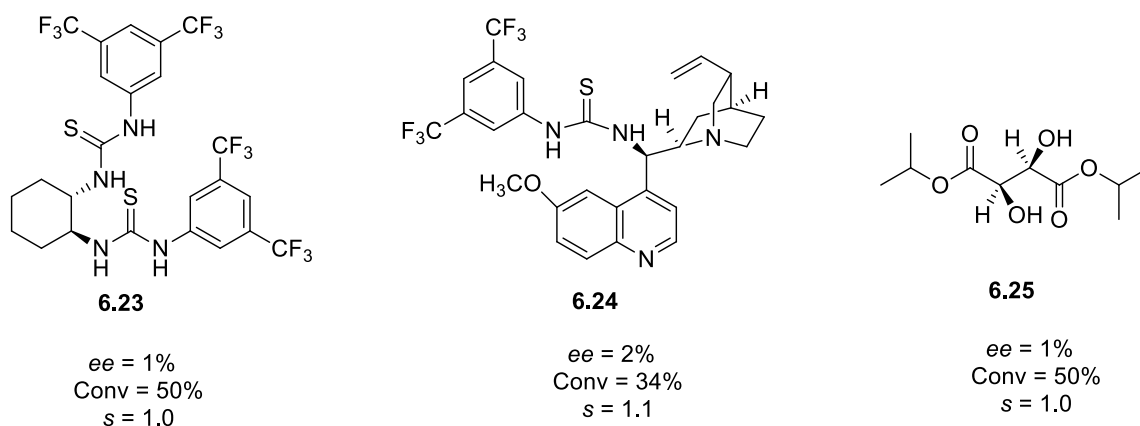
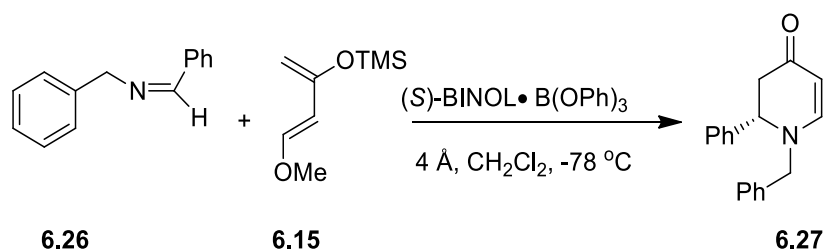


Figure 6.3 Catalyst with Hydrogen bonding capability

After examining several chiral Lewis acid systems and other catalysts with imines **6.15** and **6.21** and obtaining little to no selectivity, we decided to investigate the efficiency of our in situ catalyst formations. We were worried that the boron catalyst complexes were not forming since we could not reproduce Yamamoto's work. Several different methods were performed to synthesize the BINOL-B(OPh)₃ complex and the boronate ester from BINOL and phenyl boronic acid, but ¹H NMR spectra was inconclusive regarding complex

formation. Finally, we decided to use the BINOL/B(OPh)₃ system with a published reaction in order to test for complex formation. A benzyl imine **6.26** was made and reacted with Danishefsky's diene **6.15** using B(OPh)₃ -BINOL **6.13** complex, where product **6.27** with a 67% *ee* was obtained compared to the reported *ee* of 85% (Scheme 6.8).¹⁸ These results show that the BINOL/B(OPh)₃ complex seems to be forming, but it is not an efficient catalyst for the kinetic resolution.



Scheme 6.8 Asymmetric reaction of benzyl imine and Danishefsky's diene

In conclusion, different chiral Lewis acids and other catalysts were screened for the kinetic resolution of amines via imines. No improvement in selectivity factor was observed. In the future, different chiral Lewis acid systems including various boron and metal sources like substituted boronic acids as well as different substituted BINOL like ligands can be investigated to achieve selectivity. It was known from experiments and modeling studies that the substituent on the 3,3'-position of the BINOL influences enantioselectivity in a strong way, when used in conjunction with boron/metal compounds. These as well as other chiral sources can also be tested to determine their selectivity in these reactions.

6.5 Experimental

All reactions were carried out in oven dried glassware under nitrogen. Air sensitive and moisture sensitive liquids and solutions were transferred using syringe. Aza-Diels-Alder reactions were carried out at -78 °C using a cryocool. All thin layer chromatography plates were observed under uv lamp (254 nm or 365 nm). All Solvents including THF, dichloromethane, and toluene were dried by passing through a column of activated alumina before use and stored over molecular sieves. All reagents were purchased and used as is, unless otherwise noted. Premium grade silica gel 32-63 µm was used. Column chromatography was performed using silica gel as a stationary phase. Enantiomeric excess was determined by using chiral HPLC technology. ¹H NMR was obtained using a 300 MHz NMR and ¹³C was obtained using a 75.46 MHz NMR. Samples were prepared using CDCl₃ and spectra were obtained with reference to the solvent peak 7.26 ppm for ¹H and 77.0 ppm for ¹³C at 25 °C. Data for ¹H NMR spectra was reported as follows: chemical shift (δ, ppm), multiplicity (s = singlet, d = doublet, t = triplet, q = quartet, m = multiplet, dd = doublet of doublets) and coupling constant in (Hz). Data for ¹³C was reported in terms of chemical shifts and number of carbons.

General Procedure for Calculation of Conversion and Selectivity Factor:

Conversion was calculated by using *ee* of recovered starting material (*ee*^s) and product (*ee*^p) by using the following equation.

$$\% C = \frac{ee_s}{ee_s + ee_p}$$

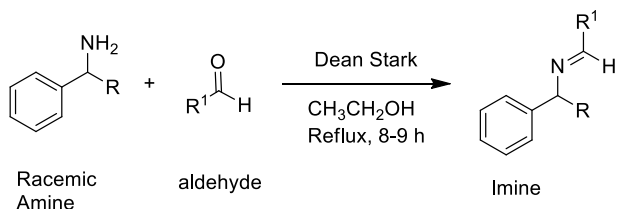
%C = Conversion
ee_s = enantiomeric excess of the recovered starting material
ee_p = enantiomeric excess of the product

Selectivity factor ($s = k_{fast}/k_{slow}$) determined by using the following equation.

$$S = \ln[(1-C) (1-ee(ee^s))] / \ln[(1+C) (1+ee(ee^s))]$$

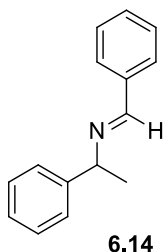
6.5 Experimental Procedure:

General method for the preparation of imines (Scheme 6.7) :



All imines were prepared using the following general protocol and spectral data matched for those published in the literature. An oven dried 50 mL round bottom flask was charged with a stir bar and 35 mL of ethanol under nitrogen. Racemic amine (20 mmol, 1.0 equiv) and aldehyde (20 mmol, 1.0 equiv) was added to the round bottom flask and the resulting mixture was allowed to reflux at 60-70 °C and water was removed using a Dean-Stark apparatus. The reaction mixtures were allowed to reflux for 7-8 h. At the end of the reaction, solvent was removed under reduced pressure. The resulting oil was used without further purification.

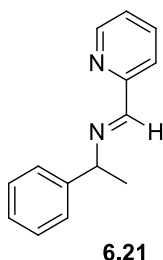
Preparation of (E)-N-benzylidene-1-phenylethanamine (6.14) :



Imine **6.14** was made using the above general protocol by mixing phenylethyl amine (2.57 mL, 20 mmol) and benzaldehyde (2.03 mL, 20 mmol). Spectral data for **6.14**: ^1H NMR

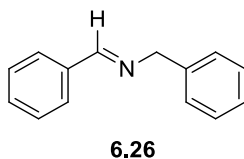
(CDCl₃) δ 1.60 (3H, d, J=6.6 Hz), 4.57 (1H, q, J=6.6 Hz). 7.7-7.82 (2H, m), 8.39 (1H, s);
¹³C NMR (CDCl₃) δ 22.9, 67.9, 124.8, 124.9, 126.4, 126.6, 126.7, 128.7, 134.5, 143.3,
 157.6 HPLC condition to separate racemic mixture was 10% IPA in 90% hexane using
 OD-H Column. *t*R 6.58 and 7.73

Preparation of (E)-1-phenyl-N-(pyridine-2-ylmethylene) ethanamine (6.21):



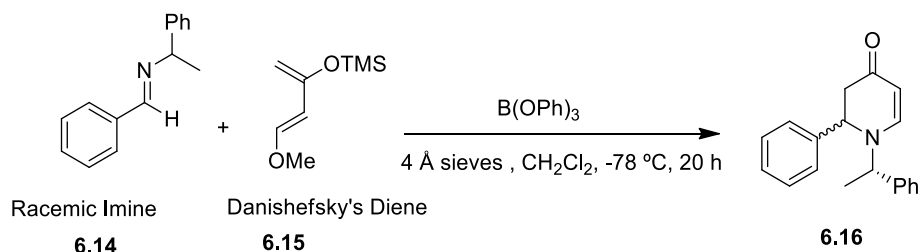
Imine **6.21** was made using the above general protocol by mixing 1-phenylethylamine (2.57 mL, 20 mmol) and pyridine 2-benzaldehyde (1.90 mL, 20 mmol). Spectral data for **6.21**: ¹H NMR (CDCl₃) δ 1.61 (d, 3H, J = 6.9Hz), 4.64 (q, 1H, , J = 6.6 Hz), 7.2-7.7 (m, 6H), 7.73 (t, 1H), 8.10 (d, 1H, J = 7.8 Hz), 8.46(s, 1H), 8.63 (d, 1H, J = 6.6 Hz); ¹³C NMR (CDCl₃): δ 24.5, 69.6, 121.5, 124.7, 126.7, 127.0, 128.5, 136.5, 144.6, 149.3, 154.8, 160.4.

Preparation of (E)-N-benzylidene-1-phenylmethanamine (6.26):



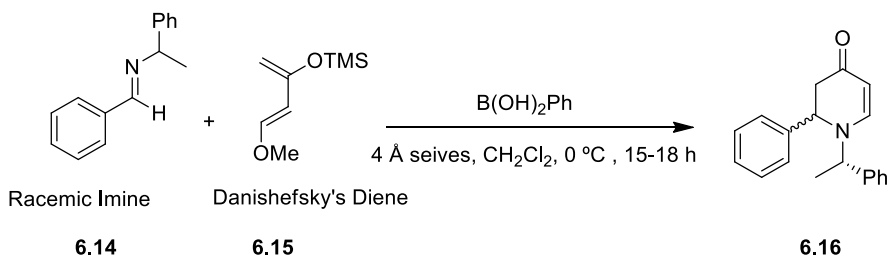
Imine **6.26** was made using the above general protocol by mixing benzyl amine (2.17 mL, 20 mmol) and benzaldehyde (2.03 mL, 20 mmol). Spectral data for **6.26**: ¹H NMR (CDCl₃) δ 4.86 (s, 2H), 7.28-7.47(m, 2H), 7.80-7.84 (m, 2H), 8.42(s,1H). ¹³C NMR (CDCl₃): δ 64.8, 126.7, 127.7, 128.0, 128.2, 128.3, 130.5, 135.9, 139.1, 161.7.

Control experiments for aza-Diels-Alder reaction of imine 6.15 with B(OPh)₃ compound:



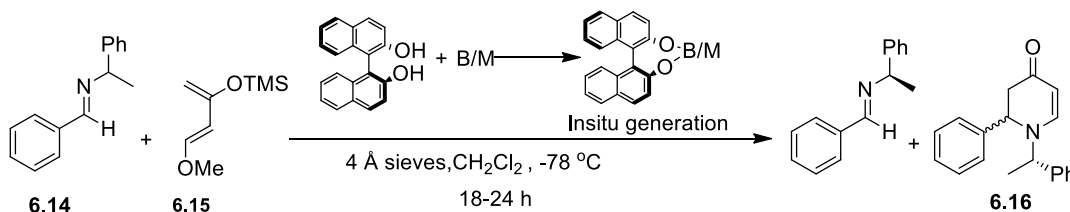
To an oven dried four dram vial, 4 Å powdered molecular sieves were added followed by 10 mL dichloromethane under a nitrogen atmosphere and an addition of B(OPh)_3 (51 mg, 0.35 mmol). After stirring at room temperature for 1 h, the resulting mixture was cooled to $0\text{ }^\circ\text{C}$, then a solution of imine **6.14** (73 mg, 0.35 mmol) in CH_2Cl_2 (1 mL) was added. After stirring for 10 minutes at $0\text{ }^\circ\text{C}$, the mixture was cooled to $-78\text{ }^\circ\text{C}$, and a solution of Danishefsky's diene (0.084 mL, 0.42 mmol or 0.042 mL, 0.21 mmol) in 1 mL CH_2Cl_2 was added dropwise. The mixture was allowed to stir at $-78\text{ }^\circ\text{C}$ for 18-20 h. The solution was washed with water and a sat. NaHCO_3 solution, and then dried over Na_2SO_4 . Solvent was removed and a conversion of 43% and a dr of 20:80 was determined by ^1H NMR.

Control experiment for aza-Diels-Alder reaction of imine 6.14 with phenyl boronic acid compound:



To an oven dried four dram vial, 4Å powder molecular sieves were added followed by 10 mL dichloromethane under nitrogen atmosphere and a phenylboronic acid (43 mg, 0.35 mmol). After stirring at room temperature for 1 h, the resulting mixture was cooled to 0 °C, then a solution of imine **6.14** (73 mg, 0.35 mmol) in CH₂Cl₂ (1 mL) was added. After stirring for 10 minutes at 0 °C, a solution of Danishefsky's diene (0.084 mL, 0.42 mmol) in 1 mL CH₂Cl₂ was added dropwise. The mixture was allowed to stir at 0 °C for several hours, the solution was then washed with water and sat. NaHCO₃ solution, and then dried over Na₂SO₄. Solvent was removed and a conversion of 35% and a dr of 35:65 was determined via ¹H NMR.

Aza-Diels-Alder reaction of imine 6.14 with chiral boron/metal compound:

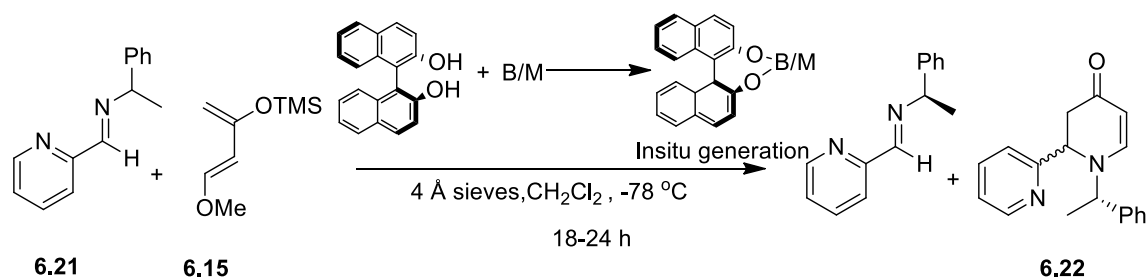


To an oven dried four dram vial, 4Å powder molecular sieves were added using 10 mL dichloromethane under nitrogen atmosphere followed by addition of B(OPh)₃ or a metal compound (0.175 mmol) and (*S*)-BINOL (0.175 mmol, 1 equiv). After stirring at room temperature for 1 h, the resulting mixture was cooled to 0 °C, then a solution of imine **6.14** (73 mg, 0.35 mmol) in CH₂Cl₂ (1 mL) was added. After stirring for 10 minutes at 0 °C, the mixture was cooled to -78 °C, and a solution of Danishefsky's diene (0.084 mL, 0.42 mmol) in 1 mL CH₂Cl₂ was added dropwise. The mixture was allowed to stir at -78 °C for several hours. The solution was washed with water and a sat. NaHCO₃ solution, and then dried over Na₂SO₄. The solvent was removed and purification was done by silica gel

column chromatography with the eluent 70% EtOAc in hexane. The enantiomeric excess of the product was determined by using a CHIRALPAK OD-H column using a (80:20) hexane/isopropanol solvent with a flow rate of 0.600 ml/min. All four diastereomers did not separate on the chiral HPLC, but the individual products were identified by making the products from the pure *S*-imine and *R*-imine. (Enantiomer *t*R 18.9 (*S* enantiomer product), 21.3 (*S* and *R* enantiomer product), 30.1 (*R* enantiomer product))

Spectral data: ^1H NMR (CDCl_3) : δ 1.46 (d, 3H, $J = 7.2$ Hz), 2.55-2.88 (m, 2H), 4.43 (q, 1H, $J = 6.9$ Hz), 4.68 (dd, 1H, $J = 6.6, 9.0$ Hz), 5.02 (d, 1H, $J = 7.8$ Hz), 7.05 (d, 1H, $J = 7.8$ Hz), 7.09-7.42 (m, 10H).

Aza-Diels-Alder reaction of imine 6.21 with chiral boron/metal compound:

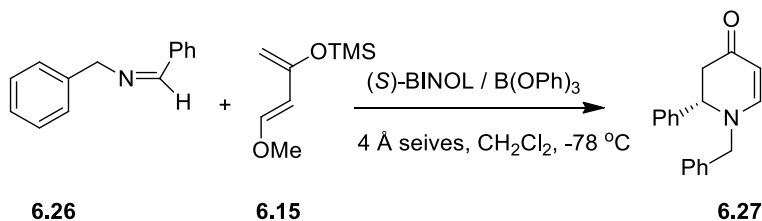


To an oven dried four dram vial, 4Å powder molecular sieves were added using 10 mL dichloromethane under nitrogen atmosphere followed by addition of $\text{B}(\text{OPh})_3$ or a metal compound (0.175 mmol) and (*S*)-BINOL (0.175 mmol, 1 equiv). After stirring at room temperature for 1 h, the resulting mixture was cooled to 0°C , then a solution of imine **6.21** (74 mg, 0.35 mmol) in CH_2Cl_2 (1 mL) was added. After stirring for 10 minutes at 0°C , the mixture was cooled to -78°C , and a solution of Danishefsky's diene (0.042 mL, 0.21 mmol) in 1 mL CH_2Cl_2 was added dropwise. The mixture was allowed to stir at -78°C for several hours. The solution was washed with water and a sat. NaHCO_3 solution, and then

dried over Na₂SO₄. Solvent was removed and purification was done by silica gel column chromatography using 60% EtOAc in hexane. The enantiomeric excess was determined by using CHIRALPAK OD-H column using an 80:20 hexane/isopropapol solvent with a flow rate of 0.600 ml/min. The products in the HPLC were identified by making the individual products from pure *S*-imine and *R*-imine. 22.7 (product of *S* enantiomer), 25.2 (product of *S* enantiomer), 30.6 (Product of *R* enantiomer mixture), 31.9 (product of *R* enantiomer)

Spectral data: ¹H NMR (CDCl₃) δ 1.44 (d, 3H, *J* = 6.6 Hz), 2.64-2.88 (m, 2H), 4.43 (q, 1H, *J* = 6.9 Hz), 4.77 (dd, 1H, *J* = 5.1, 5.4 Hz), 4.91 (d, 1H, *J* = 7.8 Hz), 7.05 (d, 1H, *J* = 7.8 Hz), 7.10-7.32 (m, 7H), 7.32-7.59 (m, 1H), 8.50 (d, *J* = 3.6 Hz, 1H); MS: M⁺ = 278. tR 22.7

aza-Diels-Alder reaction of imine 6.26 with Chiral Boron-(*S*)-BINOL (6.13) compound:



To an oven dried four dram vial, 4Å powder molecular sieves were added using 10 mL dichloromethane under nitrogen atmosphere followed by addition of B(OPh)₃ (101 mg, 0.35 mmol) and (*S*)-BINOL (100 mg, 0.35 mmol). After stirring at room temperature for 1 h, the resulting mixture was cooled to 0 °C, then a solution of imine (68 mg, 0.35 mmol) in CH₂Cl₂ (1 mL) was added. After stirring for 10 minutes at 0 °C, the mixture was cooled to -78 °C, and a solution of Danishefsky's diene (0.084 mL, 0.42mmol) in 1 mL CH₂Cl₂ was added dropwise. The mixture was allowed to stir at -78 °C for several hours. The

solution was washed with water and a sat. NaHCO_3 solution, and then dried over Na_2SO_4 . Solvent was removed and purification was done by silica gel column chromatography to afford pure product (22% yield). The enantiomeric excess of the product was determined by using a CHIRALPAK AD-H column using a (90:10) hexane/isopropanol solvent with the flow rate of 1.0 ml/min. Spectral data: ^1H NMR (CDCl_3) δ 2.68 (dd, 1H, $J=7.8, 16.5$ Hz), 2.87 (dd, 1H, $J=6.9, 16.5$ Hz), 4.13 (d, 1H, $J=15.0$ Hz), 4.36 (d, 1H, $J=15.3$ Hz), 4.52 (t, 1H, $J=7.5$ Hz), 5.09 (d, 1H, $J=7.5$ Hz), 7.11-7.39 (m, 1H).

6.6 References

- (1) Pamies, O.; Ell, A. H.; Samec, J. S. M.; Hermanns, N.; Backvall, J. E. An efficient and mild ruthenium-catalyzed racemization of amines: application to the synthesis of enantiomerically pure amines. *Tetrahedron Lett.* **2002**, *43*, 4699-4702.
- (2) Hartwig, J. Chiral Amine Synthesis; Nugent, T. C., Eds.; Wiley-VCH: Germany, 2010
- (3) Keith, J. M.; Larrow, J. F.; Jacobsen, E. N. Practical considerations in kinetic resolution reactions. *Adv. Synth. Catal.* **2001**, *343*, 5-26.
- (4) Hohn, M.; Bornscheuer, U. T. Biocatalytic routes to optically active amines. *Chemcatchem* **2009**, *1*, 42-51.
- (5) Gotor-Fernandez, V.; Gotor, V. Biocatalytic routes to chiral amines and amino acids. *Curr Opin Drug Disc* **2009**, *12*, 784-797.
- (6) Arseniyadis, S.; Subhash, P. V.; Valleix, A.; Mathew, S. P.; Blackmond, D. G.; Wagner, A.; Mioskowski, C. Tuning the enantioselective N-acetylation of racemic amines: A spectacular salt effect. *J. Am. Chem. Soc.* **2005**, *127*, 6138-6139.
- (7) Arseniyadis, S.; Valleix, A.; Wagner, A.; Mioskowski, C. Kinetic resolution of amines: A highly enantioselective and chemoselective acetylating agent with a unique solvent-induced reversal of stereoselectivity. *Angew. Chem., Int. Ed.* **2004**, *43*, 3314-3317.
- (8) Ie, Y.; Fu, G. C. A new benchmark for the non-enzymatic enantioselective acylation of amines: use of a planar-chiral derivative of 4-pyrrolidinopyridine as the acylating agent. *Chem. Commun.* **2000**, 119-120.
- (9) Karnik, A. V.; Kamath, S. S. Enantioselective benzylation of racemic amines using chiral benzimidazolide as a benzyloxylation agent. *Tetrahedron-Asymmetr* **2008**, *19*, 45-48.
- (10) Kolleth, A.; Cattoen, M.; Arseniyadis, S.; Cossy, J. Non-enzymatic acylative kinetic resolution of primary allylic amines. *Chem. Commun.* **2013**, *49*, 9338-9340.
- (11) Kolleth, A.; Christoph, S.; Arseniyadis, S.; Cossy, J. Kinetic resolution of propargylamines via a highly enantioselective non-enzymatic N-acylation process. *Chem. Commun.* **2012**, *48*, 10511-10513.

- (12) Arai, S.; Bellemin-Laponnaz, S.; Fu, G. C. Kinetic resolution of amines by a nonenzymatic acylation catalyst. *Angew. Chem., Int. Ed.* **2001**, *40*, 234-236.
- (13) Arp, F. O.; Fu, G. C. Kinetic resolutions of indolines by a nonenzymatic acylation catalyst. *J. Am. Chem. Soc.* **2006**, *128*, 14264-14265.
- (14) Seidel, D. The Anion-Binding Approach to Catalytic Enantioselective Acyl Transfer. *Synlett* 2014, *25*, eFirst
- (15) De, C. K.; Klauber, E. G.; Seidel, D. Merging nucleophilic and hydrogen bonding catalysis: An anion binding approach to the kinetic resolution of amines. *J. Am. Chem. Soc.* **2009**, 061.
- (16) Mittal, N.; Sun, D. X.; Seidel, D. Kinetic resolution of amines via dual catalysis: Remarkable dependence of selectivity on the achiral cocatalyst. *Organic letters* **2012**, *14*, 3084-3087.
- (17) Klauber, E. G.; De, C. K.; Shah, T. K.; Seidel, D. Merging nucleophilic and hydrogen bonding catalysis: An anion binding approach to the kinetic resolution of propargylic amines. *J. Am. Chem. Soc.* **2010**, *132*, 13624-13626.
- (18) Klauber, E. G.; Mittal, N.; Shah, T. K.; Seidel, D. A dual-catalysis/anion-binding approach to the kinetic resolution of allylic amines. *Org. Lett.* **2011**, *13*, 2464-2467.
- (19) Min, C.; Mittal, N.; De, C. K.; Seidel, D. A dual-catalysis approach to the kinetic resolution of 1,2-diaryl-1,2-diaminoethanes. *Chem. Commun.* **2012**, *48*, 10853-10855.
- (20) Hsieh, S. Y.; Binanzer, M.; Kreituss, I.; Bode, J. W. Expanded substrate scope and catalyst optimization for the catalytic kinetic resolution of N-heterocycles. *Chem. Commun.* **2012**, *48*, 8892-8894.
- (21) Binanzer, M.; Hsieh, S. Y.; Bode, J. W. Catalytic kinetic resolution of cyclic secondary amines. *J. Am. Chem. Soc.* **2011**, *133*, 19698-19701.
- (22) Birman, V. B.; Jiang, H.; Li, X.; Guo, L.; Uffman, E. W. Kinetic resolution of 2-oxazolidinones via catalytic, enantioselective N-acylation. *J. Am. Chem. Soc.* **2006**, *128*, 6536-6537.
- (23) Fowler, B. S.; Mikochik, P. J.; Miller, S. J. Peptide-catalyzed kinetic resolution of formamides and thioformamides as an entry to nonracemic amines. *J. Am. Chem. Soc.* **2010**, *132*, 2870-2871.

- (24) Suarez, A.; Downey, C. W.; Fu, G. C. Kinetic resolutions of azomethine imines via -catalyzed [3+2] cycloadditions. *J. Am. Chem. Soc.* **2005**, *127*, 11244-11245.
- (25) Lensink, C.; Devries, J. G. Diastereoselective hydrogenation and kinetic resolution of imines using rhodium diphosphine catalyzed hydrogenation. *Tetrahedron-Asymmetr* **1993**, *4*, 215-222.
- (26) Yun, J. S.; Buchwald, S. L. Efficient kinetic resolution in the asymmetric hydrosilylation of imines of 3-substituted indanones and 4-substituted tetralones. *J. Org. Chem.* **2000**, *65*, 767-774.
- (27) Wang, M.; Huang, Z.; Xu, J.; Chi, Y. R. N-heterocyclic carbene-catalyzed $[3+4]$ cycloaddition and kinetic resolution of azomethine imines. *J. Am. Chem. Soc.* **2014**, *136*, 1214-1217.
- (28) Carry, F. A.; Sundberg, R. J. Advanced Organic Chemistry, 4th Ed.; Springer: New York, 2004; Chp 6
- (29) Tietze, L. F.; Ketschau, G. Hetero Diels-Alder reaction in organic chemistry, Springer-Verlag Berlin Heidelberg: Germany, 1997.
- (30) Hattori, K.; Yamamoto, H. Asymmetric aza-Diels-Alder reaction catalyzed by Effect of biphenol and binaphthol ligand. *Synlett* **1993**, 129-130.
- (31) Hattori, K.; Yamamoto, H. Asymmetric aza-Diels-Alder reaction - Enantioselective and diastereoselective reaction of imine mediated by chiral Lewis acid. *Tetrahedron* **1993**, *49*, 1749-1760.